THE DEVELOPMENT OF NOVEL ANTIMICROBIAL PEPTIDES AND VARIOUS STRATEGIES TO IMPROVE THEIR ACTIVITY AND BIOCOMPATIBILITY

by

Prashant Sandeep Kumar

B.Sc., The University of British Columbia, 2011

A THESIS SUBMITTED IN PARTIAL FULFILLMENT OF

THE REQUIREMENTS FOR THE DEGREE OF

DOCTOR OF PHILOSOPHY

in

THE FACULTY OF GRADUATE AND POSTDOCTORAL STUDIES

(Chemistry)

THE UNIVERSITY OF BRITISH COLUMBIA

(Vancouver)

July 2018

The following individuals certify that they have read, and recommend to the Faculty of Graduate and Postdoctoral Studies for acceptance, the dissertation entitled:

The Development Of Novel Antimicrobial Peptides And Various Strategies To Improve Their Activity And Biocompatibility

---

submitted by Prashant S. Kumar in partial fulfillment of the requirements

the degree of Doctor Of Philosophy

in Chemistry

Examining Committee:

Suzana K. Straus, Chemistry

Co-supervisor

Jayachandran N. Kizhakkedathu, Pathology and Laboratory Medicine

Co-supervisor

Katherine S. Ryan, Chemistry

Supervisory Committee Member

Russ Algar, Chemistry

University Examiner

Dirk Lange, Medicine

University Examiner

Additional Supervisory Committee Members:

Hongbin Li, Chemistry

Supervisory Committee Member

Abstract

With the advent of antibiotic resistance and crisis, it is crucial to find substitutes to conventional antibiotics. Antimicrobial peptides (AMPs) are considered to be viable alternatives, because they are broad spectrum and bacteria develop little or no resistance towards AMPs. Interestingly, only few AMPs are used as therapeutics, due to problems such as host toxicity, protease cleavage and short half-life. Therefore, there is a need to improve the efficacy of AMPs by the use of D-peptides and/or delivery vehicles. The introduction of the thesis describes the diversity and various mechanisms of action (MOA) of AMPs. The issues and ways to improve the efficacy of AMPs, which forms the foundation of this thesis, are also discussed.

Recently, hyperbranched polyglycerol (HPG) has gained attention due to its excellent biocompatibility, multifunctionality and long blood circulation time. The body of the thesis describes a methodology to covalently attach aurein 2.2 and its mutants to HPG and study the influence of the molecular weight on the antimicrobial activity. A peptide array was used to design tryptophan and arginine mutants of aurein 2.2. Mutant peptide 77 had significantly superior antimicrobial and antibiofilm activity compared to aurein 2.2 but was more toxic. We found that HPG can be used as a general scaffold to alleviate the toxicity of the peptides, however the antimicrobial activity of the peptides decrease as the molecular weight of HPG increases.

The conjugates/peptides were tested in an *in vivo* mice skin infection (abscess) model. Surprisingly, peptide 73 and aurein 2.2 has similar efficacy *in vivo* indicating both the antimicrobial activity and toxicity, i.e. therapeutic index, are important. The conjugates (HPG-73c) were not active in mice abscess model, whereas 73c and D-73 encapsulated in micelles composed of DSPE-PEG2000 had excellent activity suggesting the release of the peptide from

the delivery vehicle is necessary for *in vivo* activity. Without encapsulation D-73 was too toxic. A bacterial expression system was used to produce isotopically (^{15}N) labeled aurein 2.2 and its interaction with whole bacterial cells was examined by nuclear magnetic resonance (NMR) and scanning electron microscopy (SEM) confirming the MOA. Finally, the results presented will be discussed in the broad context of designing AMPs for therapeutics and understanding their MOA.

Lay Summary

Antibiotic resistance has become a major public health concern. Indeed, some studies report that ABR could lead to 10 million deaths per year by 2050, making it crucial to find timely alternatives to currently used antibiotics. Antimicrobial peptides (AMPs) have shown great promise, because bacteria develop no or low resistance to AMPs. However, only few antimicrobial peptides are commercially available for use. This is due to problems with toxicity, short half-life, and rapid kidney clearance. This thesis focuses on developing strategies to improve the antimicrobial activity and properties of AMPs, by developing more active peptides and using delivery systems, such as biocompatible polymers and encapsulating agents. The activity of the peptides was tested using resistant bacteria, as well as in a mouse skin infection (abscess) model. Finally, a new method was developed to study how these peptides interact with whole bacterial cells, in order to understand how they function. Overall, the findings presented in this thesis lay the foundation for the future development of biocompatible AMPs, an essential tool to combat ABR.

Preface

Ethics approval was received from UBC for studies conducted at the Centre for Blood Research (UBC Ethics approval no: H10-01896). Animal experiments were performed in accordance with The Canadian Council on Animal Care (CCAC) guidelines and were approved by the University of British Columbia Animal Care Committee (certificate number A14-0363). This research project was conducted under the supervision of Dr. Suzana K. Straus (Department of Chemistry, UBC, Vancouver) and Dr. Jayachandran N. Kizhakkedathu (Centre for Blood Research, UBC, Vancouver).

A version of Chapter 1 has been published as a first authored, invited review paper in the journal *Biomolecules* (DOI: 10.3390/biom8010004). I was responsible for conducting the literature review and writing the review paper which was edited by my supervisors.

Chapter 2 is based on the study published in the journal *ACS Biomacromolecules* (DOI: 10.1021/bm5018244) and describes the effect of conjugation of aurein peptides to hyperbranched polyglycerol (HPG) on antimicrobial activity, biocompatibility and structure. I was responsible for writing the paper which was edited by my supervisors. I was responsible for designing the experiments with my supervisors, synthesizing the peptides and conjugates and running most of the experiments except the following: Rajesh A. Shenoi synthesized the 44,000 Dalton HPG; Michael Nguyen synthesized the aurein 2.2 peptide under my supervision; and Benjamin Lai ran the complement activation and cell toxicity studies.

Chapter 3 is based on the study published in the journal *ACS Applied Material and Interfaces* (DOI: 10.1021/acsami.7b09471). This work examines the influence of the peptide sequence and HPG molecular weight on the antimicrobial activity and biocompatibility. I was responsible for writing the paper which was edited by my supervisors. I designed the peptide

array with Suzana K. Straus, synthesising the polymers, peptides and conjugates. Srinivas Abbina synthesized the 100,000 Dalton HPG. Allen Takayesu synthesized peptide 73 and 77 under my supervision. Manu Thomas Kalathottukaren performed the blood coagulation studies (aPTT and PT) and Usama Abbasi ran the cell toxicity studies.

Chapter 4 is based on the study conducted in collaboration with Dr. Bob Hancock's laboratory at the Centre for Microbial Diseases and Immunity Research, UBC, Vancouver. Studies in this chapter investigated the antibiofilm activity and efficacy of the peptides in mice abscess model. I was responsible for designing and synthesizing all the peptides and conjugates and running the experiments except for all the *in vivo* mice studies which were conducted by Daniel Pletzer and all the antibiofilm experiments which were done by John Cheng.

Chapter 5 is based on the overexpression, purification and esterification of aurein 2.2. The expressed isotopically labelled peptide was then utilized to probe the interaction of aurein 2.2 with whole bacterial cells by nuclear magnetic resonance (NMR) and scanning electron microscopy (SEM). The plasmid used for expression in this chapter was kindly provided by Dr. Hans J. Vogel from the University of Calgary. I was responsible for designing the experiments with my supervisors. All the experiments were also conducted by me with help from Suzana K. Straus for the NMR experiment. Allen Takayesu conducted some of the expression experiments under my supervision.

Publications

1) **Kumar, P**.; Kizhakkedathu, J.; Straus, S. Antimicrobial Peptides: Diversity, Mechanism of Action and Strategies to Improve the Activity and Biocompatibility In Vivo. ***Biomolecules*** 2018, *8*, 4, doi:10.3390/biom8010004.

2) **Kumar, P**.; Takayesu, A.; Abbasi, U.; Kalathottukaren, M. T.; Abbina, S.; Kizhakkedathu, J. N.; Straus, S. K. Antimicrobial Peptide–Polymer Conjugates with High Activity: Influence of Polymer Molecular Weight and Peptide Sequence on Antimicrobial

Activity, Proteolysis, and Biocompatibility. ***ACS Appl. Mater. Interfaces*** 2017, acsami.7b09471, doi:10.1021/acsami.7b09471.

3) **Kumar, P**.; Shenoi, R. A.; Lai, B. F. L.; Nguyen, M.; Kizhakkedathu, J. N.; Straus, S. K. Conjugation of Aurein 2.2 to HPG Yields an Antimicrobial with Better Properties. ***Biomacromolecules*** 2015, *16*, 913–923, doi:10.1021/bm5018244.

4) Abbina, S.; Vappala, S.; **Kumar, P**.; Siren, E. M. J.; La, C. C.; Abbasi, U.; Brooks, D. E.; Kizhakkedathu, J. N. Hyperbranched polyglycerols: recent advances in synthesis, biocompatibility and biomedical applications. ***J. Mater. Chem. B*** 2017, *5*, 9249–9277, doi:10.1039/C7TB02515G.

5) Wenzel, M.; Senges, C. H. R.; Zhang, J.; Suleman, S.; Nguyen, M.; **Kumar, P**.; Chiriac, A. I.; Stepanek, J. J.; Raatschen, N.; May, C.; Krämer, U.; Sahl, H.-G.; Straus, S. K.; Bandow, J. E. Antimicrobial Peptides from the Aurein Family Form Ion-Selective Pores in *Bacillus subtilis*. ***ChemBioChem*** 2015, *16*, 1101–1108, doi:10.1002/cbic.201500020.

6) Sang, Y.; Tait, A. R.; Scott, W. R. P.; Creagh, A. L.; **Kumar, P**.; Haynes, C. A.; Straus, S. K. Probing the Interaction between U24 and the SH3 Domain of Fyn Tyrosine Kinase. ***Biochemistry*** 2014, *53*, 6092–6102, doi:10.1021/bi500945x.

Table of Contents

Abstract ..... **iii**

Lay Summary ..... **v**

Preface ..... **vi**

Table of Contents ..... **ix**

List of Tables ..... **xvii**

List of Figures ..... **xviii**

List of Symbols ..... **xxiii**

List of Abbreviations ..... **xxiv**

Acknowledgements ..... **xxvii**

Dedication ..... **xxix**

Chapter 1: Introduction **1**

1.1 Antibiotics 1

1.1.1 History of antibiotics 1

1.1.2 Structure of Bacterial Cell and Membrane 2

1.1.3 Categories of antibiotics 3

1.1.4 Antibiotic resistance 4

1.2 Antimicrobial peptides 5

1.2.1 Antimicrobial peptides: history and diversity 5

1.2.2 Categories of antimicrobial peptides 9

1.2.3 Common properties of antimicrobial peptides 12

1.2.4 Mechanism of antimicrobial peptide action 14

1.2.4.1 Direct killing: membrane permeabilizing mechanism of action 15

1.2.4.2 Direct killing: non membrane targeting mechanisms of action 20
1.2.4.3 Immune modulation mechanism of action 22
1.2.5 Aurein peptides 23
1.2.6 Challenges with antimicrobial peptides 24
1.3 Strategies to improve antimicrobial peptides 25
1.3.1 Chemical modification of AMPs 25
1.3.2 Delivery systems for AMPs 28
1.4 Hyperbranched polyglycerol 31
1.5 Thesis rationale, hypotheses and aims 34
1.5.1 Development of novel antimicrobial conjugates 34
1.5.2 Development of potent novel antimicrobial peptides and conjugates 35
1.5.3 *In vivo* efficacy of the peptides and the conjugates in mice models 36
1.5.4 Interaction of aurein 2.2 with whole bacterial cells by NMR. 37
1.6 Summary 39
Chapter 2: Conjugation of aurein 2.2 to HPG yields an antimicrobial with better properties. 40
2.1 Synopsis 40
2.2 Background 41
2.3 Methods 43
2.3.1 Peptide Synthesis and Purification 43
2.3.2 Synthesis of HPG 44
2.3.3 Amine Modification of HPG 44
2.3.4 Conjugation of Peptide with amine-modified HPG 45

2.3.5 Characterization of HPG Peptide Conjugates 45
2.3.6 MIC Determination 46
2.3.7 Blood Compatibility Analysis 47
2.3.7.1 Platelet Activation Analysis: Flow Cytometry 47
2.3.7.2 Platelet Aggregation Studies 48
2.3.7.3 Red Blood Cell Lysis Studies 48
2.3.7.4 Complement Activation Analysis: CH50 Assay 49
2.3.7.5 Blood Coagulation by Activated Partial Thromboplastin Time (aPTT) and Partial Thromboplastin Time (PT) Analysis 50
2.3.8 Cell Toxicity analysis 51
2.3.9 Biomembrane Interaction by CD Spectroscopy 52
2.4 Results and Discussion 53
2.4.1 Synthesis of Conjugates 53
2.4.2 Antimicrobial Activity of the Bioconjugates 55
2.4.3 Peptide Secondary Structure on Bioconjugates 56
2.4.4 Blood Compatibility of the Peptide and Peptide Conjugates 58
2.4.5 Cell Compatibility of the Peptide and Conjugates 65
2.5 Summary 66
Chapter 3: Antimicrobial peptide-polymer conjugates with high activity: Influence of polymer molecular weight and peptide sequence on antimicrobial activity, proteolysis and biocompatibility 68
3.1 Synopsis 68
3.2 Background 69

3.3 Methods 70
3.3.1 Peptide array 70
3.3.2 Peptide synthesis and purification 71
3.3.3 Synthesis of HPG 71
3.3.4 Amine Modification of HPG 72
3.3.5 Conjugation of peptide with HPG-amine 73
3.3.6 Synthesis of PEG 77c conjugate 74
3.3.7 Antimicrobial activity measurements (minimum inhibitory concentration or MIC) 74
3.3.8 MIC determination after tryptic degradation 74
3.3.9 Biocompatibility analysis 75
3.3.10 Biomembrane interaction: CD spectroscopy 75
3.4 Results and Discussion 75
3.4.1 Discovery of potent peptides using peptide array based on aurein peptide 75
3.4.2 Synthesis of aurein 2.2Δ3-cys and peptide 77c conjugates 77
3.4.3 Antimicrobial activity of the conjugates 79
3.4.4 Resistance to proteolysis: tryptic degradation 82
3.4.5 Peptide secondary structure on bioconjugates 84
3.4.6 Cell compatibility of the peptides and conjugates 85
3.4.7 Blood compatibility of the peptide and peptide conjugates 89
3.5 Summary 97
Chapter 4: The *in vitro* biofilm activity and the *in vivo* efficacy of the novel peptides and the polymer conjugates. 98
4.1 Synopsis 98

4.2 Background 98
4.3 Materials and methods 101
4.3.1 Peptide synthesis and purification 101
4.3.2 Synthesis of the bioconjugate 101
4.3.3 Antimicrobial activity measurements: MIC determination 101
4.3.4 Biofilm studies 102
4.3.5 Red blood cell lysis 102
4.3.6 Mouse skin infection model 103
Bacterial strains and growth conditions for animal studies 103
Ethics statement 103
Cutaneous mouse infection model 103
Statistical analysis 104
4.4 Results and Discussion 104
4.4.1 Antibacterial activity of the novel peptides *in vitro* 104
4.4.2 Efficacy of the peptides against *Staphylococcus aureus* biofilms 107
4.4.3 Tolerance of the peptides 109
4.4.4 *In vitro* therapeutic index of the peptides 110
4.4.5 Efficacy of peptides in a mouse abscess model 111
4.4.6 Peptide aggregation 116
4.4.7 Efficacy of the HPG conjugates in the mouse abscess model 117
4.4.8 Peptide design paradigms 118
4.5 Summary 119

Chapter 5: Overexpression, purification and esterification of aurein 2.2 utilized to probe the interaction of aurein 2.2 with whole bacterial cells by NMR. 121

5.1 Synopsis 121

5.2 Background 121

5.3 Methods and materials 124

5.3.1 Expression of Calmodulin-aurein fusion protein in E.coli 124

5.3.2 SDS PAGE 125

5.3.3 Purification of Calmodulin-aurein fusion protein in *E.coli* 125

5.3.4 Digestion of Calmodulin-aurein fusion protein 126

5.3.5 MALDI-TOF 126

5.3.6 Peptide purification by RP-HPLC 127

5.3.7 Peptide Esterification 127

5.3.8 MIC Assays 127

5.3.9 2D NMR 127

5.3.10 Scanning electron microscope studies 128

5.4 Results And Discussion 128

5.4.1 Expression and purification of CaM-aurein 2.2 128

5.4.2 Cleavage of CaM-aurein 2.2 and purification of aurein 2.2 130

5.4.3 Chemical esterification of aurein 2.2 retains antimicrobial activity. 132

5.4.4 Whole cell NMR and SEM 134

5.5 Summary 137

Chapter 6: Conclusions and Future work 139

6.1 Conclusions 139

6.2 Future work 143

Bibliography 148

Appendix A 168

A.1 HPLC trace of Aurein 2.2Δ3-cys 168

A.2 Proton NMR of amine functionalized HPG 168

A.3 Proton NMR of HPG-bifunctional linker 169

A.4 UV spectra of the HPG-bifunctional linker 169

A.5 HPLC purification of the conjugate 170

A.6 Proton NMR of HPG-Aurein 2.2Δ3-cys 170

A.7 Size exclusion chromatography of conjugates 171

A.8 CD spectroscopy of Aurein 2.2Δ3-cys 171

A.9 CD spectroscopy of the conjugates 172

A.10 Platelet aggregation by the bioconjugates 172

Appendix B 174

B.1 Proton NMR of HPG-phthalimide 174

B.2 Proton NMR of HPG-Amine 174

B.3 Proton NMR of HPG maleimide 175

B.4 Proton NMR of HPG 77c 175

B.5 Proton NMR of PEG 77c 176

B.6 Bacteria killing and RBC lysis in whole blood/bacteria mixture 176

B.7 Bacteria killing in serum/bacteria mixture 178

B.8 Maldi of Matrix 178

B.9 aPTT analaysis of 77c and the conjugates 179

B.10 Thromboelastometry of conjugates and peptides 179

B.11 aPTT analaysis of 77c and the conjugates 180

Appendix C 181

C.1 Toxicity and precipitation of D-peptides at various concentrations in saline..... 181

C.2 Toxicity and precipitation of D-peptides at various concentrations in DSPE-PEG2000 182

C.3 Average hydrodynamic size of peptide 73c in water and DSPE-PEG2000. 183

Appendix D 184

D.1 MS/MS spectra of aurein 2.2 and diesterified aurein 2.2 184

List of Tables

Table 1.1: Mechanism of antibiotic action and acquired resistance for different of antibiotic classes. 6

Table 1.2: Classes of antimicrobial peptides based on structure 10

Table 1.3: Antimicrobial peptide in clinical trials 25

Table 2.1: Sequence and molecular weight of the peptides and the bioconjugates made ……...54

Table 2.2: Secondary structure of Aurein 2.2Δ3-cys and HPG-Aurein 2.2Δ3-cys in various environments determined by CD spectroscopy (representative spectra shown in Figure 2.3)..... 58

Table 3.1: Antimicrobial activity (MICs) of selected peptides identified in the peptide array….71

Table 3.2: Characteristics of the peptides and the HPG conjugates used in this study[@]. 80

Table 3.3: Alpha helical content (%) of the various conjugates studied here, as determined from fits from the CD spectra (Figure 3.4). 87

Table 4.1: Various properties of some of the peptides used in this studies…….105

Table 4.2: Antimicrobial activity of the peptides. 105

Table 4.3: Anti-biofilm activity of the peptides..... 108

Table 4.4: Therapeutic index of the peptides..... 112

Table 4.5: Average hydrodynamic size of peptide 73c..... 116

Table 5.1: Antimicrobial activity of expressed and synthetic aurein 2.2…….133

List of Figures

Figure 1.1: Cell envelope of Gram postive and Gram negative bacteria.. 2

Figure 1.2: The β lactam ring of the generalized penicillin molecule.. 4

Figure 1.3: Sources of antimicrobial peptides (total 2818) as of September 2017 from the antimicrobial peptide database. 7

Figure 1.4: Structural diversity of AMPs. 11

Figure 1.5: Various mechanism of action of antimicrobial peptides.. 15

Figure 1.6: Initial interaction of cationic AMPs with the multicellular animal (left) or bacterial (right) membrane. RBC: red blood cell.. 17

Figure 1.7: Proposed mechanism of action for AMPs in bacteria.. 19

Figure 1.8: Structure of lipid II molecules with pyrophosphate sugar moiety circled in red. 21

Figure 1.9: Chemical modifications AMPs. 28

Figure 1.10: Various polymers used for AMP conjugation. 30

Figure 1.11: Generic structure of HPG. 32

Figure 2.1: Synthesis of HPG.. 42

Figure 2.2: Synthetic route for the conjugation of the aurein peptide with hyperbranched polyglycerol (HPG). 53

Figure 2.3: CD spectra of the HPG-Aurein 2.2Δ3-cys 5% in PBS buffer and lipids (1:1 POPC/POPG) and the peptide under the same conditions. 57

Figure 2.4: Influence of free aurein peptide and HPG peptide conjugates concentration on red blood cell lysis. 60

Figure 2.5: Influence of free aurein peptide and HPG peptide conjugates concentration on complement activation.. 62

Figure 2.6: Influence of free aurein peptide and HPG peptide conjugates concentration on platelet activation. 63

Figure 2.7: Influence of free aurein peptide and HPG peptide conjugates concentration on intrinsic pathway of blood coagulation. 65

Figure 2.8: Cell biocompatibility of the peptides and the conjugates against. 66

Figure 3.1: Helical wheels for some of the peptides generated in the array……..77

Figure 3.2: Synthetic scheme for the conjugation of the peptides with HPG.. 78

Figure 3.3: MALDI-TOF mass spectra of 77c, 22k 77c and trypsin after 3 hours of digestion... 83

Figure 3.4: CD Spectra of the conjugates in phosphate buffer and POPC/PG (1:35). 86

Figure 3.5: Fibroblast cell viability upon exposure to free peptides and HPG peptide conjugates 88

Figure 3.6: Red blood cell lysis upon exposure to free peptides and HPG peptide conjugates.... 90

Figure 3.7: Platelet activation upon exposure to free peptides and HPG peptide conjugates 92

Figure 3.8: Complement activation upon exposure to free peptide and HPG peptide conjugates. 94

Figure 3.9: Prothrombin time upon exposure to free aurein peptide and HPG peptide conjugates 96

Figure 4.1: Red blood cell lysis upon exposure to free peptides and HPG peptide conjugates...110

Figure 4.2: RBC lysis vs log of peptide concentration curves to extrapolate the concentration at which the peptides cause 50% RBC lysis (LD_{50}). 111

Figure 4.3: Infection and therapeutic treatment of mouse cutaneous abscesses. All mice were infected with MRSA USA300 and treated with saline solution, aurein and peptide 73 (dose = 5 mg/kg) 1 h post-bacterial infection.. 113

Figure 4.4: Therapeutic treatment of mouse cutaneous abscesses with D and L peptides. 115

Figure 4.5: Therapeutic treatment of mouse cutaneous abscesses with HPG-73c conjugates. .. 118

Figure 5.1: Calmodulin (CaM)-aurein 2.2 fusion construct with TEV protease cut site…….123

Figure 5.2: Expression and purification of CaM-aurein 2.2. 129

Figure 5.3: MALDI-TOF of the cleavage mixture.. 131

Figure 5.4: HPLC purification of the cleaved CaM-aurein 2.2.. 131

Figure 5.5: MALDI-TOF of the diesterified aurein 2.2.. 133

Figure 5.6: $^{1}H,^{15}N$-HSQC spectra of whole *S. aureus* cells with the aurein peptides. 135

Figure 5.7: CD spectra of expressed peptides..... 136

Figure 5.8: SEM of *S. aureus* after incubating for 1 h with the expressed peptides..... 137

Figure 6.1: Design of HPG-73 conjugate that would lead to the release of peptide 73 at the site of infection. ……..……146

Figure A.1: HPLC purification of the Aurein 2.2Δ3cys. Peptide elutes between 55-57min…...168

Figure A.2: Proton NMR (in D_2O) of amine modified HPG. 168

Figure A.3: Proton NMR (in deuterated DMSO) of HPG-bifunctional Linker..... 169

Figure A.4: UV-Vis of HPG-Bifunctional linker. 169

Figure A.5: Size exclusion HPLC purification of the bioconjugates..... 170

Figure A.6: Proton NMR (in D_2O) of HPG-Aurein 2.2Δ3-cys..... 170

Figure A.7: Size exclusion chromatographs of HPG-Aurein 2.2Δ3-cys and HPG-Bifunctional linker. 171

Figure A.8: CD spectra of the Aurein 2.2Δ3-cys in and trifluroethanol (TFE) and lipids(POPC/POPG)..... 171

Figure A.9: CD spectra of the HPG-Aurein 2.2Δ3-cys in PBS buffer, Trifluroethanol (TFE) and lipids(POPC/POPG)..... 172

Figure A.10: Platelet aggregation by the bioconjugates.. 172

Figure B.1: ^{1}H NMR (in 100% DMSO-d6) of phthalimide modified 22k HPG…….174

Figure B. 2: ^{1}H NMR (in 100% DMSO-d6) of 22k HPG-NH_2 after deprotection of the phthalimide. 174

Figure B.3: ^{1}H NMR (in 100% DMSO-d6) of 22k HPG maleimide..... 175

Figure B.4: ^{1}H NMR (in 100% DMSO- d6) of 22k HPG 77c..... 175

Figure B. 5: ^{1}H NMR (in 100% D_2O) of 5k mPEG 77c 176

Figure B.6a: Bacterial colony forming units per milliliters (CFU/mL) in whole blood in presence of peptide/conjugates. 176

Figure B.6b: Percent RBC lysis in the whole blood in presence of bacteria and peptide/conjugate. 177

Figure B.7: The ability for the peptide and conjugates to kill bacteria in serum..... 178

Figure B.8: Appendix B.8: MALDI of matrix..... 178

Figure B.9: Influence of free peptide and HPG peptide conjugates on activated Partial Thromboplastin Time (aPTT) 179

Figure B.10: Typical thromboelastometry of the HEPES-buffered saline (HBS), 22K 77c and 77c..... 180

Figure B.11: Whole blood clotting time by Thromboelastometry of the 22k 77c and 77c 180

Figure C. 1: CD-1 mice were injected with 50 ul of different peptide concentrations on the left

and right side of the dorsum. The skin inspected three days post injection……..181

Figure C.2: CD-1 mice were injected with 50 ul of different peptide concentrations on the left and right side of the dorsum. The skin inspected three days post injection. No visible peptide/conjugate precipitation at various concentration in DSPE-PEG2000..... 182

Figure C.3: Average hydrodynamic size and the intensity percent of peptide 73c in water and DSPE-PEG2000. 183

Figure D.1: MS/MS spectra of aurein 2.2 and diesterified aurein 2.2…….184

List of Symbols

°C	Degree Celsius
g	Gram
h	Hour
Hz	Hertz
K	Kelvin
kg	Kilogram
mg	Milligram
MHz	Megahertz (10^6 Hertz)
mL	Milliliter
mM	Millimolar
µg	Microgram
µL	Microliter
nm	Nanometer
nM	Nanomolar
s	Second

List of Abbreviations

^{1}H NMR	Proton Nuclear Magnetic Resonance
^{31}P NMR	Phosphorus-31 Nuclear Magnetic Resonance
ABR	Antibiotic resistance
AD	Anno domini
AMP	Antimicrobial peptides
ANOVA	Analysis of variance
aPTT	Activated partial thromboplastin time
BCA	Bicinchoninic acid
CA	California
Ca	Community acquired
CD	Circular Dichroism
$CHCl_3$	Chloroform
D_2O	Deuterated Water
DD	D-alanyl-D-alanine
DHPC	1,2-dihexanoyl-sn-glycero-3-phosphocholine
DLS	Dynamic light scattering
DMF	Dimethylformamide
DMPC	1,2-dimyristoyl-sn-glycero-3-phosphocholine
DMPG	1,2-dimyristoyl-sn-glycero-3-[phospho-rac-(1-glycerol)]
DMSO	Dimethyl sulfoxide
DNA	Deoxyribonucleic acid
DPC	Dodecylphosphocholine
DSC	Differential Scanning Calorimetry
DSPC	1,2-Distearoyl-sn-glycero-3-phosphocholine
DSPE	1,2-Distearoyl-sn-glycero-3-phosphoethanolamine
DSPG	1,2-Distearoyl-sn-glycero-3-phosphoglycerol
DSPE-PEG2000	1,2-distearoyl-sn-glycero-3-phosphoethanolamine-N-[amino(polyethylene glycol)-2000]
EDTA	Ethylenediaminetetraacetic acid

ELISA	Enzyme linked immunosorbent assay
FBS	Fetal bovine serum
FDA	Food and Drug Administration
HDP	Host Defense Peptide
HEPES	N-2-hydroxyethylpiperazine-N'-2-ethanesulfonic acid
HIT	Heparin-induced thrombocytopenia
HPG	Hyperbranched polyglycerol
HPLC	High Performance Liquid Chromatography
HUVEC	Human Umbilical Vein Endothelial Cells
IDR	Innate defense regulator peptide
ITC	Isothermal titration calorimetry
IU	International unit
kDa	Kilo Dalton
MALDI-TOF	Matrix-Assisted Laser Desorption/Ionization-Time of flight spectrometry
MBEC	Minimal biofilm eradication concentration
MBIC	Minimal biofilm inhibitory concentration
MCP	Monocyte Chemoattractant Protein
MDR	Multidrug resistance
MIC	Minimal inhibitory Concentration
MOA	Mechanism of action
MOPS	4-morpholinepropanesulfonic acid
mPEG	Methoxypolyethylene glycol
MRSA	Methicillin-resistant Staphylococcus aureus
MS/MS	Tandem mass spectrometry
MW	Molecular weight
OCD	Oriented Circular Dichroism
OD	Optical Density
PBMC	Peripheral Blood Mononuclear Cell
PBS	Phosphate-buffered saline
PC	Phosphatidylcholine

PDI	Polydispersity index
PE	Phosphatidylethanolamine
PEG	Polyethylene glycol
PG	Phosphatidylglycerol
POPC	1-palmitoyl-2-oleoyl-sn-glycero-3-phosphocholine
POPE	1-palmitoyl-2-oleoyl-sn-glycero-3-phosphoethanolamine
POPG	1-palmitoyl-2-oleoyl-sn-glycero-3-[phospho-rac-(1-glycerol)]
ppm	Parts per million
PPP	Platelet-poor Plasma
PRP	Platelet-rich Plasma
PS	Phosphatidylserine
PT	Prothrombin time
RBC	Red blood cell
REDOR	Rotational Echo Double Resonance
Rh	Hydrodynamic radius
RI	Retro-inverso
RNA	Ribonucleic acid
ROMBP	Ring opening multibranching polymerization
RP HPLC	Reverse-Phase High Performance Liquid Chromatography
RT	Room temperature
SDS	Sodium Dodecylsulfate
SUV	Small Unilamellar Vesicle
TEG	Thromboelastography
TFA	Trifluoroacetic acid
TFE	2,2,2-trifluoroethanol
TFE-d3	Deuterated 2,2,2-trifluoroethanol
TI	Therapeutic index
UBC	University of British Columbia
US/USA	United States of America
UV	Ultraviolet

Acknowledgements

I “give thanks to the Lord, for he is good and his love endures forever” (Psalm 107:1). I trust in you, God.

This research thesis would not have been possible without the help, advice and support from numerous individuals. I would like to express my sincere gratitude to these people here. First of all, I would like to thank my supervisor Dr. Suzana K Straus and co-supervisor Dr. Jayachandran N. Kizhakkedathu, for giving me an opportunity to learn, do research and teach in their laboratory. Thank you for having confidence in me and always being there for me. A million thanks for your patience in our weekly meetings, and for constantly providing guidance and motivation.

I would like to thank my committee members, Dr. Hongbin Li, Dr. Derek P Gates, Dr. Katherine S. Ryan, for their valuable suggestions on this project, and in exam and committee meetings. Thank you Dr. Li and Dr. Ryan in particular for reading through this thesis. Dr. Donald E. Brooks, thank you very much for fruitful discussions and suggestions.

Special thanks to Dr. Rajesh A. Shenoi and Dr. Srinivas Abbina for being my mentors in the lab and sharing your knowledge. You both are an inspiration for me and other students in the Kizhakkedathu laboratory. I would like to thank Benjamin Lai, Dr. Manu Thomas Kalathottukaren, Dr. Frederico Rosell, Dr. Evan Haney, Irina Chafeeva, Iren Constantinescu, and Derrick Horne, for providing me excellent training on various techniques used for this project. I am grateful to Dr. Daniel Pletzer, Dr. John Cheng and Dr. Bob Hancock who provided invaluable guidance with interpretation of research findings through our collaboration. Thank you Dr. Hans J. Vogel for providing the plasmid for the studies in Chapter 5.

I would also like to thank my students, Allen Takayesu, Michael Nguyen, Sayak Subhra Panda, José Ausencio Álvarez Huerta, Marty Yue, Waleed Aljehani, Aparna Mallaredy for their contribution in various projects and giving me a chance to mentor them and improve my leadership skills.

My sincerest gratitude to Usama Abbasi, Dr. Imran Ul-Haq, Dr. Jasmine Hamilton, , Dr. Anilkumar Parambath, Dr. Mahsa Alizadeh, Dr. Johan Janzen, Dr. Andrew Tait, Dr. Yurou Sang, Kevin Cooley, Matthew Drayton, Chantal Mustoe, Nigare Raheem, Sonja Horte, Dr. David Yang, Vincent Leung, Dr. Kai Yu, Yan Mei, Dr. Nima Khademmohtaram, Dr. Narges Hadjesfandiari, Erika Siren, Chanel La, Sreeparna Vappala, Na Li (April), Erika Das, Dr. Rafi Chapnian, Dr. Madhab Bagpai, Joseph Lee, Jin Zhang, Rui Zhang, Htet Ei Bo, Angela Dodd, Ruqaiba Desmond, Jung Hwan Bae (David), Selina Suleman, Marie Weinhart, Ainge Chang, Kyle Scoten, Kelly Hutchinson, Minnie Jiang, Cian Zybutz, Ethan Lee, Celebi Wan, and all past lab members of Brooks, Kizhakkedathu and Straus laboratories, for providing support and creating a fun-filled and positive work environment.

I would also like to thank all my family and friends, here in Canada and also in Fiji, for their love and support. Special thanks to my friends and members from the Acts 29 church. My sincere gratitude to the biology and chemistry department of Langara College, especially Dr. Shirley Wacowich-Sgarbi who provided the platform for my first ever research experience.

I am most grateful to my parents, especially my mother, Mohini Kumar, and my younger brother, for their unconditional love and prayers.

To my Lord and savior, Jesus Christ,

for his everlasting reckless love.

To my mother, Mohini Kumar;

for every sacrifice you have made for us.

For God so loved the world that He gave His one and only Son,

that whoever believes in Him shall not perish

but have eternal life.

(John 3:16)

Chapter 1: Introduction[a]

1.1 Antibiotics

1.1.1 History of antibiotics

Antibiotics are defined as therapeutic agents that are used to treat and prevent bacterial infections. The antibiotic can either kill bacteria and/or prevent bacterial growth. Although the first antibiotic was discovered in the 19th century, the use of antibiotics as therapeutic agents dates back to AD 350 by the Nubians who unknowingly used tetracycline based compounds[1]. Interestingly ancient Chinese and Greeks also used herbal medicine to combat bacterial infections. Egyptians would apply moldy bread to infected wounds[2]. In 1907 arsphenamine was synthesized by Alfred Berthelm in Paul Ehrlich's lab. Ehrlich hypothesized that screening many compounds would eventually lead to the discovery of a 'magic bullet' that would kill the microbe but not the patient [3]. Arsphenamine was eventually used to treat syphilis patients.

Many microorganisms also produce antibiotics to protect their environment niche and inhibit bacterial infection. In 1928 Sir Alexander Fleming noticed that the zone immediately around the *Penicillium* mold (fungi) inhibited *Staphylococcus* growth. He hypothesized the mold secreted an active compound to inhibit bacterial growth. The active compound secreted by the mold was penicillin which was further developed and purified by Ernst Chain and Howard Florey and initially used in 1942 during World War II (WWII)[4]. The antibiotics field experienced a golden era as many families

[a]A version of Chapter 1 has been published**.** **Kumar, P**.; Kizhakkedathu, J.; Straus, S. Antimicrobial Peptides: Diversity, Mechanism of Action and Strategies to Improve the Activity and Biocompatibility In Vivo. ***Biomolecules*** 2018, *8*, 4, doi:10.3390/biom8010004.

of antibiotics such as aminoglycosides, sulfonamides, cephalosporins and fluoroquinolones were discovered in the next 20 years. These new discoveries lead to extensive therapeutic research and the commercial industry against bacterial infections. Interestingly, various families of the antibiotics target different components of the bacteria which will be described in detail in section 1.1.3.

1.1.2 Structure of Bacterial Cell and Membrane

It is important to understand the basic structure and components of the bacterial cell before looking into the mechanism of action of certain antibiotics. Bacterial cells are divided into two broad classes i.e. Gram positive and Gram negative. Gram negative bacteria are generally characterized by their cell envelope which consists of a cell membrane, thin peptidoglycan (cell wall) and a bacterial outer membrane (Figure 1.1a)[5]. The area between the cell and outer membrane is known as the periplasmic space where many lipoproteins are located. Gram negative bacteria are also characterized by the presence of lipopolysacchride (LPS) on the outer membrane.

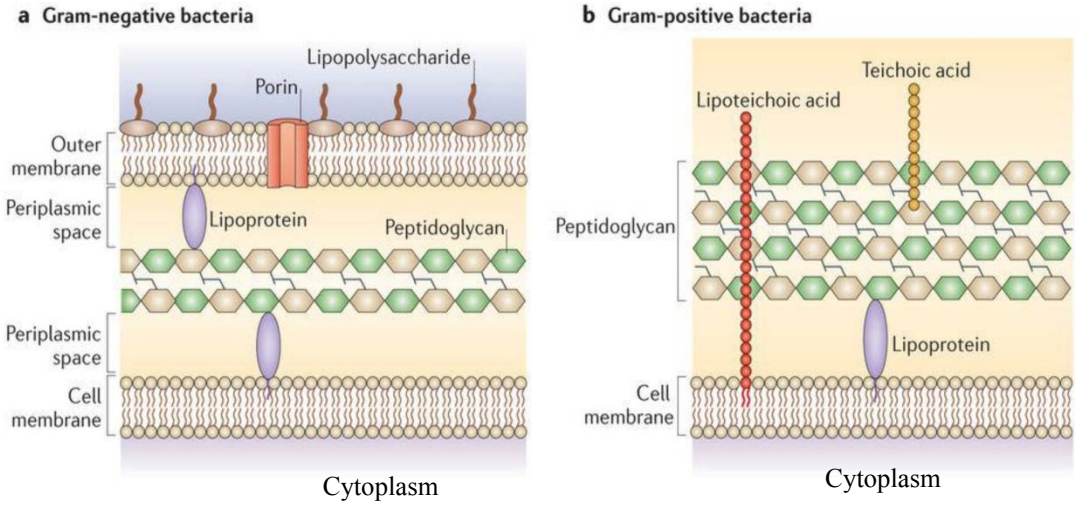

Figure 1.1: Cell envelope of Gram postive and Gram negative bacteria. Figure used with permission from Brown et. al. Extracellular Vesicles in Gram-Positive Bacteria, Mycobacteria and Fungi. Nat. Rev. Microbiol. 13 (10), 620–630 (2015).

On the other hand, the cell envelope of Gram positive bacteria is comprised of an inner cell membrane and a thick peptidoglycan (cell wall) layer. The cell wall is composed of the peptidoglycan and different types of teichoic acid. Intracellular structures in Gram positive and Gram negative bacteria are very similar. Most bacteria consist of closed circular chromosomal DNA floating in the cytoplasm and ribosomes to facilitate protein synthesis. Common extracellular structures include the capsule and flagella[6,7].

1.1.3 Categories of antibiotics

Antibiotics can be categorized according to their mechanism of action. There are hundreds of antibiotics[8] which can be natural, semi-synthetic or synthetic making classification important. Antibiotics usually kill or inhibit the growth of the bacteria by interfering with a major pathway or by interacting with a specific structural component. The mechanism of action of the most common classes of antibiotics is summarized in Table 1.1.

Penicillin is the name given to a group of antibiotics which include penicillin G, penicillin V, ampicillin. The structural similarity is the β lactam ring (Figure 1.2) which is necessary to inhibit the cell wall synthesis in bacteria. The β lactam moiety binds to DD (D-alanyl-D-alanine)-transpeptidase, an enzyme that normally facilitates the peptidoglycan cross-linking. This binding interaction leads to weakening of the cell wall, leading to bacterial cell lysis due to the osmotic pressure[9]. Interestingly, tetracyclin-based antibiotics such as methacyclin work synergistically with penicillin as penicillin weakens the peptidoglycan and facilitates the entry of methacyclin into the bacteria cells to inhibit protein synthesis [10].

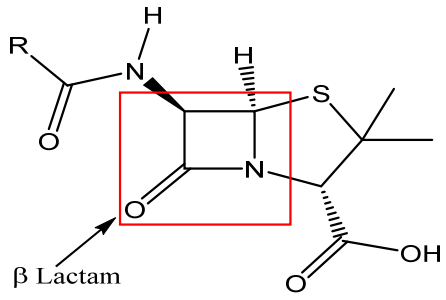

Figure 1.2: The β lactam ring of the generalized penicillin molecule. The R group moiety is different for Penicillin G, penicillin V, ampicillin and other penicillins. Image created using ChemDraw software.

1.1.4 Antibiotic resistance

Antibiotic resistance (ABR) is a natural phenomenon and was observed as early as the 1940s. For instance, penicillin was introduced as a therapeutic agent in 1942. Well before this, however, the β lactamase enzyme that destroys penicillin was identified in 1940[11]. All ABR is genetically encoded and can be classified into two types: intrinsic or acquired resistance[12]. In intrinsic resistance, the bacteria have an innate ability to resist the antibiotic. For example, Gram negative bacteria show resistance to vancomycin because the antibiotic is too large to permeate the outer membrane. Some bacterial species have chromosomal DNA that also encodes for a efflux pump that enables them to remove the antibiotic from the cell[13]. In contrast, in acquired resistance (Table 1.1), the bacteria modify themselves such that they can now resist the antibiotic to which they were susceptible to earlier. Acquired resistance is mediated by mutations in the chromosomal DNA or horizontal gene transfer[14]. Non lethal mutations in the chromosomal DNA can arise by mistakes made by the DNA polymerase during DNA replication which might be beneficial for the bacteria if the mutation modifies the antibiotic target (e.g. rifampin and fluoroquinolones (ciprofloxanin)) (Table 1.1). In one of the horizontal gene transfer mechanisms (conjugation), a specific gene coding ABR (e.g β lactamases genes (enzyme that cleaves the β

lactam ring)) is located on a small circular DNA, known as a plasmid, which can be transferred from one bacterium to another. This allows the bacteria that have just received the new plasmid to become resistant. Interestingly, most of the multidrug resistance (MDR) efflux pumps that were previously on chromosomal DNA are now found on plasmids[15].

ABR is one of the greatest threats to human health in the future as it has been estimated that by 2050 ten million people may die per year due to ABR[16]. In the European Union, the current cost of treating ABR bacterial infections is 1.5 billion Euros per year [13]. In addition to the ABR crisis, there were only a few new antibiotics developed in the past decade[17]. On average only one antibiotic has been developed per year in the past 15 years. Multiple drug resistant bacteria have become a global concern leading to an urgent need to discover and develop novel antibiotics.

1.2 Antimicrobial peptides

1.2.1 Antimicrobial peptides: history and diversity

Antimicrobial peptides (AMPs), also known as host defense peptides, are virtually found in all forms of life. Antimicrobial peptides are produced by all organisms ranging from bacteria to plants, vertebrates and invertebrates (Figure 1.3). In bacteria the AMPs benefit individual bacterial species by killing other bacterial species that may compete for nutrients and the same environmental niche. Bacterial AMPs synthesized by ribosomes are known as bacteriocins and can be classified into two categories: lantibiotics and non-lantibiotics[18,19]. Lantibiotics are AMPs containing the non-natural amino acid lanthionine. Nisin, a lantibiotic, was one of the first AMPs isolated and characterized from *Lactococcus lactis* in 1947[20]. It is active against a variety of Gram positive bacteria with a minimum inhibitory concentration (MIC) in the nanomolar range and has been used as a food preservative for 50 years with no significant development of

Table 1.1: Mechanism of antibiotic action and acquired resistance for different antibiotic classes.

Mechanism of action	Antibiotic class (examples)	Mechanism of acquired resistance
Interfering of cell wall synthesis[21]	1. β lactams a) Penicillin (penicillin, ampicillin) b) Cephalosporins (cefotaxine) c) Carbapenems (imipenem) d) Monobactams (aztreonam) 2. Glycopeptides (vancomycin)	• β lactamases produced by bacteria that cleave the β lactam ring • Modified or low affinity DD-transpeptidase • Removal by efflux pump
Inhibition of protein synthesis[12,13]	1. Tetracyclins (methacyclin) 2. Aminoglycosides (streptomycin) 3. Chloramphenicol 4. Lincosamide (clindamycin) 5. Macrolides (erythromycin) 6. Streptogramins (virginiamycin)	• Removal by efflux pump • Enzymatic inactivation/modification of the antibiotics • Modification of target such as ribosomes • Altered membrane permeability
Inhibition of folic acid synthesis[22]	Sulfonamides (sulfamethoxazole)	• New enzyme via acquisition of foreign genes
Inhibition of DNA replication[22]	Fluoroquinolones (ciprofloxanin)	• Modification of the target enzymes involved in DNA replication
Inhibition of RNA synthesis[12]	Rifampin	• Point mutation in the gene encoding for RNA polymerase
Disrupting of cell membrane structure or ion gradient[22]	1. Polypeptides (polymyxin, actinomycin) 2. Ionophores (gramicidin)	• Altered membrane structure • Enzymatic degradation

resistance[23]. Other bacteriocins such as mersacidin have also been studied for their possible use against antibiotic resistant Gram positive bacteria[24].

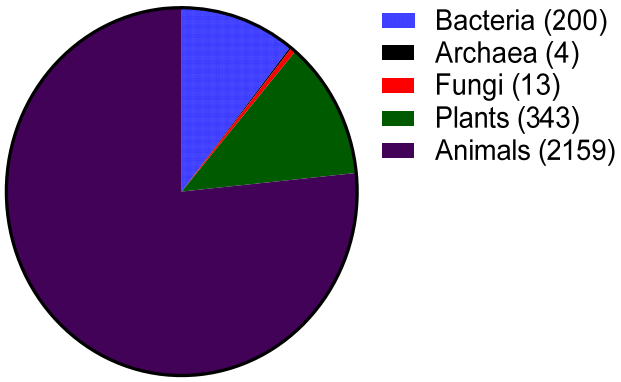

Figure 1.3: Sources of antimicrobial peptides (total 2818) as of September 2017 from the antimicrobial peptide database. Image created using GraphPad Prism software from numbers obtained from http://aps.unmc.edu/AP/ on September 20, 2017

Most AMPs reported to date are from eukaryotic origins such as plants, animals, and fungi (Figure 1.3). Since 1885, fluids such as blood, sweat, saliva plasma, white blood cell secretions and granule extracts have been prized for their antimicrobial properties[25]. However, it was not till 1981 that Hans Boman reported that the hemolymph (plasma and blood) of silk moth (*Hyalophora cecropia*) contained AMPs known as cecropins[26]. These peptides are cationic, amphipathic and have broad spectrum activity (i.e. are active against multiple types of microorganisms such a Gram positive and Gram negative bacteria and fungi). The field grew further when Rober Leher, Shunji Natori and Michael Zasloff isolated and described defensins[27] (mammalian macrophages), sacrotoxins[28] (fly Larvae) and magainins[29] (skin's of frogs (*Xenopus Laevis*)), respectively.

In eukaryotes, AMPs play an important role in innate immunity (first line of defense). Plants lack adaptive immunity (B cell and T cell mediated immunity) and hence AMPs play a

fundamental role in their protection against infection by bacteria and fungi. The presence of genes encoding for plant AMPs can be found in variety of plant species. Interestingly all plant AMPs are cysteine rich and contain many disulphide bonds[30]. The best studied groups of plant AMPs include the thionins[31], plant defensins[32] and cyclotides[33]. Plant AMPs can be found in leaves, flowers, seeds and tubers[23].

Similar to plants, invertebrates lack an adaptive immune system and hence are completely dependent on the innate immune system for protection against infection. AMPs have been found in all invertebrates examined to date, which mostly includes insects and marine invertebrates[34]. AMPs can be found in the hemolymph, hemocytes (blood cells), phagocytes (white blood cells) and epithelial cells of these creatures[23]. As mentioned earlier, the first AMP (cecropins) from eukaryotes was discovered in silk moth, which is also found in fruit flies (*Drosophila).* Many other marine invertebrates such as shrimp, oysters and horseshoe crabs express AMPs constitutively[35,36] (i.e. a gene is transcribed and translated continually to make a protein or peptides). Tachyplesin and polyphemusin are two potent AMPs produced by horseshoe crabs which possess antibacterial and antifungal activity at low micromolar range[37]. Interestingly, like some other AMPs, polyphemusin also shows antiviral activity against human immunodeficiency virus (HIV)[38].

Although vertebrate immunity consists of both the innate and adaptive immune systems, AMPs have been isolated and characterized from a variety of vertebrates such as fish, mammals and amphibians, indicating the crucial role of AMPs in innate immunity. Vertebrate AMPs can be isolated from a variety of cells, such as granules of white blood cells (phagocytes, neutrophils, macrophages, natural killer cells), epithelial tissue situated in the mouth, lungs, or skin, and bodily fluids[39–41]. Interestingly, amphibian skin glands have been a rich source of AMPs, with

more than 500 AMPs reported to date[23]. Most vertebrate AMPs show direct antimicrobial activity at high concentration such as in the granules of white blood cells. However, some vertebrate AMPs have also shown to perform critical functions in immune modulation and controlling inflammation[42–47]. The two most prominent groups of AMPs in vertebrates are cathelicidins and defensins, which will be discussed further in the next section.

1.2.2 Categories of antimicrobial peptides

Antimicrobial peptides are a distinct and diverse class of molecules. With over 2800 peptides sequences reported to date, it is important to categorize AMPs. AMPs can be categorized in many different ways, which can be based on the structure, sequence, or mechanism of action. As the activity of the peptides is dependent on the structure and the sequence, it is important to take both of these properties into account while categorizing AMPs. In this thesis, we will be focusing on eukaryotic cationic AMPs, as not many eukaryotic AMPs are anionic.

The first subgroup contains AMPs that adopt an alpha helical structure and which are predominantly found in the extracellular matrix of frogs and insects. Most of these peptides are unstructured in aqueous solution but become structured when in contact with trifluoroethanol, lipids, micelles and liposomes (Figure 1.4). An extensively studied human AMP which is a member of cathelicidins is LL-37 (Table 1.2). Cathelicidins are one of the most diverse AMPs of vertebrates, mainly found in mammals such as humans, mice, sheep, goat, horses and bovines[48]. Cathelicidin AMPs range from 12-80 amino acids and can adopt a variety of other structures (Table 1.2). In addition to their antimicrobial activity, cathelicidins such as LL-37 play an important role in immunomodulatory and inflammation responses[44].

Table 1.2: Classes of antimicrobial peptides based on structure

Category[a]	Peptides	Unique structural/sequence feature	Source
α helical peptides	Aurein 1-2[49,50]	Amidated C-terminus	Frogs
	Mellitin[44], Brevinin 1[51]	Amidated C-terminus	Bees
	Maculatins[52]	-	Frogs
	Citropin[53]	Amidated C-terminus	Frogs
	Buforin II[54]	Amidated C-terminus	Frogs
		-	Toad
	Cathelicidins[48] • LL-37 • BMAP-27,28,34 • Magainins • Cecropin	Amidated C-terminus - - Amidated C-terminus	Humans Bovine Frogs Insect
β sheet peptides	Cathelicidins[48] • Protegrins • Bactenecin	Cysteine rich Disulphide forming loop/Arginine rich	Pigs Bovine
	Defensins[b,41,55–57] • α defensins • β defensins • θ defensins	Three disulphide bonds Three disulphide bonds Three disulphide bonds and cyclic	Mammals Mammals Gorilla
	Tachyplesins[37] and Polyphemusin[58]	Cysteine/arginine rich and amidated C-terminus	Horse shoe crabs
Extended/ flexible	Cathelicidins[48] • PR-39 • Tritrpticin • Indolicidin • Crotalicidin 15-34	Proline and arginine rich Tryptophan and arginine rich Tryptophan and amidated C-terminus Lysine rich	Pigs Pigs Bovine Snakes
	Histatins[59]	Histidine rich and amidated C-terminus	Humans

[a] Classification is based on the predominant structure, some peptides might have mixed alpha helix and β sheet

[b] Analogues of defensins are also found in insects, plants and fungi and not restricted to mammals.

Another good example are the α helical magainins (Table 1.2), which were originally isolated from the African clawed frog *Xenopus laevis* and are active against Gram positive and Gram negative bacteria, fungi, yeast and viruses[60]. The structure and function relationship of the magainins has been well studied[61,62]. These AMPs were the first to be tested in the clinic, but ultimately failed[23]. However, the magainin analogue pexiganan is currently in clinical trials[63]. Most of the alpha helical peptides require amidation at the C-terminus for higher antimicrobial activity (Table 1.2). The amidation of the C-terminus enhances the electrostatic interaction between the positively charged peptide and the negatively charged bacterial membrane. This interaction stabilizes the helical structure at the membrane interface[64].

The second subclass of AMPs predominantly adopts a β-sheet structure (Figure 1.4). This class includes AMPs such as protegrins (from the cathelicidin family), defensins and tachyplesins. Interestingly nearly all β-sheet AMPs contain cysteine residues that are conserved and form disulphide bonds. In defensins, the disulfide bonds provide structural stability and minimize protease degradation[65]. β sheet AMPs are more structured in solution and do not

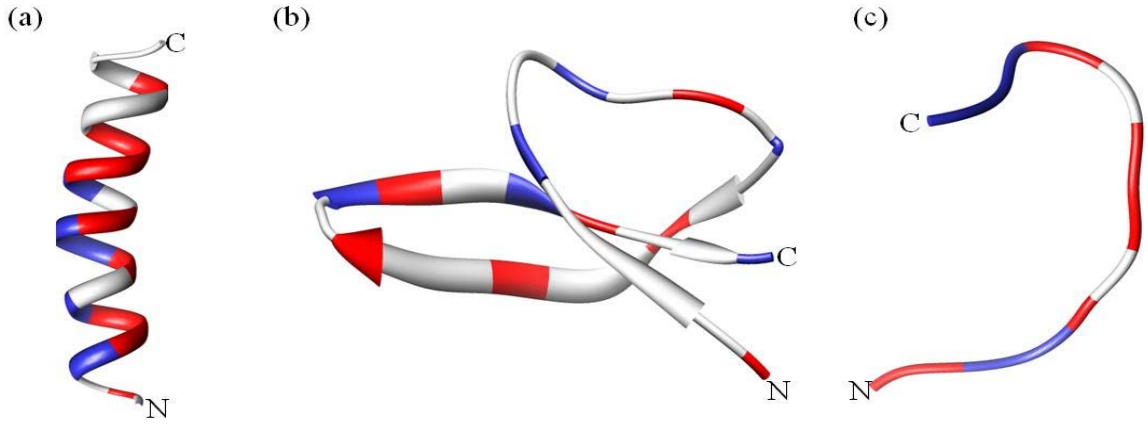

Figure 1.4: Structural diversity of AMPs. (a) the α-helical magainin, (b) β-sheet human defensin 5 and (c) extended coil indolicidin. Positively charged residues are colored blue whereas hydrophobic residues are red. The N and C termini are indicated. The figure was generated using CHIMERA[66–69] and PowerPoint.

undergo major structural changes when going from an aqueous environment to a membrane environment[70]. Defensins are the largest group of AMPs that are further categorized in sub-families on the basis and location of the disulphide bond (Table 1.2). Defensins are also involved in antibacterial, antifungal, antiviral, immune and inflammation responses[44]. Knockout and transgenic mice experiments have indicated that α defensins are critical for protection against *Escherichia coli*[71] and *Salmonella enteric*[72]. Tachyplesins and polyphemusin (arginine rich, ~30% by sequence) are other β-sheet AMPs that were isolated from hemocytes of horseshoe crabs[51,58].

The third and last subclass of AMPs has a unique extended coil structure. Most of the AMPs in this category are from the cathelicidin family and consist of 2 or more proline residues, which are known to break secondary structural elements such as α-helices or β-sheets[73]. Indolicidin is a tryptophan rich AMP isolated from bovine neutrophils and consists of only 13 amino acids[74]. Nuclear magnetic resonance (NMR) and circular dichroism (CD) studies reveal that indolicidin forms a unique membrane-associated peptide structure with well defined extended structure in the presence of micelles[74,75] (Figure 1.4c). In a more recent study, Falcao et al[76] dissected the crotalicidin peptide and discovered that the C-terminus fragment (crotalicidin 15-34) showed activity against Gram negative bacteria and tumors. NMR studies of the active crotalicidin 15-34 revealed that the AMP adopts mostly an extended structure (83%) and was only 17% α-helical. The N-terminus (crotalicidin 1-14) was fully α- helical but inactive.

1.2.3 Common properties of antimicrobial peptides.

Although AMPs are a diverse group of molecules in terms of sequence, structure and sources, there are several properties that are common to almost all AMPs. Firstly, most AMPs

display a net positive charge (cationic) ranging from +2 to +13 and may contain a specific cationic domain. The cationic nature can be attributed to the presence of lysine and arginine (and sometimes histidine) residues. Many studies have demonstrated the correlation between charge and antimicrobial activity of AMPs[77–82]. Increasing the charge of magainin 2 from +3 to +5 improved the antibacterial activity against both Gram positive and Gram negative bacteria, but an increase to +6 or +7 lead to increased hemolytic activity and loss of antimicrobial activity[78]. The loss of antimicrobial activity may be due to the fact that an extremely strong interaction between the peptide and the phospholipid head group would prevent translocation of the peptide into the inner leaflet of the membrane[83].

Secondly, hydrophobicity is a key feature for all AMPs and is defined as the percent of hydrophobic residues such as valine, leucine, isoleucine, alanine, methionine, phenylalanine, tyrosine and tryptophan in the peptide sequence (typically 50% for AMPs). Hydrophobicity governs the extent to which the water-soluble AMPs will be able to partition into the membrane lipid bilayer. It is required for membrane permeabilization; however, excessive levels of hydrophobicity can lead to mammalian cell toxicity and loss of antimicrobial selectivity[83–85]. Chen et al. examined the influence of hydrophobicity in a synthetic α helical AMP ($V13K_L$) on the antimicrobial activity and hemolysis of human red blood cells (RBCs)[85]. The results suggest that there is an optimal hydrophobicity needed for good antimicrobial activity. Sequences with hydrophobicities below and very much above this threshold made the peptides inactive[85]. The decrease in activity when the hydrophobicity is high may be due to the increased likelihood of dimerization, thereby preventing access of the peptide to the bacterial membrane. Additionally, increasing the hydrophobicity of the non polar face of the amphipathic α helix also enhances the

lysis of RBCs. This may be due to the membrane discrimination mechanism as peptides with higher hydrophobicity penetrate deeper into the hydrophobic core of the RBC membrane[85].

Another feature shared by all antimicrobial peptides is amphipathicity. Amphipathicity refers to the relative abundance of hydrophilic and hydrophobic residues or domains within the AMPs. It can be thought of as the balance between the cationic and hydrophobic residues, not just at the primary sequence level, but also in terms of the 2D or 3D structure of the AMPs. Amphipathicity can be achieved by a number of peptide conformations such as the ones listed in Table 1.2, but the most elegant example is the α helix. The α helix allows the peptide to form two "faces", namely the polar and nonpolar face referring to the arrangement of the hydrophobic and hydrophilic side chains of the residues in the helix. Amphipathicity of AMPs can be reflected by calculating the hydrophobic moment which is the vector sum of individual amino acid hydrophobicity, standardized to an ideal helix[83] (calculated using many websites such as http://www.bioinformatics.nl/emboss-explorer/). Interestingly, for α-helical AMPs it was previously thought that disruption of the amphipathicity leads to an increase in antimicrobial activity and reduction in RBC lysis[59,86–89], however, a recent study by Zhang et al. on melittin related peptides demonstrated that increased amphipathicity also leads to a decrease in RBC lysis[90] suggesting a complicated relationship between amphipathicity, hydrophobicity and net charge. It would seem rather that the different parameters play a unique role, depending on the peptide sequence.

1.2.4 Mechanism of antimicrobial peptide action

Antimicrobial peptides are unique molecules and their mechanism of action (MOA) has been studied extensively since they were discovered. It is important to understand the MOA of these AMPs to facilitate further development as therapeutic agents. It was originally thought that

membrane targeting was the only mode of action, but there is increasing evidence now that AMPs have other MOA[56] (Figure 1.5). The MOA can be divided into two major classes: direct killing and immune modulation. The direct killing mechanism of action can be further divided into membrane targeting and non-membrane targeting, which will be the focal point of the following sections.

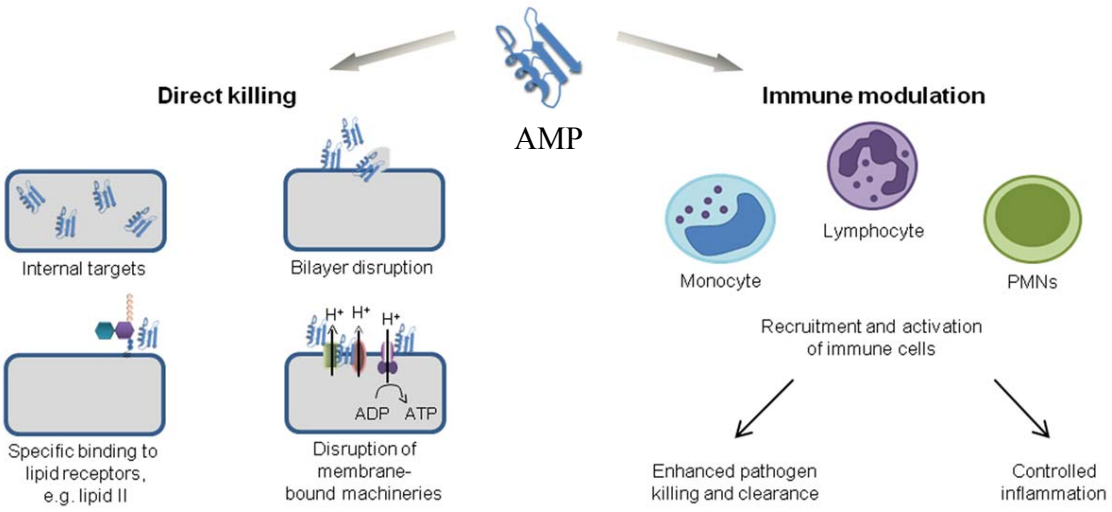

Figure 1.5: Various mechanisms of action of antimicrobial peptides. Figure adapted with permission from Ulm, H et. al. Antimicrobial Host Defensins – Specific Antibiotic Activities and Innate Defense Modulation. Front. Immunol. 3, 249 (2012).

1.2.4.1 Direct killing: membrane permeabilizing mechanism of action

The membrane targeting AMPs can have receptor mediated or non-receptor mediated interactions. The receptor mediated pathway mostly includes AMPs produced by bacteria and which are active *in vitro* in the nanomolar range, such as nisin[91]. The nisin peptide has two domains: the first domain binds with high affinity to the lipid II molecule, a membrane anchored cell wall precursor. The second region is the membrane-embedded pore forming domain. Mesentericin is another example of a receptor mediated membrane targeting AMP[92].

Most vertebrate and invertebrate AMPs target the membrane without specifically interacting with receptors. These AMPs are typically active *in vitro* against microbes at micromolar concentrations[93] and function by interacting with the components of the membrane. The outer surface (Figure 1.1) of Gram positive bacteria and Gram negative bacteria contains teichoic and lipopolysaccharide, each conferring net negative charge on the surface allowing the initial electrostatic attraction with cationic AMPs[83,93]. More importantly, AMPs target a fundamental difference in design between bacterial membrane and membrane of multicellular animals. The outer monolayer (leaflet) (Figure 1.6) of the lipid bilayer in bacterial membranes is mostly made up of lipids with negatively charged head groups such as phosphatidylglycerol (PG) and cardiolipin[94] whereas the outer leaflet of the animal membranes are made up of zwitterionic phospholipids such as phosphatidylcholine (PC), sphingomyelin and other neutral components such as cholesterol[95]. Most of the lipids with negatively charged head groups are in the inner leaflet facing the cytoplasm in animal membranes[95,96]. The positively charged AMP has strong electrostatic interaction with the negatively charged phospholipids on the outer leaflet of the bacterial membrane (Figure 1.6).

Moreover, some AMPs are even sensitive to other properties of the lipids and not just the charge [97,98]. Magainins can induce leakage more effectively in liposomes made of PG, an anionic phospholipid found predominantly in bacterial membrane compared to liposomes composed of negatively charged phosphatidylserine (PS), a major phospholipid of animal membranes[97]. Lipids have different shapes depending on the size of the head group and hydrophobic tails. PS

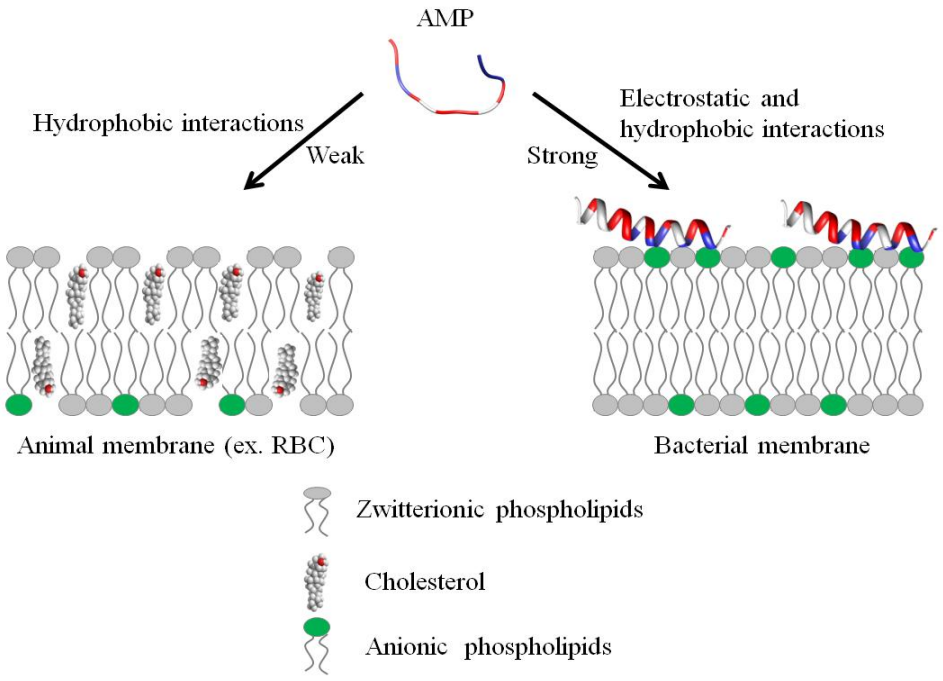

Figure 1.6: Initial interaction of cationic AMPs with the multicellular animal (left) or bacterial (right) membrane. RBC: red blood cell. Figure created using PowerPoint and Chimera.

and PG have molecular shape similar to a cone and cylinder respectively and hence display different membrane curvature properties[99]. The specific interactions are not only limited to anionic lipids as AMPs, such as plant cyclotides, can also bind specifically to zwitterionic lipid such as phosphatidylethanolamine (PE), which is abundantly present at the surface of bacterial membranes and also found in great quantity in the inner cytoplasmic leaflet of the animal membranes[100,101]. These studies suggest that membrane charge is not the only factor that is important for the initial interaction but other properties such as for example membrane curvature may also play an important role[97,102,103].

After the initial electrostatic and hydrophobic interactions, the AMPs accumulate at the surface and self assemble on the bacterial membrane after reaching a certain concentration[104,105]. At this stage various models have been used to describe the action of AMPs. The models can be

classified under two broad categories: transmembrane pore and non-pore models. The transmembrane pore models can be further subdivided into the barrel-stave pore and toroidal pore models. In the barrel stave model, the AMPs are initially oriented parallel to the membrane but eventually insert perpendicularly in the lipid bilayer[106](Figure 1.7a). This promotes lateral peptide-peptide interactions, in a manner similar to that of membrane protein ion channels. Peptide amphipathic structure (α and/or β sheet) is essential in this pore formation mechanism as the hydrophobic regions interact with the membrane lipids and hydrophilic residues form the lumen of the channels[107,108] (ring like a barrel pore). A unique property associated with AMPs in this category is a minimum length of ~22 residues (α helical) or ~8 residues (β sheet) to span the lipid bilayer. Only a few AMPs, such as alamethicin[109], pardaxin[110,111] and protegrins[107], have been shown to form barrel stave channels.

Furthermore, in the toroidal pore model, the peptides also insert perpendicularly in the lipid bilayer but specific peptide-peptide interactions are not present[109]. Instead the peptides induce a local curvature of the lipid bilayer with the pores partly formed by peptides and partly by the phospholipid head group (Figure 1.7b). The dynamic and transient lipid-peptide supramolecule is known as the "toroidal pore". The distinguishing feature of this model as compared to the barrel-stave pore is the net arrangement of the bilayer: in the barrel-stave pore, the hydrophobic and hydrophilic arrangement of the lipids is maintained, whereas in toroidal pores model the hydrophobic and hydrophilic arrangement of the bilayer is disrupted. This provides alternate surfaces for the lipid tail and the lipid head group to interact with. As the pores are transient upon disintegration, some peptides translocate to the inner cytoplasmic leaflet entering the cytoplasm and potentially targeting intracellular components[112]. Other features of the toroidal pore include ion selectivity and discrete size[83]. A number of AMPs such as magainin

2[70], lacticin Q[70], aurein 2.2[113] and melittin[70,109] have been shown to form toroidal pores. Both pore forming models (toroidal pore and barrel stave) lead to membrane depolarization and eventually cell death.

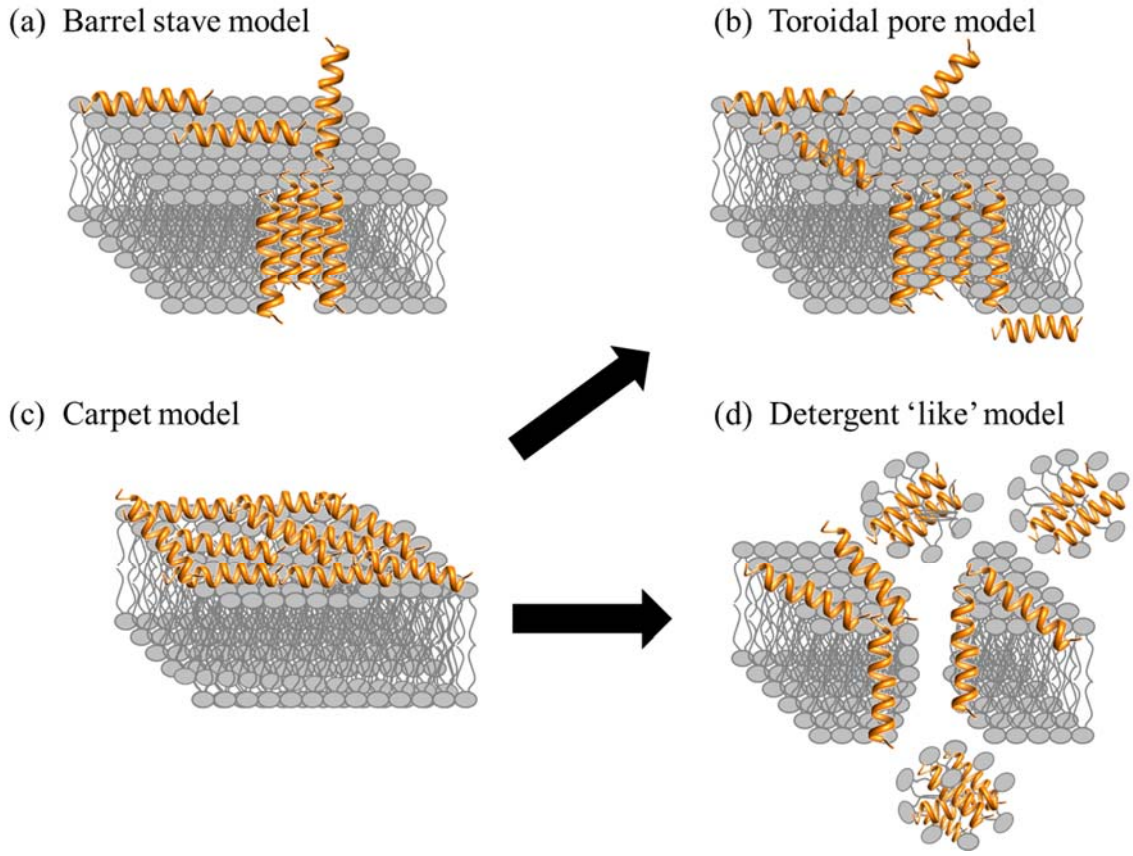

Figure 1.7: Proposed mechanisms of action for AMPs in bacteria. This figure was generated using Microsoft PowerPoint and Chimera.

AMPs can also act without forming specific pores in the membrane. One of these models is designated as the carpet model[70,93,83]. In this case, the AMPs adsorb parallel to the lipid bilayer and reach a threshold concentration to cover the surface of the membrane, thereby forming a "carpet" (Figure 1.7c). This leads to unfavorable interactions on the membrane surface. Consequently, the membrane integrity is lost, producing a detergent-like effect, which eventually disintegrates the membrane by forming micelles. The final collapse of the membrane bilayer

structure into micelles is also known as the detergent-like model (Figure 1.7d). The carpet model does not require specific peptide-peptide interactions of the membrane-bound peptide monomers; it also does not require the peptide to insert into the hydrophobic core to form transmembrane channels or specific peptide structures[83]. Many peptides act as antimicrobial agents despite their specific amino acid composition or the length of the sequence. Such AMPs typically act using the carpet model[93], and do so at high concentrations because of their amphiphilic nature[23]. Examples of AMPs acting by the carpet model are cecropin[114], indolicidin[53] , aurein 1.2[115], and LL-37[93] .

Overall, there are a number of models to describe the MOA of AMPs. In addition to those given above, there are other related models such the Shai-Huang-Matsazuki model, the interfacial activity model, and the electroporation model[70]. Some models do not make the specific distinctions shown in Figure 1.7. For example, it has been suggested that the carpet-like mechanism is a prerequisite step for the toroidal pore model[70]. Most studies to elucidate the MOA of AMPs involve the use of model membranes. The mode of action of only a few AMPs has been investigated with whole bacterial cells using imaging techniques[116,117]. It is possible that different results may be obtained using different membrane models or assay conditions, i.e. that the models described here may or may not translate directly to what is occurring in bacteria.

1.2.4.2 Direct killing: non membrane targeting mechanisms of action

The non-membrane targeting AMPs can be divided into two broad categories: those that target the bacterial cell wall and those that have intracellular targets (Figure 1.5). Similarly to conventional antibiotics like penicillin, AMPs can also inhibit cell wall synthesis. Although most conventional antibiotics bind to specific proteins/enzymes involved in the synthesis of the cell wall components, AMPs often interact with various precursor molecules that are required for cell

wall synthesis. One molecule that is a prime target is the highly conserved lipid II, a precursor molecule in the synthesis of the cell wall[118]. For instance, AMPs such as defensins bind to the negatively charged pyrophosphate sugar moiety of the lipid II molecule[119] (Figure 1.8). The binding event can further promote formation of pores and membrane disruption[118]. AMPs such as the human β defensin 3[119] and α defensin 1[120] rely on selective binding to lipid II to confer bactericidal activity.

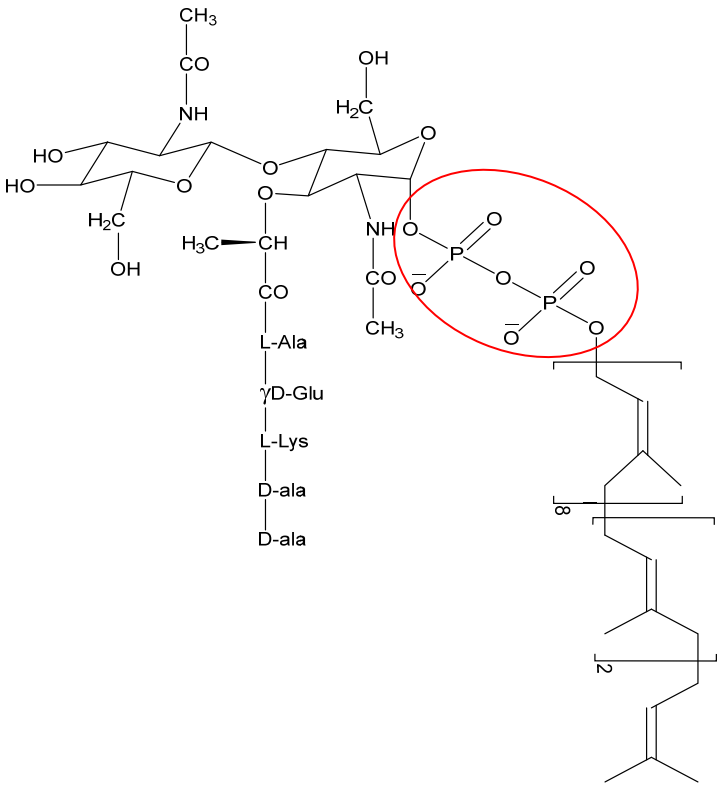

Figure 1.8: Structure of lipid II molecules with pyrophosphate sugar moiety circled in red. This figure was generated using Chemdraw.

When AMPs were first discovered, it was thought that they could not have intracellular targets. Studies with the original α helical peptides such as magainin, cecropin and melittin showed that an all D-amino acid version of these peptides was equipotent compared to the natural all L-amino acid peptides[121], supporting the idea that stereospecific targets such as

proteins or DNA/RNA were not required for antibacterial activity, further confirming that AMPs target the membrane[98]. However, subsequent studies revealed that other AMPs with all-D or all-L amino acids did not have equal activity[122]. Now it is well established that several AMPs have intracellular targets as some AMPs do not cause membrane permeabilization at the minimal effective concentration, but still cause bacterial death[107].

Mechanistically, these AMPs interact with the cytoplasmic membrane first and then accumulate intracellularly, where they can block critical cellular processes. Many novel mechanisms involving intracellular targets, such as inhibition of protein/nucleic acid synthesis and disruption of enzymatic/protein activity, have been discovered[107]. For example, buforin II, an histone derived AMP from frogs, translocates through the bacterial membrane without permeabilization and binds to the DNA and RNA of *E.coli*[54]. Human α defensin 5 also translocates into the cytoplasm of *E.coli* and accumulates at the cell division plate and at opposite poles suggesting part of the antibacterial activity might be due to the targets in the cytoplasm. Indolicidin[123], human β defensin 4[124], human α defensin 1[57] and PR-39[125] have also been shown to target intracellular components in the bacterial cell.

1.2.4.3 Immune modulation mechanism of action

In addition to direct killing of microbes, AMPs can also recruit and activate immune cells (Figure 1.5), resulting in enhanced microbial killing and/or control of inflammation[42,126,127]. As AMPs are produced by many immune cells such as neutrophils and macrophages, they are one of the first molecules that encounter invading microbes[23]. In an infection, it is important to produce an immune response to attract other immune cells and also control inflammation. Interestingly some AMPs can produce a variety of immune responses, such as activation, attraction, and differentiation of white blood cells, stimulation of angiogenesis (formation of new blood

vessels), reduction of inflammation by lowering the expression of proinflammatory chemokines, and controlling the expression of chemokines and reactive oxygen/nitrogen species[46,42,126,128,129].

The human AMPs such LL-37 and β defensins have the ability to attract (chemoattract) many immune cells such as mast cells[130], leukocytes[131] and dentritic cells[132]. Innate defense regulators (IDR) which are synthetic versions of natural AMPs, such IDR-1 and IDR-1018, also suppress pro-inflammatory cytokines in mice infection models[133,134]. IDR-1018 has also shown promise in reducing the inflammation response in severe malaria, without having direct anti-malaria activity. Mice treated with a combination of anti-malaria agents and IDR-1018 demonstrated a reduction in the harmful neural inflammation which otherwise leads to death. Although most AMPs have been shown to interact with innate immune system components such as neutrophils and macrophages, there is evidence that they are also involved in modulation of the adaptive immune system, i.e. the T and B cells. The exact mechanisms are not well understood[42], however, some studies show that AMPs may act as vaccine adjuvants[129,135]. Interestingly, all these studies show that AMPs work in many independent or co-operative "multi-hit"[136] mechanisms of action, making AMPs ideal candidates for future development.

1.2.5 Aurein peptides

Aurein peptides are secreted from the granular dorsal glands of the Australian Green and Golden Bell Frog *Litoria aurea* and the Southern Bell Frog *L. raniformis*. There are more than 30 aurein peptides from five different families, ranging from the short active aurein peptides (aurein 1-3) to the longer peptides such aurein 4.1 and 5.1 which are not active[50]. Most aurein peptides are active against Gram positive bacteria such as *Staphylococcus aureus* and *Staphylococcus epidermidis*. Some peptides, such as aurein 1.2, 3.2 and 3.3, display their strongest activity against 30-50 different types of cancer[49]. Most of the active aurein peptides are

amidated at the C-terminus and usually adopt an α-helical structure when in contact with phospholipids or a membrane-mimetic environment[50,64,113,115,137].

The mechanism of action and structure of aurein 2.2 has been extensively studied in recent years. Earlier studies with aurein 2.2 have shown that it is important to study the bilayer perturbation in membrane models made from PC and PG rather than PC alone, indicating that electrostatic interactions are important in the lipid–peptide interaction[137]. In a POPC/POPG (1:1) membrane model, the peptides induce toroidal pores. In contrast, in a DMPC/DMPG (1:1) membrane model, the peptides work in a detergent like model indicating the importance of the hydrophobic thickness of the lipid bilayer and the membrane composition[113,138]. The truncation of the N-terminus leads to the loss of antimicrobial activity but makes the peptide immunomodulatory[139]. In a more recent study, Wenzel et al. showed that aurein 2.2 forms ion selective pores, permitting the translocation of ions such as potassium and magnesium. In addition aurein 2.2 also causes membrane permeabilization, which disrupts the membrane potential and decreases the energy supply of the cells leading to cell death[140].

1.2.6 Challenges with antimicrobial peptides

Although many eukaryotic AMPs have been identified and characterized, not many have made it to clinical trials (Table 1.3) and only a few have been approved by the US Food and Drug Administration (FDA). Most AMPs in clinical trials are analogues of natural AMPs, but there are some that are completely synthetic (e.g. IMX942). The majority of AMPs in clinical trials are limited to topical applications, due to the systemic toxicity, the susceptibility of the peptides to protease degradation and the rapid kidney clearance[23,105,141] of these peptides if they are ingested. Oral administration of AMPs can lead to proteolytic digestion by enzymes in the digestive tract such as trypsin and pepsin. Systemic administration results in short half lives *in*

vivo, protease degradation and cytotoxic profiles in blood[43]. Many strategies have been investigated to circumvent these issues and to improve the efficacy of AMPs. These include chemical modification of AMPs[142] and the use of delivery vehicles[143]. These strategies will be discussed in more detail below.

Table 1.3: Antimicrobial peptide in clinical trials[43,126,144,63]

Peptide	Progress	Application	AMP analogue (host)
Pexiganan	Phase III	Topical application for diabetic foot ulcers	Magainin (frogs)
OP145	Phase I/II	Bacterial ear infection	LL-37 (humans)
Omiganan	Phase III	Topical cream for prevention of cathether infection, severe acne, rosacea, atopic dermatitis	Indolicidin (bovine)
PAC 113	Phase II	Mouth wash for fungal/yeast infection	Histatin (humans)
Iseganan	Phase III	Treatment of inflammation and ulceration of digestive system mucous membrane	Protegin-1 (pigs)
IMX942	Phase II	Intravenous administration against hospital-acquired bacterial infections	Synthetic analogue of IDR-1

1.3 Strategies to improve antimicrobial peptides

1.3.1 Chemical modification of AMPs

Various chemical modifications of AMPs have been utilized to improve the stability of peptides against proteolytic digestion including the use of D-amino acids, cyclization, acetylation and peptidomimetics. Incorporation of non natural D-amino acids into AMP sequences reverses the stereochemistry of the peptide and hence prevents protease degradation, as enzymes are stereospecific.

In a recent study, Zhao et al. isolated a lysine rich AMP from the venom of the social wasp (*Polybia paulista*), MPI, which was active against Gram positive and Gram negative bacteria and also fungi[145]. In order to prevent proteolytic digestion by trypsin the authors designed two peptides, one with all the amino acids replaced with D-amino acids, D-MPI, and the other peptide with only the lysine residues substituted with D-amino acid (Figure 1.9a), D-lys-MPI, because trypsin cleaves after positively charged amino acids such as lysine[145]. Interestingly, both the peptides, D-MPI and D-lys-MPI were resistant to trypsin digestion, however only D-MPI was equipotent in terms of activity when compared to MPI. D-lys-MPI was inactive because the secondary structure was destabilized upon introduction of single D-amino acids. D-MPI adopted a right handed α-helical conformation, whereas the D-lys-MPI did not adopt any regular structure.

In a similar study, D-BMAP28, a peptide from bovine myeloid, was made proteolytically stable by replacing all amino acids by the D- counterparts. D-BMAP28 remained equipotent in terms of both its antimicrobial and immunomodulatory activities when compared to BMAP38[146]. Moreover, Falciani et al. reported that another AMP, D-M33, was more active against biofilms formed by Gram positive bacteria, as compared to M33[147]. Overall, the use of D-amino acids in AMPs leads to retention of the antimicrobial activity, while preventing proteolysis. This confirms that these AMPs interact with the bacterial membrane without making use of specific receptors[43], since the stereochemistry of the amino acids has no impact on membrane binding. Finally, it should be emphasized that the synthesis of peptides containing D-amino acids is very costly[148]. Alternative strategies are thus important to reduce the economic impact.

These alternative approaches are many and variable. For instance, the substitution of positively-charged arginine in a sequence with other charged non natural amino acids, such as L-

orthothine and L-homoarginine (Figure 1.9b), also increases proteolysis stability of AMPs[149]. Moreover, acetylation of the N-terminus also increases the proteolytic stability of peptides as it blocks the activity of aminopeptidases; however, this leads to removal of a positive charge which in most cases decreases the antimicrobial activity[150,151]. Cyclization of peptides by different methods also prevents protease degradation (Figure 1.9c). Cyclization by joining the backbone N and C termini or by disulfide bridges similar to human defensins are common strategies used to increase serum stability of AMPs[152]. In a recent study, click chemistry was developed for specific cyclization of certain amino acids[153]. The results suggested that the α helical structure was critical for activity as the i, i+4 cyclization (1st and 4th amino acid cyclized) retained the structure and activity compared to i, i+6 cyclization, which was not structured and inactive.

Further strategies include the use of peptidomimetics: peptide-like polymers made from a backbone that is altered when compared to a peptide[154–156]. The main concept in peptidomimetics is to maintain the activity of the peptidomimetics by conserving the 2D and 3D spatial arrangement of the side chains, but modify the backbone to prevent proteolysis degradation. Some examples of peptidomimetics include peptoids, ceragenins, oligoacyllysines and β-peptides[155,156]. Peptoids are isomers of peptides in which the side chain is bonded to the backbone nitrogen instead of the alpha carbon making them resistant to protease degradation[157] (Figure 1.9d). Peptoids derived from pexiganan have been shown not only to mimic the 1D structure but also mimic the 2D structure, function and mechanism of action of pexiganan[158]. CD studies confirmed that peptoids adopt α-helical structure in the presence of phospholipids, whereas X-ray reflectivity showed peptoids bind to the membrane and are membrane active[158]. Cyclization of peptoids also enhances the membrane permeation properties leading to better antimicrobials[159].

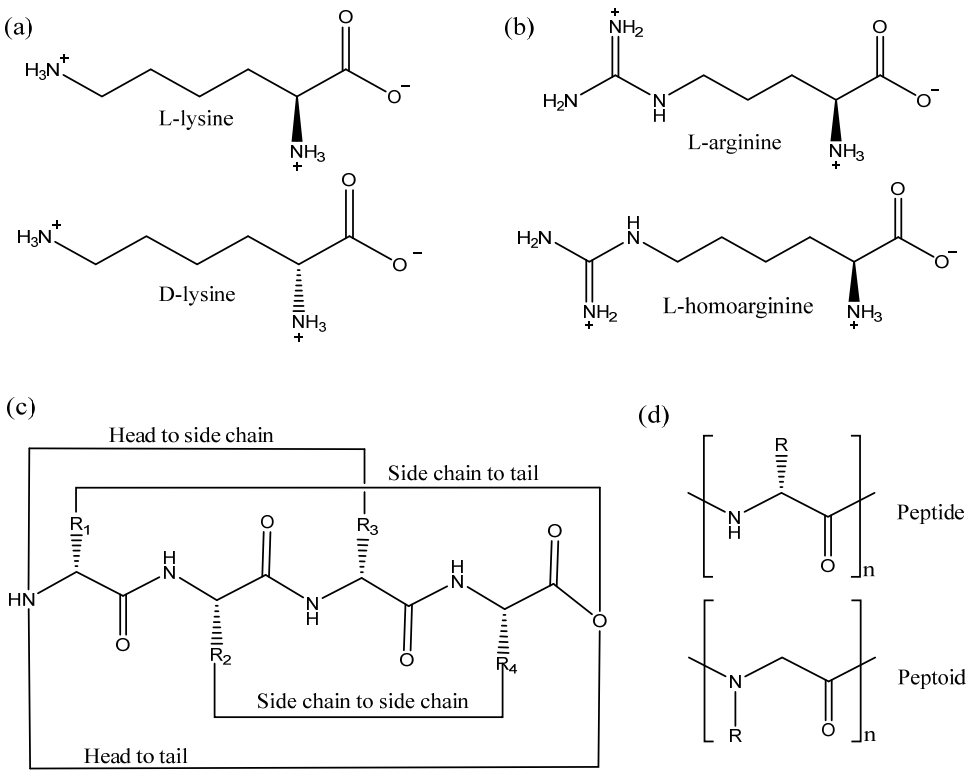

Figure 1.9: Chemical modifications of AMPs. (a) Use of D amino acids such as lysine, (b) Use of non natural amino acids such as L-homoarginine, (c) Various cyclization strategies. (d) 1-dimensional structural difference between a peptide and peptoid. This figure was generated using ChemDraw.

1.3.2 Delivery systems for AMPs

Another important strategy to improve the properties of AMPs is to use delivery systems, i.e. systems ranging from inorganic and polymer materials, surfactant/lipid self assembly systems to peptide self assembly systems[143,160] which can be used to improve the stability, toxicity, half-life and release profile of AMPs. The AMPs can be covalently attached to the delivery system or non-covalently encapsulated by these different types of systems. From their mechanism of action, it is well known that AMPs interact with lipids and hence lipid-based delivery systems of peptides are well studied[161]. The encapsulation of LL37 within liposomes composed of DSPC/DSPE-PEG/cholesterol ensured enhanced bioactivity and reduced toxicity towards cell

cultures[162]. In a similar study, DSPC/DSPG liposomes were found to encapsulate nisin and protect it from extreme alkaline/acidic conditions and elevated temperature[163]. Other nanoparticles for encapsulation of AMPs include DNA cages, metal particles, polymeric systems, carbon nanotubes and mesoporous silica particles[160,164].

As mentioned above, in addition to encapsulation, AMPs can be covalently attached to various molecules, e.g. PEG (Figure 1.10a). PEGylation is a process by which a polyethylene glycol chain is added to a biomolecule. PEGylation is one of the most extensively investigated strategies to improve the performance of proteins, peptides and other biomolecules. The advantages of PEGylation include reduced non-specific uptake in tissue, reduced cell toxicity, increased blood half-life and reduced proteolytic degradation[160,165]. Many AMPs such as tachyplesin I[166], magainin 2[167], and nisin[168] have been PEGylated, leading to improved properties. However, this improvement is often at the expense of the antimicrobial activity. For instance, PEGylation of the cyclic peptide tachyplesin and of magainin reduced toxicity towards CHO-K1 cells, but also decreased antimicrobial activity towards *E. coli* and *S. epidermidis*. Interestingly, PEGylation of nisin via the amine group of lysine lead to a conjugate that was inactive. It was hypothesized that the amino group of the lysine residue is needed to bind to the pyrophosphate of the lipid II molecule, hence the loss of activity. In other words, the site and nature of the conjugation chemistry[168] has an impact on the properties of the resulting compounds. Finally, PEGylation of KYE28 revealed that increasing the length of PEG lead to a partial loss in antimicrobial activity, but also to a strong decrease in hemolysis and to improved selectivity in blood and bacteria mixtures[169]. Important drawbacks of linear PEG is its relatively large hydrodynamic size, high intrinsic viscosity in aqueous conditions which increases with

increase in molecular weight (and limits the generation of concentrated peptide formulations) and the lack of multiple functionality [40].

Alternatively, AMPs can also be conjugated to biopolymers such as chitosan and hyaluronic acid, which have multiple functional groups for the attachment of peptides (Figure 1.10b and c). Chitosan is a linear biocompatible, biodegradable carbohydrate polymer with some antimicrobial activity[170]. Conjugation of the short and moderately active anolin to chitosan increased the antimicrobial activity of the conjugate and abolished the hemolytic activity[171]. In general, the antimicrobial activity increased in proportion to the number of peptides attached to the chitosan polymer. Recently, click chemistry has been used as an interesting approach to attach AMPs to chitosan at specific sites[172].

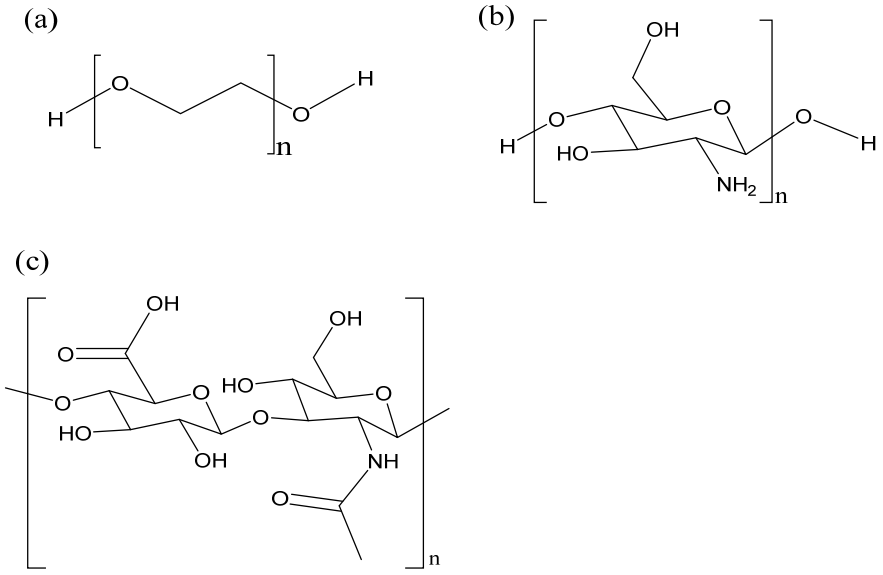

Figure 1.10: Various polymers used for AMP conjugation. (a) polyethylene glycol, (b) chitosan, (c) hyaluronic acid. Image created using ChemDraw.

Another biocompatible, biodegradable linear carbohydrate polymer utilized for AMP conjugation is hyaluronic acid. In contrast to PEGylation, conjugation of nisin to hyaluronic acid results in a conjugate which maintains antimicrobial activity[173]. The hyaluronic-nisin conjugates

were mostly active against Gram positive bacteria, and in the presence of EDTA the antimicrobial activity extended towards Gram negative bacteria. The EDTA binds to divalent cations such as Mg^{2+} and disturbs the lipopolysacchride-divalent cation interaction, disintegrating the outer membrane of the Gram negative bacteria, making it more susceptible to the hyaluronic-nisin conjugate.

1.4 Hyperbranched polyglycerol

Recently hyperbranched polyglycerol (HPG), a synthetic polymer, has gained a lot of attention in the research community due to its excellent biological properties[174]. HPG was originally synthesized by cationic ring opening multi branching polymerization (ROMPB) but due to various limitations, such as multiple side reactions, anionic ROMBP with slow monomer addition has been utilized thereafter[175–177]. The synthesis of high molecular weight HPG (>100,000 Da) usually requires an emulsifying agent such as 1,4 dioxane as a solvent[178] due to the poor mixing that arises because the viscosity of the solution increases as polymerization proceeds[177]. HPG has been used in many biomedical applications due to the ease in its synthesis, globular structure, and various hydroxyl groups available for functionalization, low viscosity, high solubility and excellent biocompatibility.

HPG has excellent blood compatibility compared to PEG. Studies by the Brooks and Kizhakkedathu groups demonstrated that HPG had no effect on red blood cell aggregation and lysis, platelet activation and aggregation, complement activation, and blood coagulation[179–181]. In contrast, similar molecular weight PEG aggregate red blood cells, activate platelets and the complement system and alter blood coagulation[181]. Additionally, high and low molecular weight HPG are also compatible with many different types of cells in cell culture models such as fibroblasts[182], human umbilical vein endothelial cells (HUVEC)[181], human peritoneal

mesothelial[182] cells and H9e2 cells[183]. More importantly, the *in vivo* profile of HPG looks promising in different models: for instance, hydrophobically modified[184], cationic[185] or drug conjugated[186,187] HPGs were all well tolerated in mice and found to be non toxic.

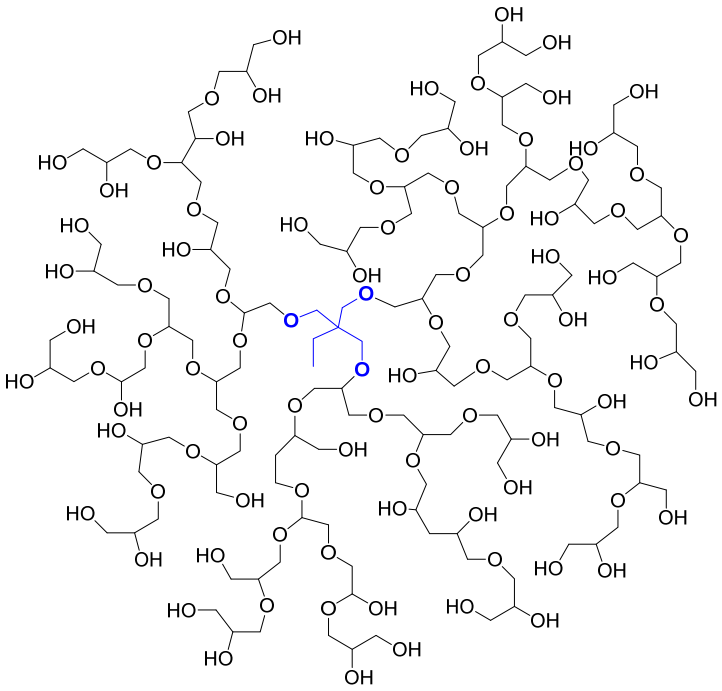

Figure 1.11: Generic structure of HPG. Image created using ChemDraw.

Furthermore, the pharmacokinetic properties of HPG and modified HPG have been well studied. The circulation half-life for 100kDa HPG is much longer (~40 hrs) compared to similar molecular weight PEG and linear polyglycerols (LPGs)[181]. The circulation half-life can be fine-tuned by varying the molecular weight[181,188] and/or by incorporating ketal linkages[189] in the HPG backbone. The repeated injection of the HPG modified red blood cells in mice models suggest that mice do not generate an immune response to the HPG molecule, unlike what was observed for PEG[190]. Although HPG has excellent *in vivo* biocompatibility, high molecular weight HPG is known to accumulate in liver and other organs[187]; however, the accumulation is lower compared to other polymers of similar molecular weight[191].

Moreover, due to its excellent cell tolerance, blood and *in vivo* biocompatibility, HPG has been utilized for many biomedical applications such as the development of long circulating drug conjugates[186,187], anticoagulant neutralizing agents[185,192], modification of red blood cell surface[193,194], as an osmotic agent in peritoneal dialysis[195] and for cell/organ preservation[196]. There are only a few examples of HPG conjugated peptides used for biomedical applications. For instance, Freund and co-workers utilized the multivalency effect of HPG by conjugating many peptides to the HPG scaffold[197]. The proline rich peptide used is a binding partner to FBP21, a protein involved in splicing of pre-mRNA in the nucleus of eukaryotic cells. The binding affinity was enhanced by nearly 9-fold once the peptides were conjugated to HPG compared to free peptides[197]. In another example, Zhang *et al*. conjugated a very short peptide, denoted RGD (arginine-glycine-aspartic acid), to HPG polymer for its use in antiplatelet therapy[198]. RGD is known to bind to platelet integrin GPIIbIIIa and interrupts platelet-fibrinogen binding and platelet aggregation during thrombosis[198]. Conjugation of the RGD peptides to high molecular weight HPG increased the platelet inhibitory function by 2-3 orders of magnitude. Moderate levels of conjugated peptides could lead to suitable candidates for the development of an antithrombotic drug.

Additionally, Haag and co-workers conjugated a tolerogenic peptide to HPG to increase the bioavailability and efficacy in vaccination strategies. Tolerogenic peptides have the ability to provide immunological tolerance[199]. The tolerogenic peptide pOVA is presented via the major histocompatibility complex II (MHCII) of the antigen presenting cell (APC) and recognized by T-cells. The uptake, storage and stability of the HPG-pOVA conjugates were dependent on the linkage chemistry. The degradable ester linked conjugates had superior properties compared to amide linked polymers. The authors also speculated that the linker structure might additionally

target the conjugates to specific APC and favor a tolerogenic T-cell response. These conjugates are promising novel candidates for vaccines that could be used for the treatment of autoimmune diseases and allergies[199].

1.5 Thesis rationale, hypotheses and aims

The emergence of antibiotic resistant microbes (Table 1.1) and the limited discovery and development of new antibiotics is one of the greatest threats to human health[16]. Although antimicrobial peptides can be used as alternatives or synergistically with antibiotics to treat antibiotic resistant microbes, there are several limitations associated with the use of AMPs. These limitations include systemic toxicity, proteolytic degradation and short circulation half-lives[23,105,141], for example. Although aurein 2.2 shows good activity against Gram positive bacteria *in vitro*, it is however, toxic towards peripheral blood mononuclear cells (PMBCs)[139].

The main objectives of this thesis are hence: 1) to develop ways to increase the biocompatibility of aurein 2.2 while maintaining sufficient antimicrobial activity via polymer conjugation approaches, specifically conjugation to hyperbranched polyglycerols (HPG); 2) to investigate the influence of polymer molecular weight and peptide sequence on the antimicrobial activity; 3) to determine the efficacy of the optimal peptide and polymer peptide conjugate in mice models of infection, and 4) to establish Nuclear Magnetic Resonance (NMR) methodology that can be used in the future to study the mechanism of action of the peptides. These will be described briefly below.

1.5.1 Development of novel antimicrobial conjugates

In recent years different polymer systems have been developed to alleviate the limitations associated with AMPs but lead to a significant decrease in the activity of peptides[169,171,173170]. Our laboratory has pioneered the synthesis and characterization of HPG, and has shown that it is

a highly biocompatible polymer[185,186,200]. Studies reported in **Chapter 2** uncover the molecular design of the HPG-aurein 2.2 conjugates, and the influence of peptide density and structure on their antimicrobial activity. We hypothesize *that conjugation of multiple aurein 2.2 peptides to HPG would decrease the toxicity of the peptides but will maintain the antimicrobial activity due to the multivalent presentation and compact nature of HPG.* To test this hypothesis, the specific aims are to:

1. Develop a methodology to synthesize the HPG-aurein 2.2 conjugate with different number of peptides per polymer.
2. Compare the antimicrobial activity of the HPG-aurein 2.2 conjugates.
3. Measure the toxicity of the HPG-aurein 2.2 conjugates against various blood components and mammalian cells.
4. Correlate the activity of the HPG-aurein 2.2 conjugates to the peptide structure using biomembrane mimicking phospholipid vesicles.

1.5.2 Development of potent novel antimicrobial peptides and conjugates

Many studies have designed mutants of natural AMPs to increase the antimicrobial activity of peptides. Increasing the charge of the peptide is a common strategy used to enhance antimicrobial activity[87]. Although making single amino acid mutations in a peptide sequence and purifying them is a laborious task, it has been used for decades to design AMP analogues[139]. A more efficient method to generate peptide analogues is SPOT synthesis of peptides on cellulose membrane which enables the screening of hundreds or even thousands of peptides at once[201–203]. It has been shown previously that polymer scaffold molecular weight could influence the activity of peptides conjugated due to the increased molecular volume and changes in the peptide

conjugation density[204]. Moreover, the molecular weight of HPG can be fine tuned for various biomedical applications.

Studies reported in **Chapter 3** provide insight into the influence of peptide sequence and polymers molecular weight on antimicrobial activity, blood and cell toxicity, and stability against proteolytic degradation of the conjugates. *It is hypothesized that the tryptophan and arginine mutation of the aurein 2.2, the parent peptide, would lead to novel peptides with potent antimicrobial activity and conjugation of the peptide to the polymers will result in conjugates with excellent antimicrobial activity and biocompatibility.* The specific aims for this chapter are to:

1. Design and screen an antimicrobial peptide array containing arginine and tryptophan mutants.
2. Synthesize various molecular weights of HPG and conjugate them with novel peptides.
3. Evaluate the antimicrobial activity and toxicity of the conjugates and the novel peptides.
4. Determine the proteolytic susceptibility and structure-function relationship of the best candidate conjugate.

1.5.3 *In vivo* efficacy of the peptides and the conjugates in mice models

An abscess is a common skin condition caused by bacterial infection and is characterized by the accumulation of pus in the skin which normally appears red, swollen and tender and may cause severe pain[205]. In 2005, approximately 3.2 million people with abscesses were treated in hospital emergency departments in the US alone[206]. Abscesses are treated by surgically draining the pus and treating with antibiotics to prevent spreading and reoccurrence[207]. Antibiotics do not work within the abscess due to limited penetration, high bacterial loads and low pH[208]. Methicillin resistant *Staphylococcus aureus* (MRSA) is an example of a bacterial species that

causes difficult to treat abscesses. Mansour et al. have shown that MRSA in abscess and biofilm conditions produce similar stress response which can be targeted in mice by antimicrobial peptide DJK-5[207]. In another study, D-amino acid AMPs eradicate biofilms formed by multi-resistant *Pseudomonas aeruginosa* in invertebrate (*Caenorhabditis elegans* and *Galleria mellonella*) survival models[209].

The novel peptides developed in **Chapter 3** showed enhanced *in vitro* antimicrobial activity against *S. aureus* compared to the aurein peptides. Studies reported in **Chapter 4** investigate the *in vivo* efficacy of the peptides and the conjugates in mice abscess models. *Our hypothesis is that the novel peptides and their conjugates will be effective in preventing abscesses in mice models, and the D-amino acid version of the peptides will further enhance their in vivo efficacy.* The specific aims to test this hypothesis are to:

1. Evaluate the efficacy of the various novel peptide analogues in a mouse abscess model.
2. Conjugate the most active peptide to HPG and evaluate in mouse abscess model.
3. Design the D-amino acid version of the most active peptide and evaluate its *in vivo* efficacy.

1.5.4 Interaction of aurein 2.2 with whole bacterial cells by NMR.

The mechanism of action (MOA) of aurein 2.2 has been well studied and many techniques such as NMR, CD spectroscopy and leakage assays[117,139] have been developed to understand the bacterial killing action of AMPs. Although the MOA of some AMPs is well understood, most studies use model membrane systems such as supported bilayers, liposomes, vesicles and micelles showing that AMPs damage the membrane or form membrane pores via various mechanisms such as toroidal pore, barrel stave or detergent models as described in section 1.2.4.2. Hence, the main killing action of AMPs is thought to target the bacterial cell

membrane, but as mentioned earlier, AMPs may also target the cell wall or other intracellular components[160]. To date only a few studies have explored the membrane/cell wall-peptide or peptide-intracellular component interactions in living cells[116]. Therefore, it is important to investigate the detailed structural interaction between AMPs and their targets in living cells to further understand their MOA.

NMR is one of the most powerful techniques that can used to elucidate the detailed structural interactions between AMPs with potential molecular targets such as membranes, proteins and nucleotides[210]. To date only a few whole cell NMR experiments have been reported to determine the interactions of AMPs with different bacterial components. Solid state NMR studies (cross-polarization magic-angle spinning, CPMAS) of whole planktonic cells were able to detect the total ^{13}C and ^{15}N composition of intact *S. aureus* cells and pinpoint the general MOA[211]. On the other hand, isotopic labeling of peptides instead of the bacterial cells can be used to determine the specific interaction of AMPs with live bacterial cells. Chemical isotopic labeling of the AMPs is not practical due to high cost; however, recombinant expression of AMPs in bacteria has been recently well developed by the Hans J. Vogel lab, using a calmodulin fusion construct [210]. A common disadvantage with AMPs expressed in bacteria is their free C-terminus whereas most AMPs, including aurein 2.2, require an amidated C-terminus to display potent antimicrobial activity.

Studies reported in **Chapter 5**, describe a methodology to express and purify aurein 2.2 in a bacterial expression system and chemically modify the carboxyl C-terminus to restore the activity which was then used to probe the interaction of aurein 2.2 with whole bacterial cells by NMR. The specific aims are to:

1. Express, purify and cleave the isotopically (^{15}N) labeled calmodulin-aurein fusion protein.
2. Esterify the carboxyl C-terminus of expressed aurein 2.2 and measure the antimicrobial activity.
3. Develop a preliminary 2D NMR methodology to study the interaction of ^{15}N labeled aurein 2.2 with whole bacterial cells.

1.6 Summary

Overall, these studies will provide fundamental information of AMP-polymer conjugates which can be used to design novel drug candidates with better antimicrobial activity, and can be further developed into antibiotics that can combat the ABR crisis. It also provides a useful tool to understand the mechanism of other AMPs and conjugates in the future.

Chapter 2: Conjugation of aurein 2.2 to HPG yields an antimicrobial with better properties[b]

2.1 Synopsis

Aurein 2.2 is an antimicrobial peptide (AMP) whose mechanism of action is quite well understood and with good activity against Gram positive bacteria. It is, however, cytotoxic. Recently, hyperbranched polyglycerol (HPG) has been gaining a lot of attention as an alternative to PEG due to its excellent biocompatibility. In this Chapter, I report the synthesis of HPG conjugates of antimicrobial peptides. Aurein 2.2 peptide was conjugated to high molecular weight HPG with varying number of peptides per polymer and their biocompatibility and antimicrobial activities were investigated. The antimicrobial activity of the peptide and its conjugates were determined by measuring the minimal inhibition concentration (MIC) against *S. aureus* and *S. epidermidis*. The interaction of aurein 2.2 peptide and the conjugates with model bacterial biomembranes was investigated using CD spectroscopy to understand the mode of action of the conjugates. The biocompatibility of the AMP-polymer conjugates was investigated by measuring the red cell lysis, platelet activation and aggregation, complement activation, blood coagulation, and cell toxicity. Results presented in this chapter show that the size of the conjugates and the peptide density influence the biocompatibility of the antimicrobial conjugates. These results will help to further define the properties of HPG-AMP conjugates and set the stage for development of better therapeutic agents.

[b]A version of Chapter 2 has been published**.** **Kumar, P**.; Shenoi, R. A.; Lai, B. F. L.; Nguyen, M.; Kizhakkedathu, J. N.; Straus, S. K. Conjugation of Aurein 2.2 to HPG Yields an Antimicrobial with Better Properties. ***Biomacromolecules*** 2015, *16*, 913–923, doi:10.1021/bm5018244.

2.2 Background

As outlined in Chapter 1, it has become increasingly important to find substitutes to conventionally used antibiotics. Antimicrobial peptides (AMP) are considered to be viable alternatives because they have a broad antimicrobial spectrum and are unique, since bacteria develop little or no resistance towards AMPs[212–214]. Aurein 2.2 (GLFDIVKKVVGALGSL-$CONH_2$) has also been extensively studied[113,137,138,215]. It has been shown that the N-terminus is essential for activity; however, the truncation of the C-terminus by three residues (GLFDIVKKVVGAL-$CONH_2$) has no effect on structure and function.

Although AMPs are promising therapeutic agents, only a few are used for systemic therapy. Examples of AMPs in clinical trials are arenicin and the lantibiotics MU1140 and NVB302, used to treat infections related to Gram-positive bacteria[63]. The small number of AMPs currently being used is due to problems such as unknown toxicity against host cells, short circulation half-life due to protease digestion and rapid kidney clearance[167,216]. In order to circumvent these issues, researchers are investigating ways to conjugate AMPs to biocompatible polymers to alter their residence time in the body and their tissue distribution.

A number of studies in the literature have demonstrated how polyethyleneglycol (PEG) can be used as a polymer to conjugate peptides and proteins (PEGylation) in order to improve efficacy and tissue distribution *in vivo*[167,217]. A polymer that has recently gained a lot of attention is hyperbranched polyglycerol (HPG). HPGs have been used for the conjugation of biomolecules due to their ease of one-pot synthesis (Figure 2.1), excellent biocompatibility (equal or better than PEG) and long blood circulation, which is molecular-weight dependent[181,218,219]. Other beneficial characteristics of HPG are described in detail in section 1.3.

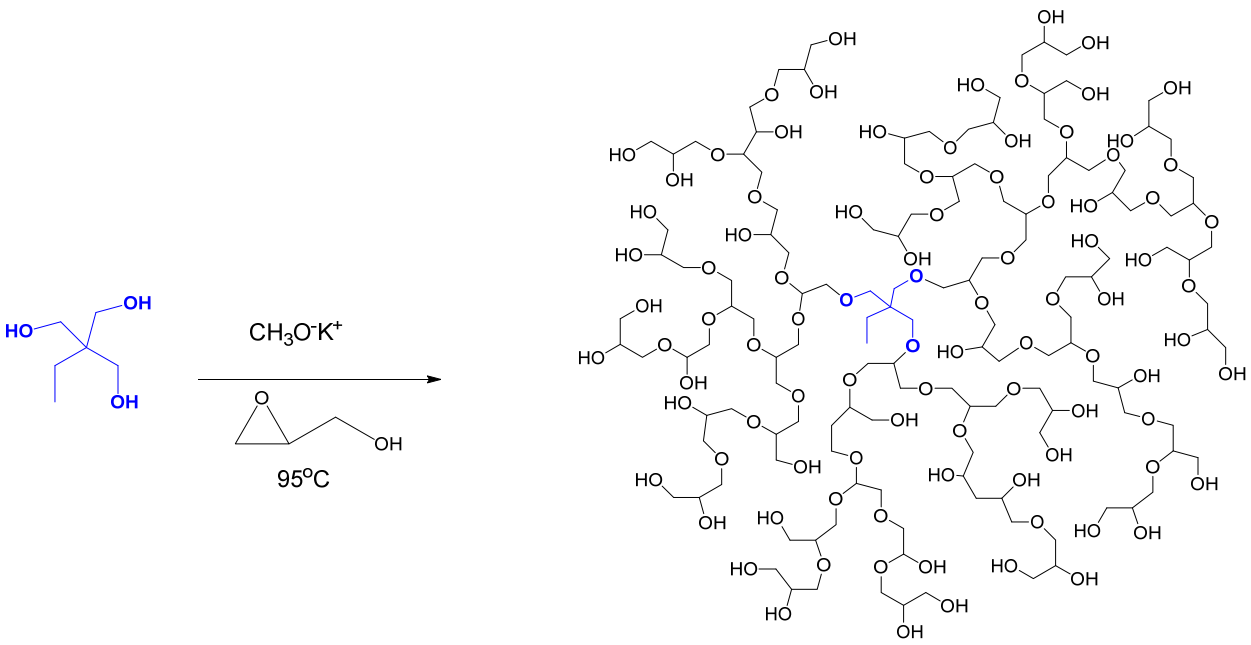

Figure 2.1: Synthesis of HPG. Anionic ring opening polymerization of the 1,1,1-Tris(hydroxymethyl) propane initiator. Figure generated using ChemDraw.

In this chapter, we investigated the utility of HPG in the generation of antimicrobial peptide conjugates. We hypothesized that conjugation of AMPs to HPG would enhance the biocompatibility of the antimicrobial peptides without considerably diminishing their antimicrobial properties. The multifunctionality of the HPG would allow the conjugation of multiple peptides per scaffold. The C-terminus of aurein 2.2 was conjugated to HPG (HPGylation). The antimicrobial activity of conjugates was measured against *S. aureus* and *S. epidermidis* in comparison to the unconjugated peptides. Solution CD spectroscopy was used to examine the interaction of the conjugates with model biomembranes to understand their mode of action. Biocompatibility of the conjugates was investigated using hemocompatibility measurements including red blood cell lysis, platelet activation and aggregation, complement activation and blood coagulation, as well as cell toxicity tests.

2.3 Methods

All chemicals were purchased from Sigma Aldrich Canada Ltd. (Oakville, ON) and used without further purification, unless indicated otherwise. Glycidol was purified by vacuum distillation and stored at 4 ºC. Cellulose ester dialysis membranes were obtained from Spectra/Por Biotech (Rancho Dominguez, CA, US). Pierce BCA protein assay kit was purchased from Thermo Fisher Scientific Inc. (Rockford, IL, US). POPC (1-palmitoyl-2-oleoyl-sn-glycero-3-phosphocholine, purity > 99%) and POPG (1-palmitoyl-2-oleoyl-sn-glycero-3-phosphoglycerol, purity > 99%) were purchased from Avanti Polar Lipids (Alabaster, AL, US) and used without further purification.

2.3.1 Peptide Synthesis and Purification

Aurein 2.2Δ3 (GLFDIVKKVVGAL-$CONH_2$) and aurein 2.2Δ3-cys (GLFDIVKKVVGALC-$CONH_2$) were synthesized (using Fmoc chemistry) using a solid phase peptide synthesizer from CS Bio Co. (Menlo Park, CA, US), as previously described[113,137,138,215]. The first residue at the C-terminus was double-coupled to the Rink resin to produce C-terminally amidated peptides. The crude products were purified by preparative reverse phase high performance liquid chromatography on a Waters 600 system (Mississauga, Ontario, Canada) monitored using a UV detector at 229 nm and using a Phenomenex (Torrance, CA, US) C4 preparative column (20.0 μm, 2.1 cm x 25.0 cm). The mobile phase was composed of two buffers (A and B) with gradient flow. Buffer A was composed of 90% ddH_2O, 10% acetonitrile, 0.1% TFA and buffer B was made up of 10% ddH_2O, 90% acetonitrile, 0.1% TFA. The peptides were purified to > 95% purity (Appendix A.1). The identity of the peptides was confirmed by MALDI-time of flight mass spectrometry, for aurein 2.2Δ3 (theoretical mass: 1357.70 Da;

experimental: 1357.67 Da) and aurein 2.2Δ3-cys (theoretical mass: 1460.83 Da; experimental: 1460.49 Da).

2.3.2 Synthesis of HPG

Synthesis of hyperbranched polyglycerol (HPG) was carried out as described in a previous report[220]. Briefly (Figure 2.1), the reaction was carried out in a three-necked glass reaction flask with a mechanical stirrer, an automatic dosage pump and temperature control under argon. 1,1,1-tris(hydroxymethyl) propane (0.24 g) was partially (10%) deprotonated with potassium methoxide (25 wt% in methanol, 0.22 mL). Methanol was removed under vacuum for 5 h. The flask was heated to 95ºC and glycidol (18 mL) was added dropwise for 12 h and stirred for another 4 h. Polymer was dissolved in methanol and precipitated three times from acetone. The polymer was dissolved in water and purified by dialysis against water by using a regenerated cellulose membrane (MWCO 1000) and characterized by gel permeation chromatography (GPC) using DAWN-EOS multi-angle light scattering (MALLS) (Wyatt technology Inc., Santa Barbara CA, USA) in conjunction with an optilab RI detector. The mobile phase used was 1.0 M $NaNO_3$ with a dn/dc value of 0.12 mL/g used for molecular weight calculation.

2.3.3 Amine Modification of HPG

HPG (44000 g/mol, 0.5 g) was dissolved in N-methyl pyrrolidinone (NMP) and reacted with 0.004 g of sodium hydride (NaH) in a glove box for 4 h at room temperature (2.5% of the hydroxyl groups are deprotonated to get 15 amine groups eventually). The azido-epoxide compound was added to the solution and stirred for 15 h at 70 ºC. The polymer solution was then cooled to room temperature (22 ºC) and precipitated three times from cold diethyl ether and centrifuged to yield the azide functionalized HPG. HPG-azide was reacted with triphenyl phosphine (0.060 g) and water (0.025 mL) in tetrahydrofuran for 15 h at room temperature to

reduce the azide group and generate the amine-functionalized HPG. To obtain the 5% amine modified polymer twice the molar ratio of reagents was used when compared to the 2.5% modification described above. The products were characterized by proton NMR.

2.3.4 Conjugation of Peptide with amine-modified HPG

The amine-functionalized HPG (2.5%) (0.01 g, 44000 g/mol) was reacted with activated ester of iodoacetic acid (iodoacetic acid N-hydroxysuccinimide ester) (0.001 g) in dimethylformamide (DMF) at room temperature (22 ºC) for 15 h. The resulting solution was dialyzed (MWCO 1000) for 24 h to remove the unreacted reagents. The product was characterized using proton NMR, UV-Vis and GPC.The iodoacetamide modified HPG (0.01 g. 44000 g/mol) was further reacted with sulfhydryl containing aurein 2.2Δ3-cys (GLFDIVKKVVGALC-$CONH_2$) (0.005 g, 1460.49 g/mol) at pH 8.0 in PBS (phosphate buffered saline):acetonitrile mixture 50:50 (V:V). To obtain the HPG-Aurein 2.2Δ3-cys 5% conjugate, twice the molar ratio of iodoacetamide modified HPG and aurein 2.2Δ3-cys were used when compared to 2.5%. The HPG conjugated peptide was purified by size exclusion chromatography using a Waters 600 system (Mississauga, ON, Canada) with a 229 nm UV detector and CATSEC column (CATSEC 300, Eprogen) (Appendix A.6). The mobile phase used was 0.2 M NaCl in 20% ethanol/water mixture. The product was further characterized by proton NMR and GPC.

2.3.5 Characterization of HPG Peptide Conjugates

Absolute molecular weights of the conjugates were determined by GPC on a Waters 2690 separation module fitted with a DAWN-EOS multi-angle light scattering (MALLS) (Wyatt technology Inc., Santa Barbara CA, USA) in conjunction with an optilab RI detector[181]. The mobile phase used was 1.0 M $NaNO_3$ with a dn/dc value of 0.12 mL/g used for the molecular weight calculation. NMR spectra were recorded on a Bruker 300 and 500 MHz NMR

spectrometers by using deuterated solvents (Cambridge Isotope Laboratories, 99.8 %D) with the solvent peak used as a reference. The peptide concentration was determined with the Pierce BCA protein assay kit.

2.3.6 MIC Determination

The MICs for the peptides and the conjugates were determined based on previously described methodology with minor modification[113,137,138,215]. Five milliliters of Mueller Hilton Broth (MHB) was inoculated with the bacterial strain (*S. aureus* C622 and *S. epidermidis* C621) and incubated overnight at 37 ºC. The day of the experiment, serial dilutions of the peptides at 2× the required concentration in sterile water in a polypropylene 96-well plate (Thermo Fisher Scientific Inc. Rockford, US) was made. First, the peptides/conjugates were diluted in equal volumes of sterile water to get 2× the required maximal concentration. Secondly, serial doubling dilutions were made in sterile water to get the peptides at 2× the required test concentrations, e.g. 1000, 500, 250….16.5 µg/ml. With a multichannel pipettor, 50 µL/well of the 2x peptide dilutions were added to columns 2 to 11 of the 96-well plates. For each strain, the OD_{600} (absorbance of the bacterial cells at 600 nm) was measured and a 1:50 dilution of the overnight cultures were made to get 2-7×10^5 CFU/ml knowing that C622 has 7.3×10^8 CFU/OD and C621 has 3×10^8 CFU/OD. Colony forming units (CFU) is a rough estimate of the number of viable bacterial cells. With a multichannel pipette, 50 µL of the diluted bacteria (diluted in 2× MHB) was added to columns 2 to 12 of the plates containing 50 µL/well of the 2× peptide dilutions. Column 12 was the bacterial growth control. MHB was added to column 1 as a media control. The plates were incubated at 37 ºC overnight and the MIC was checked after 18-24 h. The MIC was determined visually as the lowest concentration where no growth is observed.

2.3.7 Blood Compatibility Analysis

Blood was withdrawn from consenting unmedicated donors into a 3.8% sodium citrated tube with a blood/coagulant ratio of 9:1 or serum tube at the Centre for Blood Research, University of British Columbia. Serum was prepared by centrifuging whole blood samples in serum tubes at 1200*g* for 30 min in an Allegra X-22R centrifuge (Beckman Coulter, Canada). Platelet rich plasma (PRP) and platelet poor plasma (PPP) were prepared by centrifuging citrated whole blood samples at 150*g* for 20 min and 1200*g* for 30 min, respectively. Red blood cell (RBC) suspension was prepared by washing packed RBC with PBS three times to yield 80% hematocrit. The polymer/peptide stock solutions were made in PBS (with final concentrations as indicated in figure captions).

2.3.7.1 Platelet Activation Analysis: Flow Cytometry

The level of platelet activation was quantified by flow cytometry[194]. Ninety microliters of PRP was incubated at 37 °C with 10 μL of stock polymer/peptide samples (final concentration indicated in figure captions). After 1 h, aliquots of the incubation mixtures were removed for assessment of the platelet activation state. Five microliters of post-incubation platelet/polymer mixture, diluted in 45 μL PBS buffer, was incubated for 20 minutes in the dark with 5 μL of monoclonal anti-CD62-PE (Immunotech, Marseille, France). The reaction was then stopped with 0.3 mL of phosphate-buffered saline solution. The level of platelet activation was analyzed in a BD FACS Canto II flow cytometer (Becton Dickinson, ON, Canada) by gating platelet-specific events based on their light scattering profile. Activation of platelets was expressed as the percentage of platelet activation marker CD62P-PE (phycoerythrin) fluorescence detected in the 10,000 total events counted. Duplicate measurements were done; the mean of which was

reported. One U/mL of human thrombin (SigmaAldrich, Oakville, ON, Canada) was used as a positive control for the flow cytometric analysis.

2.3.7.2 Platelet Aggregation Studies

To evaluate the influence of the conjugates on platelets, a microplate platelet aggregation assay was performed. Platelet concentration in platelet-rich plasma (PRP) was made to 2.5×10^8 cells/mL. For all other samples, aggregation was quantified by mixing 10 µL of HPG-peptide conjugates with 90 µL of PRP. The absorbance was then measured at 595 nm at an interval of 15 seconds for 20 minutes with shaking at 37 °C using a Spectramax PLUS plate reader (Molecular devices, Sunnyvale, CA, US). Platelet aggregation was induced by adding 5 µM adenosine diphosphate (positive control). The full experimental procedure and analysis were previously published[221]. The percentage of aggregation was calculated using the formula:

$$\% \text{ of aggregation} = \text{Abs}_{\text{PRP}} - \text{Abs}_{\text{sample}} / \text{Abs}_{\text{PRP}} - \text{Abs}_{\text{PPP}}$$

where PRP= Platelet rich plasma, PPP= Platelet poor plasma, and Abs= Absorbance.

2.3.7.3 Red Blood Cell Lysis Studies

Ten microliters of each of the stock polymer conjugate/peptide concentrations were mixed with 90 µL of 10% hematocrit RBC suspension and incubated for 1 h at 37 °C. The complete lysis of red blood cells by dH_2O is used to define the 100% lysis point and phosphate-buffered saline mixed with the hematocrit acts as the normal control (minimal lysis). The percent of red blood cell lysis was measured by using the Drabkin method[222]. Five microliters of the washed blood cells/polymer conjugate/peptide solution was added to 1 mL of Drabkin's solution. After centrifugation, 50 µL of supernatant of the blood/polymer solution was also subjected to 1 mL of Drabkin's solution. The difference in optical density (OD) was measured using a light

spectrophotometer at 540 nm. The percent of red blood cell lysis in the sample was the OD of the supernatant divided by the OD of blood/polymer solution[222].

The selectivity of the conjugates was also tested by using a combined blood and bacteria experiment[169,223]. Bacterial suspensions (*S. aureus* C622 and *S. epidermidis* C621) were diluted to $2x10^6$ CFU/mL in MHB. Forty five microliters of the diluted bacterial suspension were added to 45 μL of 50% citrated blood (1:1 whole blood:PBS). Ten microliters of peptide conjugate (125 μg/mL final concentration) was added to the mixture and incubated for 1 h at 37 °C. Ten microliters of the incubation mixture was serial diluted in MHB and plated on Mueller Hilton agar, followed by incubation at 37 °C for 18-24 h for cfu determination. Percent lysis was also analyzed for the mixture by Drabkin's method as described above.

2.3.7.4 Complement Activation Analysis: CH50 Assay

A hemolytic assay was performed to analyze the level of complement activation by the polymers, peptides and the conjugates. Two incubation steps were utilized. First, ten microliters of stock polymer conjugate/peptide solutions (final concentration of the conjugate in μg/mL is indicated in the figure captions) were incubated and reacted with 90 μL of GVB^{2+} (Gelatin veronal buffer) diluted human serum, at 37 °C. After 1 h incubation, the polymer conjugated-treated serum (60 μL) was diluted with 120 μL of GVB^{2+} buffer. The diluted serum was then incubated in equal volume with the antibody-sensitized sheep RBC (EA cells, Comptech, TX, US) for 1 h at 37 °C, in order to measure the amount of complement activity remaining. Heat-aggregated IgG (final concentration 5 mg/mL) and PBS were also incubated with GVB^{2+}-diluted human serum for 1 h at 37 °C, as the positive and negative controls, respectively. All reactions were stopped by the addition of 0.3 mL of GVB-EDTA. Control tubes containing equal volumes of EA cells and GVB^{2+} buffer were subject to either GVB-EDTA (blank control) or dH_2O (100%

lysis control). Intact EA cells were spun down at 8000 rpm for 3 min and the supernatants were sampled.

Percentage EA lysis was calculated using average absorbance values as follows:

$$\%EA\ lysis = (OD_{540,\ test\ sample} - OD_{540,\ blank})/(OD_{540,\ 100\%\ lysis} - OD_{540,\ blank}) \times 100.$$

Percentage of complement activated (consumed) by the polymer/conjugate samples was expressed as: 100 %- % EA lysis[224].

2.3.7.5 Blood Coagulation by Activated Partial Thromboplastin Time (aPTT) and Partial Thromboplastin Time (PT) Analysis

aPTT and PT assays were performed as previously described[224]. Sodium citrate anticoagulated PPP was used for aPTT and PT analysis. The influence of peptide and peptide conjugate on the coagulation cascade was examined by mixing PPP with the polymer conjugate/peptide solution (9:1 V/V; varying final concentration depends on stock concentration used) at 37 °C. Control experiments were performed with phosphate-buffered saline solution with PPP. For the aPTT and PT analyses, the coagulation reagents actin FSL and Innovin thromboplastin (Siemens Healthcare, Marburg, Germany) were used, respectively. Each experiment was repeated in triplicates on the STart®4 coagulometer (Diagnostica Stago, France). The average values of the clotting time were obtained from at least three different donors.

For aPTT analysis, 180 μL of PPP was added to 20 μL of stock polymer/peptide solution (final concentration indicated in figure captions) at room temperature. Actin FSL (200 μL) was added and 100 μL of the polymer conjugate/peptide-PPP-reagent mixture was then added into a cuvette-strip and warmed to 37 °C for 180 s. Fifty microliters of pre-warmed 0.025 M $CaCl_2$ was then added to the cuvette and the time for clot formation was measured and recorded.

For PT analysis, 180 μL of PPP and 20 μL of stock polymer solution were mixed at room temperature. Fifty microliters of the mixture was then added into a cuvette-strip and warmed up at 37 °C for 60 s. One hundred microliters of Innovin thromboplastin (pre-warmed at 37°C) was then added to the cuvette and the time for clot formation was measured and recorded.

2.3.8 Cell Toxicity analysis

Human umbilical vascular endothelial cells (HUVEC), and fibroblasts (3T3) were used to examine the effect of bioconjugates on cell viability. All cell lines were cultured in their respective growth media at 37 °C under a humidified 95%:5% (V/V) mixture of air and CO_2. HUVEC cell line is cultured in endothelial cell growth medium (EGM-2 BulletKit, Lonza), and fibroblast is cultured in Dulbecco's modified eagle medium (DMEM, Lonza) with 10% fetal bovine serum (FBS, Lonza).

Before the addition of peptide/bioconjugate samples to the cells, each cell line was plated into separate tissue culture-treated 96 well assay plates (approximately 3000 cells/well) overnight to allow for cell attachment to the well surface. The polymers were dissolved in respective growth media for the targeting cell lines and were incubated with the cells for 48 h. Starting with an initial peptide/bioconjugates concentration of 250 μg/mL, serial dilutions of the polymer solutions with media was performed to examine the effect of concentration on cells. Fifty percent DMSO was used as a positive control for toxicity measurements.

After a 48 h incubation period, cell viability was measured by adding 20 μL of the 3-[[4,5-dimethylthiazol-2-yl]-5-[3-carboxymethoxyphenyl]-2-[4-sulfophenyl]-2H-tetrazolium] (MTS) reagent (CellTiter 96® AQueous One Solution Cell Proliferation Assay, Promega) to each of the wells. The colorimetric absorbance was measured at two wavelengths, 490 nm and 600 nm. Cells only treated with basic growth media were used as the baseline and was expressed

as 100% viable. The viability of HUVEC and fibroblast after exposure to the bioconjugates or 50% DMSO was expressed as the percentage of the viable cells compared to medium-treated cells.

2.3.9 Biomembrane Interaction by CD Spectroscopy

Circular dichroism (CD) experiments were conducted using a JASCO J-810 spectropolarimeter at 25 ºC, as previously described[113,137,138,215]. For the samples prepared with lipids, the procedure outlined in[113,137,138,215] was used. Briefly, samples with a constant peptide concentration of 75 μM were prepared in different peptide to lipid (P/L) molar ratios of 1:35 and 1:70, using the 1:1 lipid mixtures of POPC/POPG. Appropriate amounts of lipids in chloroform were dried using a stream of nitrogen gas to remove most of the chloroform and vacuum dried overnight in a 5.0 ml glass vial. After adding 450.0 μL of ddH_2O and 50 μL of peptide stock solution in ddH_2O to the dried lipids, the mixture was sonicated in a water bath for a minimum of 30 min (until the solution was no longer turbid) to ensure lipid vesicle formation. Two hundred microliters of sample was placed in a 1 mm path length for the CD measurements. The spectra were obtained over a wavelength range of 190 nm - 280 nm. Continuous scanning mode with a response time of 1 second with 0.5 nm steps, bandwidth of 1.5 nm and a scan speed of 200 nm/min were used. Spectra were corrected by subtracting the background (example PBS spectrum) from the sample spectrum. To improve the signal-to-noise ratio, an average of 10 scans was obtained. The helical content was calculated using three fitting programs (CDSSTR[225], CONTINLL[226], and SELCON3[227]) and an average was reported.

2.4 Results and Discussion

2.4.1 Synthesis of Conjugates

For the synthesis of the conjugates, a C-terminus truncated peptide with an additional cysteine at the C terminus (aurein 2.2Δ3-cys (GLFDIVKKVVGALC-$CONH_2$)) was used. The C-terminus was chosen for the cysteine addition and truncation because it was previously shown that the N-terminus is critical for activity of aurein peptides, whereas the C-terminus is not[215]. The cysteine residue is incorporated in order to facilitate the conjugation chemistry (Figure 2.2). The insertion of the cysteine residue and the truncation of the C-terminus did not affect the antimicrobial activity against the tested strains (Table 2.1) as the minimum inhibitory concentrations (MIC) are similar to previously reported values[113,138,215].

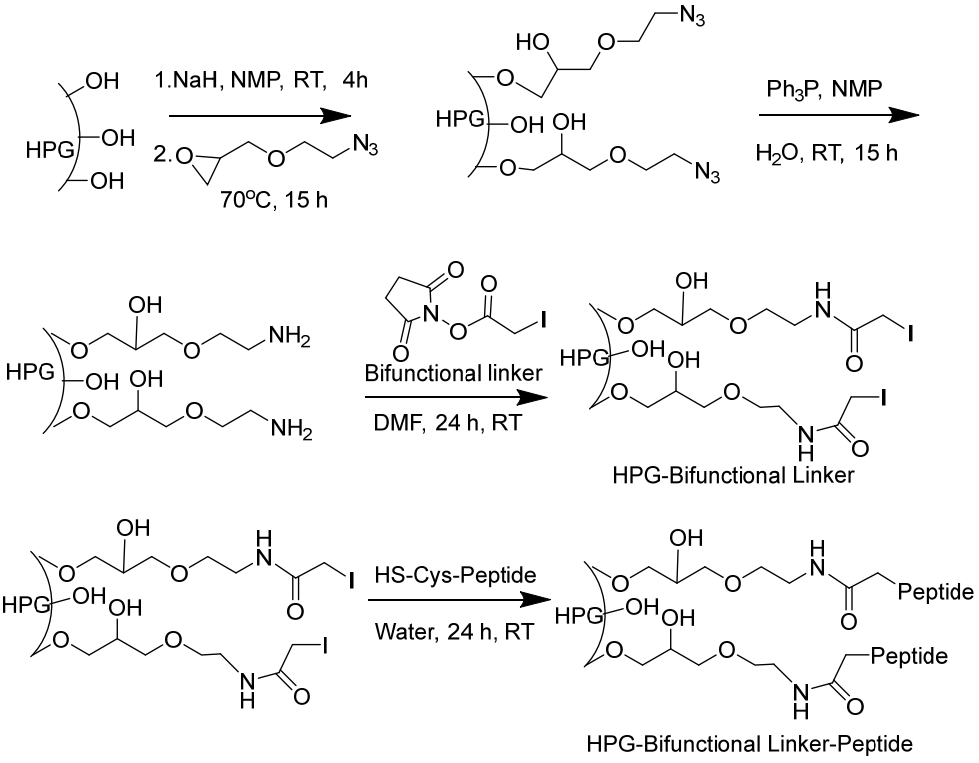

Figure 2.2: Synthetic route for the conjugation of the aurein peptide with hyperbranched polyglycerol (HPG). Only some of hydroxyl groups of HPG are represented explicitly for clarity. Figure created using ChemDraw.

Table 2.1: Sequence and molecular weight of the peptides and the bioconjugates made in this study.

	Sequence	Molecular weight	PDI (M_w/M_n)	MIC[c] *S.aureus* (μg/mL)	MIC[c] *S. epidermidis* (μg/mL)	MIC (*S.aureus*)/5% Hemolysis[d]
Aurein 2.2Δ3	GLFDIVKKVVGAL	1358[a]	-	16	32	-
Aurein 2.2Δ3-cys	GLFDIVKKVVGAL**C**	1461[a]	-	16	16	0.50
HPG-Bifunctional linker	-	44000[b]	1.1	>1000	>1000	-
HPG-Aurein2.2Δ3-cys(2.5%)	-	56000[b] (7- 8 peptides)	1.3	125	150	<0.50
HPG-Aurein2.2Δ3-cys (5%)	-	69000[b] (17-18 peptides)	1.4	110	120	0.88

[a]Molecular weight determined by MALDI-time of flight mass spectrometry.
[b]Molecular weight determined by GPC analysis.
[c]MICs reported are the most frequent values observed (n = 3 or more).
[d]MIC (*S. aureus*)/ Concentration at which 5% hemolysis is observed (from Figure 2.4).
A smaller number indicates higher activity with respect to hemolysis.
All peptides used in this chapter had an amidated C-terminus.

HPG (44 kDa) was synthesized using anionic polymerization (Figure 2.1). Some of the hydroxyl groups were further modified to an azide functionality and finally reduced to an amine containing polymer (Figure 2.2), which showed characteristic proton NMR signals (Appendix A.2). The amine modified HPG was then reacted with a bifunctional linker (iodoacetic acid *N*-hydroxysuccinimide ester) yielding the HPG-bifunctional linker species. HPG-bifunctional linker showed characteristic amide peaks (Appendix A.3) and absorbed light in the UV region (Appendix A.4) due to the addition of the iodoacetamide group.

The HPG-bifunctional linker was finally conjugated to aurein 2.2Δ3-cys to yield the peptide conjugate. To ensure that all the unreacted peptides are removed, the bioconjugate was

purified using size exclusion HPLC (Appendix A.5) and characterized by proton NMR (Appendix A.6).

After conjugation, the molecular weight of the parent was increased from 44kDa to 56kDa as determined by GPC analysis (Appendix A.7) upon peptide conjugation, which indicated approximately 7-8 peptides molecules per HPG molecule (Table 2.1). The PDI of HPG-Aurein 2.2Δ3-cys (2.5%) conjugate did not change considerably (PDI= 1.3) in comparison to HPG-bifunctional linker (PDI= 1.1) indicating that there is a uniform distribution of peptides on the polymer molecules (Table 2.1). For HPG-Aurein 2.2Δ3-cys (5%) conjugate, the molecular weight increased from 44kDa to 69kDa indicating 17-18 peptides per HPG molecule. The PDI of this conjugate was 1.4.

2.4.2 Antimicrobial Activity of the Bioconjugates

It is crucial to determine the peptide concentration of the HPG-conjugate to compare the bioconjugate and free peptide activity. The peptide concentration was determined using the BCA protein assay kit. Table 2.1 summarizes the MIC values for the free aurein 2.2Δ3-cys peptide and the HPG-Aurein 2.2Δ3-cys bioconjugates against clinical Gram positive bacteria (*S. aureus* (C621) and *S. epidermidis* (C622)). The HPGylated peptide (both 2.5% and 5%) showed approximately 7 fold weaker antimicrobial activity compared to the free peptide against *S. aureus.* In the case of *S. epidermidis*, it was in the range 3 to 7-fold weaker for conjugates. This was expected as polymer conjugation to AMPs is known to decrease the antimicrobial activity[166–168]. Interestingly, the decrease in activity is similar to magainin (5-10 fold), another alpha helical antimicrobial[167]. The decrease in activity could be due to various reasons such as interaction of the peptides with the polymer chain or modification of peptide folding, solubility and hydrophobicity. The decrease in antimicrobial activity of the HPGylated peptides is less

prominent when compared to PEGylated tachyplesin 1 (32-64 fold decrease in activity relative to free AMP) and nisin (inactive)[166,168]. However, important differences should be noted as in these examples the molecular weight of PEG was 5 kDa and a mono-PEGylated species was used, in contrast to HPG (44 kDa with 7-8 peptides or 17-18 peptides). Interestingly, the 2.5% and 5% conjugates showed similar antimicrobial activity, suggesting that a threshold number of peptide per HPG molecule is needed for antimicrobial activity. We anticipate that the optimization of the polymer molecular weight and structure of the polymer would further modulate the antimicrobial activity of the conjugates.

2.4.3 Peptide Secondary Structure on Bioconjugates

To further understand and correlate the antimicrobial activity of the HPG-conjugates, we investigated the secondary structure of the aurein peptide conjugated to HPG using CD spectroscopy (Figure 2.3). Cationic AMPs are unfolded in an aqueous environment but adopt secondary structure upon interaction with a lipid membrane. Electrostatic and hydrophobic interactions are important for this to occur. After initial electrostatic interaction with the negatively charged head groups of the outer leaflet of the membrane phospholipids, the peptides insert into the membrane. The thermodynamically favorable hydrophobic-hydrophobic interaction with the interfacial membrane lipids leads to the alpha helical conformation of many AMPs[212–214]. Aurein 2.2 adopts an alpha-helical structure when in contact with lipids[113,138,215]. CD data (Figure 2.3; Appendix A.8) confirmed that aurein 2.2Δ3-cys also adopts alpha helical structure in the presence of TFE and POPC/POPG (1:1) lipid vesicles. Peptide to lipid (P/L) ratios of 1:35 and 1:70 (mol/mol) were tested. The percentage of alpha helical content (Table 2.2) is similar to the parent peptide aurein 2.2, within the error inherent in CD[113,138,215].

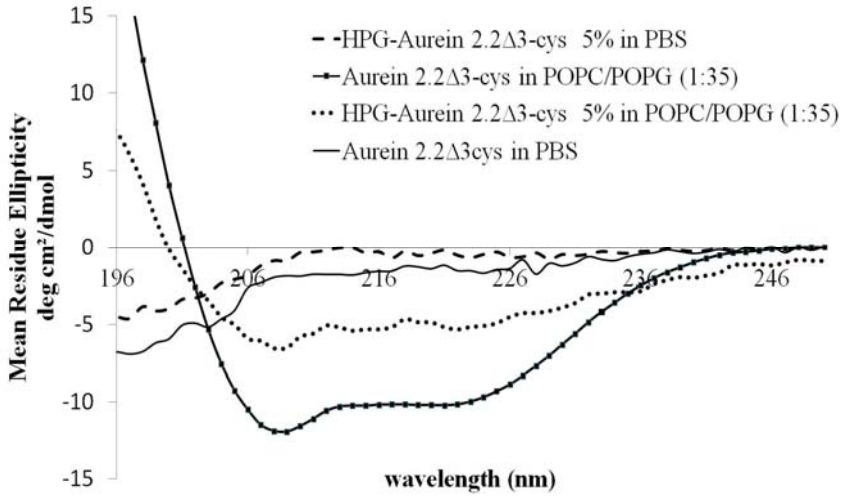

Figure 2.3: CD spectra of the HPG-Aurein 2.2Δ3-cys 5% in PBS buffer and lipids (1:1 POPC/POPG and the peptide under the same conditions. In the presence of lipids, the peptides and peptide conjugates adopt an alpha helical structure. Figure generated using Graphpad prism.

Aurein 2.2Δ3-cys conjugated to HPG was still able to form alpha helices (Figure 2.3; Appendix A.9) but to a much lesser extent (Table 2.2). For the 2.5% conjugate, the helicity in the presence of TFE, POPC/POPG (P/L=1:35), and POPC/POPG (P/L=1:70) was found to be 35%, 31% and 19%, respectively. The 5% conjugate (Appendix A.8 and A.9) was slightly more structured in TFE and POPC/POPG lipids (Table 2.2). Overall for both the conjugates, the percent helical content is at least 3 fold lower when compared to peptide only (Table 2.2). This indicates that HPGylation of aurein 2.2Δ3-cys peptide alters or destabilizes the secondary structure of the peptide, which is consistent with the literature data on PEGylation of the magainin 2 analogue[167]. A decrease in alpha helical content may correlate with the decrease in antimicrobial activity, as demonstrated for peptides conjugated to polymer brushes[228].

Table 2.2: Secondary structure of Aurein 2.2Δ3-cys and HPG-Aurein 2.2Δ3-cys in various environments determined by CD spectroscopy (representative spectra shown in Figure 2.3).

	Environment	α helical content (%)[a]
Aurein 2.2Δ3-cys	PBS	15±5
	Trifluoroethanol	98±5
	POPC/POPG (1:35)[b]	96±5
	POPC/POPG (1:70)[b]	84±8
HPG-Aurein2.2Δ3-cys (2.5%)	PBS	10±5
	Trifluoroethanol	35±8
	POPC/POPG (1:35)[b]	31±13
	POPC/POPG (1:70)[b]	19±13
HPG-Aurein2.2Δ3-cys (5%)	PBS	12±5
	Trifluoroethanol	42±8
	POPC/POPG (1:35)[b]	36±13
	POPC/POPG (1:70)[b]	28±13

[a]average from three software programs: CDSSTR[225], CONTINLL[226], and SELCON3[227].
[b]P/L ratios

2.4.4 Blood Compatibility of the Peptide and Peptide Conjugates

Since HPG-aurein conjugates are designed as agents to be administered intravenously, and will interact with blood immediately upon administration, the determination of their interaction with blood components will provide important information on the biocompatibility of the conjugates. There are limited studies available in the literature on the interaction of different blood components with cationic AMPs or its conjugates with polymers. It is also important to understand whether the decoration of cationic AMPs on HPG would alter their blood interaction. Thus we tested the interaction of HPG conjugates with various blood components by measuring the red cell lysis, platelet aggregation and activation, complement activation and blood coagulation.

Previous studies have demonstrated that the toxicity of AMPs can be correlated with their ability to lyse red blood cells. Recently, Zhao et al. used a computational approach to develop

peptides with improved antimicrobial activity while minimizing red blood cell lysis[229]. To study the interaction of conjugates with RBCs, washed RBCs were incubated with the conjugates at 37 °C and the percent lysis was measured. Aurein 2.2Δ3-cys causes RBC lysis at concentrations as low as 62.5 μg/mL, whereas HPG-Aurein 2.2Δ3-cys (2.5%) was not cytotoxic at this concentration (Figure 2.4a). Even at twice the new MIC value (250 μg/mL) of this conjugate, HPG-Aurein 2.2Δ3-cys (2.5%) shows no change in RBC lysis (Figure 2.4a) compared to control buffer, demonstrating the improvement in biocompatibility. However, as more peptide groups are attached, as in HPG-Aurein 2.2Δ3-cys (5%), an increase in lysis is seen (Figure 2.4a) indicating more peptide-like characteristics. These results suggest an optimal number of peptides are needed to enhance biocompatibility and retain antimicrobial activity. The charge and hydrophobic masking effect of HPG may contribute to the diminished toxicity of the conjugates towards RBCs. It is also possible that the peptides cannot permeate the RBC membrane due to the steric hindrance introduced by the large HPG moiety. A similar trend has been observed upon polymer conjugation of the synthetic AMP CaLL[230].

To mimic the situation in a systemic infection situation and to demonstrate whether HPGylated aurein peptides show selectivity towards bacterial cells in the presence of whole blood, hemolysis and antimicrobial activity were monitored in the same sample. In the combined (blood and bacteria) experiments, there was a further decrease in hemolysis as a general trend, with the conjugated peptides (both 2.5% and 5%) now showing hemolysis comparable PBS (Figure 2.4b). Even at this high concentration (125 μg/mL) the conjugates showed selectivity towards bacterial cells (Figure 2.4c) with no significant hemolysis (Figure 2.4b). Bacterial counts were not detectable in these experiments. These findings are similar to those seen for PEGylated

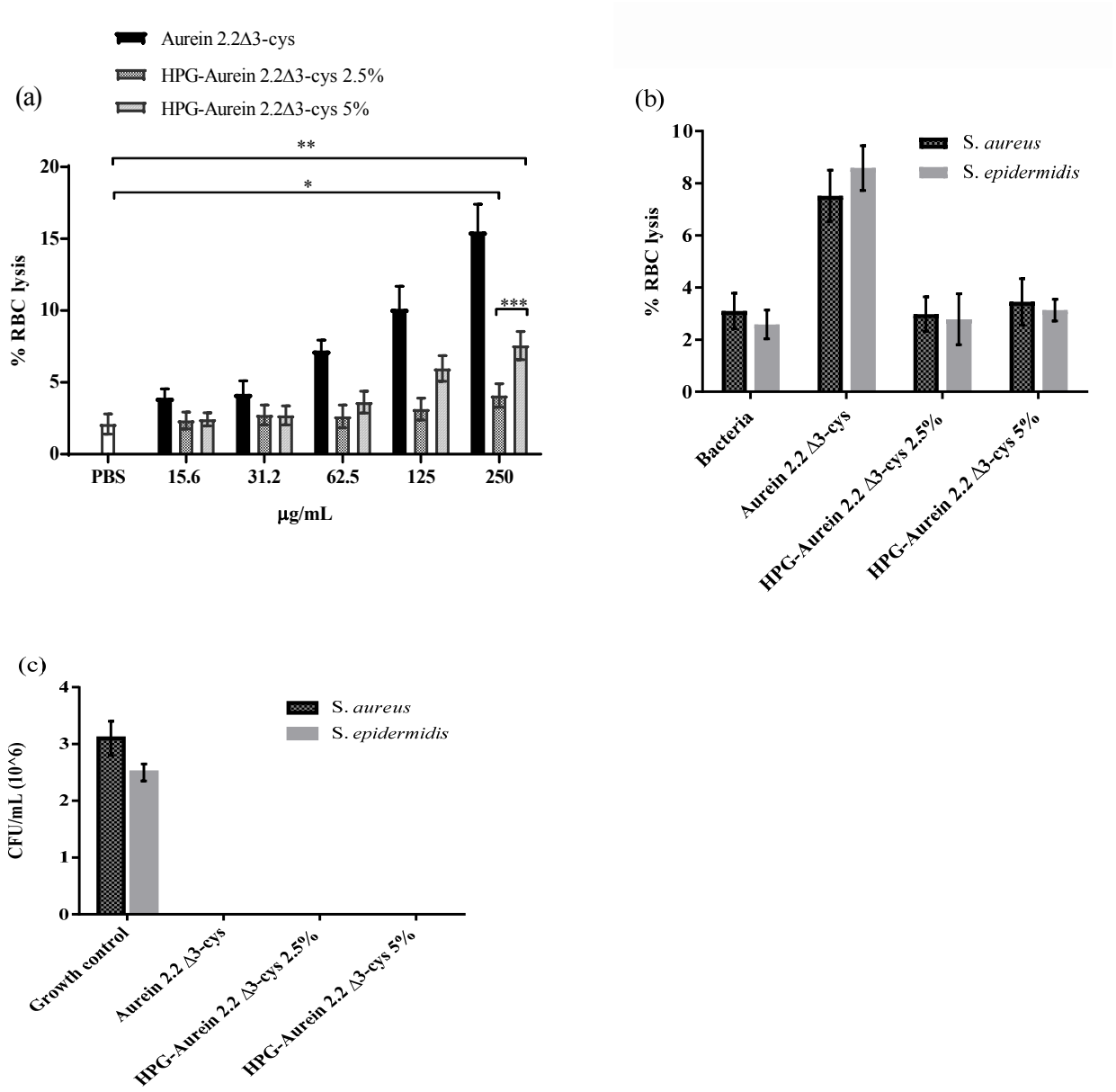

Figure 2.4: (a) Influence of free aurein peptide and HPG peptide conjugates concentration on red blood cell lysis. Hemolysis of free peptides and peptides conjugated to HPG at various concentrations after incubation for 1 h with washed red blood cells at 37 °C. Positive control was water and PBS buffer was used as normal control. *P=0.0316; **P=0.0011; ***P=0.0073. (b) Combined RBC lysis in the presence of bacterial cells. Peptide/conjugates (125 µg/mL) were added to the 50% citrated RBC/bacterial mixture (1:1). (c) Bacterial Colony forming unit per milliliters (CFU/mL) of the same samples were also observed. No bacterial counts were detected for the HPGylated and free peptides. Figure generated using Graphpad prism.

KYE28 (peptide derived from Heparin cofactor II), which also showed an improved hemolysis profile in the presence of whole blood[169].

The complement system is part of the innate immune system and is involved in the first line of defense. It is comprised of as many as 30 different proteins circulating in the blood. Upon activation by foreign molecules, these proteins are cleaved and release anaphylatoxins which in turn can cause inflammation. To investigate whether the HPGylated peptide activated the complement system, the amount of complement activation was measured by a complement consumption analysis using a modified antibody-sensitized sheep erythrocyte complement lysis (CH50) assay[231]. The bioconjugates were incubated with human serum followed by the addition of antibody-sensitized sheep erythrocytes. Lysis of the antibody-sensitized sheep erythrocyte which was measured by hemoglobin release indicated the percent complement consumption. HPGylated and free peptides do not activate complement at the tested concentrations (Figure 2.5) indicating that these conjugates are not interacting with the complement system. Unmodified HPG also showed no complement activation[181].

Platelets are involved in blood clotting. Activation of platelets can lead to thrombotic complications i.e. formation of blood clots inside blood vessels. It has been shown that cationic polymers and peptides activate platelets[185]. Thus we investigated whether HPG-aurein conjugate can induce platelet activation and aggregation in human PRP (platelet rich plasma). Platelet activation was measured from the expression of a glycoprotein P-selectin CD62 on the surface of platelets. Monoclonal anti-CD62P-FITC (fluorescently labelled) antibody based flow cytometry analysis was used for this purpose.

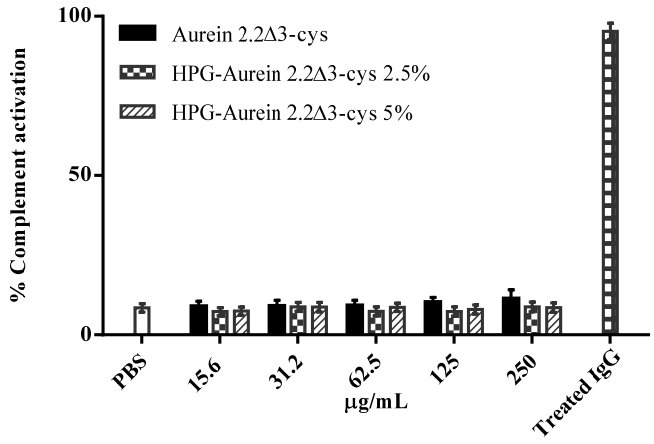

Figure 2.5: Influence of free aurein peptide and HPG peptide conjugates concentration on complement activation. Complement activation in human serum was measured by a complement consumption assay (CH50) using antibody-sensitized sheep red blood cells. The percentage of complement proteins consumed is reported. Heat-aggregated Immunoglobulin G (IgG) (final concentration 5 mg/mL) was used a positive control and PBS buffer as a normal control. Figure generated using Graphpad prism. Results are courtesy of Benjamin Lai.

The influence of the concentration of HPG conjugates and the peptide on platelet activation (% expression of CD62P) is given in Figure 2.6a. Results show that the extent of platelet activation by HPGylated and free peptides was very similar to buffer control (Figure 2.6a), indicating that the bioconjugates did not induce platelet activation at the tested concentrations. A similar observation was seen for the platelet aggregation analysis (Figure 2.6b). To test the extent of aggregation by the bioconjugates, adjusted PRP was incubated with peptides or conjugates and the absorbance was measured for 20 minutes. As the aggregation increases more light can pass through and the measured absorbance decreases (Appendix A.10).

Quantification of the percent platelet aggregation in the last 5 minutes (plateau phase) is shown in Figure 2.6b. Results show that the free peptides and the conjugates did not cause platelet aggregation, as the values were comparable to the buffer control.

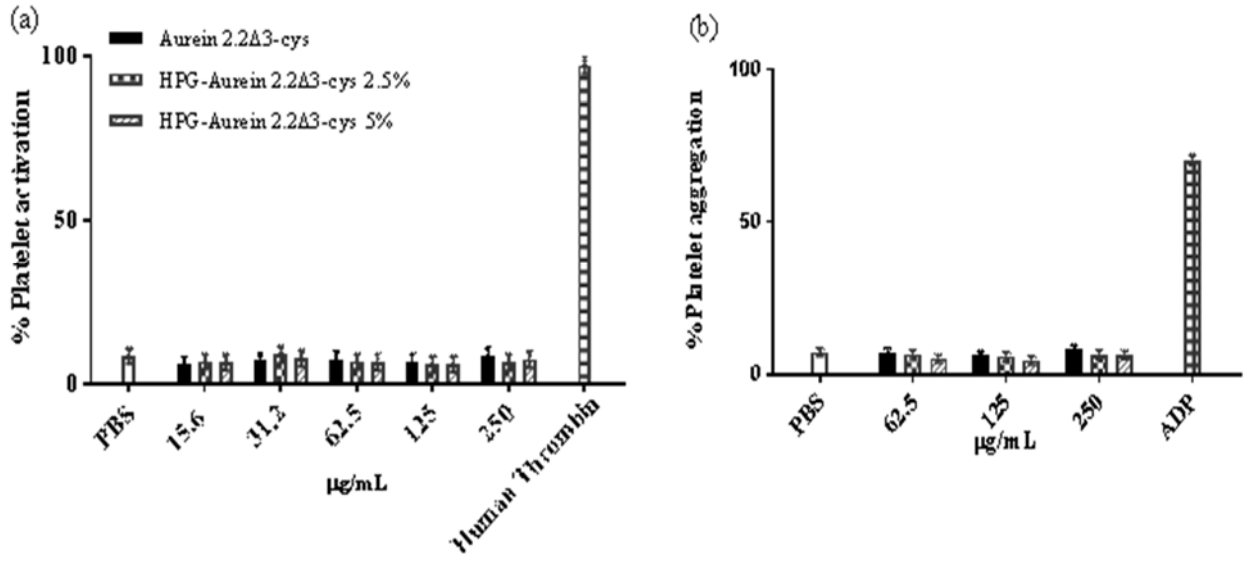

Figure 2.6: (a) Influence of free aurein peptide and HPG peptide conjugates concentration on platelet activation. Platelet activation was measured in human platelet rich plasma by counting platelets (flow cytometry) that expressed the activation marker CD62P using the monoclonal anti-CD62-PE antibody. Human thrombin and PBS buffer were used as positive and negative controls, respectively. (b) Influence of free aurein peptide and HPG peptide conjugates concentration on platelet aggregation. The peptides and bioconjugates were incubated with adjusted platelet rich plasma (PRP) for 20 minutes. Absorbance at the plateau phase was used to calculate percent aggregation (see Appendix A.10). ADP (5 µM) was used as a positive control and PBS buffer as normal control. Figure generated GraphPad prism.

Blood coagulation in the presence of free peptide and conjugates were studied by measuring the blood clotting time using a clinical coagulation assay[224]. This test provides important information on the pro- or anti-coagulant activities of the AMP conjugates. Cationic

peptides and polymers were shown to influence the blood coagulation by, in most cases, delaying the onset of coagulation[185,220]. The conjugates/peptides were incubated with human PPP (platelet poor plasma) and the clotting time was measured by aPTT (activated partial thromboplastin time), which measures the intrinsic pathway of blood coagulation. Clotting time is the time it takes for a fibrin clot to form once thromboplastin reagent and calcium chloride is added. The peptide and the conjugates did not significantly affect the aPTT values when compared to PBS control (Figure 2.7a) at all the concentrations tested. The extrinsic pathway of blood coagulation in the presence of peptide conjugates and free peptides was probed by measuring the prothrombin time (PT). Aurein 2.2Δ3-cys prolonged PT at concentrations as low as 125 μg/mL, whereas HPG-Aurein 2.2Δ3-cys (both 2.5% and 5%) did not significantly change the PT at this concentration (Figure 2.7b). At 250 μg/mL (twice the new MIC), HPG-Aurein 2.2Δ3-cys (2.5%) did not alter clotting time as significantly as the free peptides. However, upon increase in the peptide density, the coagulation time increased at the highest concentration tested (Figure 2.7b) in comparison to the control buffer, suggesting the importance of peptide density on the conjugates. This also suggests a way to further improve the properties of the conjugates. The mechanism by which the free peptide and the conjugate influence the extrinsic pathway of coagulation needs to be further investigated. A possible explanation for the observations made here could be that the hydrophobic and electrostatic interactions between the peptides and clotting factors result in delayed coagulation. However, in the conjugate, the hydrophobic masking effect of HPG may contribute to the diminished interaction with clotting factors, leading to the observed unchanged clotting time. More experiments are needed, however, to confirm this hypothesis.

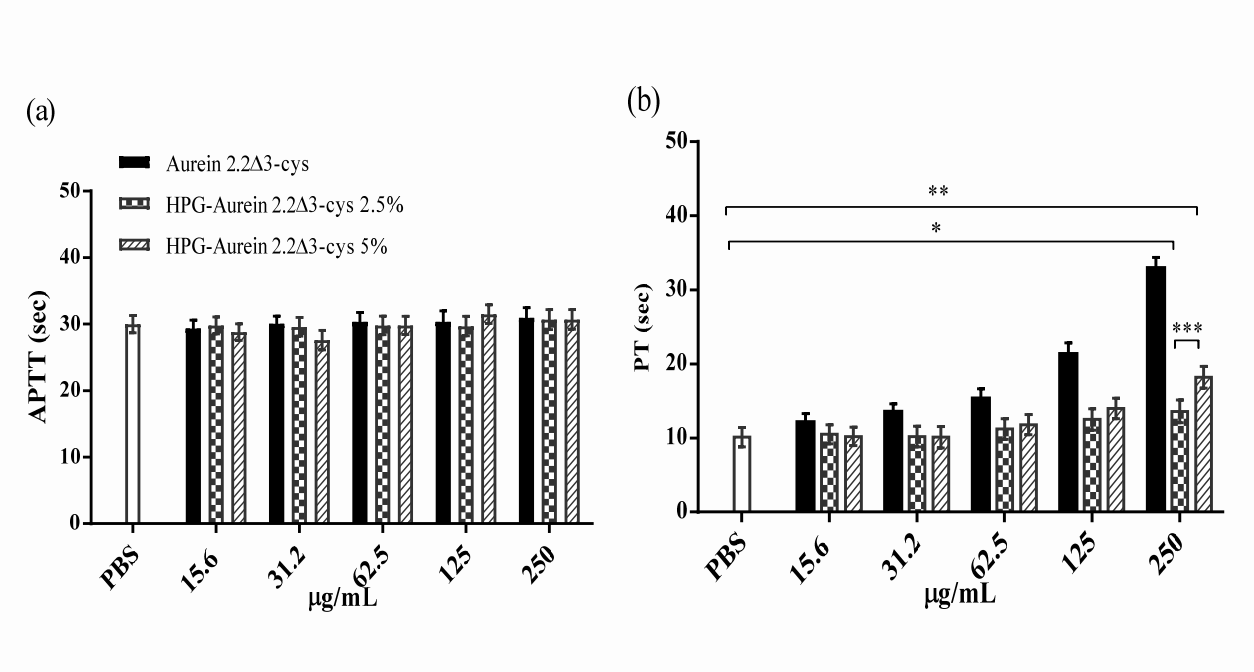

Figure 2.7: (a) Influence of free aurein peptide and HPG peptide conjugates concentration on intrinsic pathway of blood coagulation. Intrinsic pathway blood coagulation was monitored by measuring the activated partial thromboplastin time (aPTT) in human plasma at 37 ºC. PBS buffer was used as a negative control. (b) Influence of free aurein peptide and HPG peptide conjugates concentration on extrinsic pathway of blood coagulation. Prothrombin Time (PT) was measured by incubating peptide and conjugates with human plasma at 37 ºC. *P=0.0395; **P=0.0018; ***P=0.0198. Figure generated using Graphpad prism.

2.4.5 Cell Compatibility of the Peptide and Conjugates

The cell compatibility of the peptides and the conjugates was assessed by incubating HUVECs and fibroblasts with various peptide/conjugate concentrations for 48 h and measuring the viable cells by the MTS assay (Figure 2.8). Aurein 2.2Δ3-cys caused a decrease in cell viability at concentrations as low as 31.2 µg/mL (HUVEC) and 125 µg/mL (fibroblasts), whereas HPG-Aurein 2.2Δ3-cys (2.5% and 5%) were nontoxic at twice the new MIC concentration (250 µg/mL). An explanation for these observations is that the HPGylated peptides could not permeate the cell walls effectively because of the steric hindrance introduced by the

large HPG moiety, similar to that observed for PEGylated tachyplesin and magainin[166,168]. Another synthetic AMP CaLL also showed enhanced cell compatibility[230]

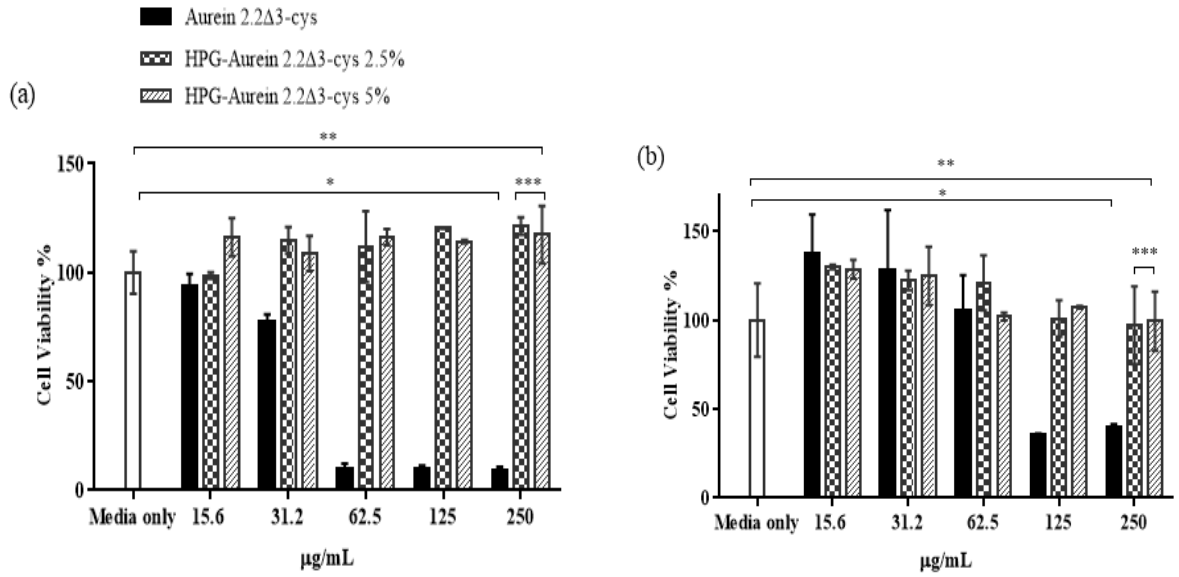

Figure 2.8: Cell biocompatibility of the peptides and the conjugates against (a) human umbilical vein endothelial cells *P<0.0001; **P=0.1372; ***P=0.6501 and (b) fibroblasts *P=0.0070; **P=0.9725; ***P=0.8895 measured by the MTS assay after 48 h of incubation. Figure generated using GraphPad prism. Results are courtesy of Benjamin Lai.

2.5 Summary

In this chapter, I describe the first design of a multifunctional HPG-peptide conjugate based on the alpha helical AMP aurein 2.2 and the examination of the effect of HPGylation on the antimicrobial activity, interaction with blood components and structure of the peptide. The conjugates were well characterized for composition and molecular weight. The HPGylation of aurein 2.2Δ3-cys decreased the antimicrobial activity (~3-7-fold) and the alpha helical content (~3 fold). The biomembrane interaction of the HPG conjugate depends on the amount of peptide substitution; the higher the peptide density the higher the interaction. On the other hand, the HPGylation of the aurein 2.2 decreased the interaction with blood components especially to red

blood cells and the blood coagulation system; the peptide density on the HPG is an important contributing factor. HPGylated and free aurein 2.2 did not aggregate or activate platelets nor did they activate the complement system. Finally, the HPGylated peptides were also non-toxic to HUVECs and fibroblasts. The results presented here also demonstrate the importance of optimizing the peptide density on the HPG scaffold to provide optimal antimicrobial activity without generating toxicity. Future work will examine the interdependence of the peptide and HPG scaffold properties by examining the mechanism of action of the conjugates, as was done for the parent peptide alone[113,138,215] (Chapter 5). Parameters to vary include the HPG molecular weight. PEG analogs will also be made for direct comparison. Finally, the results presented here demonstrate the potential of using HPG-peptide conjugates in the design of a variety of important biomolecules, such as e.g. conjugates with anti-inflammatory activities derived from peptides with immunomodulating properties[230].

Chapter 3: Antimicrobial peptide-polymer conjugates with high activity: Influence of polymer molecular weight and peptide sequence on antimicrobial activity, proteolysis and biocompatibility[c]

3.1 Synopsis

In this chapter we report the synthesis, characterization, activity and biocompatibility of a novel series of antimicrobial peptide-polymer conjugates. Using the parent peptide aurein 2.2, we designed a peptide array (~100 peptides) with single and multiple W and R mutations and identified antimicrobial peptides (AMPs) with potent activity against *S. aureus*. These novel AMPs were conjugated to hyperbranched polyglycerol (HPG) of different molecular weights and number of peptides to improve their antimicrobial activity and toxicity. The cell and blood compatibility studies of these conjugates demonstrated better properties than the AMP alone. However, conjugates showed lower antimicrobial activity in comparison to peptides, as determined from minimal inhibition concentrations (MICs) against *Staphylococcus aureus* but considerably better than the available polymer-AMP conjugates in the literature. In addition to measuring MICs and characterizing the biocompatibility, CD spectroscopy was used to investigate the interaction of the novel conjugates with model bacterial biomembranes. Moreover, the novel conjugates were exposed to trypsin to evaluate their stability. It was found that the conjugates resist proteolysis in comparison to unprotected peptides. The peptide-conjugates were active in serum and whole blood. Overall, the results show that combining a

[c]A version of Chapter 3 has been published**. Kumar, P**.; Takayesu, A.; Abbasi, U.; Kalathottukaren, M. T.; Abbina, S.; Kizhakkedathu, J. N.; Straus, S. K. Antimicrobial Peptide–Polymer Conjugates with High Activity: Influence of Polymer Molecular Weight and Peptide Sequence on Antimicrobial Activity, Proteolysis, and Biocompatibility. ***ACS Appl. Mater. Interfaces*** 2017, acsami.7b09471, doi:10.1021/acsami.7b09471.

highly active AMP and low molecular weight HPG yields bioconjugates with excellent biocompatibility, MICs below 100 μg/ml, and proteolytic stability which could potentially improve its utility for *in vivo* applications.

3.2 Background

In Chapter 2, antimicrobial peptide aurein 2.2 was covalently attached to a 44 kDa HPG scaffold. It was found that peptide density on the conjugate is important for determining biocompatibility and efficacy. Although the antimicrobial activity of aurein 2.2 is improved compared to PEG conjugates, there was a 7-8-fold decrease (16 μg/ml to 110-120 μg/ml) in MIC. Thus further improvements in the activity are desired.

In this chapter, we therefore investigate strategies to improve the activity of the AMP-HPG bioconjugates, while preserving biocompatibility. We initially used a peptide array, where tryptophan (W) and arginine (R) mutations were introduced, to create more active mutants of aurein 2.2. These more active AMPs were then conjugated to HPGs of different molecular weights (22 kDa to 105 kDa). The antimicrobial activities of the newly identified and most active peptide and its HPG conjugates were measured against *S. aureus* and compared to the unconjugated peptides. In addition to the biocompatibility measurements, we investigated the resistance against tryptic degradation of the HPG conjugates as compared to the free peptides. Solution CD spectroscopy was used to examine the peptide secondary structure when bioconjugates interacted with model biomembranes in order to understand their mode of action. Overall, these studies aimed to devise improved bioconjugates and to further our understanding of the parameters that are important for obtaining optimal properties.

3.3 Methods

All chemicals were sourced from Sigma Aldrich Canada Ltd. (Oakville, ON) and used without further purification, except for glycidol, which was purified by vacuum distillation. 1-palmitoyl-2-oleoyl-sn-glycero-3-phosphocholine (POPC) and 1-palmitoyl-2-oleoyl-sn-glycero-3-phosphoglycerol (POPG) were purchased from Avanti Polar Lipids (Alabaster, AL). Pierce BCA protein assay kit was bought from Thermo Fisher Scientific Inc. (Rockford, IL). Dialysis membrane was obtained from Spectra/Por Biotech (Rancho Dominguez, CA).

3.3.1 Peptide array

Considering the importance of charge, hydrophobicity and amphipathicity a peptide array with tryptophan (W) and arginine (R) mutations was designed using the aurein 2.2Δ3 peptide as the framework. Tryptophan and arginine were chosen because they have special characteristics that allow them to interact with each other and the bacterial membrane[232]. The helical wheel projection was used as a guide to ensure that the amphipathic nature of the peptides was preserved. We started with a single mutation by replacing the lysine (K) residues with R or hydrophobic residues with W, followed by multiple R and W mutations. Quantitative structure-activity relationship (QSAR) have been used previously to design AMPs with better antimicrobial activities. This method requires a large dataset from a systematic peptide array with thousands of peptides [233] so a more targeted approach was used here.

Arrays of peptides were SPOT-synthesized on cellulose membranes by Kinexus Inc. (Vancouver, BC, Canada), as described previously[234,202]. Each cellulose spot was assumed to have a peptide density of 150 nmol based on Pierce BCA protein assay kit and a purity of ~70%. Peptides were dissolved in 200 μL of autoclaved water and the solution was incubated at room

temperature for ~4 h with gentle shaking to solubilize the peptide from the cellulose membrane. The stock peptide solutions were serially diluted and used for the antimicrobial screens described below. From the array, some of the most active peptides (Table 3.1) were synthesized using solid phase peptide synthesis and purified (95% purity), as described in Chapter 2.3.1. The antimicrobial activity of the peptides synthesized in house was verified and found to be consistent with those found for the peptides in the array (Table 3.1).

Table 3.1: Antimicrobial activity (MICs) of selected peptides identified in the peptide array.[@]

Peptide	MIC *S. aureus* (μg/mL)
1. GLFDIVKKVVGAL (parent peptide)	32
24. GLWDIWKKWWGWL	16
34. GLFDIVRRVVRAL	16
77. RLWDIVRRVWGWL	4
91. GLWDIWRRWWRWL	8

[@] The parent peptide, aurein 2.2, was used as a template. The other peptides in the library were obtained by incorporating arginine (R) and tryptophan (W) residues at various locations. All peptides used in this chapter had an amidated C-terminus.

3.3.2 Peptide synthesis and purification

Solid phase peptide synthesis (Fmoc) was used to synthesize aurein 2.2Δ3-cys and its RW mutants (Table 3.1), as previously described[113-215] with details given in Chapter 2.3.1.

3.3.3 Synthesis of HPG

Synthesis and characterization of hyperbranched polyglycerol (HPG) with different molecular weights was carried out as previously reported[235,220] and in Chapter 2. Briefly, For 22

kDa HPG, 1,1,1-tris(hydroxymethyl) propane (0.240 g) was partially (10%) deprotonated with CH_3OK (25 wt% in methanol, 0.22mL). Methanol removed under vacuum for 5 h. The flask was heated to 95 ºC and glycidol (9mL) was added dropwise for 12 h and stirred for another 4 h. For 44 kDa HPG, glycidol (20mL) was added dropwise for 15 h. For 105 kDa HPG, glycidol (50mL) was also added dropwise for 15 h. The workup protocol, absolute molecular weight and polydispersity of the HPGs were determined using gel permeation chromatography (GPC) coupled with multi angle light scattering (MALS) as described in Chapter 2.3.2

3.3.4 Amine Modification of HPG

HPG was vacuum dried for overnight at 70 °C prior to the reaction. A flame dried round bottom flask was loaded with dried HPG (22 kDa, 200 mg) in anhydrous DMF (20 mL) under Ar. To this solution, NaH (3 eq, w.r.t. targeted -OH groups; 15 mg) was added slowly and stirred at RT for 2 h. To the obtained white cloudy solution, *N*-glycidylphthalimide (1.5 eq; 54 mg) was added and stirred for another 20 h at 70 °C. The reaction mixture was quenched with dilute HCl (pH ~7) and the resulting reaction mixture was concentrated approximately 3 times the initial concentration. The polymer was purified by precipitation from acetone, followed by dialysis against water (MWCO – 10000 Da, 24 h). The polymer was lyophilized and the number of phthalimide groups on HPG was determined by ^{1}H NMR (Appendix B.1). The HPG-phthalimide was deprotected to HPG amine by refluxing it with hydrazine (20 eq, 35 wt. % in H_2O; 383 mg) in methanol (20 mL) for 24 h. The reduction of HPG-phthalimide was confirmed by ^{1}H NMR (Appendix B.2) and the resulting HPG amine was purified by dialysis and lyophilized. The number of amine groups was equivalent to phthalimide groups on HPG. For 44 kDa (200 mg), 3 eq of NaH (13 mg), 1.5 eq of *N*-glycidylphthalimide (55 mg) of and 20 eq, 35 wt.% in H_2O

hydrazine (335 mg). For 105 kDa (200 mg), 3 eq of NaH (9 mg), 1.5 eq of *N* glycidylphthalimide (34 mg) of and 20 eq, 35 wt. % in H_2O hydrazine (210 mg).

3.3.5 Conjugation of peptide with HPG-amine

The HPG-amine (0.014 g, 22000 g/mol) was reacted with 3-(maleimido)propionic acid N-hydroxysuccinimide ester (0.009 g) in dimethylformamide (DMF) at room temperature (22 ºC) for 24 h. The reaction mixture was dialyzed in DMF (MWCO 1000) for 24 h to remove the unreacted 3-(maleimido)propionic acid N-hydroxysuccinimide ester. ^{1}H NMR was used to characterize the product (Appendix B.3). The maleimide modified HPG (0.010g, 22000 g/mol) was reacted with sulfhydryl containing aurein2.2Δ3-cys (GLFDIVKKVVGALC-$CONH_2$) (0.007g, 1460.49 g/mol) or its RW mutant (peptide 77c, 0.009 g, 1857.34 g/mol) in DMF for 24 hours. The resulting conjugate was purified by size exclusion chromatography (Waters 600 system Mississauga, Ontario, Canada) using a CATSEC column (CATSEC 300, Eprogen)[181] and a UV detector (229 nm) with a mobile phase composed of 0.5M NaCl in 20% ethanol/water mixture. The product was further characterized by GPC and ^{1}H NMR (Appendix B.4). The maleimide to thiol-maleimide conversion for 22k 77c and 22k aurein 2.2Δ3-cys was 70% and 80%, respectively. The unreacted maleimide was quenched with ethanethiol. For 44k 77c, 44k HPG amine (10 mg), 2 eq of 3-(maleimido)propionic acid N-hydroxysuccinimide ester (5 mg) was added, followed by 1.2 eq of peptide 77c (9 mg). The maleimide to thiol-maleimide conversion was 57%. For 44k aurein 2.2Δ3-cys, 1.2 eq of aurein 2.2Δ3-cys peptide (8 mg) was added. In this case, the maleimide to thiol-maleimide conversion was between 79%.

For 105k 77c, 105k HPG amine (10 mg), 2 eq of 3-(maleimido)propionic acid N-hydroxysuccinimide ester (2 mg) was added, followed by 1.2 eq of peptide 77c (10 mg). The

maleimide to thiol-maleimide conversion was 51%. For 105k aurein 2.2Δ3-cys, 1.2 eq of aurein 2.2Δ3-cys peptide (8 mg) was added. Here, the maleimide to thiol-maleimide conversion was 67%. The conjugates were characterized for their molecular weights by GPC-MALS, conjugation efficiency by ^{1}H NMR and bicinchoninic acid (BCA) protein assay as described in Chapter 2.3.4 and 2.3.5

3.3.6 Synthesis of PEG 77c conjugate

The mPEG-maleimide (5k) was purchased from advanced polymer materials Inc. (Montreal, Canada). The mPEG maleimide (0.01 g) was dissolved in 1 mL of acetonitrile and added to sulfhydryl containing peptide 77c (0.004 g, 1857.34 g/mol) dissolved in 1 mL of DMF and stirred for 24 h. The PEG conjugated peptide was purified the same way as the HPG conjugated peptide (described above) using a size exclusion CATSEC 100 column and characterized by ^{1}H NMR (Appendix B.5).

3.3.7 Antimicrobial activity measurements (minimum inhibitory concentration or MIC)

The MICs of the peptides/conjugates against *S. aureus* were measured based on previously described methodology[235;113,138,215] and Chapter 2.3.6.

3.3.8 MIC determination after tryptic degradation

To determine whether conjugation of the AMP with HPG prevents or alters degradation of the peptides by trypsin, we incubated the peptides/conjugates with trypsin. Trypsin (3 µg) was added to peptide 77c (200 µg/mL solution) and the 22K-77c conjugate (200 µg/mL solution) and incubated at 37 °C for 3 h. After 3 h, the MALDI spectra of the two solutions were acquired. The trypsin-digested samples without purification were used for determination of the MIC of the peptides/conjugates, as described in Chapter 2.3.6.

3.3.9 Biocompatibility analysis

The biocompatibility of conjugates and peptides were evaluated by measuring the cell viability against mouse embryonic fibroblasts (3T3-L1) by MTT (3-(4,5-dimethylthiazol-2-yl)-2,5-Diphenyltetrazolium) assay. The blood compatibility of the conjugates were determined by measuring their effect on blood coagulation, effects on platelets, complement activation and red blood cell lysis using human blood. The blood was obtained from unmedicated consenting donors; the protocol was approved by the clinical ethical committee of the University of British Columbia. Detailed protocols are described in sections 2.3.7 to 2.3.12.

3.3.10 Biomembrane interaction: CD spectroscopy

As previously described[113,138,215], a JASCO J-810 spectropolarimeter was used to conduct circular dichroism experiments at 25 ºC. A 1mm cuvette was filled with 200 µL of sample and the spectra were obtained over a wavelength range of 190 nm - 250 nm. A continuous scanning mode was employed with a response time of 1 second, bandwidth of 1.5 nm, 0.5 nm steps, and a scan speed of 200 nm/min. An average of 5 scans was obtained to improve the signal to noise ratio. The spectra were corrected by subtracting the background (e.g. phospholipid spectrum) from the sample spectrum. An average alpha helical content was reported by calculating the output %helix from three fitting programs (CDSSTR, CONTINLL, and SELCON3)[236] and averaging these three numbers.

3.4 Results and Discussion

3.4.1 Discovery of potent peptides using peptide array based on aurein peptide

Trytophan and arginine have unique properties that allow them to interact with each other and the bacterial membrane[232]. The cation-π interactions between the residues allow maximum

hydrogen bonding for the arginine side chain and allow the peptide to penetrate deeper into the bacterial membrane[232]. Using the parent peptide aurein 2.2, with three residues removed from the C-terminus, we designed a peptide array (~100 peptides) with single and multiple W and R mutations. Previous work had shown that truncation of aurein 2.2 by three residues at the C-terminus has minimal impact on its activity[138]. In order to determine how the mutations impact antimicrobial activity, the sequences were plotted as helical wheels[237] (Figure 3.1). Interestingly, changing single hydrophobic residues, e.g. F or V, for W does not improve activity (Figure 3.1b). However, adding a W near the interface of the hydrophobic/hydrophilic boundary results in a peptide that is 2x more active. Positioning the tryptophan at this interface may help the peptide anchor into the membrane better, as W is known to snorkel[238]. Mutation of the lysine residues for arginine (Figure 3.1c) at single positions (K7 or K8) has a surprising negative impact on activity. The mutation of G11R is most likely beneficial as this introduces a positive charge in close proximity to the negatively charged D4. Active AMPs typically have multiple positive charges[239]. From the peptide array, we identified peptide 77 (Figure 3.1d) that was 8 fold more active (MIC of 4 μg/mL) than the parent peptide (Table 3.1). A comparison of peptides with multiple mutations (Figures 3.1d, 3.1e, 3.1f) shows that clear trends are difficult to extract. Peptides 77 and 91 have the same number of R residues (and hence the same overall charge), yet peptide 91 is less active (Table 3.1). The addition of more W residues in peptide 91 does not appear to be beneficial, when comparing to peptide 77. Finally, although peptides 87 and 77 have the same number of mutations, their difference in activity is dramatically different. Overall, an examination of the sequence indicates that both the position and number of R and W residues play a critical role with respect to the activity of AMPs.

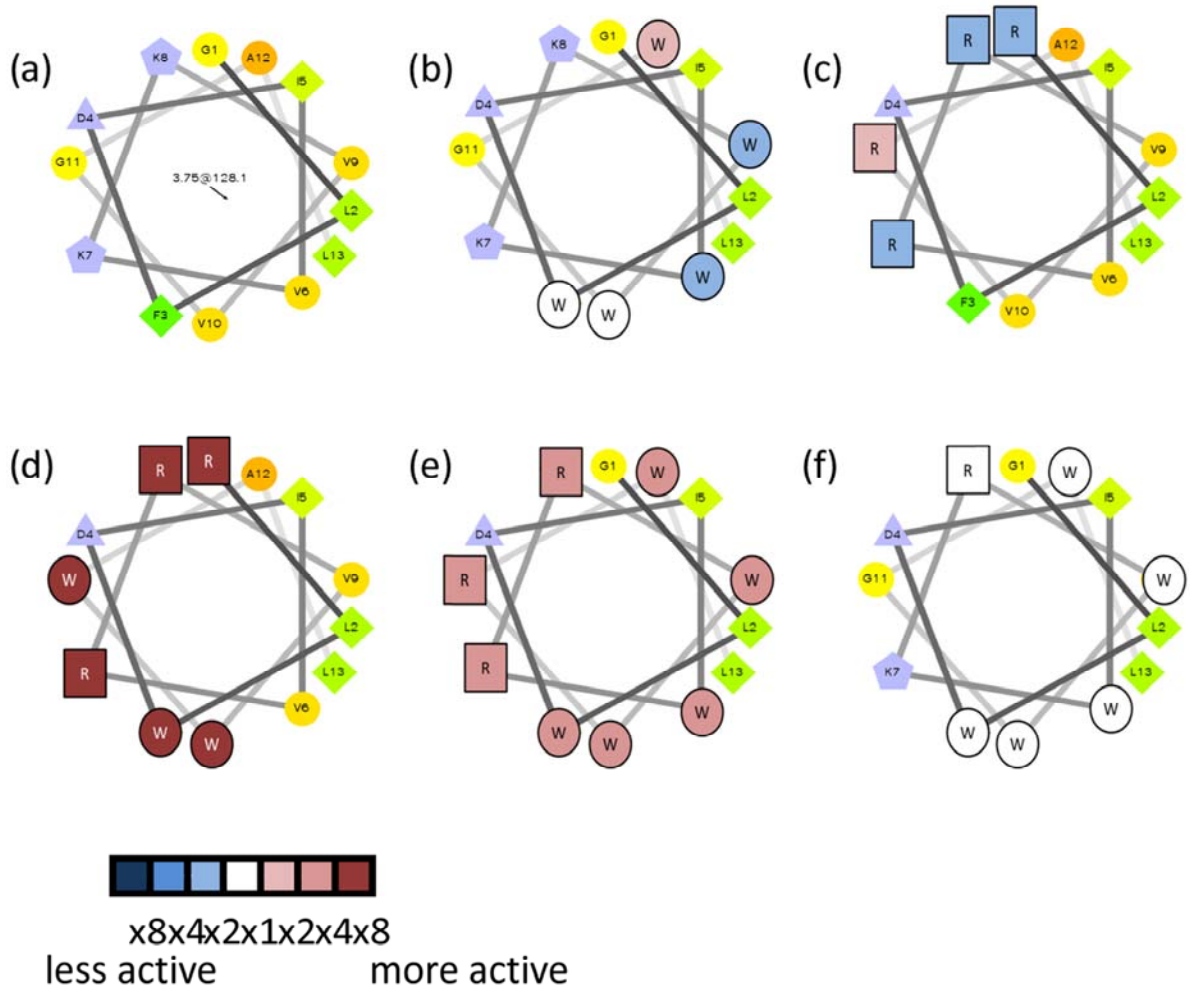

Figure 3.1: Helical wheels for some of the peptides generated in the array from a) the parent peptide aurein 2.2-Δ3. The helical wheel for aurein 2.2-Δ3 was generated using the script available at http://rzlab.ucr.edu/scripts/wheel/wheel.cgi. In b), single mutations of W are shown, along with the fold increase/decrease in MIC, as indicated in the legend. In c), single mutations in R are shown. In d)-f), some of the more active peptides are illustrated: d) peptide 77, which is 8x more active than the parent peptide; e) peptide 91, which is 4x more active; and f) peptide 87, which is just as active as aurein 2.2-Δ3. Figure created by Suzana K. Straus and used here with her permission.

3.4.2 Synthesis of aurein 2.2Δ3-cys and peptide 77c conjugates

To develop the HPG conjugates, peptides with an additional cysteine at the C terminus were synthesized to facilitate the conjugation (Figure 3.2). Since the N-terminus is critical for activity of aurein peptides[138,215], the C-terminus was chosen for the cysteine addition. The

addition of the cysteine residue had minimal to no impact on the antimicrobial activity of the peptides (Table 3.2).

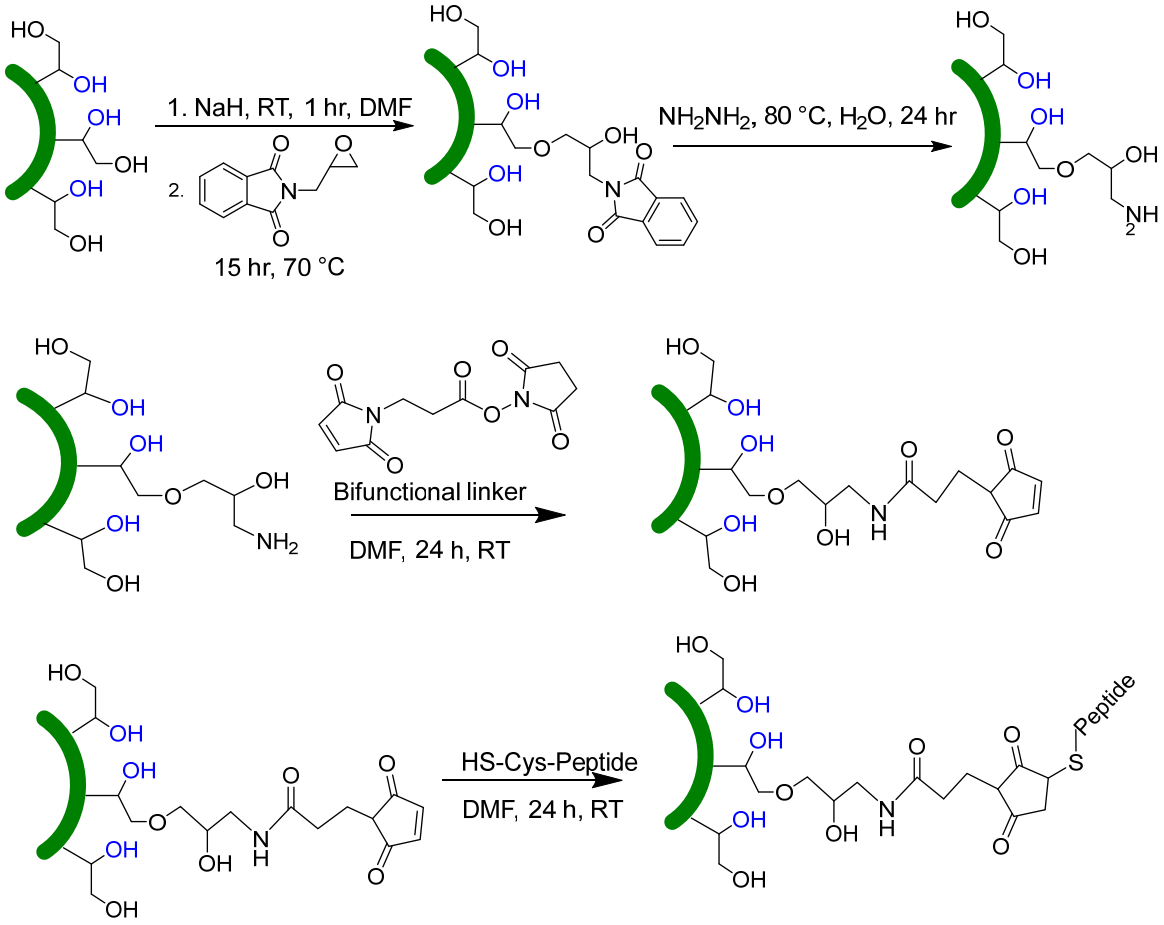

Figure 3.2: Synthetic scheme for the conjugation of the peptides with HPG. Only a small number of hydroxyl groups of HPG are shown to ensure clarity. A new amine modification protocol and bifunctional linker was used for accurate quantification of the amine and maleimide groups, respectively. This also ensured water free reactions as peptide 77c was not as readily soluble in water as aurein 2.2Δ3-cys. Figure generated using ChemDraw.

A general scheme for the HPG-AMP conjugate synthesis is shown in Figure 3.2. HPGs (22, 44 and 105 k) were synthesized by polymerization of glycidol via anionic ring opening and were modified to generate primary amine functionality[240]. This was further modified with a bifunctional linker (3-(maleimido) propionic acid N-hydroxysuccinimide ester) to generate maleimide groups on HPG. Aurein 2.2Δ3-cys and peptide 77c were each conjugated to this

scaffold via Michael type addition of the thiol group of the peptide and maleimide groups on HPG. The number of maleimide groups on the polymer was varied for the generation of conjugates with different number of peptides (Table 3.2). The bioconjugate was purified using size exclusion chromatography and characterized by proton NMR. The NMR data for the precursors and the final conjugates are shown in Appendix B.3 and B.4. The molecular weight of the HPG conjugates increased compared to the parent polymer (Table 3.2) with a molecular weight distribution (PDI) in the range of 1.2 to 1.5. The PDI of the conjugates did not increase considerably compared to the parent HPG suggesting a uniform distribution of the peptides on the polymer molecule. The number of peptides on the conjugates was determined by determining the peptide concentration obtained from a BCA protein kit and the conjugate molecular weight (Table 3.2). For a given molecular weight scaffold, the number of aurein 2.2Δ3-cys and peptide 77c remained similar, and thus comparisons were made for their activity and biocompatibility (see below).

3.4.3 Antimicrobial activity of the conjugates

Table 3.2 summarizes the minimal inhibitory concentration (MIC) values for the free peptides and their bioconjugates against clinical Gram positive strain *S. aureus* (C622). The MIC value of the conjugates is with respect to peptide concentration. The MIC value obtained for 44k aurein 2.2Δ3-cys of 150 μg/ml is close to the previously obtained value for the HPG- aurein2.2Δ3-cys (5%) of 110 μg/ml[235]. These two samples contain a similar number of peptides. In terms of fold decrease in activity relative to the free peptide (calculated using the 95% confidence interval values[241] in Table 3.2), this translates into values of 4-5 for the conjugate reported here versus 5-8 for the conjugate in Chapter 2. This suggests that the difference in conjugation chemistry used here results in a slightly better conjugate, but the more striking result of this work is that we were

able to synthesize a conjugate (22k 77c) with an MIC of 50 μg/mL, which is one of the most active polymer-AMP conjugates reported to date in literature[166,167,235].

Table 3.2: Characteristics of the peptides and the HPG conjugates used in this study[@].

Peptide/conjugates	Number of peptide groups per polymer		Molecular weight	PDI	MIC *S.aureus* [c] (95% CI[d]) μg/mL	Fold decrease in activity	Number of peptides/ k Da
	GPC	NMR					
aurein 2.2Δ3-cys	-	-	1 461[a]	-	32 (26-38)	1	
peptide 77c	-	-	1 858[a]	-	8 (5-11)	1	
22k aurein 2.2Δ3-cys	8 ± 2	8 ± 1	33 000[b]	1.2	85 (74-95)	3	0.24
22k 77c	8 ± 1	7 ± 1	36 000[b]	1.3	50 (39-61)	6	0.22
44k aurein 2.2Δ3-cys	16 ± 2	15 ± 2	68 000[b]	1.4	150 (133-167)	5	0.24
44k 77c	13 ± 1	11 ± 3	67 000[b]	1.3	100 (83-117)	13	0.19
105k aurein 2.2Δ3-cys	30 ± 3	26 ± 5	148 000[b]	1.4	475 (390-560)	15	0.20
105k 77c	25 ± 4	20 ± 5	151 000[b]	1.4	325 (268-382)	41	0.16
PEG 5k-77c	-	1		1.2	125 (102-148)	16	0.20

[@] The number average molecular weights (M_n) HPGs used in this study are 22k (PDI 1.1), 44k (PDI 1.2), and 105k (PDI 1.2). For comparison, a mono-substituted PEG-peptide 77c construct was also synthesized. The number of peptides attached is indicated in brackets in the first column, as determined by GPC analysis. The sequence for aurein 2.2Δ3-cys and peptide 77c was GLFDIVKKVVGALC and RLWDIVRRVWGWLC, respectively.

[a]Molecular weight determined by MALDI-TOF.

[b]Molecular weight determined by GPC-MALLS.

[c]MICs are the most frequent values observed out of three repeats.

[d] 95% confidence intervals

Looking at the entries in Table 3.2 in general, the HPGylated peptides showed weaker antimicrobial activity compared to the free peptides. This was expected as polymer conjugation to AMPs is known to decrease their antimicrobial activity[166–168,235]. A few important observations were made based on the MIC values of the conjugates. For both peptides, with an increase in the molecular weight of the polymer scaffold, the antimicrobial activity of the conjugates decreased (Table 3.2). The activity decrease was slightly more pronounced in the case of peptide 77c conjugates than aurein 2.2Δ3-cys. This suggests that the peptide sequence plays a crucial role in determining the activity of the conjugates. However, it is important to point out that since peptide 77c is more potent than aurein 2.2Δ3-cys its conjugates had overall lower MICs. In practical terms, both the molecular weight and peptide sequence are critical factors that impact the antimicrobial activity of the conjugates. In comparison to PEG 5K 77c, the 22k 77c and 44k 77c are more active (Table 3.2).

The increase in MIC of the conjugates with increasing molecular weights of conjugates could be related to differences in the interaction of the peptides with the polymer chain, to modifications of the secondary structure of the peptide, to its hydrophobicity and solubility, or to changes in the interaction of conjugates with bacterial membrane. Based on the MIC values and peptide density (last column in Table 3.2), we can state that PEG lowers the activity of the peptide more than HPG upon conjugation. This could be possibly due to the compact structure of HPG compared to PEG[181]. Our current data as well as literature support this observation. For instance, the decrease in antimicrobial activity of 22k 77c is less prominent when compared to PEGylated AMPs like tachyplesin 1 which showed a 32-64 fold decrease in activity or nisin which became inactive upon PEGylation[166,168]. It is important to note when comparing the activities of HPGylated and

the PEGylated peptide 77c (Table 3.2) that not only is there a difference in the molecular weight of the polymer, but there is also a difference in the number of peptides attached.

We also investigated the activity of peptide and conjugates in serum and whole blood (Appendix B.6 and Appendix B.7). At the concentrations studied, both the peptide 77c and 22K 77c were effective at clearing the bacteria.

3.4.4 Resistance to proteolysis: tryptic degradation

Many strategies have been employed to limit enzymatic degradation of antimicrobial peptides for their systemic use. These include chemical modification of the peptide (side chain groups, N and C-termini,) incorporation of D amino acids, and cyclization[239,242–244]. Traditionally polymer conjugation to peptides has increased the stability of peptides against proteolytic degradation [245,246]. In the current work, we determined whether the conjugation of peptide 77c to HPG prevents the peptides from protease degradation. We incubated peptide 77c and 22K 77c with trypsin for 3 h and characterized the peptide fragments generated by MALDI-TOF mass spectrometry. We have seen that the conjugated peptide (22K 77c) did not show characteristic cleavage of the naked peptide 77c (characteristic m/z 1114, 988) when incubated with trypsin (Figure 3.3), suggesting that the conjugated peptide 77c on HPG is resistant to tryptic degradation. The additional peaks present in the MALDI spectra were from the matrix, as can be seen from the MS spectrum in Appendix B.8.

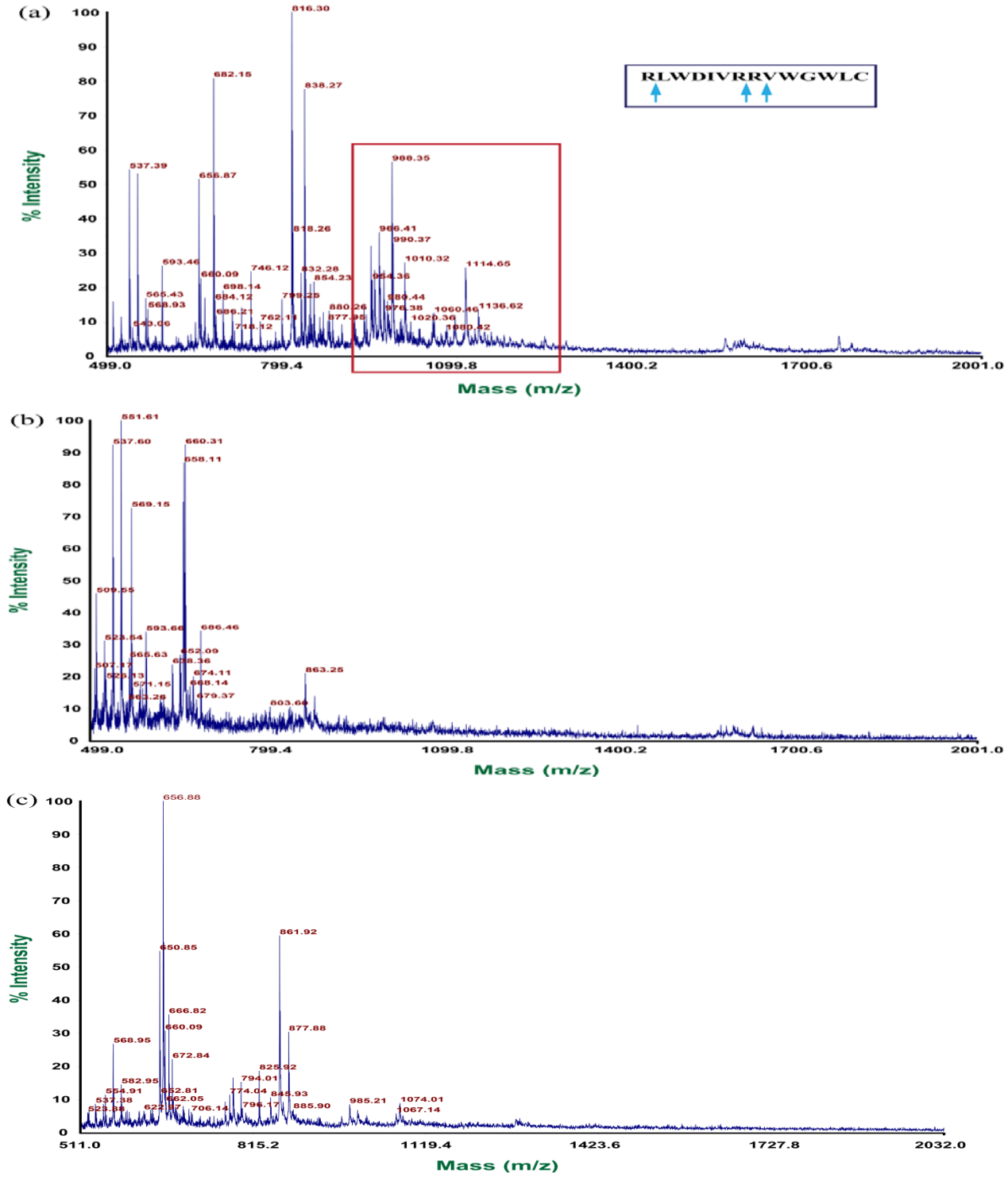

Figure 3.3: MALDI-TOF mass spectra of a) 77c, b) 22k 77c and c) trypsin after 3 hours of digestion. Trypsin was added to the peptides/conjugates and incubated at 37 °C for 3 hours, followed by MALDI characterization. Trypsin cleaves after positively charged residues such as arginine as shown in a). The peptide fragments detected for peptide 77c are highlighted in the red box in a). Figure generated using Data explorer and Adobe.

In order to validate that the degradation of the peptides leads to loss in antimicrobial activity, the MIC of the samples treated with trypsin were determined. Peptide 77c was inactive once treated with trypsin for 3 hours, whereas 22K 77c retained the same MIC (50 μg/mL) before and after trypsin treatment. This further indicates that the peptide is protected from protease degradation once conjugated to HPG and maintains activity. Trypsin alone did not possess any antimicrobial activity.

3.4.5 Peptide secondary structure on bioconjugates

To further investigate the mechanism of action of HPG-conjugates, we determined the secondary structure of the conjugates using CD spectroscopy. Typically, AMPs do not adopt secondary structure in an aqueous environment but fold upon interaction with a lipid membrane. Initially, positively charged residues interact with the negatively charged head groups found in the outer leaflet of the membrane bilayer, followed by thermodynamically favorable hydrophobic-hydrophobic interactions between the AMP and the interfacial membrane lipids, leading to the formation of a specific conformation[212–214]. In our study, both free peptides are random coil in phosphate buffer (Figure 3.4a). Interestingly, peptide 77 adopts an alpha helical conformation once conjugated to HPG in phosphate buffer without the presence of phospholipids or mimics such as trifluoroethanol (TFE). All molecular weight conjugates (22k 77c, 44k 77c and 105k 77c) of 77c adopt alpha helical structure in phosphate buffer, which indicates it is an intrinsic property of the peptide-polymer conjugate. In the presence of phospholipids, the percent helicity of the 77c conjugates increases indicating a more favorable conformation upon

interaction with a membrane mimetic (Table 3.3, Figure 3.4). However, the increase in helicity is much smaller for the conjugates than the free peptide in the presence of POPC/POPG (1:1) relative to PBS.

On the other hand, once HPGylated with various molecular weight HPG, aurein 2.2Δ3-cys remains as a random coil. It only adopts an alpha helical structure in the presence of phospholipids. Compared to the free peptide, the percent helicity for the HPGylated aurein 2.2Δ3-cys is much lower than the free aurein 2.2Δ3-cys, which is similar to previous studies[235]. HPGylation of aurein 2.2Δ3-cys peptide does not affect the structure of the peptide, whereas HPGylation of the peptide 77c enhances the secondary structure of the peptide in buffer. However, HPGylation of both peptides leads to a decrease in percent helicity in a membrane-like environment when compared to the respective free peptides (Table 3.3). Finally, the data in Table 3.3 clearly shows that the helicity for a given peptide conjugate decreases with increasing HPG molecular weight. In this case, the alpha helical content correlates well with the activity (Table 3.2).

3.4.6 Cell compatibility of the peptides and conjugates

The biocompatibility of the antimicrobial peptides and their conjugates is crucial for their use in various applications[247–249]. Therefore, the cell viability was assessed against human fibroblasts by the MTT assay. It is known from previous studies that aurein 2.2Δ3-cys is cytotoxic to fibroblasts[235]. It causes a decrease in cell viability at a concentration of 62.5μg/mL (Figure 3.5a). However, once conjugated to HPG (22k, 44K or 105k), its cell tolerance is increased irrespective of the molecular weight of the HPG used (Figure 3.5a).

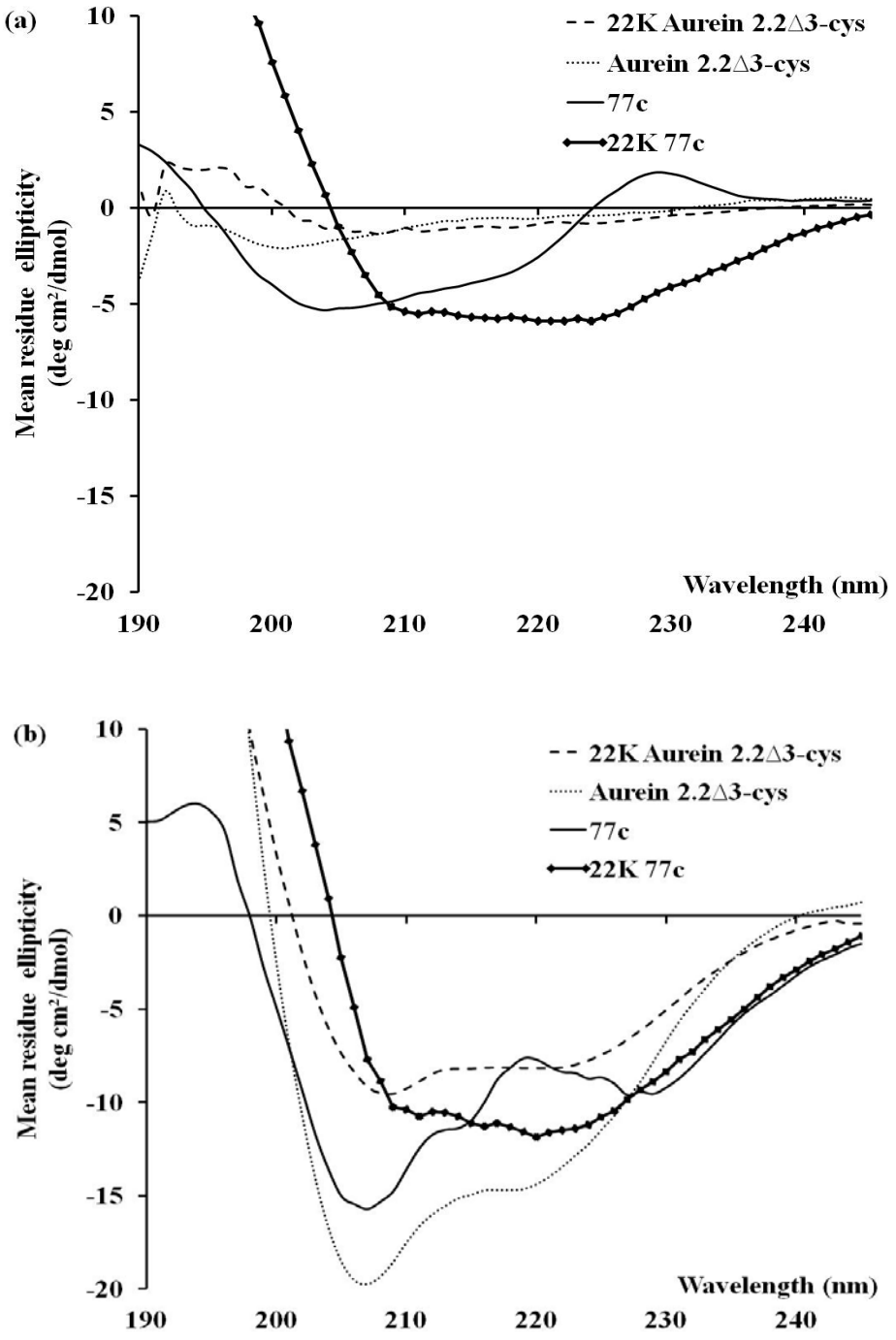

Figure 3.4: CD Spectra of the conjugates in a) phosphate buffer and b) POPC/POPG (1:35). The peptides and conjugates have a higher helical content in the presence of lipids. Interestingly, conjugation of peptide 77c to HPG results in more structured peptides. Figure generated using Graphpad prism.

Table 3.3: Alpha helical content (%) of the various conjugates studied here, as determined from fits from the CD spectra (Figure 3.4).

	PBS	POPC/POPG (1:1) Peptide/Lipid (1:35)
aurein 2.2Δ3-cys	7±5	97±5
22k aurein 2.2Δ3-cys	8±5	47±6
44k aurein 2.2Δ3-cys	4±2	40±5
105k aurein 2.2Δ3-cys	5±2	30±8
peptide 77c	8±5	73±6
22k 77c	40±5	65±6
44k 77c	31±6	52±7
105k 77c	23±4	41±8

Average values from three software programs: CDSSTR[225], CONTINLL[226], and SELCON3[227]

Peptide 77c was also toxic towards fibroblast at 2x the MIC concentrations (15.62 μg/mL). However, once HPGylated, peptide 77c (22k 77c) showed better tolerance even at concentrations of 5x the MIC (250 μg/mL). All the HPGylated peptides showed the same trend irrespective of the molecular weight of the scaffold. It is possible that the large HPG moiety prevents the HPGylated peptides from permeating through the extracellular matrix effectively, because of steric hindrance. This phenomenon has been previously observed for PEGylated magainin, tachyplesin, and a synthetic AMP CaLL[166,167,250]. Our biomembrane interaction data (Table 3.3 and Figure 3.4) support this statement; there was a significant decrease in the secondary structure formation upon conjugation of the peptides to HPG.

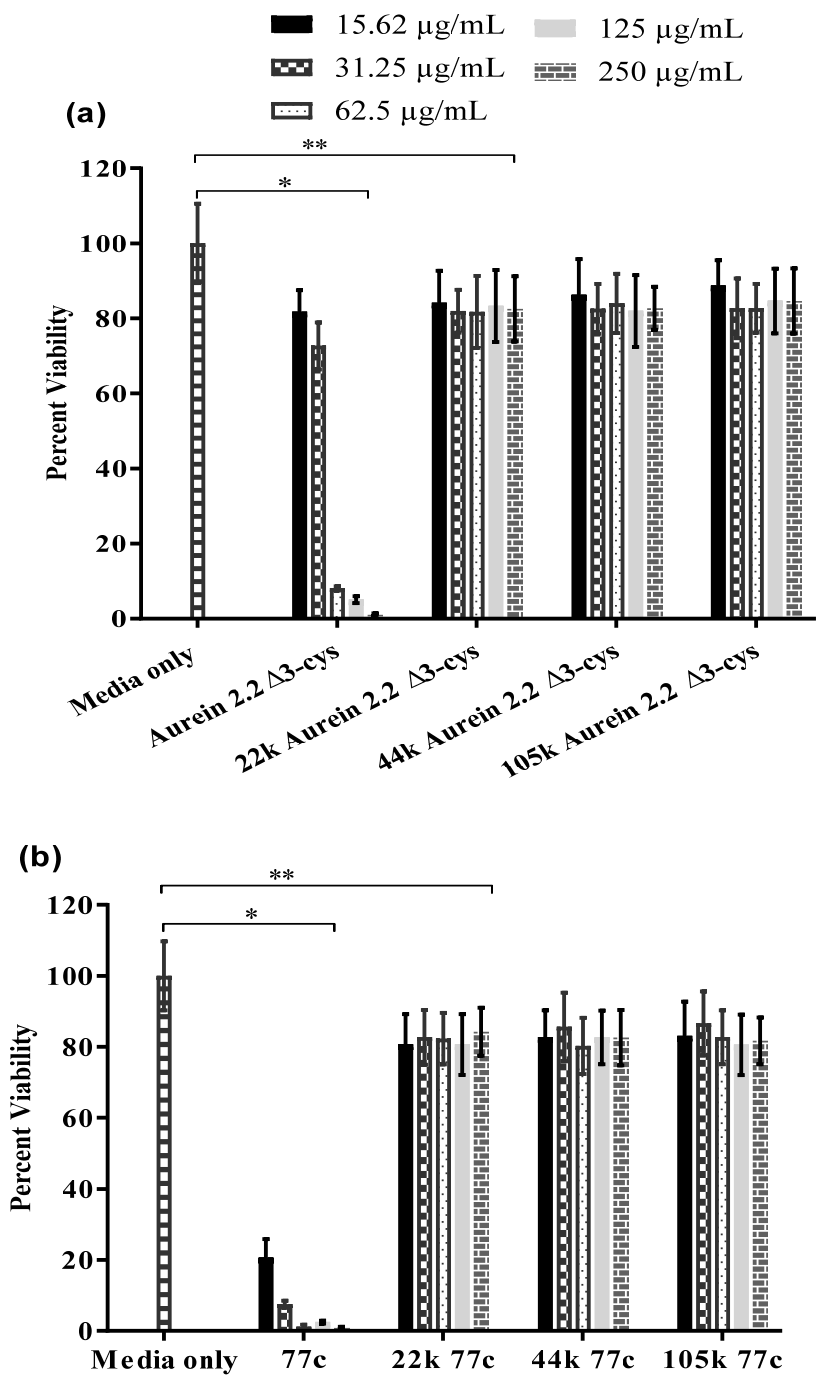

Figure 3.5: Fibroblast cell viability upon exposure to free peptides and HPG peptide conjugates. a) aurein 2.2Δ3-cys *P=0.0056; **P=0.2121. b) peptide 77c *P=0.0047; **P=0.2007. Viability of the cell after incubation with free peptides and peptides conjugated to HPG at various concentrations for 48 h at 37 °C. Figure generated using Graphpad prism. Results are courtesy of Usama Abbasi.

3.4.7 Blood compatibility of the peptide and peptide conjugates

Although the conjugates are compatible with cultured cells, it is important to determine the interaction with blood, as these conjugates will be potentially used in systemic administration. There are only a few reports in the literature on the interaction of cationic AMPs and/or conjugates[169,251] with various blood components. Moreover, researchers are actively seeking to develop peptides that minimize red blood cell lysis, as described in a recent study that used computational methods[229]. Given this importance, we sought to understand whether the attachment of two different (in terms of activity) cationic AMPs on HPG (with different molecular weight) would alter their blood interaction. Platelet activation, red cell lysis, complement activation and blood coagulation were used to test the interaction of HPG conjugates with different blood components. For all the experiments volume ratio of blood/plasma to peptide/conjugate was kept at 9:1 v/v.

Washed RBCs were incubated with the peptide/conjugates and the percent lysis was measured in order to investigate the interaction of conjugates with RBCs. Aurein 2.2Δ3-cys causes about 10% RBC lysis at 2x the MIC concentration (62.5 μg/mL), whereas 22k HPG-aurein 2.2Δ3-cys (MIC 85 μg/mL) was not cytotoxic at nearly 3x its new MIC concentration (250 μg/mL, Figure 3.6). Peptide 77c caused similar RBC lysis compared to aurein 2.2Δ3-cys at 2x the MIC.

At 16 μg/mL (2x the MIC), peptide 77c also caused about 10% RBC lysis, however once conjugated to 22k polymer (22K 77c, MIC 50 μg/mL), the conjugate cause 10% lysis at 5x the new MIC (250 μg/mL).

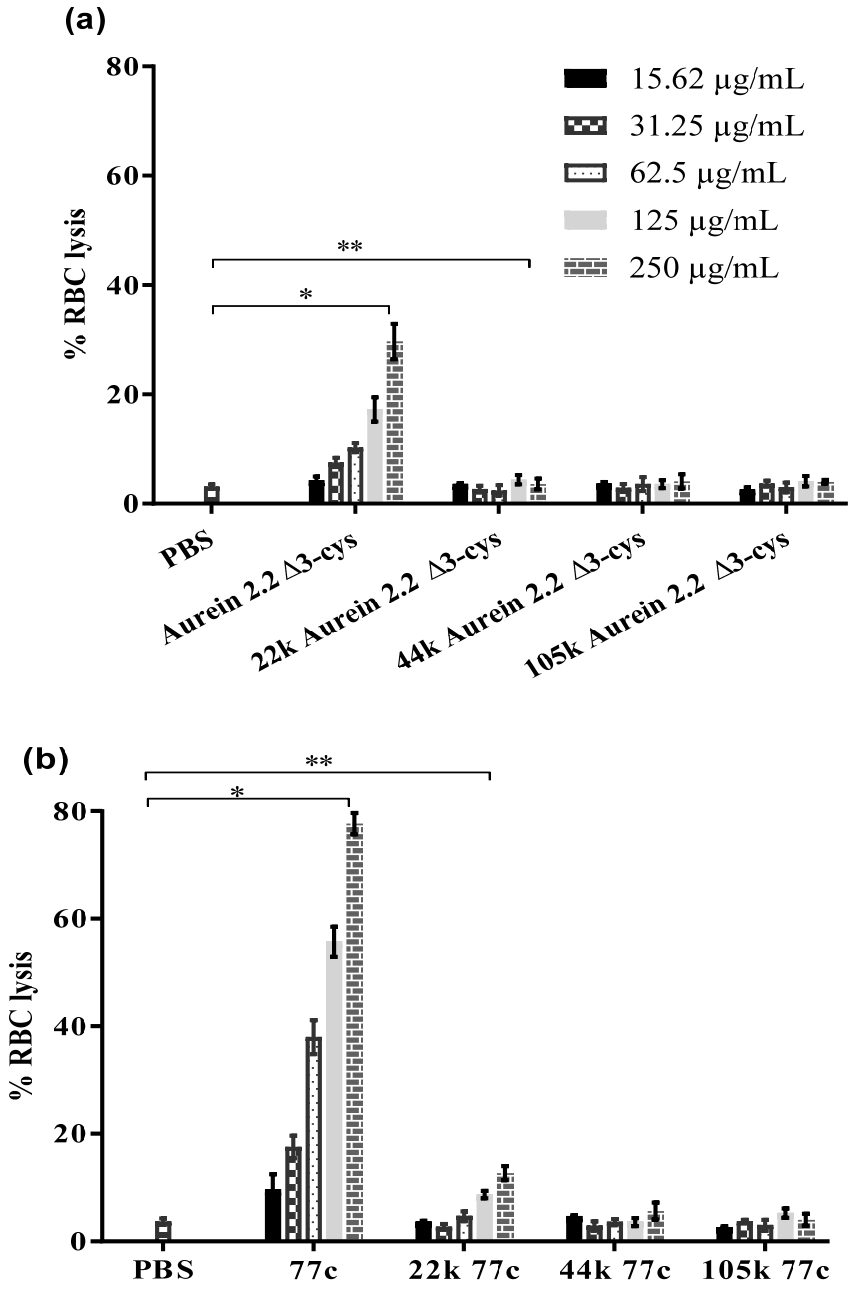

Figure 3.6: Red blood cell lysis upon exposure to free peptides and HPG peptide conjugates: a) aurein 2.2Δ3-cys *P=0.0075; **P=0.5469. b) peptide 77c *P=0.0004; **P=0.0122. Hemolysis of free peptides and HPG conjugates was measured at various concentrations, after 1h incubation at 37 °C with washed red blood cells. PBS buffer was used as normal control. Figure generated using Graphpad prism.

The data suggests that neither the activity of the peptide nor the polymer molecular weight influence the RBC lysis. The hydrophobic masking effect and charge of HPG work universally, contributing to the diminished toxicity of all the conjugates towards RBCs. A very similar observation was made upon polymer conjugation of other AMPs, such as KYE28[169] and CaLL[250].

Platelets are important players in the blood clotting cascade. Many thrombotic complications, such as the formation of blood clots inside blood vessels, can arise when platelets are activated. Cationic peptides/polymers have been shown to activate platelets[185]. Thus we examined whether the peptides/conjugates induce platelet activation in human PRP. Expressed glycoprotein P-selectin CD62 on the surface of platelets by fluorescently labeled monoclonal anti-CD62P-FITC antibody and flow cytometry was used to measure platelet activation. Aurein 2.2Δ3-cys and all of its various molecular weight conjugates do not activate platelets at the concentrations indicated (Figure 3.7a). Interestingly, peptide 77c on its own activates platelets at 250 μg/mL (30% activation), but none of the HPGylated 77c conjugates activate platelets (Figure 3.7a). Again, this suggests that HPG has the ability to mask the negative effects of the peptides, independent of HPG molecular weight.

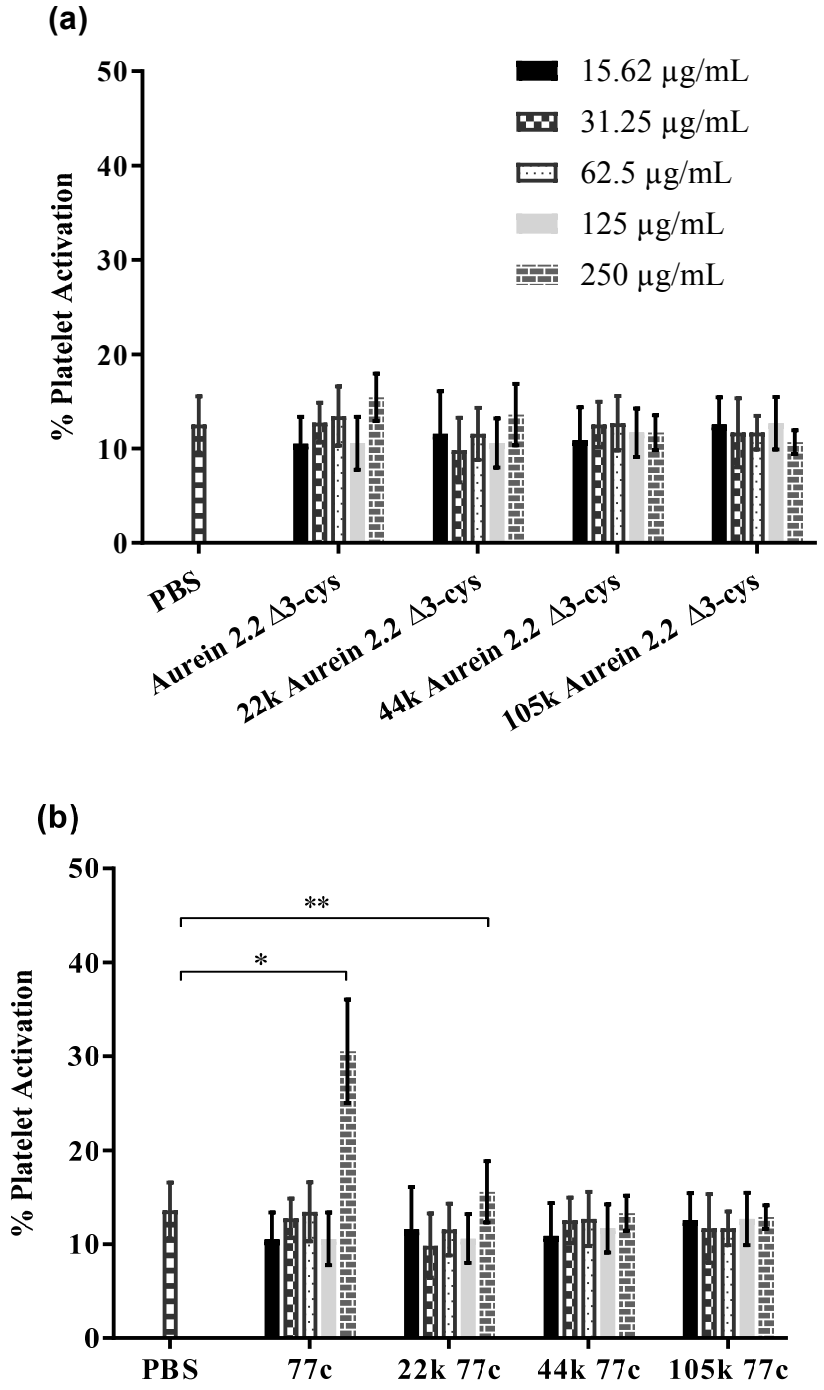

Figure 3.7: Platelet activation upon exposure to free peptides and HPG peptide conjugates: a) aurein 2.2Δ3-cys; b) peptide 77c. *P=0.0094; **P=0.5944. Human platelet rich plasma was used to measure platelet activation. Platelets that expressed the activation marker CD62P using the monoclonal anti-CD62-PE antibody were counted (flow cytometry). PBS buffer was used as a negative control. Figure generated using Graphpad prism.

The complement system is an important part of innate immunity. As many as 30 different proteins are part of this system. Complement activation upon interaction with the peptides and/or the conjugates is an indication of inflammatory potential such as histamine release and suggests blood incompatibility. Complement activation was determined by a complement consumption analysis using a antibody-sensitized sheep erythrocyte complement lysis (CH50) assay using human serum[231] to determine whether the free and HPGylated peptides had an effect on the complement system. Neither aurein 2.2Δ3-cys, peptide 77, nor the HPGylated peptides activate complement (Figure 3.8), indicating that they are all blood compatible.

Moreover, clinical coagulation assays were used to study the blood coagulation profile of the peptides and conjugates[224]. This test provides important information on the pro- or anti-coagulant activities of the peptides/conjugates. Blood coagulation was measured by clinical coagulation assays activated partial thromboplastin time (aPTT) and partial thromboplastin time (PT) in human plasma. In aPTT measurements, clotting time is taken as the time it takes for fibrin clot to form once thromboplastin reagent and calcium chloride is added. Aurein peptides were shown to influence the blood coagulation by delaying the onset of coagulation[235]. Both peptides and the conjugates did not significantly affect the aPTT values when compared to the HEPES-buffered saline (HBS) control (Appendix B.9).

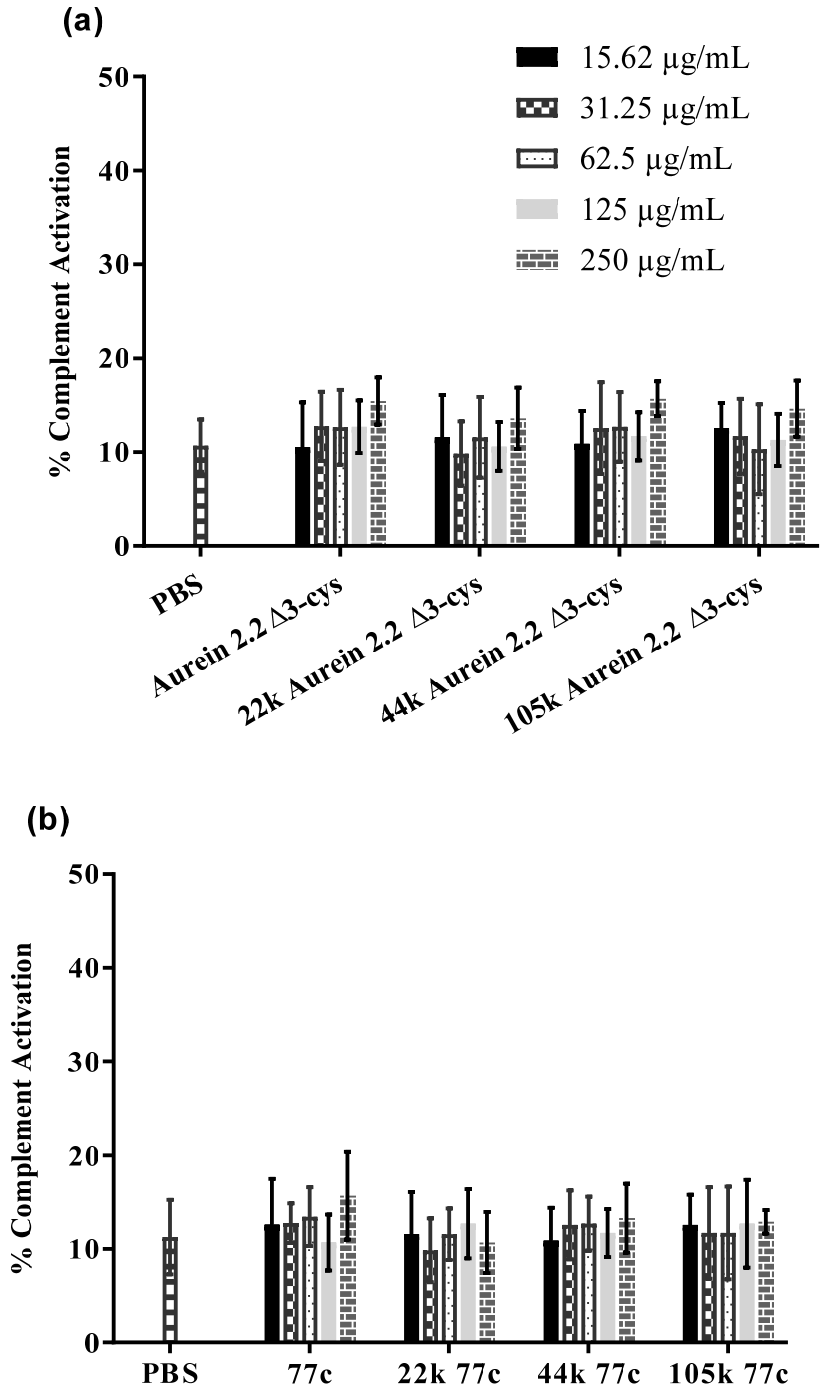

Figure 3.8: Complement activation upon exposure to free peptide and HPG peptide conjugates: a) aurein 2.2Δ3-cys; b) peptide 77c. A complement consumption assay (CH50) was used to determine complement activation, using antibody-sensitized sheep red blood cells and human serum. The percentage of consumed complement proteins is shown. PBS buffer was used as a normal control. Figure generated using Graphpad prism.

Prothrombin time (PT) was measured to characterize the extrinsic pathway of blood coagulation upon addition of free peptides and conjugates. Cationic peptides and polymers have been shown to delay prothrombin time[185,220]. Interestingly, peptide 77c has no impact on PT whereas aurein 2.2Δ3-cys prolonged PT at concentrations as low as 125 μg/mL, suggesting that peptide 77c is not changing the blood coagulation profile compared to aurein 2.2Δ3-cys. None of the conjugates showed any changes in the PT (Figure 3.9). In the conjugates, HPG may mask the hydrophobic nature of the peptides and prevent non-specific interactions with blood coagulation proteins, which leads to normal prothrombin time.

To further investigate the influence of our peptide and its conjugates on whole blood clotting profile, we used rotational thromboelastometry (ROTEM) measurements in human whole blood. Representative ROTEM traces are shown in Appendix B.10 and clotting time is shown in Appendix B.11. Both the peptide and conjugate (peptide 77c and 22K 77c) showed similar clotting profile as the buffer control suggesting that the conjugate or peptide is not altering the blood coagulation profile. The clotting time of the peptide and conjugates is also not significantly different from the buffer control under these conditions.

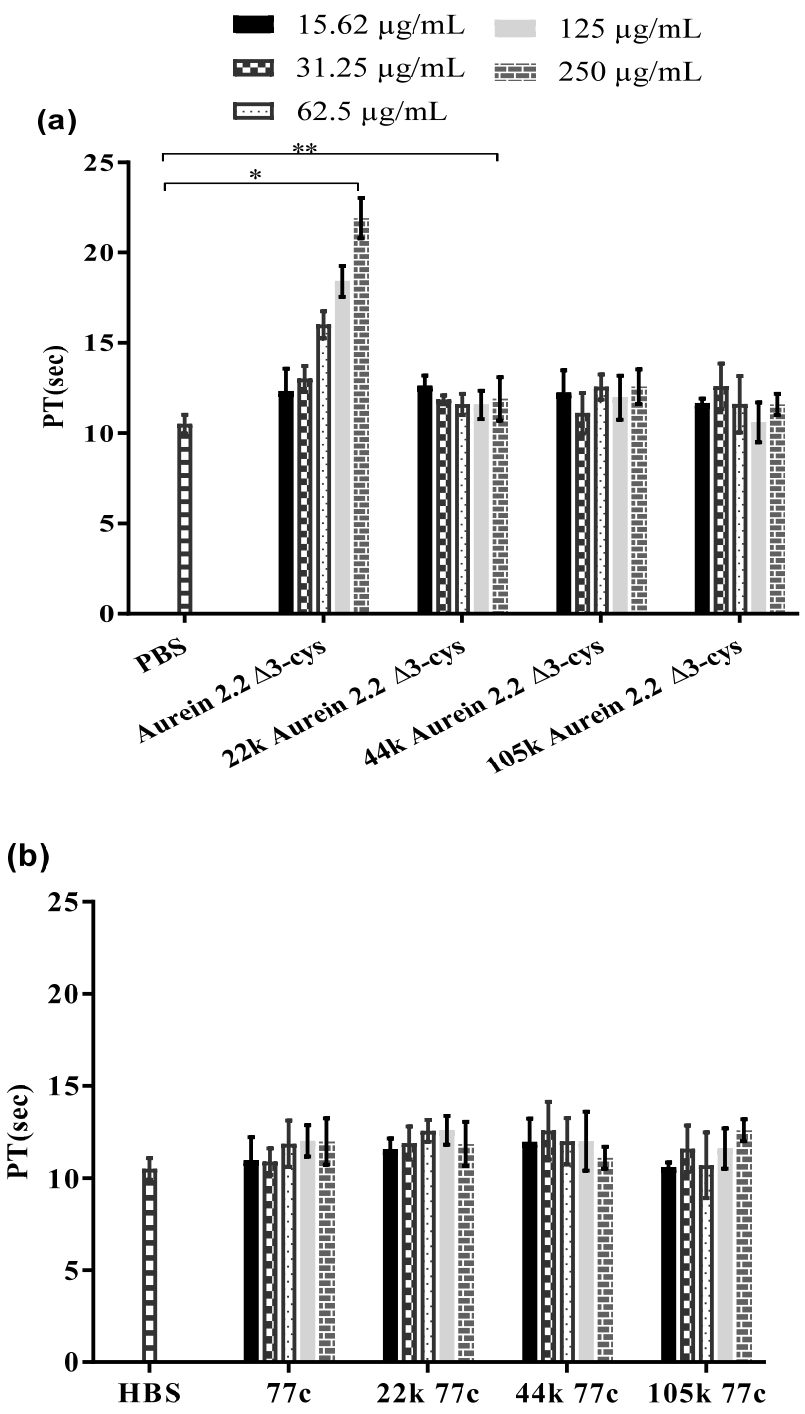

Figure 3.9: Prothrombin time upon exposure to free aurein peptide and HPG peptide conjugates: a) aurein 2.2Δ3-cys *P=0.0067; **P=0.2803. b) peptide 77c. Prothrombin time (PT) was measured by incubating peptide and conjugates with platelet poor plasma at 37 °C. Figure generated using Graphpad prism. Results are courtesy of Dr. Manu Thomas Kalathottukaren.

3.5 Summary

In this chapter, we examined how the parameters such as peptide sequence and size of HPG impact the antimicrobial activity and blood compatibility of AMP/HPG bioconjugates. Specifically, we designed a R and W mutant peptide library derived from the previously studied aurein 2.2 peptide and obtained peptide 77 that was 4-8 fold more active compared to the parent peptide. We conjugated both aurein 2.2 and the new peptide to HPGs of varied molecular weight and examined the effect of HPGylation on the antimicrobial activity, structure and interaction with blood components. Overall, HPGylation of both peptides decreased the antimicrobial activity, with the best molecular weight being 22k, where a factor of 3-6 in the increase in MICs was observed. More importantly, we obtained a bioconjugate with the best MIC value reported in literature to date, namely 50 μg/ml. This bioconjuate (22K 77c) also showed resistance to tryptic digestion and maintained antimicrobial activity compared to the free peptide. HPGylation decreased the alpha helical content of both peptides in a membrane environment; however, in buffer HPGylated peptide 77c adopted an alpha helical structure compared to HPGylated aurein 2.2Δ3-cys which was random coil. Even though the activity and structure of the peptides are different, HPGylation reduced the interaction with red blood cells and platelets. All HPGylated peptides were biocompatible with fibroblast cells, demonstrating their non-toxic behavior compared to the free peptides. The results presented here demonstrate that it is possible to optimize peptide sequence and HPG molecular weight to obtain bioconjugates with excellent properties. The results suggest that conjugating highly active peptides with low molecular weight HPG is the best strategy.

Chapter 4: The *in vitro* biofilm activity and the *in vivo* efficacy of the novel peptides and the polymer conjugates.

4.1 Synopsis

In Chapter 3, we developed novel peptides and conjugates with good antimicrobial activity. In order to determine their usefulness as potential therapeutic agents and more importantly, to determine whether HPG-conjugation could be part of a broader strategy to help develop novel antimicrobial agents, it is important to test the activity of these peptides and bioconjugates developed in Chapter 3 in biofilm inhibition and eradication, and in wound healing. To this end, we describe the evaluation of antimicrobial, anti-biofilm, toxicity, and *in vivo* activity in a mice abscess model in this chapter. As discussed in Chapter 1, other strategies to increase the efficacy of AMPs include the use of D-amino acids (Chapter 1.3.1). Hence, we also conducted activity tests on peptides where the sequence was preserved but the L-amino acids were replaced by their D- counterparts. Likewise, we investigated peptides where both the order of sequence and the use of D-amino acids were combined.

4.2 Background

As described in Chapter 1, antimicrobial peptides are sometimes also referred to as host defense peptides (HPDs) in order to reflect their multi-faceted activities. Up to this point, we have examined the activity of aurein peptides, their derivatives and the HPG conjugates in terms of their ability to act against planktonic bacteria. However, many AMPs also display activity against bacteria in other forms such as in biofilm. A biofilm is a dense assembly of surface adhered bacteria localized in an extracellular polymeric substance (EPS) made from polysaccharides, DNA and proteins[252]. The EPS typically blocks the transport of the antibiotics

through the biofilm making biofilms particularly antibiotic resistant[252] and consequently difficult to treat. It has been reported previously that some AMPs are also effective in clearing bacteria and enhance the wound healing in different skin infections. For instance, AMPs show potential for all of these activities, e.g. D-M33 posses good antibiofilm activity (Chapter 1.3.1), whereas DJK-5 displays both antibiofilm activity and wound healing properties in skin infection models[207] (Chapter 1.3). Since antibiofilm activities of AMPs were already presented in Chapter 1, we will not discuss them again here but rather focus on wound healing.

Cutaneous abscesses are one of the most common skin conditions that are caused by bacterial infection and are characterized by the accumulation of pus in the skin, leading to lesions that normally appear red and swollen and that may cause severe pain[205]. Although both Gram positive and Gram negative bacteria cause abscesses, community associated methicillin resistant *Staphylococcus aureus* (Ca MRSA) is the most common agent[253]. A Ca-MRSA strain that has been frequently recovered is USA 300[254]. In 2005, approximately 3.2 million people with abscesses were treated in hospital emergency departments in the USA alone[206]. Abscesses are treated by surgically draining the pus and treating with antibiotics to prevent spreading and reoccurrence[207]. Common antibiotics used to treat MRSA abscesses are trimethoprim-sulfamethoxazole and tetracyclines, however, antibiotics do not work within the abscess due to limited penetration, high bacterial loads and low pH[208]. As many bacterial strains are also acquiring antibiotic resistance, there is an urgent need for alternatives and adjuncts.

More recently, AMPs have been utilized to treat skin infections caused by multidrug resistant pathogens[255,256]. Interestingly most AMPs in clinical trials to date have been used as topical antibacterial agents for skin related infections. AMPs have many advantages over

traditional antibiotics: they display broad-spectrum antimicrobial and immunomodulatory activity; they can neutralize virulence factors; and finally, they show low or no resistance to the treatment. Interestingly, Mansour et al. have shown that abscess and biofilm caused by MRSA (USA 300) produces a similar stress response which can be targeted in mice by antimicrobial peptide DJK-5[207]. The DJK-5 peptide was initially developed for a screen of anti-biofilm peptides. Moreover, in a similar study, AMPs such as WR12 and IK8 showed good anti-biofilm activity and were used effectively as topical antibacterial agents for the treatment of MRSA associated skin infections in mice models[255]. Interestingly D-IK8 peptide showed the best activity against intracellular MRSA. Finally, in another study, D-amino acid AMPs eradicate biofilms formed by multi-resistant *Pseudomonas aeruginosa* in invertebrate (*C. elegans* and *G. mellonell*) survival models[209].

Although AMPs have various activities, not many have been FDA approved due to their toxicity, the susceptibility of peptides to protease degradation and the rapid kidney clearance[23,105,141]. Many strategies have been investigated to circumvent these issues and to improve the efficacy of AMPs. These include chemical modification of AMPs[142] and the use of delivery vehicles[143] as discussed in Chapter 1.3. The use of D amino acids prevents protease degradation. On the other hand toxicity can be mitigated by either conjugation of AMPs to polymers such as HPG (Chapter 3) or encapsulation of the peptides using delivery vehicles such as liposomes or micelles. The encapsulation of LL37 within liposomes composed of DSPC/DSPE-PEG/cholesterol ensured enhanced bioactivity and reduced toxicity in cell cultures[162]. In Chapter 3, we developed peptide 77 and its HPG conjugates that showed enhanced *in vitro* antimicrobial activity against *S. aureus* compared to the aurein peptides. In this Chapter, we investigate the *in vitro* anti-biofilm and *in vivo* activity of peptide 73 and other peptides that

are closely related to 77 but more active *in vivo* when compared to 77. Our hypothesis is that novel peptides will be effective in healing abscesses in mouse models, and their conjugates will mitigate the toxicity of the AMPs *in vivo*. The D-amino acid version of peptide 73 (D-73) and retro-inverso (RI-73, D amino acid with the sequence reversed) may further enhance its *in vivo* efficacy. We also examined the role of encapsulation of the novel peptides using the abscess mouse model. Finally, the resulting data will allow us to determine the relationship between the *in vitro* and *in vivo* activity of the peptides/conjugates. Such information is important in the design of functional AMPs, with potential clinical applications.

4.3 Materials and methods

All chemicals were purchased from Sigma Aldrich Canada Ltd. (Oakville, ON) and used without further purification except for glycidol, which was purified by vacuum distillation. Dialysis membrane was obtained from Spectra/Por Biotech (Rancho Dominguez, CA).

4.3.1 Peptide synthesis and purification

Solid phase peptide synthesis (Fmoc) was used to synthesize aurein 2.2, aurein 2.2Δ3-cys and its RW mutants (Table 4.1), as previously described[113,215,257] with details given in Chapter 2.3.1 and 3.3.2.

4.3.2 Synthesis of the bioconjugate

Synthesis and characterization of HPG-73c was carried out as described in Chapter 3.3.3 to 3.3.5.

4.3.3 Antimicrobial activity measurements: MIC determination

The MICs of the peptides/conjugates against *S. aureus* were measured based on previously described methodology[235;113,138,215] found in Chapter 2.3.6.

4.3.4 Biofilm studies

The bioluminescence- and biofluorescence-based static microtiter plate assays were established in a similar fashion as previously described [258]. Briefly, an overnight culture was diluted to an OD = 0.01 in tryptic soy broth supplemented with 1% glucose (w/v) or in BM2 supplemented with 0.4% glucose (w/v), 0.5 mM Mg^{2+}, and, for USA300-*lac*::lux/USA300 GFP or PAO1 lux/PAO1 GFP strains, respectively, and then 90 µL was added to each well of a 96-well Costar polypropylene plate (Corning Inc., Corning, NY) containing 10 µL of peptide diluted in water or water alone. Each peptide was evaluated for antibiofilm activity at concentrations of 64, 32, 16, 8, 4, 2, 1 and 0.5 µg/mL. After overnight growth, the planktonic cells were washed away with deionized water and the remaining adhered biomass was resuspended in 150 µL of 10% LB/ 90% PBS (v/v) solution by pipetting up-and-down (withdrawing the liquid up and squirting it back down). Total biofilm mass was quantified by measuring luminescence or fluorescence (eGFP, λ_{ex} = 488 nm, λ_{em} = 530 nm) using a microtiter plate reader (Bio-Tek Instruments Inc., Winooski, VT). The percent biofilm inhibition was calculated in relation to the amount of biofilm grown in the absence of peptide (defined as 100%) and the media sterility control (defined as 0% growth). Results from three separate biological replicates were averaged.

4.3.5 Red blood cell lysis

Blood was withdrawn from consenting unmedicated donors into a 3.8% sodium citrated tube with a blood/coagulant ratio of 9:1 or serum tube at the Centre for Blood Research, University of British Columbia. Red blood cell (RBC) suspension was prepared by washing packed RBC with PBS three times to yield 80% hematocrit. Detailed protocols of the red blood lysis studies can be found in Chapter 2.3.9.

4.3.6 Mouse skin infection model

Bacterial strains and growth conditions for animal studies

Bacterial strains used in this study were the *Pseudomonas aeruginosa* laboratory wild type strain PAO1[259], the *P. aeruginosa* Liverpool Epidemic Strain isolate LESB58[260], and the *Staphylococcus aureus* LAC (USA300) strain[261]. All organisms were cultured in double Yeast Tryptone (dYT), shaking at 250 rpm, at 37 °C. Bacterial growth was monitored using a spectrophotometer at the optical density of 600 nm (OD_{600}).

Ethics statement

Animal experiments were performed in accordance with The Canadian Council on Animal Care (CCAC) guidelines and were approved by the University of British Columbia Animal Care Committee (certificate number A14-0363). Mice used in this study were female outbred CD-1. All animals were purchased from Charles River Laboratories (Wilmington, MA), were 7 weeks of age, and weighed about 25 ± 3 g at the time of the experiments. 1 to 3% isoflurane was used to anesthetize the mice. Mice were euthanized with carbon dioxide.

Cutaneous mouse infection model

The abscess infection model was described earlier[262]. Briefly, all bacterial strains were grown to an OD_{600} of 1.0 in dYT broth and subsequently washed twice with sterile PBS and adjusted to 1×10^7 CFU/ml for *P. aeruginosa* PAO1 and 5×10^7 CFU/ml for *P. aeruginosa* LESB58 and *S. aureus* LAC, respectively. The fur on the backs of the mice was removed by shaving and application of chemical depilatories. A 50 μL bacterial suspension was injected into the right side of the dorsum. All utilized peptides were tested for skin toxicity prior efficacy testing. Concentrations used were 5 mg/kg for L-73, D-73 and RI-73. Peptides or saline (50 μL) were directly injected subcutaneously into the infected area [intra-abscess (IA) injection] at 1 h

post infection. The progression of the disease/infection was monitored daily and abscess lesion sizes (visible dermonecrosis) on day three measured using a caliper. Swelling/inflammation was not considered in the measurements. Skin abscesses were excised (including all accumulated pus), homogenized in sterile PBS using a Mini-Beadbeater-96 (Biospec products) for 5 min and bacterial counts determined by serial dilution. Experiments were performed at least 3 times independently with 3 to 4 animals per group.

Statistical analysis

Statistical evaluations were performed using GraphPad Prism 7.0 (GraphPad Software, La Jolla, CA, USA). *P*-values were calculated using one-way ANOVA, Kruskal-Wallis multiple-comparison test followed by the Dunn procedure. Data was considered significant when *p*-values were below 0.05 or 0.01 as indicated.

4.4 Results and Discussion

4.4.1 Antibacterial activity of the novel peptides *in vitro*

We explored the antimicrobial activity of a range of peptides derived from aurein 2.2: aurein 2.2, aurein 2.2Δ3 (where the last 3 residues at the C-terminus are removed from aurein 2.2), peptide 77 and 77c (which was discussed in Chapter 3) and the new peptide 73, a D-amino acid version (D-73) and a retro-inverso version (RI-73). The sequences of some of these peptides and their hydrophobicity are given in Table 4.1. The peptides listed above were tested against a standard *S. aureus* strains, MRSA USA 300 strain and *P. aeruginosa*. MICs are listed in Table 4.2.

As can be seen from the activities, the novel peptides 73 and 77 are 4 times more active against C622 strain of *S. aureus* (MIC, 4 μg/mL) compared to the parent aurein 2.2 peptide

(MIC, 16 μg/mL) and 8 times more active than the peptides it was derived from (aurein 2.2Δ3, MIC, 32 μg/mL). These peptides both have increased charge (+2 to +3) and hydrophobicity (Table 4.1), suggesting that this may be a contributing factor to increased activity. A similar trend was seen in magainin 2 where increasing the charge of magainin 2 from +3 to +5 improved its antibacterial activity against Gram positive bacteria[78]. As hydrophobicity governs the extent to which the water-soluble AMPs will be able to partition into the membrane lipid bilayer, it is key to maintain a threshold hydrophobicity as sequences with hydrophobicity below and very much above this threshold made the peptides inactive and toxic respectively[85]. Interestingly peptides like 73 and 77 are composed of tryptophan and arginine residues that have unique properties that allow them to interact with each other and the bacterial membrane which may also explain the increase in activity of the peptides[263,232].

Table 4.1: Various properties of some of the peptides used in this studies

Peptide	Molecular weight	Net charge	Hydrophobicity[a]	Hydrophobicity moment[a]
Aurein 2.2Δ3 (GLFDIVKKVVGAL)	1357.68	+2	0.632	0.73
Aurein 2.2 (GLFDIVKKVVGALGSL)	1614.97	+2	0.617	0.603
73 (RLWDIVRRWVGWL)	1755.10	+3	0.815	0.753
77 (RLWDIVRRVWGWL)	1755.10	+3	0.815	0.721
73c (RLWDIVRRWVGWLC)	1857.24	+3	0.866	0.670

[a] Calculated from heliquest http://heliquest.ipmc.cnrs.fr/

All peptides used in this chapter had an amidated C-terminus.

Table 4.2: Antimicrobial activity of the peptides.

Peptide	MIC *S. aureus* C622 (µg/mL)	MIC* Ca-MRSA (USA300-*lac*::lux) (µg/mL)	MIC* *P. aeruginosa* (PA01 lux) (µg/mL)
Aurein 2.2 (GLFDIVKKVVGALGSL)	16	32	>64
Aurein 2.2Δ3 (GLFDIVKKVVGAL)	32	64	>64
73 (RLWDIVRRWVGWL)	4	4	64
73c (RLWDIVRRWVGWLC)	16	16	>64
77 (RLWDIVRRVWGWL)	4	4	64
D-73 (rlwdivrrwvGwl)	4	4	16
RI-73 (lwGvwrrvidwlr)	4	4	64
22k -73c (7-8 peptides)	50	-	-

* MIC results are courtesy of Dr. John Cheng from the Hancock lab

Moreover, the D and retro-inverso (RI) versions of peptide 73 (Table 4.2) had similar activity compared to 73 suggesting that the use of D amino acids does not affect the antimicrobial activity of these peptides similar to lysine rich D-MPI peptide[145]. This indicates that peptide 73 interacts with the bacteria without making use of specific receptors since the stereochemistry of the amino acids has no impact on the antimicrobial activity[43]. Peptide D-73 also showed the best antimicrobial activity against *P. aeruginosa* with an MIC of 16 µg/mL (Table 4.2). The addition of a cysteine to the C-terminus of the peptide 73 decreases its antimicrobial activity drastically by 4 fold (MIC from 4 to 16 µg/mL, Table 4.2). Addition of a cysteine residue might promote

disulfide bridges that affect the antimicrobial activity of the peptide. Cathelicidin-derived peptides, E6 and Tet20 also show a decrease in antimicrobial activity when a cysteine is added at the C-terminus[264].

4.4.2 Efficacy of the peptides against *Staphylococcus aureus* biofilms

Biofilms are one of the most complex and dense assembly of cells that display emergent properties such as antibiotic resistance that are not present in free-living bacteria[265]. The formation of a biofilm is a major virulence factor of *S.aureus*. Biofilm is made of a complex matrix which protects the deeply positioned bacteria from antibiotics and host immune defense[266]. This eventually leads to the release of the bacteria in the host which can cause recurring and chronic infections[255]. Given the serious consequences of biofilms and the fact that it has been previously reported that some AMPs can lead to the inhibition and/or eradication of biofilms, we wanted to assess if our peptides are active against *S.aureus* biofilms.

Firstly, we evaluated our peptides as an agent to inhibit *S. aureus* biofilm by measuring the minimum biofilm inhibitory concentration (MBIC). Peptides 73 and 77 were both more effective at inhibiting 85% of the biofilm formation with an MBIC of 2 μg/mL compared to the aurein peptides (Table 4.3). The addition of a cysteine to the C-terminus of peptide 73 also decreased its ability to inhibit biofilm formation, in analogy to the MIC data presented in the previous section. In addition, the D-peptides (D-73 and RI-73) also maintain the inhibitory properties (MBIC, 2 and 4 μg/mL, respectively).

Inhibition of bacterial growth is important but it is also critical that the peptides can eradicate biofilms too. In general the trend for biofilm eradication is similar to that observed for MBICs,

but higher concentrations of the peptide are generally needed to eradicate biofilm. For example peptide 73 has a MBIC of 2 μg/mL and MIC of μ μg/mL but a MBEC of 16 μg/mL (Table 4.3). Unlike peptide 73, aurein 2.2 does not possess a strong anti-biofilm activity.

Table 4.3: Anti-biofilm activity of the peptides.

Peptide	**$MBIC_{85}$ Ca-MRSA USA300 GFP (μg/mL)**	**$MBIC_{85}$ *P. aeruginosa* (PA01 lux) (μg/mL)**	**$MBEC_{80}$ (μg/mL) Ca-MRSA USA300 GFP (μg/mL)**
Aurein 2.2 (GLFDIVKKVVGALGSL)	16	>64	>64
Aurein 2.2Δ3 (GLFDIVKKVVGAL)	32	>64	>64
73 (RLWDIVRRWVGWL)	2	>64	16
73c (RLWDIVRRWVGWLC)	8	64	-
77 (RLWDIVRRVWGWL)	2	>64	-
D-73 (rlwdivrrwvGwl)	2	32	32
RI-73 (lwGvwrrvidwlr)	4	16	32
22k -73c (7-8 peptides)	50	-	-

*All $MBIC_{85}$ (Peptide concentration when 85% of the biofilm is inhibited) and $MBEC_{80}$ (Peptide concentration when 80% of the biofilm is eradicated) results are courtesy of Dr. John Cheng from the Hancock lab

Generally, the MBECs reported in Table 4.3 are much higher than the MIC: for example peptide, 73 has a MBEC of 16 μg/mL which is 8x the MIC, indicating it is more difficult to eradicate

than to inhibit biofilms. In a similar study, peptide WR12 which is also a W and R rich peptide needed 8x the MIC to eradicate 80% of the *S.aureus* biofilm[255].

4.4.3 Tolerance of the peptides

Host toxicity is one of the major limitations of AMPs that has prevented advancement of these drugs into clinical trials. Similar to studies done in Chapters 2 and 3, we evaluated the toxicity of the peptides by measuring the red blood cell lysis at 37 °C for 1 hour. None of the peptides caused any significant RBC lysis near the MIC and MBIC. For example, aurein 2.2 and 73 are not lytic (similar lysis to PBS buffer <5%) at 25 μg/mL and 12.5 μg/mL respectively. However, at higher concentrations (100 μg/mL) peptides 73, 73c, and 77 are more toxic compared to the original aurein peptide (Figure 4.1). Interestingly, D-73 and RI-73 have similar antimicrobial activity compared to peptide 73, but they are both more toxic towards RBCs (Figure 4.1). RI-73 is the most toxic peptide causing approximately 65% lysis of RBCs at 100 μg/mL. Such a tendency has been previously observed in the literature: for instance, the RI version of certain cell penetrating peptides also caused severe cell toxicity[267], whereas the original peptide did not. Our collaborators also tested toxicity of these peptides in different cells lines (data not shown). A similar toxicity trend to these seen in Figure 4.1 was observed using the LDH release assay with PBMCs (peripheral blood mononuclear cells).

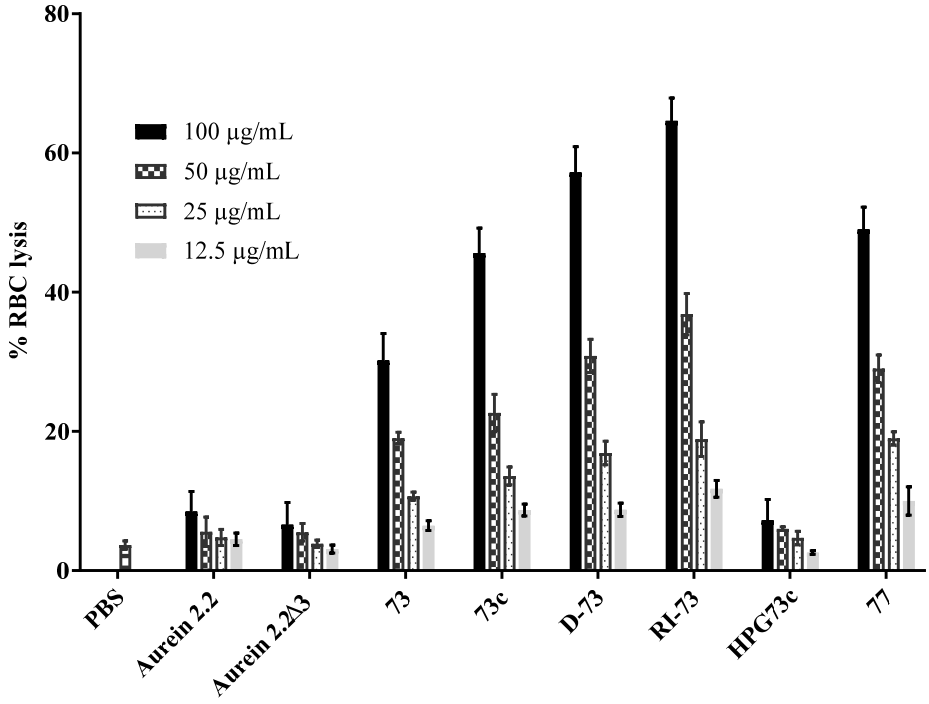

Figure 4.1: Red blood cell lysis upon exposure to free peptides and HPG peptide conjugates: Hemolysis of the free peptides and the HPG conjugates was measured at various concentrations, after 1h incubation at 37 °C with washed red blood cells. PBS buffer was used as normal control. The experiment was repeated three times. Figure generated using Graphpad prism.

4.4.4 *In vitro* therapeutic index of the peptides

The therapeutic index (TI) which is a ratio of the concentration at which the peptide causes 50% toxicity (RBC lysis or cell viability) and the MIC is a parameter used to represent the specificity of the peptides for bacterial versus mammalian cells[268]. A plot of Log [peptide concentration] versus percent RBC lysis with a non linear regression (Graphpad Prism) was used to determine the 50% lysis concentration (also known as LD_{50}) (Figure 4.2). Aurein 2.2 and peptide 73 have the best therapeutic index (42 and 55 respectively) *in vitro* compared to the other peptides. The therapeutic index for some peptides in DSPE-PEG2000 was also examined. The

DSPE-PEG2000 encapsulated peptides were less toxic *in vitro* but the antimicrobial activity also decreased and a clear trend was not visible (Table 4.4).

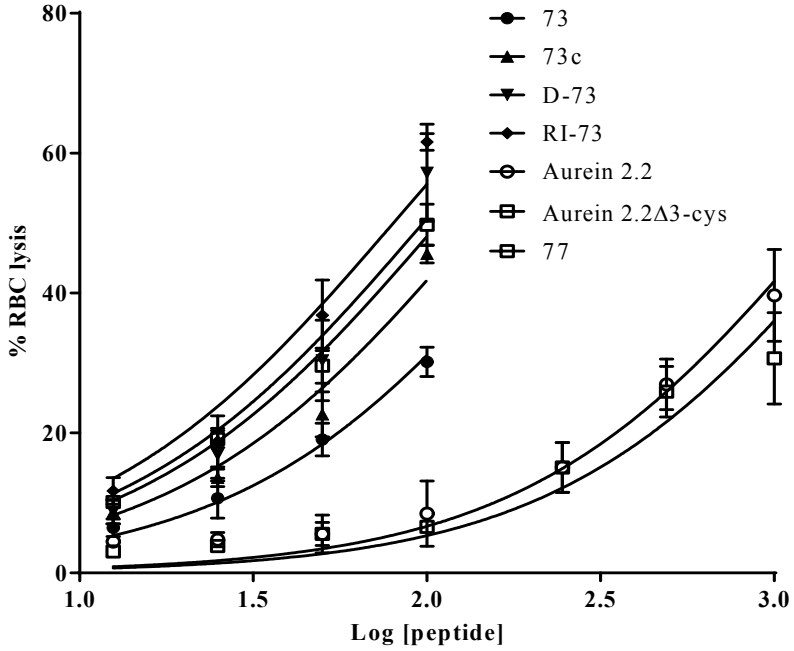

Figure 4.2: RBC lysis vs log of peptide concentration curves to extrapolate the concentration at which the peptides cause 50% RBC lysis (LD_{50}). Figure generated using Graphpad prism with a hyperbolic non linear fit, % RBC lysis =100/(1+10^(($LogLD_{50}$-X))), where X is the Log [peptide].

4.4.5 Efficacy of peptides in a mouse abscess model

As these novel peptides displayed good antimicrobial and antibiofilm activity and no toxicity at MIC, we conducted *in vivo* studies in a mouse abscess model[207,262]. Briefly, mice were injected with community acquired USA 300 MRSA strain and treated with a single subcutaneous [intra-abscess (IA)] injection of peptides or saline 1 hour post infection. The abscess area (visible dermonecrosis) and the intra abscess bacterial count were determined 3 days post infection to

evaluate the efficacy of the peptides. Peptides 73 and 77 have the same hydrophobicity, charge and *in vitro* antimicrobial activity but only peptide 73 significantly decreased the lesion size by

Table 4.4: Therapeutic index of the peptides

Peptide	MIC CA-MRSA (µg/mL)	50% RBC lysis (µg/mL)	Therapeutic index [50% RBC lysis]/MIC
Aurein 2.2 (GLFDIVKKVVGALGSL)	32	1350	42
Aurein 2.2Δ3 (GLFDIVKKVVGAL)	64	1577	25
73 (RLWDIVRRWVGWL)	4	221	55
73c (RLWDIVRRWVGWLC)	16	139	9
77 (RLWDIVRRVWGWL)	4	107	27
D-73 (rlwdivrrwvGwl)	4	97	24
RI-73 (lwGvwrrvidwlr)	4	80	20
22k -73c (7-8 peptides)	50*	>1500	>30
73 in DSPE-PEG2000	40	941	23
73c in DSPE-PEG2000	625	850	1.36
D-73 in DSPE-PEG2000	30	795	27

*MIC against ***S. aureus*** **C622**

approximately 3 fold compared to saline control in the mouse model (Figure 4.3a). Moreover, mice treated with peptide 73 also showed a 10-fold reduction in bacteria recovered from the abscess site (Figure 4.3b). The *in vivo* difference in activity between peptide 73 and 77 might be due to the fact that peptide 77 is more toxic *in vitro* (Figure 4.1) and also *in vivo* (Appendix C),

which might lead to inactivation or clearance of the peptide *in vivo*. The TI (Table 4.3) for peptide 73 (TI=55) is 2-fold better compared to 77 (TI=27), correlating with the *in vivo* activity and indicating the fine balance needed in terms of the *in vitro* toxicity and antimicrobial activity for optimum *in vivo* activity. Interestingly, aurein 2.2 which is the natural parent peptide isolated from Australian frog (skin) has similar activity as peptide 73 in reducing lesion size and viable bacteria counts (Figure 4.3). Aurein 2.2 has both lower antibacterial activity and toxicity *in vitro* and has a TI of 42 which is similar to peptide 73 (TI=55), again correlating well with the *in vivo* activity.

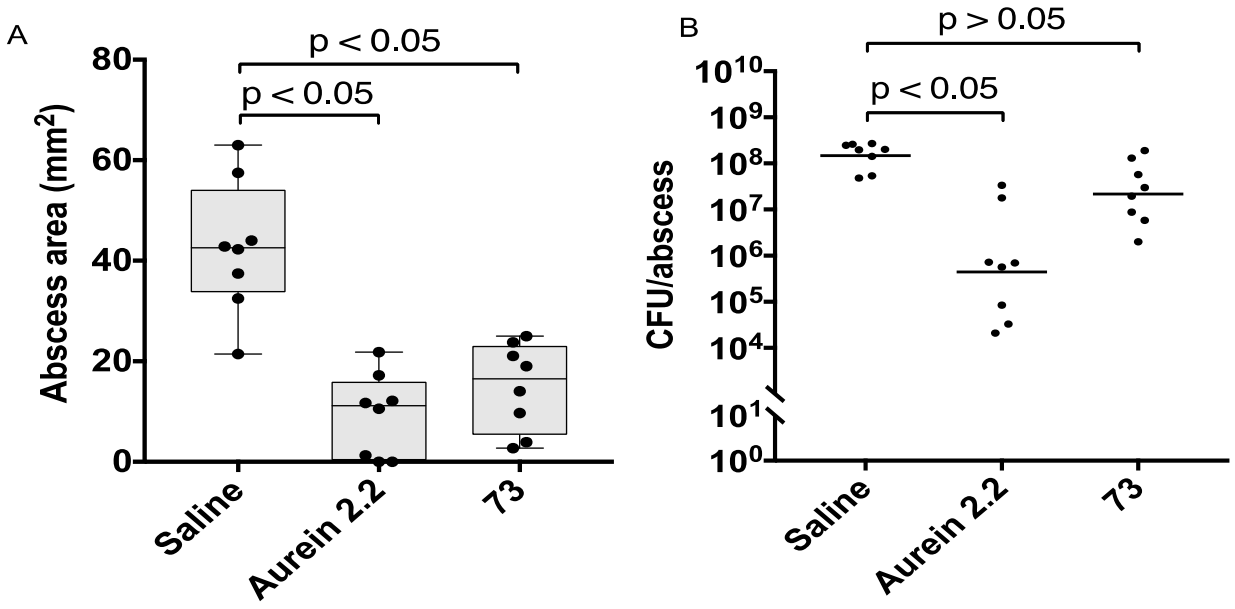

Figure 4.3: Infection and therapeutic treatment of mouse cutaneous abscesses. All mice were infected with MRSA USA300 and treated with saline solution, aurein and peptide 73 (dose = 5 mg/kg) 1 h post-bacterial infection. Lesion sizes and CFU counts were determined 3 days postinfection. The experiment was repeated at least twice. Results are courtesy of Dr. Daniel Pletzer from the Hancock lab.

In addition to peptide 73, the two versions of the peptide containing D-amino acids, namely D-73 and RI-73, were also tested in the mouse model. Unfortunately both the peptide D-73 and RI-7 were toxic and precipitated at 5 mg/kg in saline solution under the skin (Appendix C.1). This is consistent to the *in vitro* toxicity profile, as both peptide D-73 and RI-73 are more toxic compared to the L versions (Figure 4.1). Many stragegies have been used to alleviate the toxicity of AMPs but the easiest way is by encapsulation. DSPE-PEG2000 has been previously utilized to encapsulate LL-37 by the formation of liposomes to increase the bicompatability[162]. This encapsulation strategy was attempted here, but instead of making liposomes, we dissolved D-73 and RI-73 in DSPE-PEG2000 and evaluated the toxicity and precipitation *in vivo*. Interestingly dissolving these peptides in DSPE-PEG2000 prevented any precipitation and toxicity at various concentrations (Appendix C.2) due to the formation of miclles. The activity of various peptides dissolved in DSPE-PEG2000 in the mouse abcess model is summarized in Figure 4.4. Of the two D peptides, D-73 significantly decreased the lesion size and bacterial count in the abscess, whereas RI-73 was similar to the DSPE-PEG2000 control. D-73 also perfomed better than peptide 73 suggesting the benefit of using D-peptides as long as the toxicity is alleviated. Aurein 2.2Δ3, from which peptide 73 is derived, was not effective in the mouse model. Peptide 73c, which had solubility issues in saline but good solublilty in DSPE-PEG2000, was as effective as D-73 in reducing lesion size and viable bacterial counts.

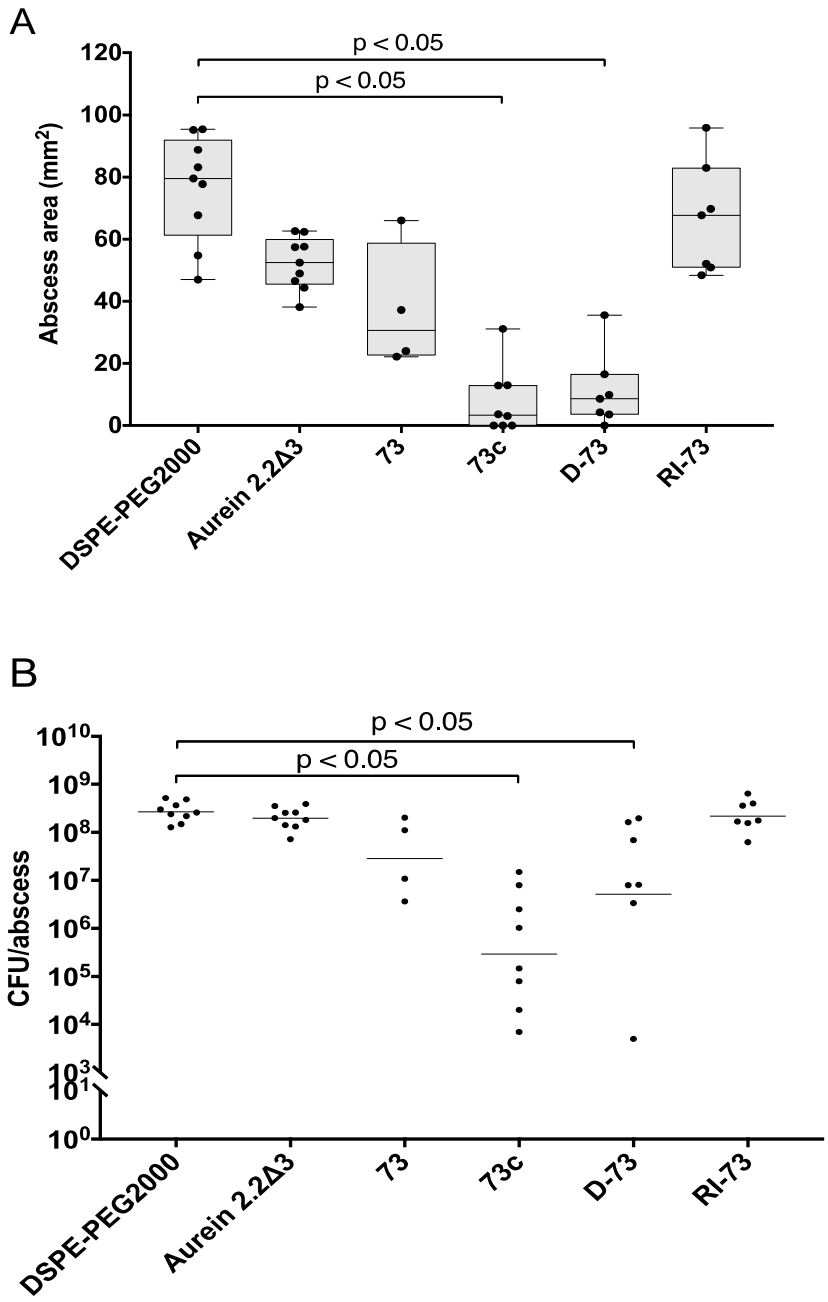

Figure 4.4: Therapeutic treatment of mouse cutaneous abscesses with D and L peptides. All mice were infected with MRSA USA300 and treated with DSPE-PEG2000 solution and various peptides dissolves in DSPE-PEG2000 solution (5 mg/kg) 1 h post-bacterial infection. Lesion sizes and CFU counts were determined 3 days postinfection. The experiment was repeated at least two times. Results are courtesy of Dr. Daniel Pletzer from the Hancock lab (UBC).

4.4.6 Peptide aggregation

Tryptophan and arginine containing AMPs have been well known to aggregate which may relate to its toxicity[269]. Peptide 73c was one of the most active peptide in the mice abscess model when dissolved in PEG but had poor solubility in water and saline solution. To investigate the aggregation behavior of peptide 73c the average hydrodynamic diameter (H_d) was measured in water and DSPE-PEG2000 at 3 mg/mL (concentration injected in abscesses). From Table 4.5 (and also Appendix C.3), it can be concluded that peptide 73c forms aggregates of various sizes with an average H_d of 329 nm and a large standard deviation (100 nm). Upon encapsulation with DSPE-PEG2000, most (74%) of the peptide 73c forms micelles with a H_d of 11.9 nm, whereas 26% still exists in the aggregate state. In another study, DSPE-PEG2000 encapuslated cabozantinib, an anticancer drug, also had an H_d of 11 nm[270]. The formation of micelles may account for the decreased toxicity and increased solubility of peptide 73c and hence better efficacy *in vivo*. However, in the future it would be beneficial to increase the concentration of DSPE-PEG2000 or use a better encapsulationg agent to increase the loading efficiency.

Table 4.5: Average hydrodynamic size of peptide 73c

	Average hydrodynamic size (nm)	**Standard deviation (nm)**	**% intensity**
73c in deionised water	329	100	90
73c in DSPE-PEG2000	11.9	1.6	74
	254	30	26

4.4.7 Efficacy of the HPG conjugates in the mouse abscess model

Results from Chapter 2 and 3 suggest that the HPG peptide conjugates were non toxic and showed moderate antimicrobial activity against *S. aureus*. These conjugates made use of aurein 2.2Δ3 or peptide 77, which the mouse abscess model shows to be less effective than some of the other peptides tested (Figure 4.2 and 4.3). Since peptide 73c showed good activity upon encapsulation, a conjugate consisting of peptide 73c and 22K HPG was synthesized and the *in vivo* efficacy was evaluated. HPG-73c was not toxic and did not precipitate under the skin at concentrations as high as 30 mg/kg (9 mg/kg peptide 73c equivalent) in saline, but the solution was cloudy indicating that solubility is an issue. HPG-73c was not effective in reducing the lesion size or bacterial counts in the mouse abscess model (Figure 4.5). This may be due to the fact, as observed in Chapter 3, that conjugation has an impact on antimicrobial activity (recall the 6-7 fold increase in MIC). Compared to the free peptides shown in Figure 4.4, the HPG conjugate was already tested at a higher concentration (30 mg/kg) to try to account for the lower MIC of the bioconjugate. However, this higher concentration is most likely still low (i.e. when comparing dosage of 5 mg/kg for an MIC of 4 μg/mL (free peptide) versus 30 mg/kg for an MIC of 50 μg/mL for conjugate). As mentioned above, going to higher concentrations is problematic, firstly because the solubility is poor, but also in terms of the high amount of material required. It is difficult to speculate whether a really high dose would lead to a statistically significant change in the abscess size and bacterial count.

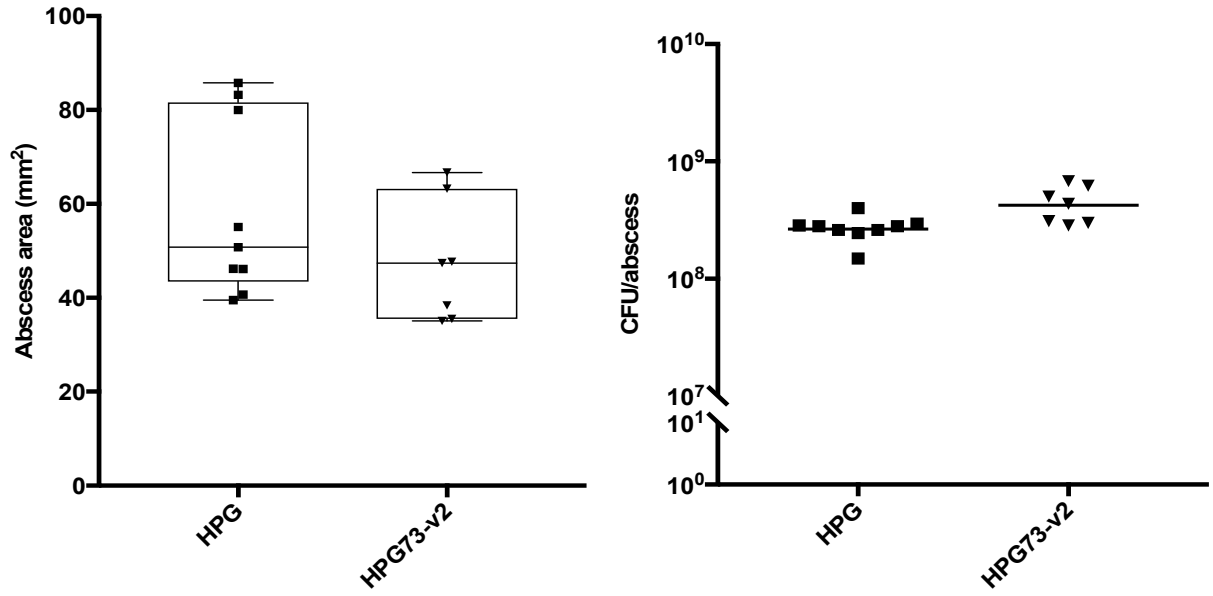

Figure 4.5: Therapeutic treatment of mouse cutaneous abscesses with HPG-73c conjugates. All mice were infected with MRSA USA300 and treated with HPG solution and HPG73c (30 mg/kg) 1 h post-bacterial infection. Lesion sizes and CFU counts were determined 3 days postinfection. The experiment was repeated at least two times. Results are courtesy of Dr. Daniel Pletzer from the Hancock lab (UBC).

4.4.8 Peptide design paradigms

Determining the MIC of the peptides is one of the most prominent parameters used in the screening of AMPs. Although it is a good starting point, the peptide with the best MIC does not always guarantee that the peptide would be more effective in different animal models such as the mouse abscess model. For example, peptide 73 has a better MIC than aurein 2.2 but has similar activity in the abscess model. The data presented in this chapter strongly suggests that it is important to test the peptides in animal models to better understand the efficacy of the peptides *in vivo* before further development of the AMPs. It is also worth screening the toxicity of the

peptides and determining the therapeutic index *in vitro*, as it correlates well with the activity *in vivo* for our mice abscess model.

As discussed in Chapter 1.3 there are many strategies to improve the activity of AMPs. One of the easiest and most frequent strategies used to improve the activity of AMPs is the use of D-peptides to prevent proteolytic degradation. Peptide D-73 and RI-73 have similar MICs compared to 73 but could not be administered *in vivo* because of the toxicity issues. The toxicity of the D-73 peptides was mitigated by the use of DSPE-PEG2000 as a non covalent delivery vehicle which enabled the peptides to be released and effectively treat the abscess; however RI-73 was still ineffective in mice. Interestingly, the use of D-peptides also improved the *in vivo* efficacy of other peptides such as DJK-5[207] and D-IK8[255].

Another strategy used to improve the efficacy of AMPs is the use of covalent attachment to polymer molecules (conjugation). Similarly to the results presented in Chapter 3, the conjugation of peptide 73c to HPG alleviated the toxicity but the conjugates were not effective in the abscess model at the concentrations tested. One approach would be to increase the dosage but the solubility of the conjugate might limit this option. A better strategy would require the peptides to be released at the site of infection either by enzymatic cleavage or a degradable linker, similar to the DSPE-PEG2000 formulation used for 73c and D-73. Recently, an immunomodulatory peptide pOVA when conjugated to HPG via a cleavable ester linkage had superior properties compared to the non cleavable amide linkage[199].

4.5 Summary

In this chapter, we successfully demonstrated the antibacterial and antibiofilm activity of various novel peptides and conjugates. The therapeutic index of the peptides *in vitro* correlated

well with the *in vivo* activity in a mouse abscess model indicating the fine balance needed between antimicrobial activity and toxicity. This was particularly evident in the case of peptide 73, with its superior antimicrobial activity but higher toxicity, as compared to aurein 2.2. Peptide 73c and D-73 were the most active peptides *in vivo* when used in a formulation with DSPE-PEG2000 which aided in alleviating the toxicity of both the peptides. Although conjugation of peptide 73c to HPG also mitigated the toxicity of the peptide, the conjugate was not effective *in vivo* indicating that the release of the peptide may be an important step for an *in vivo* active formulation.

Chapter 5: Overexpression, purification and esterification of aurein 2.2 utilized to probe the interaction of aurein 2.2 with whole bacterial cells by NMR.

5.1 Synopsis

The antibiotic crisis has lead to a pressing need for alternatives such as antimicrobial peptides. Better understanding the structure and mechanism of action (MOA) of AMPs would lead to the discovery of more potent and less toxic AMPs. Many models have been utilized to describe the MOA but only a few studies have probed the interaction of AMPs with live bacterial cells. In this chapter, we use a calmodulin-aurein 2.2 (CaM-aurein 2.2) fusion construct to obtain isotopically ^{15}N labeled aurein 2.2 using a bacterial expression system. Expression of AMPs yield peptides with carboxylic acid at the C-terminus which typically renders the peptide inactive; consequently, blocking the free carboxyl at the C-terminus via esterification was required to restore the activity of aurein 2.2. The interaction of the esterified and ^{15}N labeled aurein 2.2 with live *Staphylococcus aureus* was probed using NMR (^{1}H,^{15}N-HSQC) and scanning electron microscopy (SEM). This system can be further developed and utilised to study the interaction of other AMPs and polymer conjugates with live bacteria in the future.

5.2 Background

Antimicrobial peptides such as aurein 2.2 and 73 have good antibacterial activity both *in vivo* and *in vitro*. The mechanism of action (MOA) of AMPs like aurein 2.2 has been well studied and many techniques such as NMR, CD spectroscopy and leakage assays[117,139] have been utilized to understand the bacterial killing action of AMPs. Although the MOA of some AMPs is well understood, most studies use model membrane systems such as supported bilayers,

liposomes, vesicles and micelles showing that AMPs damage the membrane or form membrane pores via various mechanisms such as toroidal pore, barrel stave or detergent models as described in Chapter 1.2.4. Hence, the main killing action of AMPs is thought to target the bacterial cell membrane, but AMPs may also target the cell wall or other intracellular components[160]. To date only a few studies have explored the membrane/cell wall-peptide or peptide-intracellular component interactions in living cells[116]. Therefore, it is important to investigate the detailed structural interaction between AMPs and its targets in living cells to further understand their MOA.

NMR is one of the most powerful techniques that can used to elucidate the detailed structural interactions between AMPs with potential molecular targets such as membranes, proteins and nucleotides[210]. To date only a few whole cell NMR experiments have been reported to determine the interactions of AMPs with different bacterial components. Solid state NMR studies (cross-polarization magic-angle spinning, CPMAS) of whole planktonic cells were able to detect the total ^{13}C and ^{15}N composition of intact *S. aureus* cells[211]. The general mode of antibiotic action could be identified as whole cells treated with fosfomycin had lower peptidoglycan composition compared to cells treated with chloramphenicol which contained a higher percentage of peptidoglycan but a reduction in the cytoplasmic protein content[211]. In a more recent study, ^{13}C and ^{15}N CPMAS NMR was used to detect ribosomes in intact whole cells which could possibly be used in the future to determine the interaction of other ribosome binding compounds[271].

Most whole cell NMR studies to date utilize isotopic labeling of the bacterial cells rather than the antimicrobial compound such as AMPs. AMPs are synthesized by solid phase peptide synthesis and chemical isotopic labeling of the AMPs is not practical due to the high cost. Few

recombinant expression systems in bacteria have been utilized to produce isotopic labeled AMPs[210,272]. Vidovic et al. used a construct in which AMP LAH4 was fused to the histone fold domain of the human transcription factor TAF12[272]. Interestingly, this fusion construct was expressed within insoluble inclusion bodies and did not require any purification and was cleaved chemically by formic acid due to the unique Asp-Pro bond. Moreover, recombinant expression of AMPs has also been developed by Ishida et al. using a calmodulin fusion construct (Figure 5.1), with a Tobacco Etch Virus (TEV) cleavage site[210]. With the development of this unique system, it is now possible to isotopically label AMPs and to study the interaction of AMPs with whole bacterial cells by NMR. NMR spectroscopy also becomes more complex when polymer conjugates are to be studied due to the signals from the polymer leading to indistinguishable overlapping signals. Isotopic labeling of the AMPs in this case will enable us to specifically observe the AMP signal only.

Figure 5.1: Calmodulin (CaM)-aurein 2.2 fusion construct with TEV protease cut site (between glutamine and glycine) and the restriction enzyme site. Figure modified from Ishida, H et. al[210].

Calmodulin is a ubiquitous calcium sensor protein found in eukaryotes. Its negative surface charge allows it to bind to many peptide sequences with positive charge and hydrophobic residues[273–275]. As most AMPs consist of a high proportion of such amino acids, having an AMP-calmodulin fusion is advantageous as this construct will prevent proteolytic degradation and toxic effects arising from AMPs during expression[210]. Ishida et al have shown that many AMPs such as indolicidin and magainin can be expressed using the calmodulin fusion construct and the

AMPs bind to calmodulin in the micromolar range[210]. The resulting AMPs are produced in milligram quantities with a carboxy C-terminus[215].

In this chapter, we used the recombinant expression system developed by Ishida et al. to express aurein 2.2 for the first time. This yielded a peptide that could still adopt an alpha helical secondary structure but did not display any antimicrobial activity due to the free carboxyl at the C-terminus. To restore the activity of aurein 2.2, which in its natural form has an amidated C terminus, the free carboxyls (C-terminus and aspartic acid) were esterified using trimethylsilyl chloride (TMSCl). Isotopically (^{15}N) labeled aurein 2.2 was expressed and esterified to yield a peptide with good antimicrobial activity. NMR studies (2-dimensional ^{15}N-^{1}H heteronuclear single quantum coherence (HSQC experiment)) with intact whole bacterial cells were performed to verify the mechanism of action and as a proof of concept that will allow us to study the detailed structure and interactions of other AMPS/conjugates with whole bacteria cell in the future.

5.3 Methods and materials

All chemicals were purchased from Sigma Aldrich Canada Ltd (Oakville, ON) unless mentioned otherwise and used without further purification. Dialysis membrane was obtained from Spectra/Por Biotech (Rancho Dominguez, CA).

5.3.1 Expression of Calmodulin-aurein fusion protein in E.coli

The pET15b plasmid containing the pCaM-Aurein2.2 construct was provided by the Hans Vogel lab (University of Calgary, Canada). The pCaM-TEV site-Aurein2.2 construct was prepared as previously described[210]. *E. coli* cells transformed with the pCaM-TEV site-Aurein2.2 construct were grown in Lysogeny broth (LB) or minimal media (M9) at 37 ^{o}C with 100 μg/L ampicillin. For the preparation of ^{15}N-labelled aurein2.2 peptide, M9 media was prepared using

$^{15}NH_4Cl$. Cultures were grown to an OD600 of 0.5-0.7 and induced for 4 hours using 0.5 mM Isopropyl β-D-1-thiogalactopyranoside (IPTG). Sodium dodecyl sulfate polyacrylamide gel electrophoresis (SDS-PAGE, see section 5.3.2 for details) was used to confirm if the induced expression was successful. Cells were harvested using centrifugation at 10,000 rpm for 10 min before being resuspended in 25 mL of 20 mM Tris-NaCl buffer (20 mM Trisaminomethane; 500 mM NaCl; pH 7.0). Two hundred microliters of 250 μM phenylmethylsulfonyl fluoride (PMSF), 25 μL DNAse and a few flakes of lysozyme were added to the resuspension mixture before French pressing three times. The supernatant was collected after centrifugation (15,000 rpm, 55 min, 4 °C) and filtered through 0.25 μm filters (Millipore).

5.3.2 SDS PAGE

One milliliter samples before and after IPTG induction were collected, centrifuged (13000 rpm, 10 min, 25 ^oC) and resuspended in 100 μL dH_2O. One hundred microliters of protein sample was mixed with 25 μL of 5X SDS sample loading buffer (Biorad) and then heated at 80 °C for 10 min. Ten microliters of each boiled sample solution as well as 10 μL of PageRuler™ protein ladder were then loaded into a premade 12% acrylamide Tris-Bis gel. SDS-PAGE sample solutions collected from the Ni-NTA washes and elutions were directly loaded onto the gel. The gel was run at a constant 120 mV for 2 hrs and stained using 50 mL of Coomassie R-250 solution for 40 min on a rocker. Gels were destained using 50 mL of premade destaining solution (30% methanol, 10% acetic acid in water) for 2 h.

5.3.3 Purification of Calmodulin-aurein fusion protein in *E.coli*

The supernatant described in section 5.3.1 was applied to a Ni-NTA $(His)_6$-tag protein binding column (GE Healthcare). Prior to the application of the supernatant, the column was cleaned with 10 mL 50 mM EDTA solution (3x), and 10 mL 0.5M NaOH (3x) before recharging

the column using 1ml of 0.1M $NiCl_2$. After loading the supernatant on to the Ni-NTA column, the column was washed with 10 column volumes of Tris-NaCl buffer until the OD_{280} of the washes were within 0.030 of the Tris-NaCl buffer blank. The His-tagged fusion protein was eluted with Tris-NaCl buffer, 400 mM imidazole, pH 7.5. The purity of the fusion protein was confirmed by SDS-PAGE. The Ni-NTA elutions were dialyzed overnight against 20 mM Tris-NaCl buffer at 4 °C (8k dialysis bag) to remove the excess imidazole.

5.3.4 Digestion of Calmodulin-aurein fusion protein

Tobacco Etch Virus (TEV) protease was prepared using the same expression protocol as described previously[276]. Prior to Tobacco Etch Virus (TEV) digestion of the eluted fusion protein, the dialyzed elutions were concentrated using 10k cut-off Amicon centrifuge tubes (4000 x rpm, 15 min, 4 ^oC) to a total final volume of 4-5 mL. Two hundred and fifty microliters of TEV protease was added for OD_{280} of 0.5 of the elutions. To this mixture EDTA and DTT were added, for a final concentration of 5 mM EDTA and 2 mM respectively. This solution was placed on a rocker for 24-48 h at 4 °C. MALDI-TOF was used to confirm the presence of the cleaved peptide and monitor the completion of the cleavage reaction. The peptide was purified using RP-HPLC.

5.3.5 MALDI-TOF

One microliter of the sample mixture was mixed with 1 μL of 5 mg/mL α-Cyano-4-hydroxycinnamic acid (CHCA) matrix solution (70% acetonitrile, 30% dH_2O, 0.1% TFA). The cleavage mixture was diluted (32-128 fold) in the α-Cyano-4-hydroxycinnamic acid solution to prevent formation of salt crystals. One microliter of each prepared sample solution was spotted onto a plate and dried completely. MALDI-TOF MS spectra were acquired using a Voyager-DE™ STR MALDI-TOF mass spectrometer.

5.3.6 Peptide purification by RP-HPLC

RP-HPLC purification of expressed aurein 2.2 was carried out using a similar protocol given in Chapter 2.3.1. Fractions were collected for each corresponding peak seen in the HPLC trace and confirmed using MALDI-TOF.

5.3.7 Peptide Esterification

Purified aurein 2.2 was esterified at the C-terminus and the aspartaic acid residue carboxylic acid moiety using the esterification protocol described previously[277]. Lyophilized peptide (1 mg) was dissolved in 2 mL of anhydrous methanol and sonicated for 10 min. 4 equivalents (450 μL) of TMSCl was added to the reaction mixture and stirred for 4 h. The progress of the reaction was monitored every 1 h using MALDI-TOF. After completion of the reaction, the solution was quenched with 6 mL dH_2O and immediately lyophilized for a second esterification reaction to ensure the peptide was diesterified. The final diesterified product was purified using RP-HPLC and characterized by MS/MS.

5.3.8 MIC Assays

The MICs of the esterified peptides against *S. aureus* (C622) were measured based on previously described methodology[113,138,215,235] and Chapter 2.3.6.

5.3.9 2D NMR

NMR spectra for solution state peptide samples were acquired on a Bruker 500 MHz instrument (Bruker Biospin, Milton, ON), operating at a ^{1}H frequency of 499.4 MHz. ^{1}H-^{15}N NMR spectra were collected using a Heteronuclear Single Quantum Coherence (HSQC) pulse sequence[278–280] at 298 K. The NMR sample was prepared to yield 0.5 mM ^{15}N labelled aurein peptide in 25% deuterated TFE and 10% D_2O (by volume), for a total sample volume of 600 μL.

For the intact whole bacterial cell studies, an overnight culture of *S. aureus* was grown in lysogeny broth (LB) and diluted to an OD_{600} of 0.8 which corresponds to approximately 10^6 CFU/mL. Two hundred fifty microliters of the bacterial sample were spun down and resuspended in 250 µL of 10 mM phosphate buffer and 50 µL was transferred to a NMR tube containing 0.35 mM (~500 µg/mL) ^{15}N aurein 2.2 (ester or carboxyl version dissolved in 10 mM phosphate) and 10% D_2O, for a total volume of 600 uL.

5.3.10 Scanning electron microscope studies

The morphology of the *S. aureus* cells in the presence of the aurein peptides was determined with SEM. Twenty microliters of expressed aurein 2.2 or diesterified aurein 2.2 (0.35 mM final concentration) were incubated with 20 µL of *S. aureus* (10^8 CFU/mL resuspended in 10 mM phosphate buffer) for 1 hour at 37 °C. Incubation mixtures were fixed using 2.5% glutaraldehyde and repeatedly washed with 0.1 M sodium cacodylate (pH=7.4), then subjected to post-fixation with 1% v/v osmium tetroxide. The fixed samples were washed three times with distilled water and dehydrated with a gradient series of ethanol (20-95% v/v). Cells were then dried with CO_2 in a Tousimis Autosamdri 815B critical-point dryer, mounted onto stubs, and gold sputter-coated for SEM using a Hitachi S-4700 field emission scanning electron microscope at various magnifications. Multiple images from different areas were captured.

5.4 Results And Discussion

5.4.1 Expression and purification of CaM-aurein 2.2

The expression of AMPs in bacteria has been previously studied using several fusion partners such as ketosteroid isomerase (KSI)[281] and small ubiquitin-related modifier (SUMO)[282]. The expression of KSI-melittin leads to inhibition of culture growth due to the toxic peptides whereas the expression of SUMO-melittin fusion results in poor culture growth after IPTG

induction[210]. On the other hand, the CaM fusion construct has been developed to express a handful of AMPs such as melittin, tritrpticin, fowlicidin, indolicidin, magainin II, human-β-defensin 2 and lactoferrampin B[210]. For the first time, we were able to express CaM-aurein 2.2 in LB and minimal media (M9). There was no "leaky" expression (expression before adding the inducer (IPTG)) of CaM-aurein 2.2 before IPTG expression as seen from the gel and a maximum protein expression level was reached between 3 to 4 h (Figure 5.2).

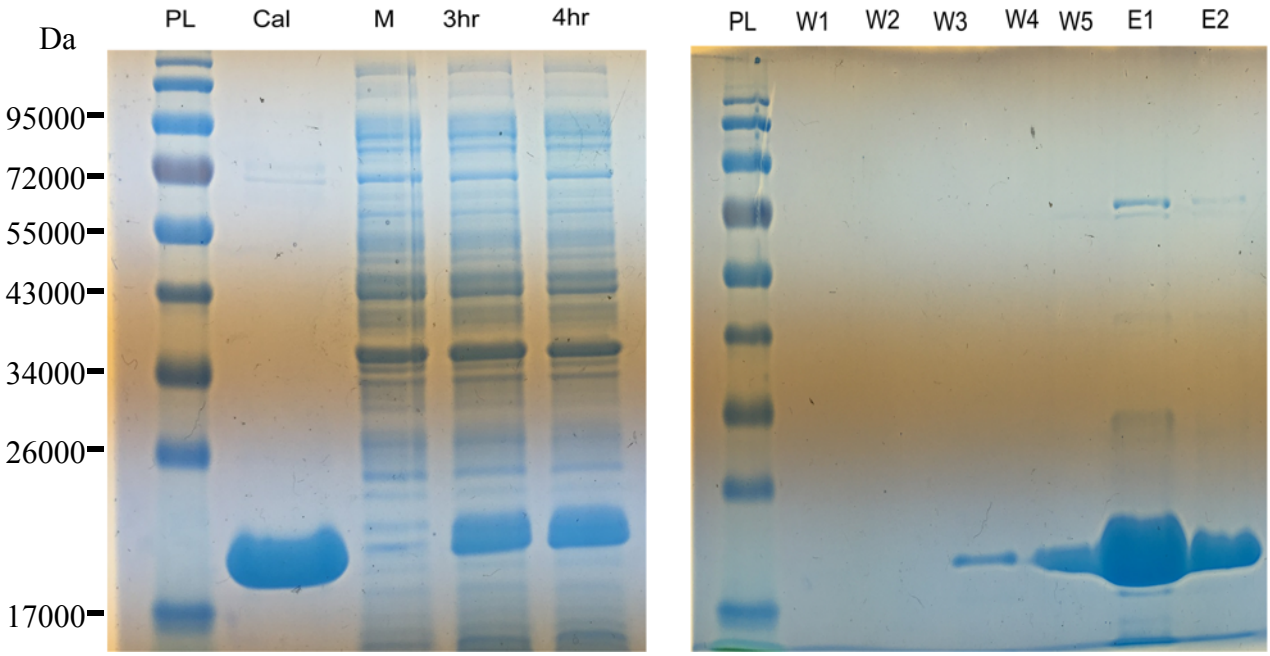

Figure 5.2: Expression and purification of CaM-aurein 2.2. SDS-PAGE (left) of samples from the *E. coli* expression cells taken at different times before and after IPTG induction (PL: protein ladder, Cal: commercial calmodulin, M: before IPTG induction). SDS-PAGE (right) of Ni-NTA column purification. After the sample was loaded, washes (W1 to W5) of the Ni-NTA resin were collected until A_{280} was similar to the buffer only (~0.03). Elution samples (E1 and E2) were collected using 400 mM elution buffer. Figure generated using PowerPoint.

Moreover, the presence of a polyhistidine $(His)_6$- tag at the N-terminus of the CaM-aurein 2.2 allowed for the purification directly via Nickel-NTA affinity chromatography (Figure 5.2). The washing with Tris-NaCl buffer removed most of the impurities. However, some high

molecular weight impurities coeluted with CaM-aurein 2.2 during the imidazole elution in the first 10 mL (E1), but the second 10 mL elution did not have any impurities. The impurities may be due to the non-specific interaction a bacterial protein containing adjacent histidine residues with the nickel-NTA or non polar interactions with the nickel-NTA resin[283]. A very high purity of the CaM-aurein 2.2 fusion protein is not necessary as the CaM-aurein 2.2 has to be cleaved and purified. As in the case for melittin, tritrpticin, fowlicidin, indolicidin, magainin II, human-β-defensin 2 and lactoferrampin, the CaM fusion system was able to mask the antimicrobial activity of aurein 2.2 and protect it from degradation during expression.

5.4.2 Cleavage of CaM-aurein 2.2 and purification of aurein 2.2

After purification, the CaM-aurein 2.2 fusion protein was dialyzed overnight in digestion buffer and subjected to TEV protease. The cleavage was monitored by MALDI-TOF and after 48 h the cleavage was complete. After optimization of the digestion buffer, complete cleavage of the fusion protein lead to the appearance of two distinct MALDI-TOF peaks, namely the CaM at 20,193 Daltons (Figure 5.3) and that for aurein 2.2 peak at 1618 Daltons (Figure 5.5). Incomplete cleavage causes the appearance of CaM-aurein 2.2 at 21,782 Daltons (Figure 5.3). Upon complete cleavage, the reaction mixture was filtered and HPLC purified. HPLC peaks were identified by MALDI-TOF and the aurein 2.2 was successfully purified (Figure 5.4). Aurein 2.2 eluted after cleaved CaM, as would be expected for a more hydrophobic peptide. The hydrophilic water soluble CaM allows the largely hydrophobic aurein 2.2 to be well solubilized during the expression and purification process. The final yield of aurein 2.2 was approximately 1-2 mg per 1 L culture (similar yields in M9 media and LB).

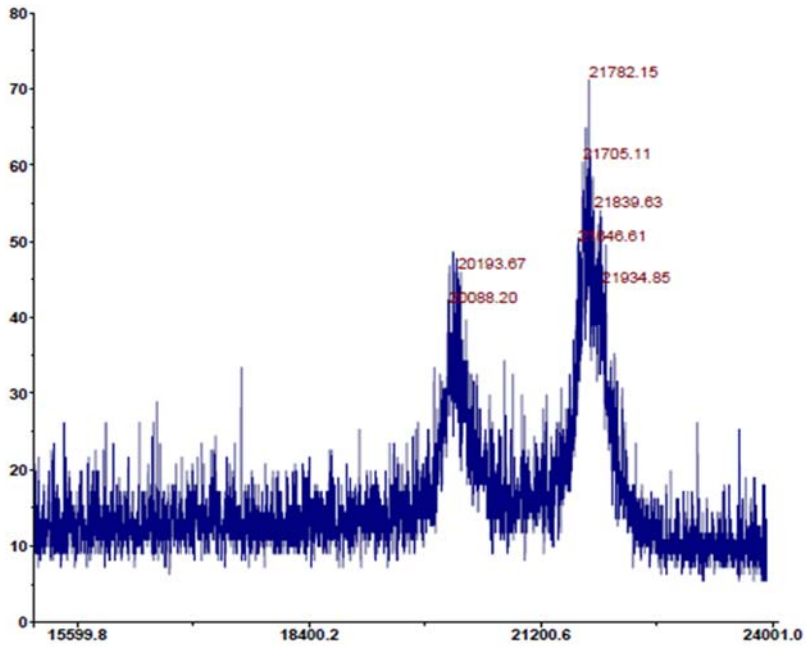

Figure 5.3: MALDI-TOF of the cleavage mixture. The peaks with maxima at m/z of 21782.15 and 20193.67 correspond to the CaM-aurein 2.2 and CaM, respectively. Figure generated using data explorer and Adobe.

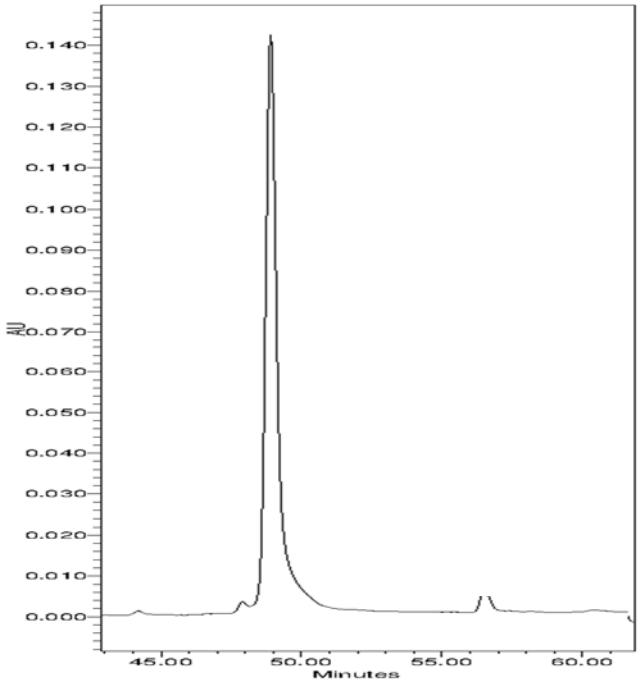

Figure 5.4: HPLC purification of the cleaved CaM-aurein 2.2. CaM elutes between 48-60 minutes, where as the more hydrophobic aurein 2.2 elutes between 56-57 minutes. Figure generated using Adobe.

5.4.3 Chemical esterification of aurein 2.2 retains antimicrobial activity.

One of the major disadvantages of expressing AMPs in most bacterial expression system is the inability to express peptides in the active amidated form. As mentioned in Chapter 1, most AMPs such as aurein 2.2 require the C-terminus to be amidated to exhibit antimicrobial activity[113,138,139,215]. Expressed aurein 2.2 consists of a carboxylic acid at the C-terminus (aurein 2.2-COOH) and was inactive against *S. aureus* (Table 5.1) with an MIC greater than 250 μg/mL compared to the synthetic amidated aurein (MIC of 32 μg/mL). Many enzymatic methods such as transacylation[284] and amidation[285] have been utilized to neutralize the negative charge of the carboxylic acid at the C-terminus of expressed peptides. These methods are usually time consuming and expensive. Using a previous reported[277] TMSCl/methanol protocol to esterify various amino acids, we were able to rapidly and selectively esterify the C-terminus and the aspartic acid of the expressed aurein 2.2 (diesterification, 2 CH_3 group, ~ +30 Daltons) (Figure 5.5) within an hour of the reaction, however monoesterified (~ +15 Daltons) products were also obtained.

Hence, to completely diesterify aurein 2.2, the reaction mixture was freeze dried and esterified with TMSCl/methanol again. The diesterification product was purified by HPLC and the antimicrobial activity was determined. The MS/MS (Appendix D.1) analysis of the purified diesterfied aurein 2.2 confirmed the addition of a CH_3 group at the aspartic acid and the C-terminus. Diesterification of aurein 2.2 partially rescued the antimicrobial activity of the expressed peptide with an MIC of 64 μg/mL compared to the synthetic amidated aurein 2.2 (32 μg/mL). Esterification of the aspartic acid could affect the structure and mechanism of action of aurein 2.2 as it has been recently suggested that aurein 2.2 forms ion selective pores in the membrane of *Bacillus subtilis* and that the aspartic acid may be involved in binding select

cations[140]. Future work should involve the selective removal of the ester from the aspartic acid or specific esterification or amidation of the C-terminus.

Table 5.1: Antimicrobial activity of expressed and synthetic aurein 2.2

Peptide	MIC *S. aureus* C622 (µg/mL)
Aurein 2.2 (synthetic) (GLFDIVKKVVGALGSL-$CONH_2$)	32
Aurein 2.2 (expressed) (GLFDIVKKVVGALGSL-COOH)	>250
Aurein 2.2 (expressed and diesterified) (GLFD*IVKKVVGALGSL-$COOCH_3$)	64

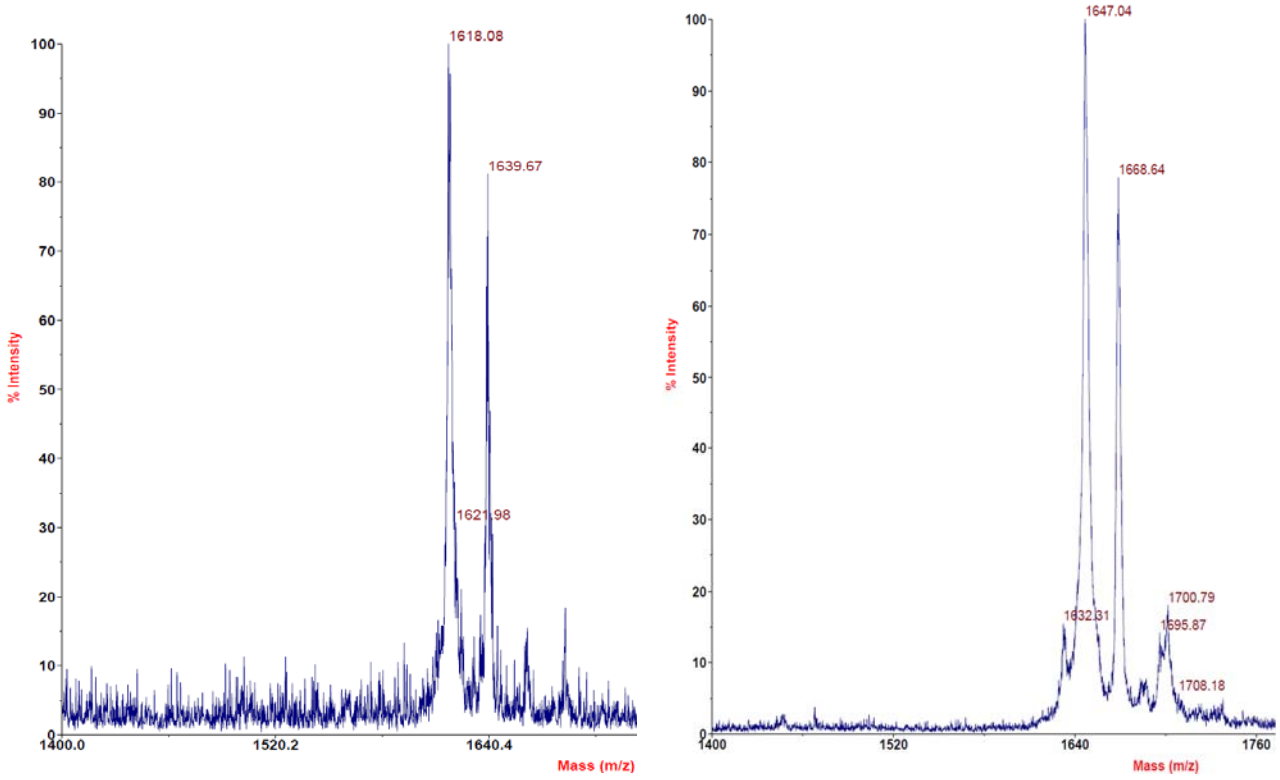

Figure 5.5: MALDI-TOF of aurein 2.2 (left) and diesterified aurein 2.2 (right). The 1618.08 (right spectra) peak corresponds to aurein 2.2-COOH. The 1647.99 peak, correspond to the diesterified aurein 2.2 and its sodium adduct (~+23) respectively. Monoesterified product is at 1632.32. Figure generated using Data explorer and Adobe.

5.4.4 Whole cell NMR and SEM

Recently a handful of studies have been reported to investigate the interaction of AMPs with living bacterial cells. Some techniques used include live cell imaging[116], CD[286] and NMR[211,271] spectroscopy. To determine the interaction of aurein 2.2 with living S. *aureus*, we incubated ^{15}N-labelled aurein 2.2 with S. *aureus* and acquired ^{1}H,^{15}N-HSQC NMR spectra at different time points. Comparing the ^{1}H,^{15}N-HSQC spectra of expressed aurein 2.2 and diesterified aurein 2.2, we can see clear differences between at the different time points (Figure 5.6). Expressed aurein 2.2 (aurein 2.2-COOH), which is inactive against S. *aureus,* does not show any differences after 1, 2 and 3 h of incubation, whereas in the spectra of diesterified aurein 2.2 the peak intensity decreased drastically with respect to time (Figure 5.6).

Amidated aurein 2.2 targets the bacterial membrane by inserting and forming ion selective pores which is consistent with the toroidal pore model[140]. The drastic decrease in peak intensity could be explained by the fact that diesterified aurein 2.2 inserts into the membrane of *S. aureus* which leads to slower tumbling of the peptide in solution and faster relaxation of transverse magnetization (short T_2) resulting in line broadeing[287]. The sharp peaks seen at the end of 3 hours when all the bacteria were killed could be from unbound peptide, freely tumbling in solution. In contrast, the aurein 2.2-COOH spectra does not show any significant decrease in peak intensity indicating the peptides do not bind and insert into the membrane and hence are inactive against *S. aureus.* Aurein 2.3-COOH, another inactive AMP against *S. aureus* does not bind to PC/PG model membranes as effectively as its amidated counterpart, despite still forming an alpha helical structure[139]. Expressed aurein 2.2-COOH shows a similar behavior as it is

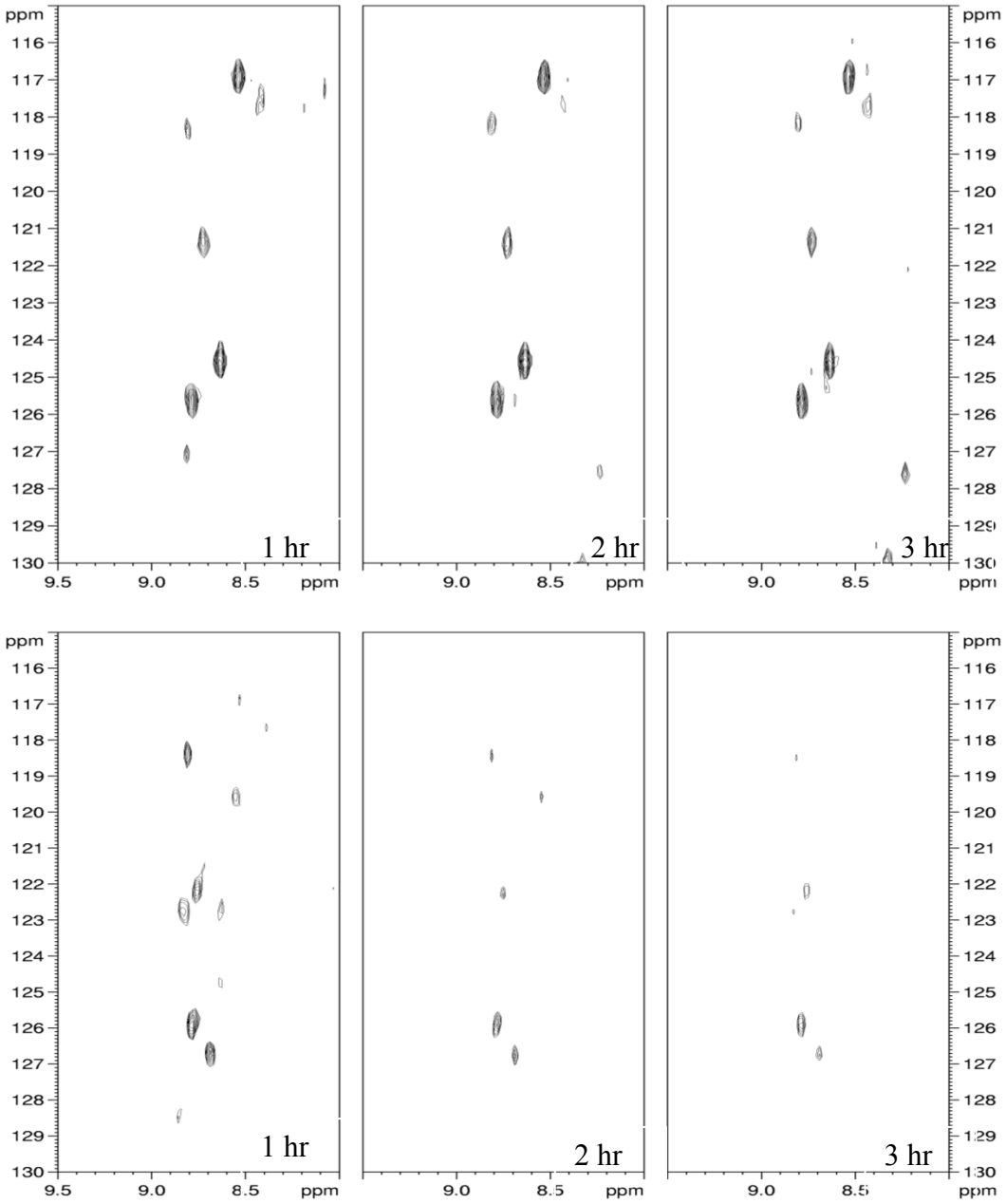

Figure 5.6: $^{1}H,^{15}N$-HSQC spectra of whole *S. aureus* cells with the aurein peptides. Aurein 2.2-COOH (top) and diesterified aurein 2.2 (bottom) were mixed with *S. aureus* cells and the spectra were acquired during 1, 2 and 3 hours of incubation. The start contour levels, number of levels and the level multiplier for aurein 2.2-COOH was $2x10^{7}$, 16 and 1.2 respectively, for all the time points whereas for diesterified aurein 2.2 they were set to $8.5x10^{7}$, 16 and 1.2 respectively.

inactive but can form alpha helical structures, whereas diesterified aurein 2.2 is active and can form an alpha helical structure (Figure 5.7). It will be interesting in the future to express an AMP that is not membrane active but has intracellular targets and study the interaction with live *S. aureus* cells via $^{1}H,^{15}N$-HSQC as intracellular protein/peptides that are more freely tumbling are easier to visualize by NMR[288,289]. The expression system could potentially also be used to determine the structure of bioconjugates of AMPs and their interaction with live bacterial cells.

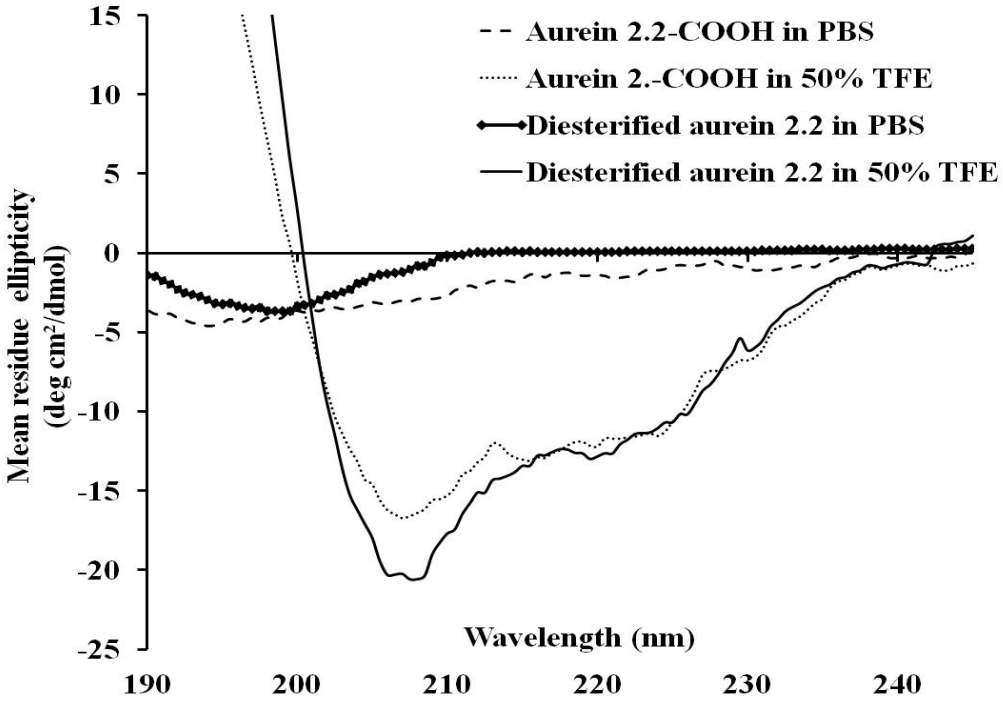

Figure 5.7: CD spectra of expressed peptides. Both aurein 2.2-COOH and diesterified aurein 2.2 adopt an alpha helical structure in trifluoroethanol (TFE). Figure generated using data Graphpad prism.

In order to visualize the *S. aureus* during the NMR experiment, we collected SEM images post 1 hour incubation with the peptides (Figure 5.8). In both the samples, the *S. aureus* seems to aggregate but clear differences can be seen. In the case of aurein 2.2-COOH, the S. *aureus* are round and intact whereas the S. *aureus* cells are smaller and lysed when treated with diesterified

aurein 2.2 (Figure 5.8). There is also more lipid and cell debris in the latter case from the ruptured cells. Similar distortions have been observed when *S. aureus* is treated with PGla, a α-helical peptide from the magainin family that can destroy bacteria by interacting with the lipid membrane[290].

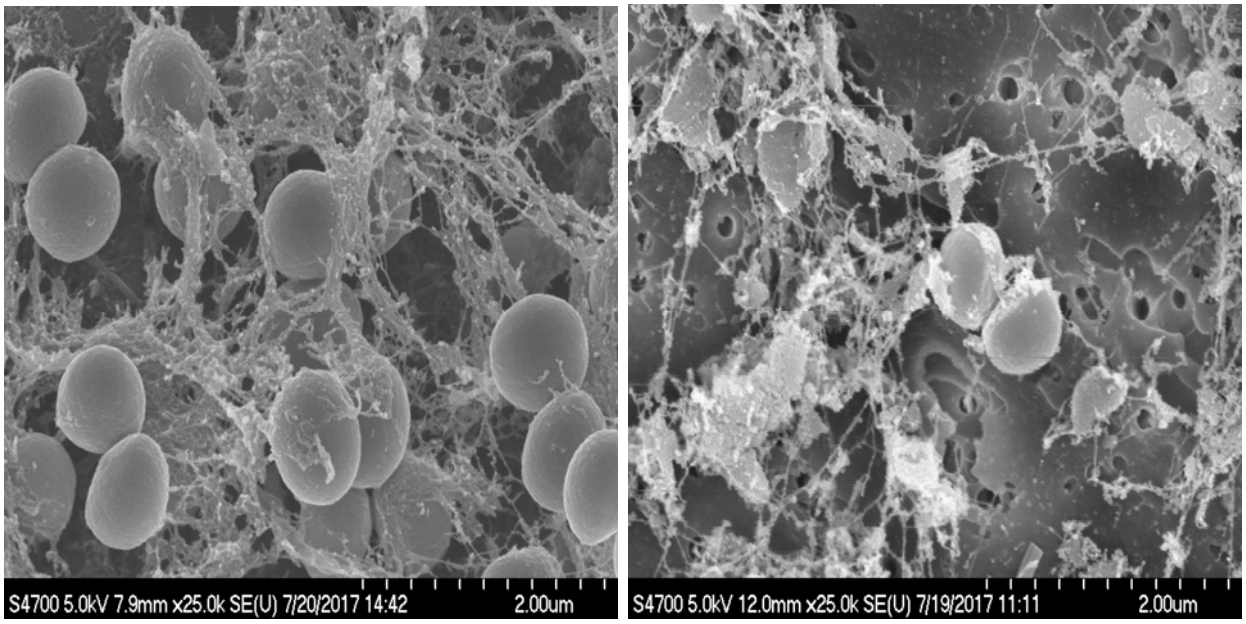

Figure 5.8: SEM of *S. aureus* after incubating for 1 h with aurein 2.2-COOH (left) and diesterified aurein 2.2 (right). The cells look smaller and compact when treated with diesterified aurein 2.2. Figure generated using PowerPoint.

5.5 Summary

In this chapter, for the first time we report a protocol for overexpression and purification of aurein 2.2 using a bacterial expression system. The aurein peptide obtained was inactive against *S. aureus* because of the free carboxylic acid at the C-terminus. Diesterification of the C-terminus and the aspartic acid carboxylic acids was confirmed by MALDI-TOF and MS/MS, which rescued the antimicrobial activity of the peptide against *S. aureus.* The interaction of diesterified aurein 2.2 and aurein 2.2-COOH with live *S. aureus* was probed using $^{1}H,^{15}N$-HSQC

NMR spectroscopy and it was confirmed that diesterified aurein 2,2 binds to bacterial membranes, whereas aurein 2.2-COOH does not interact with the bacterial membrane, in agreement with previously reported results. SEM studies further confirmed that diesterified aurein 2.2 causes significant morphological changes of the bacterial membrane, whereas aurein 2.2-COOH does not. This system will not only allow us to just study the structure of the AMPs and bioconjugates but collect dynamic NMR data with living cells in the future.

Chapter 6: Conclusions and Future work

6.1 Conclusions

Antimicrobial peptides are unique molecules that are promising candidates to treat multidrug resistant organisms[291]. Interestingly, AMPs have many mechanisms of action and can also display antiviral[51] and anticancer activities[292]. Although many AMPs have been identified and characterized, not many were able make it to clinical trials and only a few have been approved by the US Food and Drug Administration (FDA) due to issues with toxicity, protease cleavage and rapid kidney clearance[23,105,141]. Over the last decade, different strategies have been utilized to resolve these issues to improve the efficacy of AMPs to push forward their development as therapeutic agents. This thesis examined various approaches from designing new AMPs, using delivery systems for AMPs to decrease the toxicity and studying the mechanism of action of AMPs.

The conjugation of AMPs to polymers like PEG leads to improved characteristics such as lower toxicity, prevention of proteolytic cleavage and increased blood half-life[160]. We hypothesized that conjugation of aurein 2.2 would have similar benefits. In Chapter 2, we developed the chemistry and for the first time conjugated aurein 2.2 to hyperbranched polyglycerol (HPG), a biocompatible polymer. We were able to demonstrate that the conjugation lead to decreased toxicity of AMPs toward mammalian cells such as fibroblasts and to blood components such as red blood cells, complement system and platelets. The neutral charge and hydrophobic masking effect of HPG likely contributes to the diminished toxicity of the conjugates. Although the antimicrobial activity of the aurein 2.2 conjugates was decreased, it was not as severe as PEG conjugates reported in the literature[166–168]. This may be due to the fact that multiple peptides were attached to HPG compared to PEG which typically has one or two

peptides per polymer molecule; hence a polymer with multiple functional groups is advantageous over a polymer with limited functionalities.

Furthermore in Chapter 3, we hypothesized that the strategic design of a peptide array would yield at least a few peptides with significantly better antimicrobial activity. From the array we got two hits, peptide 73 and 77 which had specific arginine and tryptophan substitutions and were 4 times more active than aurein 2.2. Although arginine and tryptophan substitutions generally lead to an increase in activity[232], the specific correlation between activity and the location of these substitutions are more complicated to predict. Hence SPOT synthesis arrays were a good strategy as they permit the synthesis and testing of many peptides. Indeed, many of the peptides in the array were not as active as the parent peptide. Software programs such as quantitative structure-activity relationship (QSAR), could have been used to design AMPs with better antimicrobial activities but an initial dataset, which comes from the systematic peptide array, is required[233]. This chapter also described the successful conjugation of a more active peptide such as 77c to HPG and showed that this leads to a conjugate with higher antimicrobial activity and alleviation of the toxicity, as was the case in Chapter 2. The conjugates were also resistant to proteolytic degradation. This suggests that HPG could be used as a generic polymer scaffold for various AMPs.

AMPs have been conjugated to various polymers such as PEG, chitosan, hyaluronic acid[293] but the influence on polymer molecular weight on activity and biocompatibility of the AMPs has not been investigated to date. The remainder of the studies in Chapter 3 showed that a decrease in molecular weight of HPG leads to increase in activity, but does not have any significant effect on the biocompatibility, again suggesting the usefulness of HPG (22K HPG-77

being the most active). Finally, through our search for more active HPG conjugates, we have also made AMPs (peptide 73 and 77) which have diverse activities.

In Chapter 4, we explored the activities of peptide 73 and 77. As mentioned in Chapter 1, AMPs can have other activities such as antibiofilm and wound healing[44]. Aurein 2.2 has no antibiofilm activity, but peptide 73 and 77 were both found to be highly active against *S. aureus* biofilms. This indicates that peptides can have different activities and that the mechanism of action to kill bacteria in planktonic state and in a biofilm may be different. As the peptides and conjugates had good *in vitro* activity against *S. aureus*, we investigated the *in vivo* activity in mice abscess model. Interestingly, the *in vivo* data suggested that aurein 2.2 and peptide 73 were equally effective in mice even though their antimicrobial activity *in vitro* is very different. However, if one considers the balance between activity and toxicity, i.e. the therapeutic index, both aurein 2.2 and peptide 73 were very similar. This clearly indicates that one needs to consider the *in vivo* toxicity of AMPs and not just their antimicrobial activity during the design of these peptides[233]. It is also extremely critical to test parent peptides in an *in vivo* model before designing peptide arrays, as the parent peptide might be highly active *in vivo* (as in the case of aurein 2.2 compared to 73). In the case of aurein 2.2, further design of the peptide lead to peptide 73, which has additional antibioflim activity (which aurein 2.2 does not have). An *in vivo* antibiofilm model would be useful to determine whether this improvement is significant.

Chemical modification of AMPs such as the use of non natural[149], D-amino acids[146], and cyclization[152] has been used to prevent proteolytic cleavage and this typically leads to the improved activity of AMPs. The development of D-73 (a peptide with all D-amino acids) resulted in a peptide with similar antimicrobial activity as the parent peptide, but increased toxicity *in vitro*. The toxicity of D-73 required micellar encapsulation of the peptide within

DSPE-PEG2000 to exhibit any activity *in vivo*. The encapsulation of peptide within the micelle masks the toxicity of the D-peptides. As the encapsulation formulation for D-73 is as effective as peptide 73 without a delivery system, one could conclude that the synthesis or purchase of expensive D-peptides does not necessarily yield a better drug candidate. On the other hand, the micellar encapsulation was very effective in general as it does not only improve the toxicity, but also increases the solubility of the peptides (e.g. as for peptide 73c). In other words, a careful choice of amino acid sequence and formulation needs to be taken into account when developing an optimal antimicrobial with good activity and low toxicity.

In recent years, many covalent delivery systems have been designed to further the pursuit of developing AMPs[160]. Although the attachment of AMPs to polymers also improves various *in vitro* properties such as toxicity, solubility and protease cleavage, as seen in Chapter 2 and 3, the best *in vitro* conjugate (22k HPG-73c) was ineffective in the mouse abscess model. However, the non covalent micellar encapsulation delivery systems discussed above were very effective. The data suggests that the better strategy requires peptides to be released from the delivery system to effectively kill bacteria and heal abscesses. Again it is important to investigate the effectiveness of the conjugates both in an *in vivo* and *in vitro* model, as the activities can differ drastically.

Finally, as described in Chapter 1.2, it is important to study the mechanism of action of AMPs in order to understand how they function and to help in the design of better AMPs. As a proof of concept, we showed in Chapter 5 how AMPs can be expressed and how the antimicrobial activity of the expressed aurein 2.2 can be rescued by simple esterification. This approach could be extended to a range of expression systems developed to produce AMPs[284,285]. We demonstrated that obtaining active isotopically labeled AMPs is feasible. This opens the door

for various whole cell NMR experiments. With whole cell $^{1}H,^{15}N$-HSQC NMR experiments, we were able to confirm the mechanism of action of aurein 2.2, which binds to the bacterial membrane. Future whole cell experiments may provide new insight into the differences in mechanism of action of various peptides and conjugates, in particular in the case where the mechanism of action of the AMPs involves intracellular targets.

6.2 Future work

Studies in this thesis have revealed significant insight into the *in vitro* and *in vivo* activities of AMPs, which has in turn opened many avenues to explore. In Chapter 3, we developed peptide 73 on the basis of the *in vitro* antimicrobial activities alone, however, in Chapter 4 the *in vivo* data indicated that the toxicity profiles also need consideration. Future development of AMPs (peptide array) should consider both the toxicity such as RBC lysis and the antimicrobial activity, i.e. the therapeutic index, so that peptides with moderate antimicrobial activities are not overlooked[294,295]. For example, the aurein 2.2 parent peptide had moderate *in vitro* activity as compared to peptide 73, but their therapeutic indices were similar and could be used to account for their similar *in vivo* activity. The peptide with the best therapeutic index should also be used as the parent peptide for further development of the AMPs (peptide arrays). In addition, as most QSAR programs used to design novel AMPs only consider the antimicrobial activity of the peptides[233], it will be useful if the method could be expanded and the therapeutic indices were also considered for a more efficient design.

In this thesis, the mechanism of action (MOA) of the peptides 73 and 77 was not investigated. Many arginine and tryptophan rich peptide target the bacterial membrane[232] but recent oriented CD results (data not shown) from our lab suggest that peptide 73 and 77 do not insert into model membranes as effectively as aurein 2.2. Membrane leakage data also indicates

that peptide 73 and 77 cause less leakage as compared to aurein 2.2. It is hence possible that peptide 73 and 77 target other bacterial components, such as the cell wall or intracellular components. The expression system utilized in Chapter 5 could be used to produce isotopically labeled 73 and 77, in order to probe the interaction with live bacteria and compare it to the results on aurein 2.2 presented in Chapter 5. Moreover, this labelling approach could be used in conjunction with experiments that rely on isotopic labelling of the bacterial cells. For instance, recent studies examined the changes in bacterial cell wall composition using solid state ^{13}C-CPMAS NMR experiments. The general MOA could be elucidated using whole cells treated with fosfomycin, a cell wall biosynthesis inhibitor, as the spectra shown a clear reduction in peptidoglycan composition. This was in contrast to cells treated with chloramphenicol, a protein synthesis inhibitor, which contained a higher percentage of peptidoglycan but a reduction in the cytoplasmic protein content[211]. Finally, for further pinpointing the MOA of peptides 73 and 77, additional methods could be used. If the peptides inhibit protein synthesis then ^{13}C and ^{15}N CPMAS NMR can be used to detect intact whole cell NMR of ribosomes and possibly the interaction of ribosomes with peptide 73 and 77[271]. AMPs such as indolicidin, an arginine and tryptophan rich peptide, target other intracellular components such DNA filamentation in *E. coli* cells and has the ability to bind DNA and membranes[296,297]. DNA binding experiments of peptide 73 and 77 could be performed by isothermal titration calorimetry (ITC) or NMR spectroscopy to determine the binding affinity. The expression system developed in Chapter 5 could be used to produce isotopically labeled 73 and NMR experiments could be used, for instance, to measure the distance between the ^{15}N in the peptide and ^{31}P in the DNA (e.g. using REDOR) and thus provide structural insight into the interactions involved. Such methods would work if the binding interactions were strong[211,298,299].

Preliminary results in Chapter 4 show that peptide 73 and 77 also display superior antibiofilm activity compared to aurein 2.2. Bacteria in biofilms regulate stress response pathways which include signaling molecules such as Guanosine 5'-diphosphate 3'-diphosphate (ppGpp) and Guanosine 5'-triphosphate 3'-diphosphate (pppGpp). Peptide 73 and 77 have similar antibiofilm activity when compared to AMPs such as DJK-5 and IDR-1018 that have been shown to bind and degrade these signaling molecules[207,300]. It would be interesting to investigate the binding interaction of peptide 73 and 77 with ppGpp and/or pppGpp and with other nucleotide signaling molecules which are involved in the cells energy transformation such as cyclic adenine monophosphate (cAMP)[301].

Furthermore, *in vivo* studies in Chapter 4 show that HPG-73c was not effective in the mouse abscess model, whereas the DSPE-PEG2000 encapsulated 73c showed excellent activity. These results indicate that the peptide needs to be released from the delivery vehicle to exhibit any antimicrobial activity *in vivo*. The development of an acid cleavable functional group such as an ester or specific enzymatic cleavable linker between peptide 73 and HPG would allow for release of the peptide at the site of infection (Figure 6.1). Many bacterial and host enzymes are released at the site of infection: for example, bacteria typically release gelatinase that are involved in tissue damage in host[302,303]. Host cells (including immune cells) also release enzymes such as the matrix metalloproteases (MMPs) which play an important role in various host responses such as combating bacterial infections, inflammatory response and tissue remodeling[304].

Figure 6.1: Design of HPG-73 conjugate that would lead to the release of peptide 73 at the site of infection. The cleavage site could be an acid cleavable functional group such as an ester or specific enzyme cleavable. Figure generated using PowerPoint.

Recently, Qi et al. developed chitosan-AMP-PEG conjugates which assembled into nanoparticles and were cleaved by bacterial (*S. aureus*) gelatinase, MMP-2 and MMP-9 to expose the peptide on the chitosan to exhibit antimicrobial activity *in vivo* and *in vitro*[305]. Although the AMP was not released in this example, a similar strategy could be used to design HPG-73 conjugates that would lead to the release of the peptides at the site of infection. An enzymatically cleavable linker would require incorporation of additional amino acids in the peptide sequence which can be easily designed during the peptide synthesis, however, it should be noted that peptide 73 was derived from aurein 2.2 which requires the N-terminus for activity[113,138,139,215], therefore, additional amino acids should most likely be incorporated at the C-terminus.

Finally, the data from Chapter 4 indicated that only 60-70% of peptide 73c was encapsulated in DSPE-PEG2000 micelles. Future studies should ensure that the DSPE-PEG2000 concentration in increased or a different micelle forming agent could be used that will allow better encapsulation efficiency (close to 100% of the peptide being encapsulated) before the *in vivo* experiments. The PEG in DSPE-PEG comes in various molecular weights (2000, 3000 and 5000) and consequently different critical micellar concentrations[306]. The effect of the PEG chain length on encapsulation efficiency of the peptide should be investigated. Moreover, DSPE-PEG2000 has been FDA approved for the delivery of Doxil® (Doxorubicin), an anticancer drug[307], however the formulation was composed of liposomes instead of micelles. Liposomal

(DSPE-PEG based) encapsulation of LL37 has also lead to improved toxicity of the peptides *in vitro*[162]; therefore it will be useful to encapsulate peptide 73c or D-73 using DSPE-PEG based liposomes in the future to determine whether this would increase the *in vivo* efficacy.

Overall, the *in vitro* studies suggested above will further our understanding on the antimicrobial and antibiofilm mechanism of action of peptide 73 and 77, whereas the *in vivo* studies will give insights into the factors that are important for development of AMPs as drugs. Both of these aspects are important for the development of new AMPs. I believe the work presented in this thesis provides some of the general guidelines for future work and hopefully will serve as an inspiration and stepping stone for the future development of AMPs into clinical trials. With the emergence of antibiotic resistance and the fact that many AMP based drugs are under development, the next decade will reveal the benefits of these novel compounds and may lead to commercial development of these agents.

Bibliography

(1) Bassett, E. J.; Keith, M. S.; Armelagos, G. J.; Martin, D. L.; Villanueva, A. R. Tetracycline-Labeled Human Bone from Ancient Sudanese Nubia (A.D. 350). *Science* **1980**, *209* (4464), 1532–1534.

(2) Forrest, R. D. Early History of Wound Treatment. *J. R. Soc. Med.* **1982**, *75* (3), 198–205.

(3) Drews, J. Paul Ehrlich: Magister Mundi. *Nat. Rev. Drug Discov.* **2004**, *3* (9), 797–801.

(4) Henderson, J. W. The Yellow Brick Road to Penicillin: A Story of Serendipity. *Mayo Clin. Proc.* **1997**, *72* (7), 683–687.

(5) Brown, L.; Wolf, J. M.; Prados-Rosales, R.; Casadevall, A. Through the Wall: Extracellular Vesicles in Gram-Positive Bacteria, Mycobacteria and Fungi. *Nat. Rev. Microbiol.* **2015**, *13* (10), 620–630.

(6) Cabeen, M. T.; Jacobs-Wagner, C. Bacterial Cell Shape. *Nat. Rev. Microbiol.* **2005**, *3* (8), 601–610.

(7) Shockman, G. D.; Barrett, J. F. Structure, Function, and Assembly of Cell Walls of Gram-Positive Bacteria. *Ann. Rev. Microbiol* **1983**, *37*, 501–527.

(8) Fischbach, M. A. Antibiotics from Microbes: Converging to Kill. *Curr. Opin. Microbiol.* **2009**, *12* (5), 520–527.

(9) Yocum, R. R.; Rasmussen, J. R.; Strominger, J. L. The Mechanism of Action of Penicillin. Penicillin Acylates the Active Site of Bacillus Stearothermophilus D-Alanine Carboxypeptidase. *J. Biol. Chem.* **1980**, *255* (9), 3977–3986.

(10) Hu, Y.; Liu, A.; Vaudrey, J.; Vaiciunaite, B.; Moigboi, C.; McTavish, S. M.; Kearns, A.; Coates, A. Combinations of β-Lactam or Aminoglycoside Antibiotics with Plectasin Are Synergistic against Methicillin-Sensitive and Methicillin-Resistant Staphylococcus Aureus. *PLoS One* **2015**, *10* (2), e0117664.

(11) Abraham, E. P.; Chain, E. An Enzyme from Bacteria Able to Destroy Penicillin. 1940. *Rev. Infect. Dis. 10* (4), 677–678.

(12) Kumar, S.; Singh, B. R. An Overview of Mechanisms and Emergence of Antimicrobials Drug Resistance. *Curr. Sci.* **2009**, *96* (11), 2307–8316.

(13) Blair, J. M. A.; Webber, M. A.; Baylay, A. J.; Ogbolu, D. O.; Piddock, L. J. V. Molecular Mechanisms of Antibiotic Resistance. *Nat. Rev. Microbiol.* **2014**, *13* (1), 42–51.

(14) Coculescu, B.-I. Antimicrobial Resistance Induced by Genetic Changes. *J. Med. Life* **2009**, *2* (2), 114–123.

(15) Davies, J.; Davies, D. Origins and Evolution of Antibiotic Resistance. *Microbiol. Mol. Biol. Rev.* **2010**, *74* (3), 417–433.

(16) Kraker de, M. E. A.; Stewardson, A. J.; Harbarth, S.; Pilcher, D.; Bellomo, R. Will 10 Million People Die a Year Due to Antimicrobial Resistance by 2050? *PLoS Med.* **2016**, *13* (11), e1002184.

(17) Ventola, C. L. The Antibiotic Resistance Crisis: Part 1: Causes and Threats. *P T* **2015**, *40* (4), 277–283.

(18) Martínez, B.; Rodríguez, A.; Suárez, E. Antimicrobial Peptides Produced by Bacteria: The Bacteriocins. In *New Weapons to Control Bacterial Growth*; Springer International Publishing: Cham, 2016; pp 15–38.

(19) Nes, I. F.; Brede, D. A.; Diep, D. B. Class II Non-Lantibiotic Bacteriocins. In *Handbook of Biologically Active Peptides*; Elsevier, 2013; pp 85–92.

(20) Mattick, A. T. R.; Hirsch, A.; Berridge, N. J. Further Observations on an Inhibitory Substance (Nisin) from Lactic Streptococci. *Lancet* **1947**, *250* (6462), 5–8.
(21) Bhattacharjee, M. K. Antibiotics That Inhibit Cell Wall Synthesis. In *Chemistry of Antibiotics and Related Drugs*; Springer International Publishing: Cham, 2016; pp 49–94.
(22) Chee-Sanford, J. C.; Mackie, R. I.; Koike, S.; Krapac, I. G.; Lin, Y.-F.; Yannarell, A. C.; Maxwell, S.; Aminov, R. I. Fate and Transport of Antibiotic Residues and Antibiotic Resistance Genes Following Land Application of Manure Waste. *J. Environ. Qual.* **2009**, *38* (3), 1086.
(23) Jenssen, H.; Hamill, P.; Hancock, R. E. W. Peptide Antimicrobial Agents. *Clin. Microbiol. Rev.* **2006**, *19* (3), 491–511.
(24) Chatterjee, S.; Chatterjee, S.; Lad, S. J.; Phansalkar, M. S.; Rupp, R. H.; Ganguli, B. N.; Fehlhaber, H. W.; Kogler, H. Mersacidin, a New Antibiotic from Bacillus. Fermentation, Isolation, Purification and Chemical Characterization. *J. Antibiot. (Tokyo).* **1992**, *45* (6), 832–838.
(25) Skarnes, R. C.; Watson, D. W. Antimicrobial Factors of Normal Tissues and Fluids. *Bacteriol. Rev.* **1957**, *21* (4), 273–294.
(26) Steiner, H.; Hultmark, D.; Engström, Å.; Bennich, H.; Boman, H. G. Sequence and Specificity of Two Antibacterial Proteins Involved in Insect Immunity. *Nature* **1981**, *292* (5820), 246–248.
(27) Patterson-Delafield, J.; Szklarek, D.; Martinez, R. J.; Lehrer, R. I. Microbicidal Cationic Proteins of Rabbit Alveolar Macrophages: Amino Acid Composition and Functional Attributes. *Infect. Immun.* **1981**, *31* (2), 723–731.
(28) Okada, M.; Natori, S. Purification and Characterization of an Antibacterial Protein from Haemolymph of Sarcophaga Peregrina (Flesh-Fly) Larvae. *Biochem. J.* **1983**, *211* (3), 727–734.
(29) Zasloff, M. Magainins, a Class of Antimicrobial Peptides from Xenopus Skin: Isolation, Characterization of Two Active Forms, and Partial CDNA Sequence of a Precursor. *Proc. Natl. Acad. Sci. U. S. A.* **1987**, *84* (15), 5449–5453.
(30) Tam, J. P.; Wang, S.; Wong, K. H.; Tan, W. L. Antimicrobial Peptides from Plants. *Pharmaceuticals (Basel).* **2015**, *8* (4), 711–757.
(31) Nawrot, R.; Barylski, J.; Nowicki, G.; Broniarczyk, J.; Buchwald, W.; Goździcka-Józefiak, A. Plant Antimicrobial Peptides. *Folia Microbiol. (Praha).* **2014**, *59* (3), 181–196.
(32) Stotz, H. U.; Thomson, J. G.; Wang, Y. Plant Defensins: Defense, Development and Application. *Plant Signal. Behav.* **2009**, *4* (11), 1010–1012.
(33) Craik, D. J. Host-Defense Activities of Cyclotides. *Toxins (Basel).* **2012**, *4* (12), 139–156.
(34) Hancock, R. E. W.; Brown, K. L.; Mookherjee, N. Host Defence Peptides from Invertebrates – Emerging Antimicrobial Strategies. *Immunobiology* **2006**, *211* (4), 315–322.
(35) Bachere, E.; Gueguen, Y.; Gonzalez, M.; de Lorgeril, J.; Garnier, J.; Romestand, B. Insights into the Anti-Microbial Defense of Marine Invertebrates: The Penaeid Shrimps and the Oyster Crassostrea Gigas. *Immunol. Rev.* **2004**, *198* (1), 149–168.
(36) Iwanaga, S.; Kawabata, S.-I. Evolution and Phylogeny of Defense Molecules Associated with Innate Immunity in Horseshoe Crab. *Front. Biosci.* **1998**, *3*, D973-84.
(37) Tincu, J. A.; Taylor, S. W. Antimicrobial Peptides from Marine Invertebrates. *Antimicrob.*

Agents Chemother. **2004**, *48* (10), 3645–3654.
(38) Masuda, M.; Nakashima, H.; Ueda, T.; Naba, H.; Ikoma, R.; Otaka, A.; Terakawa, Y.; Tamamura, H.; Ibuka, T.; Murakami, T.; Koyanagi, Y.; Waki, M.; Matsumoto, A.; Yamamoto, N.; Funakoshi, S.; Fujii, N. A Novel Anti-HIV Synthetic Peptide, T-22 ([Tyr5,12,Lys7]-Polyphemusin II). *Biochem. Biophys. Res. Commun.* **1992**, *189* (2), 845–850.
(39) Yang, D.; Biragyn, A.; Hoover, D. M.; Lubkowski, J.; Oppenheim, J. J. Multiple Roles of Antimicrobial Defensins, Cathelicidins, and Eosinophil-Derived Neurotoxin in Host Defense. *Annu. Rev. Immunol.* **2004**, *22* (1), 181–215.
(40) Bowdish, D. M. E.; Davidson, D. J.; Lau, Y. E.; Lee, K.; Scott, M. G.; Hancock, R. E. W. Impact of LL-37 on Anti-Infective Immunity. *J. Leukoc. Biol.* **2005**, *77* (4), 451–459.
(41) Yang, D.; Biragyn, A.; Kwak, L. W.; Oppenheim, J. J. Mammalian Defensins in Immunity: More than Just Microbicidal. *Trends Immunol.* **2002**, *23* (6), 291–296.
(42) Hilchie, A. L.; Wuerth, K.; Hancock, R. E. W. Immune Modulation by Multifaceted Cationic Host Defense (Antimicrobial) Peptides. *Nat. Chem. Biol.* **2013**, *9* (12), 761–768.
(43) Haney, E. F.; Hancock, R. E. W. Peptide Design for Antimicrobial and Immunomodulatory Applications. *Biopolymers* **2013**, *100* (6), 572–583.
(44) Hancock, R. E.; Haney, E. F.; Gill, E. E. The Immunology of Host Defence Peptides: Beyond Antimicrobial Activity. *Nat. Publ. Gr.* **2016**, *16*.
(45) Bowdish, D. M. E.; Davidson, D. J.; Scott, M. G.; Hancock, R. E. W. Immunomodulatory Activities of Small Host Defense Peptides. *Antimicrob. Agents Chemother.* **2005**, *49* (5), 1727–1732.
(46) Nijnik, A.; Hancock, R. Host Defence Peptides: Antimicrobial and Immunomodulatory Activity and Potential Applications for Tackling Antibiotic-Resistant Infections. *Emerg. Health Threats J.* **2009**, *2*, e1.
(47) Veldhuizen, E. J. A.; Schneider, V. A. F.; Agustiandari, H.; van Dijk, A.; Tjeerdsma-van Bokhoven, J. L. M.; Bikker, F. J.; Haagsman, H. P. Antimicrobial and Immunomodulatory Activities of PR-39 Derived Peptides. *PLoS One* **2014**, *9* (4), e95939.
(48) Kościuczuk, E. M.; Lisowski, P.; Jarczak, J.; Strzałkowska, N.; Jóźwik, A.; Horbańczuk, J.; Krzyżewski, J.; Zwierzchowski, L.; Bagnicka, E. Cathelicidins: Family of Antimicrobial Peptides. A Review. *Mol. Biol. Rep.* **2012**, *39* (12), 10957–10970.
(49) Rozek, T.; Wegener, K. L.; Bowie, J. H.; Olver, I. N.; Carver, J. A.; Wallace, J. C.; Tyler, M. J. The Antibiotic and Anticancer Active Aurein Peptides from the Australian Bell Frogs Litoria Aurea and Litoria Raniformis. *Eur. J. Biochem.* **2000**, *267* (17), 5330–5341.
(50) Rozek, T.; Bowie, J. H.; Wallace, J. C.; Tyler, M. J. The Antibiotic and Anticancer Active Aurein Peptides from the Australian Bell FrogsLitoria Aurea AndLitoria Raniformis. Part 2. Sequence Determination Using Electrospray Mass Spectrometry. *Rapid Commun. Mass Spectrom.* **2000**, *14* (21), 2002–2011.
(51) Da Mata, É. C. G.; Mourão, C. B. F.; Rangel, M.; Schwartz, E. F. Antiviral Activity of Animal Venom Peptides and Related Compounds. *J. Venom. Anim. Toxins Incl. Trop. Dis.* **2017**, *23*, 3.
(52) Niidome, T.; Kobayashi, K.; Arakawa, H.; Hatakeyama, T.; Aoyagi, H. Structure–activity Relationship of an Antibacterial Peptide, Maculatin 1.1, from the Skin Glands of the Tree Frog,Litoria Genimaculata. *J. Pept. Sci.* **2004**, *10* (7), 414–422.

(53) Sikorska, E.; Greber, K.; Rodziewicz-Motowidło, S.; Szultka, Ł.; Łukasiak, J.; Kamysz, W. Synthesis and Antimicrobial Activity of Truncated Fragments and Analogs of Citropin 1.1: The Solution Structure of the SDS Micelle-Bound Citropin-like Peptides. *J. Struct. Biol.* **2009**, *168* (2), 250–258.
(54) Park, C. B.; Kim, H. S.; Kim, S. C. Mechanism of Action of the Antimicrobial Peptide Buforin II: Buforin II Kills Microorganisms by Penetrating the Cell Membrane and Inhibiting Cellular Functions. *Biochem. Biophys. Res. Commun.* **1998**, *244* (1), 253–257.
(55) Ganz, T. Defensins: Antimicrobial Peptides of Innate Immunity. *Nat. Rev. Immunol.* **2003**, *3* (9), 710–720.
(56) Ulm, H.; Wilmes, M.; Shai, Y.; Sahl, H.-G. Antimicrobial Host Defensins – Specific Antibiotic Activities and Innate Defense Modulation. *Front. Immunol.* **2012**, *3*, 249.
(57) Lehrer, R. I.; Barton, A.; Daher, K. A.; Harwig, S. S.; Ganz, T.; Selsted, M. E. Interaction of Human Defensins with Escherichia Coli. Mechanism of Bactericidal Activity. *J. Clin. Invest.* **1989**, *84* (2), 553–561.
(58) Miyata, T.; Tokunaga, F.; Yoneya, T.; Yoshikawa, K.; Iwanaga, S.; Niwa, M.; Takao, T.; Shimonishi, Y. Antimicrobial Peptides, Isolated from Horseshoe Crab Hemocytes, Tachyplesin II, and Polyphemusins I and II: Chemical Structures and Biological Activity. *J. Biochem.* **1989**, *106* (4), 663–668.
(59) Takahashi, D.; Shukla, S. K.; Prakash, O.; Zhang, G. Structural Determinants of Host Defense Peptides for Antimicrobial Activity and Target Cell Selectivity. *Biochimie* **2010**, *92* (9), 1236–1241.
(60) Zairi, A.; Tangy, F.; Bouassida, K.; Hani, K. Dermaseptins and Magainins: Antimicrobial Peptides from Frogs' Skin-New Sources for a Promising Spermicides Microbicides-a Mini Review. *J. Biomed. Biotechnol.* **2009**, *2009*, 452567.
(61) Lamb, H. M.; Wiseman, L. R. Pexiganan Acetate. *Drugs* **1998**, *56* (6), 1047–1052.
(62) Ge, Y.; MacDonald, D. L.; Holroyd, K. J.; Thornsberry, C.; Wexler, H.; Zasloff, M. In Vitro Antibacterial Properties of Pexiganan, an Analog of Magainin. *Antimicrob. Agents Chemother.* **1999**, *43* (4), 782–788.
(63) Fox, J. L. Antimicrobial Peptides Stage a Comeback. *Nat. Biotechnol.* **2013**, *31* (5), 379–382.
(64) Mura, M.; Wang, J.; Zhou, Y.; Pinna, M.; Zvelindovsky, A. V.; Dennison, S. R.; Phoenix, D. A. The Effect of Amidation on the Behaviour of Antimicrobial Peptides. *Eur. Biophys. J.* **2016**, *45* (3), 195–207.
(65) Dhople, V.; Krukemeyer, A.; Ramamoorthy, A. The Human Beta-Defensin-3, an Antibacterial Peptide with Multiple Biological Functions. *Biochim. Biophys. Acta - Biomembr.* **2006**, *1758* (9), 1499–1512.
(66) Pettersen, E. F.; Goddard, T. D.; Huang, C. C.; Couch, G. S.; Greenblatt, D. M.; Meng, E. C.; Ferrin, T. E. UCSF Chimera?A Visualization System for Exploratory Research and Analysis. *J. Comput. Chem.* **2004**, *25* (13), 1605–1612.
(67) Pettersen, E. F.; Goddard, T. D.; Huang, C. C.; Couch, G. S.; Greenblatt, D. M.; Meng, E. C.; Ferrin, T. E. UCSF Chimera--a Visualization System for Exploratory Research and Analysis. *J. Comput. Chem.* **2004**, *25* (13), 1605–1612.
(68) Yang, Z.; Lasker, K.; Schneidman-Duhovny, D.; Webb, B.; Huang, C. C.; Pettersen, E. F.; Goddard, T. D.; Meng, E. C.; Sali, A.; Ferrin, T. E. UCSF Chimera, MODELLER, and IMP: An Integrated Modeling System. *J. Struct. Biol.* **2012**, *179* (3), 269–278.

(69) Huang, C. C.; Meng, E. C.; Morris, J. H.; Pettersen, E. F.; Ferrin, T. E. Enhancing UCSF Chimera through Web Services. *Nucleic Acids Res.* **2014**, *42* (W1), W478–W484.
(70) Lee, T.-H.; Hall, K. N.; Aguilar, M.-I. Antimicrobial Peptide Structure and Mechanism of Action: A Focus on the Role of Membrane Structure. *Curr. Top. Med. Chem.* **2016**, *16* (1), 25–39.
(71) Wilson, C. L.; Ouellette, A. J.; Satchell, D. P.; Ayabe, T.; López-Boado, Y. S.; Stratman, J. L.; Hultgren, S. J.; Matrisian, L. M.; Parks, W. C. Regulation of Intestinal Alpha-Defensin Activation by the Metalloproteinase Matrilysin in Innate Host Defense. *Science* **1999**, *286* (5437), 113–117.
(72) Salzman, N. H.; Ghosh, D.; Huttner, K. M.; Paterson, Y.; Bevins, C. L. Protection against Enteric Salmonellosis in Transgenic Mice Expressing a Human Intestinal Defensin. *Nature* **2003**, *422* (6931), 522–526.
(73) Nelson, D. L. (David L.; Cox, M. M.; Lehninger, A. L. *Lehninger Principles of Biochemistry*; W.H. Freeman and Company, 2013.
(74) Falla, T. J.; Karunaratne, D. N.; Hancock, R. E. Mode of Action of the Antimicrobial Peptide Indolicidin. *J. Biol. Chem.* **1996**, *271* (32), 19298–19303.
(75) Rozek, A.; Friedrich, C. L.; Hancock, R. E. Structure of the Bovine Antimicrobial Peptide Indolicidin Bound to Dodecylphosphocholine and Sodium Dodecyl Sulfate Micelles. *Biochemistry* **2000**, *39* (51), 15765–15774.
(76) Falcao, C. B.; Pérez-Peinado, C.; de la Torre, B. G.; Mayol, X.; Zamora-Carreras, H.; Jiménez, M. Á.; Rádis-Baptista, G.; Andreu, D. Structural Dissection of Crotalicidin, a Rattlesnake Venom Cathelicidin, Retrieves a Fragment with Antimicrobial and Antitumor Activity. *J. Med. Chem.* **2015**, *58* (21), 8553–8563.
(77) Gagnon, M.-C.; Strandberg, E.; Grau-Campistany, A.; Wadhwani, P.; Reichert, J.; Bürck, J.; Rabanal, F.; Auger, M.; Paquin, J.-F.; Ulrich, A. S. Influence of the Length and Charge on the Activity of α-Helical Amphipathic Antimicrobial Peptides. *Biochemistry* **2017**, *56* (11), 1680–1695.
(78) Dathe, M.; Nikolenko, H.; Meyer, J.; Beyermann, M.; Bienert, M. Optimization of the Antimicrobial Activity of Magainin Peptides by Modification of Charge. *FEBS Lett.* **2001**, *501* (2–3), 146–150.
(79) Lyu, Y.; Yang, Y.; Lyu, X.; Dong, N.; Shan, A. Antimicrobial Activity, Improved Cell Selectivity and Mode of Action of Short PMAP-36-Derived Peptides against Bacteria and Candida. *Sci. Rep.* **2016**, *6* (1), 27258.
(80) Gagnon, M.-C.; Strandberg, E.; Grau-Campistany, A.; Wadhwani, P.; Reichert, J.; Bürck, J.; Rabanal, F.; Auger, M.; Paquin, J.-F.; Ulrich, A. S. Influence of the Length and Charge on the Activity of α-Helical Amphipathic Antimicrobial Peptides. *Biochemistry* **2017**, *56* (11), 1680–1695.
(81) Hong, S. Y.; Park, T. G.; Lee, K. H. The Effect of Charge Increase on the Specificity and Activity of a Short Antimicrobial Peptide. *Peptides* **2001**, *22* (10), 1669–1674.
(82) Jiang, Z.; Vasil, A. I.; Hale, J. D.; Hancock, R. E. W.; Vasil, M. L.; Hodges, R. S. Effects of Net Charge and the Number of Positively Charged Residues on the Biological Activity of Amphipathic Alpha-Helical Cationic Antimicrobial Peptides. *Biopolymers* **2008**, *90* (3), 369–383.
(83) Yeaman, M. R.; Yount, N. Y. Mechanisms of Antimicrobial Peptide Action and Resistance. *Pharmacol. Rev.* **2003**, *55* (1), 27–55.

(84) Yin, L. M.; Edwards, M. A.; Li, J.; Yip, C. M.; Deber, C. M. Roles of Hydrophobicity and Charge Distribution of Cationic Antimicrobial Peptides in Peptide-Membrane Interactions. *J. Biol. Chem.* **2012**, *287* (10), 7738–7745.
(85) Chen, Y.; Guarnieri, M. T.; Vasil, A. I.; Vasil, M. L.; Mant, C. T.; Hodges, R. S. Role of Peptide Hydrophobicity in the Mechanism of Action of Alpha-Helical Antimicrobial Peptides. *Antimicrob. Agents Chemother.* **2007**, *51* (4), 1398–1406.
(86) Mihajlovic, M.; Lazaridis, T. Charge Distribution and Imperfect Amphipathicity Affect Pore Formation by Antimicrobial Peptides. *Biochim. Biophys. Acta - Biomembr.* **2012**, *1818* (5), 1274–1283.
(87) Hawrani, A.; Howe, R. A.; Walsh, T. R.; Dempsey, C. E. Origin of Low Mammalian Cell Toxicity in a Class of Highly Active Antimicrobial Amphipathic Helical Peptides. *J. Biol. Chem.* **2008**, *283* (27), 18636–18645.
(88) Chen, Y.; Mant, C. T.; Farmer, S. W.; Hancock, R. E. W.; Vasil, M. L.; Hodges, R. S. Rational Design of α-Helical Antimicrobial Peptides with Enhanced Activities and Specificity/Therapeutic Index. *J. Biol. Chem.* **2005**, *280* (13), 12316–12329.
(89) Jiang, Z.; Vasil, A. I.; Gera, L.; Vasil, M. L.; Hodges, R. S. Rational Design of α-Helical Antimicrobial Peptides to Target Gram-Negative Pathogens, Acinetobacter Baumannii and Pseudomonas Aeruginosa: Utilization of Charge, 'Specificity Determinants,' Total Hydrophobicity, Hydrophobe Type and Location as Design Para. *Chem. Biol. Drug Des.* **2011**, *77* (4), 225–240.
(90) Zhang, S.-K.; Song, J.; Gong, F.; Li, S.-B.; Chang, H.-Y.; Xie, H.-M.; Gao, H.-W.; Tan, Y.-X.; Ji, S.-P. Design of an α-Helical Antimicrobial Peptide with Improved Cell-Selective and Potent Anti-Biofilm Activity. *Sci. Rep.* **2016**, *6* (1), 27394.
(91) Breukink, E.; Wiedemann, I.; van Kraaij, C.; Kuipers, O. P.; Sahl, H. G.; de Kruijff, B. Use of the Cell Wall Precursor Lipid II by a Pore-Forming Peptide Antibiotic. *Science* **1999**, *286* (5448), 2361–2364.
(92) Fleury, Y.; Dayem, M. A.; Montagne, J. J.; Chaboisseau, E.; Le Caer, J. P.; Nicolas, P.; Delfour, A. Covalent Structure, Synthesis, and Structure-Function Studies of Mesentericin Y 105(37), a Defensive Peptide from Gram-Positive Bacteria Leuconostoc Mesenteroides. *J. Biol. Chem.* **1996**, *271* (24), 14421–14429.
(93) Shai, Y. Mode of Action of Membrane Active Antimicrobial Peptides. *Biopolymers* **2002**, *66* (4), 236–248.
(94) Zhang, L.; Rozek, A.; Hancock, R. E. Interaction of Cationic Antimicrobial Peptides with Model Membranes. *J. Biol. Chem.* **2001**, *276* (38), 35714–35722.
(95) Guilhelmelli, F.; Vilela, N.; Albuquerque, P.; Derengowski, L. da S.; Silva-Pereira, I.; Kyaw, C. M. Antibiotic Development Challenges: The Various Mechanisms of Action of Antimicrobial Peptides and of Bacterial Resistance. *Front. Microbiol.* **2013**, *4*, 353.
(96) Zasloff, M. Antimicrobial Peptides of Multicellular Organisms. *Nature* **2002**, *415* (6870), 389–395.
(97) Matsuzaki, K.; Sugishita, K.; Ishibe, N.; Ueha, M.; Nakata, S.; Koichiro Miyajima; Epand, R. M. Relationship of Membrane Curvature to the Formation of Pores by Magainin 2†. *Biochemistry* **1998**, *37* (34), 11856–11863.
(98) Epand, R. M.; Vogel, H. J. Diversity of Antimicrobial Peptides and Their Mechanisms of Action. *Biochim. Biophys. Acta - Biomembr.* **1999**, *1462* (1), 11–28.
(99) Jouhet, J. Importance of the Hexagonal Lipid Phase in Biological Membrane

Organization. *Front. Plant Sci.* **2013**, *4*, 494.
(100) Strömstedt, A. A.; Kristiansen, P. E.; Gunasekera, S.; Grob, N.; Skjeldal, L.; Göransson, U. Selective Membrane Disruption by the Cyclotide Kalata B7: Complex Ions and Essential Functional Groups in the Phosphatidylethanolamine Binding Pocket. *Biochim. Biophys. Acta - Biomembr.* **2016**, *1858* (6), 1317–1327.
(101) Phoenix, D. A.; Harris, F.; Mura, M.; Dennison, S. R. The Increasing Role of Phosphatidylethanolamine as a Lipid Receptor in the Action of Host Defence Peptides. *Prog. Lipid Res.* **2015**, *59*, 26–37.
(102) Drin, G.; Antonny, B. Amphipathic Helices and Membrane Curvature. *FEBS Lett.* **2010**, *584* (9), 1840–1847.
(103) Schmidt, N. W.; Wong, G. C. L. Antimicrobial Peptides and Induced Membrane Curvature: Geometry, Coordination Chemistry, and Molecular Engineering. *Curr. Opin. Solid State Mater. Sci.* **2013**, *17* (4), 151–163.
(104) Epand, R. M.; Walker, C.; Epand, R. F.; Magarvey, N. A. Molecular Mechanisms of Membrane Targeting Antibiotics. *Biochim. Biophys. Acta - Biomembr.* **2016**, *1858* (5), 980–987.
(105) Andersson, D. I.; Hughes, D.; Kubicek-Sutherland, J. Z. Mechanisms and Consequences of Bacterial Resistance to Antimicrobial Peptides. *Drug Resist. Updat.* **2016**, *26*, 43–57.
(106) Ehrenstein, G.; Lecar, H. Electrically Gated Ionic Channels in Lipid Bilayers. *Q. Rev. Biophys.* **1977**, *10* (1), 1–34.
(107) Brogden, K. A. Antimicrobial Peptides: Pore Formers or Metabolic Inhibitors in Bacteria? *Nat. Rev. Microbiol.* **2005**, *3* (3), 238–250.
(108) Breukink, E.; de Kruijff, B. The Lantibiotic Nisin, a Special Case or Not? *Biochim. Biophys. Acta* **1999**, *1462* (1–2), 223–234.
(109) Wimley, W. C. Describing the Mechanism of Antimicrobial Peptide Action with the Interfacial Activity Model. *ACS Chem. Biol.* **2010**, *5* (10), 905–917.
(110) Rapaport, D.; Shai, Y. Interaction of Fluorescently Labeled Pardaxin and Its Analogues with Lipid Bilayers. *J. Biol. Chem.* **1991**, *266* (35), 23769–23775.
(111) Shai, Y.; Bach, D.; Yanovsky, A. Channel Formation Properties of Synthetic Pardaxin and Analogues. *J. Biol. Chem.* **1990**, *265* (33), 20202–20209.
(112) Uematsu, N.; Matsuzaki, K. Polar Angle as a Determinant of Amphipathic α-Helix-Lipid Interactions: A Model Peptide Study. *Biophys. J.* **2000**, *79* (4), 2075–2083.
(113) Cheng, J. T. J.; Hale, J. D.; Elliot, M.; Hancock, R. E. W.; Straus, S. K. Effect of Membrane Composition on Antimicrobial Peptides Aurein 2.2 and 2.3 from Australian Southern Bell Frogs. *Biophys. J.* **2009**, *96* (2), 552–565.
(114) Sitaram, N.; Nagaraj, R. Interaction of Antimicrobial Peptides with Biological and Model Membranes: Structural and Charge Requirements for Activity. *Biochim. Biophys. Acta* **1999**, *1462* (1–2), 29–54.
(115) Fernandez, D. I.; Le Brun, A. P.; Whitwell, T. C.; Sani, M.-A.; James, M.; Separovic, F. The Antimicrobial Peptide Aurein 1.2 Disrupts Model Membranes via the Carpet Mechanism. *Phys. Chem. Chem. Phys.* **2012**, *14* (45), 15739.
(116) Gee, M. L.; Burton, M.; Grevis-James, A.; Hossain, M. A.; McArthur, S.; Palombo, E. A.; Wade, J. D.; Clayton, A. H. A. Imaging the Action of Antimicrobial Peptides on Living Bacterial Cells. *Sci. Rep.* **2013**, *3* (1), 1557.
(117) Choi, H.; Rangarajan, N.; Weisshaar, J. C. Lights, Camera, Action! Antimicrobial Peptide

Mechanisms Imaged in Space and Time. *Trends Microbiol.* **2016**, *24* (2), 111–122.
(118) Malanovic, N.; Lohner, K. Antimicrobial Peptides Targeting Gram-Positive Bacteria. *Pharmaceuticals (Basel).* **2016**, *9* (3).
(119) Münch, D. Structural Variations of the Cell Wall Precursor Lipid II in Gram-Positive Bacteria — Impact on Binding and Efficacy of Antimicrobial Peptides. *Biochim. Biophys. Acta - Biomembr.* **2015**, *1848* (11), 3062–3071.
(120) de Leeuw, E.; Li, C.; Zeng, P.; Li, C.; Buin, M. D.; Lu, W.-Y.; Breukink, E.; Lu, W. Functional Interaction of Human Neutrophil Peptide-1 with the Cell Wall Precursor Lipid II. *FEBS Lett.* **2010**, *584* (8), 1543–1548.
(121) Wade, D.; Boman, A.; Wåhlin, B.; Drain, C. M.; Andreu, D.; Boman, H. G.; Merrifield, R. B. All-D Amino Acid-Containing Channel-Forming Antibiotic Peptides. *Proc. Natl. Acad. Sci. U. S. A.* **1990**, *87* (12), 4761–4765.
(122) Vunnam, S.; Juvvadi, P.; Merrifield, R. B. Synthesis and Antibacterial Action of Cecropin and Proline-Arginine-Rich Peptides from Pig Intestine. *J. Pept. Res.* **1997**, *49* (1), 59–66.
(123) Subbalakshmi, C.; Sitaram, N. Mechanism of Antimicrobial Action of Indolicidin. *FEMS Microbiol. Lett.* **1998**, *160* (1), 91–96.
(124) Sharma, H.; Nagaraj, R.; Rodrigues, D.; Sousa, D. de; Silva, E. da; Moraes, L. de. Human β-Defensin 4 with Non-Native Disulfide Bridges Exhibit Antimicrobial Activity. *PLoS One* **2015**, *10* (3), e0119525.
(125) Boman, H. G.; Agerberth, B.; Boman, A. Mechanisms of Action on Escherichia Coli of Cecropin P1 and PR-39, Two Antibacterial Peptides from Pig Intestine. *Infect. Immun.* **1993**, *61* (7), 2978–2984.
(126) Afacan, N. J.; Yeung, A. T. Y.; Pena, O. M.; Hancock, R. E. W. Therapeutic Potential of Host Defense Peptides in Antibiotic-Resistant Infections. *Curr. Pharm. Des.* **2012**, *18* (6), 807–819.
(127) Mader, J. S.; Hoskin, D. W. Cationic Antimicrobial Peptides as Novel Cytotoxic Agents for Cancer Treatment. *Expert Opin. Investig. Drugs* **2006**, *15* (8), 933–946.
(128) Lai, Y.; Gallo, R. L. AMPed up Immunity: How Antimicrobial Peptides Have Multiple Roles in Immune Defense. *Trends Immunol.* **2009**, *30* (3), 131–141.
(129) Hancock, R. E. W.; Nijnik, A.; Philpott, D. J. Modulating Immunity as a Therapy for Bacterial Infections. *Nat. Rev. Microbiol.* **2012**, *10* (4), 243–254.
(130) Niyonsaba, F.; Iwabuchi, K.; Someya, A.; Hirata, M.; Matsuda, H.; Ogawa, H.; Nagaoka, I. A Cathelicidin Family of Human Antibacterial Peptide LL-37 Induces Mast Cell Chemotaxis. *Immunology* **2002**, *106* (1), 20–26.
(131) García, J.-R.; Jaumann, F.; Schulz, S.; Krause, A.; Rodríguez-Jiménez, J.; Forssmann, U.; Adermann, K.; Klüver, E.; Vogelmeier, C.; Becker, D.; Hedrich, R.; Forssmann, W.-G.; Bals, R. Identification of a Novel, Multifunctional Beta-Defensin (Human Beta-Defensin 3) with Specific Antimicrobial Activity. Its Interaction with Plasma Membranes of Xenopus Oocytes and the Induction of Macrophage Chemoattraction. *Cell Tissue Res.* **2001**, *306* (2), 257–264.
(132) Liu, Y. J. Dendritic Cell Subsets and Lineages, and Their Functions in Innate and Adaptive Immunity. *Cell* **2001**, *106* (3), 259–262.
(133) Nijnik, A.; Madera, L.; Ma, S.; Waldbrook, M.; Elliott, M. R.; Easton, D. M.; Mayer, M. L.; Mullaly, S. C.; Kindrachuk, J.; Jenssen, H.; Hancock, R. E. W. Synthetic Cationic Peptide IDR-1002 Provides Protection against Bacterial Infections through Chemokine

Induction and Enhanced Leukocyte Recruitment. *J. Immunol.* **2010**, *184* (5), 2539–2550.
(134) Scott, M. G.; Dullaghan, E.; Mookherjee, N.; Glavas, N.; Waldbrook, M.; Thompson, A.; Wang, A.; Lee, K.; Doria, S.; Hamill, P.; Yu, J. J.; Li, Y.; Donini, O.; Guarna, M. M.; Finlay, B. B.; North, J. R.; Hancock, R. E. W. An Anti-Infective Peptide That Selectively Modulates the Innate Immune Response. *Nat. Biotechnol.* **2007**, *25* (4), 465–472.
(135) Nicholls, E. F.; Madera, L.; Hancock, R. E. W. Immunomodulators as Adjuvants for Vaccines and Antimicrobial Therapy. *Ann. N. Y. Acad. Sci.* **2010**, *1213* (1), 46–61.
(136) Zhang, L.; Dhillon, P.; Yan, H.; Farmer, S.; Hancock, R. E. Interactions of Bacterial Cationic Peptide Antibiotics with Outer and Cytoplasmic Membranes of Pseudomonas Aeruginosa. *Antimicrob. Agents Chemother.* **2000**, *44* (12), 3317–3321.
(137) Pan, Y. L.; Cheng, J. T.; Hale, J.; Pan, J.; Hancock, R. E.; Straus, S. K. Characterization of the Structure and Membrane Interaction of the Antimicrobial Peptides Aurein 2.2 and 2.3 from Australian Southern Bell Frogs. *Biophys J* **2007**, *92* (8), 2854–2864.
(138) Cheng, J. T. J.; Hale, J. D.; Elliott, M.; Hancock, R. E. W.; Straus, S. K. The Importance of Bacterial Membrane Composition in the Structure and Function of Aurein 2.2 and Selected Variants. *Biochim. Biophys. Acta - Biomembr.* **2011**, *1808* (3), 622–633.
(139) Cheng, J. T. J. Investigating the Structure-Function Relationship of Cationic Antimicrobial Peptides and Lipopeptides, University of British Columbia, 2010.
(140) Wenzel, M.; Senges, C. H. R.; Zhang, J.; Suleman, S.; Nguyen, M.; Kumar, P.; Chiriac, A. I.; Stepanek, J. J.; Raatschen, N.; May, C.; Krämer, U.; Sahl, H.-G.; Straus, S. K.; Bandow, J. E. Antimicrobial Peptides from the Aurein Family Form Ion-Selective Pores in *Bacillus Subtilis*. *ChemBioChem* **2015**, *16* (7), 1101–1108.
(141) Vaara, M. New Approaches in Peptide Antibiotics. *Curr. Opin. Pharmacol.* **2009**, *9* (5), 571–576.
(142) Gentilucci, L.; De Marco, R.; Cerisoli, L. Chemical Modifications Designed to Improve Peptide Stability: Incorporation of Non-Natural Amino Acids, Pseudo-Peptide Bonds, and Cyclization. *Curr. Pharm. Des.* **2010**, *16* (28), 3185–3203.
(143) Nordström, R.; Malmsten, M. Delivery Systems for Antimicrobial Peptides. *Adv. Colloid Interface Sci.* **2017**, *242*, 17–34.
(144) Fjell, C. D.; Hiss, J. A.; Hancock, R. E. W.; Schneider, G. Designing Antimicrobial Peptides: Form Follows Function. *Nat. Rev. Drug Discov.* **2011**, *11* (1), 37.
(145) Zhao, Y.; Zhang, M.; Qiu, S.; Wang, J.; Peng, J.; Zhao, P.; Zhu, R.; Wang, H.; Li, Y.; Wang, K.; Yan, W.; Wang, R. Antimicrobial Activity and Stability of the D-Amino Acid Substituted Derivatives of Antimicrobial Peptide Polybia-MPI. *AMB Express* **2016**, *6* (1), 122.
(146) Kindrachuk, J.; Scruten, E.; Attah-Poku, S.; Bell, K.; Potter, A.; Babiuk, L. A.; Griebel, P. J.; Napper, S. Stability, Toxicity, and Biological Activity of Host Defense Peptide BMAP28 and Its Inversed and Retro-Inversed Isomers. *Biopolymers* **2011**, *96* (1), 14–24.
(147) Falciani, C.; Lozzi, L.; Pollini, S.; Luca, V.; Carnicelli, V.; Brunetti, J.; Lelli, B.; Bindi, S.; Scali, S.; Di Giulio, A.; Rossolini, G. M.; Mangoni, M. L.; Bracci, L.; Pini, A. Isomerization of an Antimicrobial Peptide Broadens Antimicrobial Spectrum to Gram-Positive Bacterial Pathogens. *PLoS One* **2012**, *7* (10), e46259.
(148) Davies, J. S.; Elmore, D. T. *Amino Acids, Peptides and Proteins. Volume 36, A Review of the Literature Published during 2003-2004*; RSC Pub, 2007.
(149) Berthold, N.; Czihal, P.; Fritsche, S.; Sauer, U.; Schiffer, G.; Knappe, D.; Alber, G.;

Hoffmann, R. Novel Apidaecin 1b Analogs with Superior Serum Stabilities for Treatment of Infections by Gram-Negative Pathogens. *Antimicrob. Agents Chemother.* **2013**, *57* (1), 402–409.
(150) Papanastasiou, E. A.; Hua, Q.; Sandouk, A.; Son, U. H.; Christenson, A. J.; Van Hoek, M. L.; Bishop, B. M. Role of Acetylation and Charge in Antimicrobial Peptides Based on Human β-Defensin-3. *APMIS* **2009**, *117* (7), 492–499.
(151) Jayawardene, D. S.; Dass, C. The Effect of N-Terminal Acetylation and the Inhibition Activity of Acetylated Enkephalins on the Aminopeptidase M-Catalyzed Hydrolysis of Enkephalins. *Peptides* **1999**, *20* (8), 963–970.
(152) Nguyen, L. T.; Chau, J. K.; Perry, N. A.; de Boer, L.; Zaat, S. A. J.; Vogel, H. J. Serum Stabilities of Short Tryptophan- and Arginine-Rich Antimicrobial Peptide Analogs. *PLoS One* **2010**, *5* (9), e12684.
(153) Liu, B.; Zhang, W.; Gou, S.; Huang, H.; Yao, J.; Yang, Z.; Liu, H.; Zhong, C.; Liu, B.; Ni, J.; Wang, R. Intramolecular Cyclization of the Antimicrobial Peptide Polybia-MPI with Triazole Stapling: Influence on Stability and Bioactivity. *J. Pept. Sci.* **2017**.
(154) Som, A.; Vemparala, S.; Ivanov, I.; Tew, G. N. Synthetic Mimics of Antimicrobial Peptides. *Biopolymers* **2008**, *90* (2), 83–93.
(155) Rotem, S.; Mor, A. Antimicrobial Peptide Mimics for Improved Therapeutic Properties. *Biochim. Biophys. Acta - Biomembr.* **2009**, *1788* (8), 1582–1592.
(156) Giuliani, A.; Rinaldi, A. C. Beyond Natural Antimicrobial Peptides: Multimeric Peptides and Other Peptidomimetic Approaches. *Cell. Mol. Life Sci.* **2011**, *68* (13), 2255–2266.
(157) Kapoor, R.; Wadman, M. W.; Dohm, M. T.; Czyzewski, A. M.; Spormann, A. M.; Barron, A. E. Antimicrobial Peptoids Are Effective against Pseudomonas Aeruginosa Biofilms. *Antimicrob. Agents Chemother.* **2011**, *55* (6), 3054–3057.
(158) Chongsiriwatana, N. P.; Patch, J. A.; Czyzewski, A. M.; Dohm, M. T.; Ivankin, A.; Gidalevitz, D.; Zuckermann, R. N.; Barron, A. E. Peptoids That Mimic the Structure, Function, and Mechanism of Helical Antimicrobial Peptides. *Proc. Natl. Acad. Sci. U. S. A.* **2008**, *105* (8), 2794–2799.
(159) Andreev, K.; Martynowycz, M. W.; Ivankin, A.; Huang, M. L.; Kuzmenko, I.; Meron, M.; Lin, B.; Kirshenbaum, K.; Gidalevitz, D. Cyclization Improves Membrane Permeation by Antimicrobial Peptoids. *Langmuir* **2016**, *32* (48), 12905–12913.
(160) Reinhardt, A.; Neundorf, I. Design and Application of Antimicrobial Peptide Conjugates. *Int. J. Mol. Sci.* **2016**, *17* (5), 701.
(161) Li, P.; Nielsen, H. M.; Müllertz, A. Oral Delivery of Peptides and Proteins Using Lipid-Based Drug Delivery Systems. *Expert Opin. Drug Deliv.* **2012**, *9* (10), 1289–1304.
(162) Ron-Doitch, S.; Sawodny, B.; Kühbacher, A.; David, M. M. N.; Samanta, A.; Phopase, J.; Burger-Kentischer, A.; Griffith, M.; Golomb, G.; Rupp, S. Reduced Cytotoxicity and Enhanced Bioactivity of Cationic Antimicrobial Peptides Liposomes in Cell Cultures and 3D Epidermis Model against HSV. *J. Control. Release* **2016**, *229*, 163–171.
(163) Taylor, T. M.; Gaysinsky, S.; Davidson, P. M.; Bruce, B. D.; Weiss, J. Characterization of Antimicrobial-Bearing Liposomes by ζ-Potential, Vesicle Size, and Encapsulation Efficiency. *Food Biophys. 2* (1), 1–9.
(164) Urbán, P.; Valle-Delgado, J. J.; Moles, E.; Marques, J.; Díez, C.; Fernàndez-Busquets, X. Nanotools for the Delivery of Antimicrobial Peptides. *Curr. Drug Targets* **2012**, *13* (9), 1158–1172.

(165) Veronese, F. M.; Mero, A. The Impact of PEGylation on Biological Therapies. *BioDrugs 22* (5), 315–329.
(166) Imura, Y.; Nishida, M.; Ogawa, Y.; Takakura, Y.; Matsuzaki, K. Action Mechanism of Tachyplesin I and Effects of PEGylation. *Biochim. Biophys. Acta - Biomembr.* **2007**, *1768* (5), 1160–1169.
(167) Imura, Y.; Nishida, M.; Matsuzaki, K. Action Mechanism of PEGylated Magainin 2 Analogue Peptide. *Biochim. Biophys. Acta - Biomembr.* **2007**, *1768* (10), 2578–2585.
(168) Guiotto, A.; Pozzobon, M.; Canevari, M.; Manganelli, R.; Scarin, M.; Veronese, F. M. PEGylation of the Antimicrobial Peptide Nisin A: Problems and Perspectives. *Farm.* **2003**, *58* (1), 45–50.
(169) Singh, S.; Papareddy, P.; Mörgelin, M.; Schmidtchen, A.; Malmsten, M. Effects of PEGylation on Membrane and Lipopolysaccharide Interactions of Host Defense Peptides. *Biomacromolecules* **2014**, *15* (4), 1337–1345.
(170) Kong, M.; Chen, X. G.; Xing, K.; Park, H. J. Antimicrobial Properties of Chitosan and Mode of Action: A State of the Art Review. *Int. J. Food Microbiol.* **2010**, *144* (1), 51–63.
(171) Sahariah, P.; Sørensen, K. K.; Hjálmarsdóttir, M. Á.; Sigurjónsson, Ó. E.; Jensen, K. J.; Másson, M.; Thygesen, M. B. Antimicrobial Peptide Shows Enhanced Activity and Reduced Toxicity upon Grafting to Chitosan Polymers. *Chem. Commun.* **2015**, *51* (58), 11611–11614.
(172) Barbosa, M.; Vale, N.; Costa, F. M. T. A.; Martins, M. C. L.; Gomes, P. Tethering Antimicrobial Peptides onto Chitosan: Optimization of Azide-Alkyne "Click" Reaction Conditions. *Carbohydr. Polym.* **2017**, *165*, 384–393.
(173) Lequeux, I.; Ducasse, E.; Jouenne, T.; Thebault, P. Addition of Antimicrobial Properties to Hyaluronic Acid by Grafting of Antimicrobial Peptide. *Eur. Polym. J.* **2014**, *51* (51), 182–190.
(174) Abbina, S.; Vappala, S.; Kumar, P.; Siren, E. M. J.; La, C. C.; Abbasi, U.; Brooks, D. E.; Kizhakkedathu, J. N. Hyperbranched Polyglycerols: Recent Advances in Synthesis, Biocompatibility and Biomedical Applications. *J. Mater. Chem. B* **2017**, *5* (47), 9249–9277.
(175) Tokar, R.; Kubisa, P.; Penczek, S.; Dworak, A. Cationic Polymerization of Glycidol: Coexistence of the Activated Monomer and Active Chain End Mechanism. *Macromolecules* **1994**, *27* (2), 320–322.
(176) Sunder, A.; Mülhaupt, R.; Haag, R.; Frey, H. Hyperbranched Polyether Polyols: A Modular Approach to Complex Polymer Architectures. *Adv. Mater.* **2000**, *12* (3), 235–239.
(177) Sunder, A.; Hanselmann, R.; Frey, H.; Mu, R. Controlled Synthesis of Hyperbranched Polyglycerols by Ring-Opening Multibranching Polymerization. *Macromolecues* **1999**, *32* (13), 4240–4246.
(178) Ul-haq, M. I.; Shenoi, R. A.; Brooks, D. E.; Kizhakkedathu, J. N. Solvent-Assisted Anionic Ring Opening Polymerization of Glycidol: Toward Medium and High Molecular Weight Hyperbranched Polyglycerols. *J. Polym. Sci. Part A Polym. Chem.* **2013**, *51* (12), 2614–2621.
(179) Kainthan, R. K.; Janzen, J.; Levin, E.; Devine, D. V.; Brooks, D. E. Biocompatibility Testing of Branched and Linear Polyglycidol. *Biomacromolecules* **2006**, *7* (3), 703–709.
(180) Kainthan, R. K.; Hester, S. R.; Levin, E.; Devine, D. V.; Brooks, D. E. In Vitro Biological

Evaluation of High Molecular Weight Hyperbranched Polyglycerols. *Biomaterials* **2007**, *28* (31), 4581–4590.
(181) Imran Ul-Haq, M.; Lai, B. F. L.; Chapanian, R.; Kizhakkedathu, J. N. Influence of Architecture of High Molecular Weight Linear and Branched Polyglycerols on Their Biocompatibility and Biodistribution. *Biomaterials* **2012**, *33* (35), 9135–9147.
(182) Du, C.; Mendelson, A. A.; Guan, Q.; Chapanian, R.; Chafeeva, I.; da Roza, G.; Kizhakkedathu, J. N. The Size-Dependent Efficacy and Biocompatibility of Hyperbranched Polyglycerol in Peritoneal Dialysis. *Biomaterials* **2014**, *35* (5), 1378–1389.
(183) Gao, S.; Guan, Q.; Chafeeva, I.; Brooks, D. E.; Nguan, C. Y. C.; Kizhakkedathu, J. N.; Du, C. Hyperbranched Polyglycerol as a Colloid in Cold Organ Preservation Solutions. *PLoS One* **2015**, *10* (2), e0116595.
(184) Mugabe, C.; Matsui, Y.; So, A. I.; Gleave, M. E.; Baker, J. H. E.; Minchinton, A. I.; Manisali, I.; Liggins, R.; Brooks, D. E.; Burt, H. M. In Vivo Evaluation of Mucoadhesive Nanoparticulate Docetaxel for Intravesical Treatment of Non-Muscle-Invasive Bladder Cancer. *Clin. Cancer Res.* **2011**, *17* (9), 2788–2798.
(185) Shenoi, R. A.; Kalathottukaren, M. T.; Travers, R. J.; Lai, B. F. L.; Creagh, A. L.; Lange, D.; Yu, K.; Weinhart, M.; Chew, B. H.; Du, C.; Brooks, D. E.; Carter, C. J.; Morrissey, J. H.; Haynes, C. A.; Kizhakkedathu, J. N. Affinity-Based Design of a Synthetic Universal Reversal Agent for Heparin Anticoagulants. *Sci. Transl. Med.* **2014**, *6* (260).
(186) Imran ul-haq, M.; Hamilton, J. L.; Lai, B. F. L.; Shenoi, R. A.; Horte, S.; Constantinescu, I.; Leitch, H. A.; Kizhakkedathu, J. N. Design of Long Circulating Nontoxic Dendritic Polymers for the Removal of Iron in Vivo. *ACS Nano* **2013**, *7* (12), 10704–10716.
(187) Hamilton, J. L.; Imran Ul-Haq, M.; Abbina, S.; Kalathottukaren, M. T.; Lai, B. F. L.; Hatef, A.; Unniappan, S.; Kizhakkedathu, J. N. In Vivo Efficacy, Toxicity and Biodistribution of Ultra-Long Circulating Desferrioxamine Based Polymeric Iron Chelator. *Biomaterials* **2016**, *102*, 58–71.
(188) Kainthan, R. K.; Brooks, D. E. In Vivo Biological Evaluation of High Molecular Weight Hyperbranched Polyglycerols. *Biomaterials* **2007**, *28* (32), 4779–4787.
(189) Shenoi, R. A.; Abbina, S.; Kizhakkedathu, J. N. *In Vivo* Biological Evaluation of High Molecular Weight Multifunctional Acid-Degradable Polymeric Drug Carriers with Structurally Different Ketals. *Biomacromolecules* **2016**, *17* (11), 3683–3693.
(190) Chapanian, R.; Constantinescu, I.; Medvedev, N.; Scott, M. D.; Brooks, D. E.; Kizhakkedathu, J. N. Therapeutic Cells via Functional Modification: Influence of Molecular Properties of Polymer Grafts on In Vivo Circulation, Clearance, Immunogenicity, and Antigen Protection. *Biomacromolecules* **2013**, *14* (6), 2052–2062.
(191) Chen, A. M.; Scott, M. D. Comparative Analysis of Polymer and Linker Chemistries on the Efficacy of Immunocamouflage of Murine Leukocytes. *Artif. Cells, Blood Substitutes, Biotechnol.* **2006**, *34* (3), 305–322.
(192) Kalathottukaren, M. T.; Abraham, L.; Kapopara, P. R.; Lai, B. F. L.; Shenoi, R. A.; Rosell, F. I.; Conway, E. M.; Pryzdial, E. L. G.; Morrissey, J. H.; Haynes, C. A.; Kizhakkedathu, J. N. Alteration of Blood Clotting and Lung Damage by Protamine Are Avoided Using the Heparin and Polyphosphate Inhibitor UHRA. *Blood* **2017**, *129* (10), 1368–1379.
(193) Rossi, N. A. A.; Constantinescu, I.; Brooks, D. E.; Scott, M. D.; Kizhakkedathu, J. N.

Enhanced Cell Surface Polymer Grafting in Concentrated and Nonreactive Aqueous Polymer Solutions. *J. Am. Chem. Soc.* **2010**, *132* (10), 3423–3430.
(194) Chapanian, R.; Kwan, D. H.; Constantinescu, I.; Shaikh, F. a.; Rossi, N. a. . a.; Withers, S. G.; Kizhakkedathu, J. N. Enhancement of Biological Reactions on Cell Surfaces via Macromolecular Crowding. *Nat. Commun.* **2014**, *5*, 4683.
(195) Du, C.; Mendelson, A. A.; Guan, Q.; Chapanian, R.; Chafeeva, I.; da Roza, G.; Kizhakkedathu, J. N. The Size-Dependent Efficacy and Biocompatibility of Hyperbranched Polyglycerol in Peritoneal Dialysis. *Biomaterials* **2014**, *35* (5), 1378–1389.
(196) Gao, S.; Guan, Q.; Chafeeva, I.; Brooks, D. E.; Nguan, C. Y. C.; Kizhakkedathu, J. N.; Du, C. Hyperbranched Polyglycerol as a Colloid in Cold Organ Preservation Solutions. *PLoS One* **2015**, *10* (2), 1–22.
(197) Henning, L. M.; Bhatia, S.; Bertazzon, M.; Marczynke, M.; Seitz, O.; Volkmer, R.; Haag, R.; Freund, C. Exploring Monovalent and Multivalent Peptides for the Inhibition of FBP21-TWW. *Beilstein J. Org. Chem* **2015**, *11*, 701–706.
(198) Zhang, J. G.; Krajden, O. B.; Kainthan, R. K.; Kizhakkedathu, J. N.; Constantinescu, I.; Brooks, D. E.; Gyongyossy-Issa, M. I. C. Conjugation to Hyperbranched Polyglycerols Improves RGD-Mediated Inhibition of Platelet Function in Vitro. *Bioconjug. Chem.* **2008**, *19* (6), 1241–1247.
(199) Gupta, S.; Pfeil, J.; Kumar, S.; Poulsen, C.; Lauer, U.; Hamann, A.; Hoffmann, U.; Haag, R. Tolerogenic Modulation of the Immune Response by Oligoglycerol– and Polyglycerol–Peptide Conjugates. *Bioconjug. Chem.* **2015**, *26* (4), 669–679.
(200) Kainthan, R. K.; Janzen, J.; Kizhakkedathu, J. N.; Devine, D. V; Brooks, D. E. Hydrophobically Derivatized Hyperbranched Polyglycerol as a Human Serum Albumin Substitute. *Biomaterials* **2008**, *29* (11), 1693–1704.
(201) Winkler, D. F. H.; Hilpert, K.; Brandt, O.; Hancock, R. E. W. Synthesis of Peptide Arrays Using SPOT-Technology and the CelluSpots-Method. In *Methods in molecular biology*; 2009; Vol. 570, pp 157–174.
(202) Hilpert, K.; Winkler, D. F.; Hancock, R. E. Peptide Arrays on Cellulose Support: SPOT Synthesis, a Time and Cost Efficient Method for Synthesis of Large Numbers of Peptides in a Parallel and Addressable Fashion. *Nat. Protoc.* **2007**, *2* (6), 1333–1349.
(203) Frank, R. The SPOT-Synthesis Technique. Synthetic Peptide Arrays on Membrane Supports--Principles and Applications. *J. Immunol. Methods* **2002**, *267* (1), 13–26.
(204) Patel, A.; Cholkar, K.; Mitra, A. K. Recent Developments in Protein and Peptide Parenteral Delivery Approaches. *Ther. Deliv.* **2014**, *5* (3), 337–365.
(205) Campion, E. W.; Singer, A. J.; Talan, D. A. Management of Skin Abscesses in the Era of Methicillin-Resistant Staphylococcus Aureus. *N Engl J Med* **2014**, *370*, 1039–1047.
(206) Taira, B. R.; Singer, A. J.; Thode, H. C.; Lee, C. C. National Epidemiology of Cutaneous Abscesses: 1996 to 2005. *Am. J. Emerg. Med.* **2009**, *27* (3), 289–292.
(207) Mansour, S. C.; Pletzer, D.; De La Fuente-Núñez, C.; Kim, P.; Cheung, G. Y. C.; Joo, H.-S.; Otto, M.; Hancock, R. E. W. Bacterial Abscess Formation Is Controlled by the Stringent Stress Response and Can Be Targeted Therapeutically. *EBIOM* **2016**, *12*, 219–226.
(208) Stearne, L. E. T.; Gyssens, I. C.; Goessens, W. H. F.; Mouton, J. W.; Oyen, W. J. G.; van der Meer, J. W. M.; Verbrugh, H. A. In Vivo Efficacy of Trovafloxacin against

Bacteroides Fragilis in Mixed Infection with Either Escherichia Coli or a Vancomycin-Resistant Strain of Enterococcus Faecium in an Established-Abscess Murine Model. *Antimicrob. Agents Chemother.* **2001**, *45* (5), 1394–1401.
(209) de la Fuente-Núñez, C.; Reffuveille, F.; Mansour, S. C.; Reckseidler-Zenteno, S. L.; Hernández, D.; Brackman, G.; Coenye, T.; Hancock, R. E. W. D-Enantiomeric Peptides That Eradicate Wild-Type and Multidrug-Resistant Biofilms and Protect against Lethal Pseudomonas Aeruginosa Infections. *Chem. Biol.* **2015**, *22* (2), 196–205.
(210) Ishida, H.; Nguyen, L. T.; Gopal, R.; Aizawa, T.; Vogel, H. J. Overexpression of Antimicrobial, Anticancer, and Transmembrane Peptides in *Escherichia Coli* through a Calmodulin-Peptide Fusion System. *J. Am. Chem. Soc.* **2016**, *138* (35), 11318–11326.
(211) Nygaard, R.; Romaniuk, J. A. H.; Rice, D. M.; Cegelski, L. Spectral Snapshots of Bacterial Cell-Wall Composition and the Influence of Antibiotics by Whole-Cell NMR. *Biophys. J.* **2015**, *108* (6), 1380–1389.
(212) Hancock, R. E. Cationic Peptides: Effectors in Innate Immunity and Novel Antimicrobials. *Lancet Infect. Dis.* **2001**, *1* (3), 156–164.
(213) Hancock, R. E. Mechanisms of Action of Newer Antibiotics for Gram-Positive Pathogens. *Lancet Infect. Dis.* **2005**, *5* (4), 209–218.
(214) Devine, D. A.; Hancock, R. E. W. Cationic Peptides: Distribution and Mechanisms of Resistance. *Curr. Pharm. Des.* **2002**, *8* (9), 703–714.
(215) Cheng, J. T. J.; Hale, J. D.; Kindrachuk, J.; Jessen, H.; Elliott, M.; Hancock, R. E. W.; Straus, S. K. Importance of Residue 13 and the C-Terminus for the Structure and Activity of the Antimicrobial Peptide Aurein 2.2. *Biophys. J.* **2010**, *99* (9), 2926–2935.
(216) Hancock, R. E. W.; Sahl, H.-G. Antimicrobial and Host-Defense Peptides as New Anti-Infective Therapeutic Strategies. *Nat. Biotechnol.* **2006**, *24* (12), 1551–1557.
(217) Haag, R.; Kratz, F. Polymer Therapeutics: Concepts and Applications. *Angew. Chemie Int. Ed.* **2006**, *45* (8), 1198–1215.
(218) CalderÃ^{3}n, M.; Quadir, M. A.; Sharma, S. K.; Haag, R. Dendritic Polyglycerols for Biomedical Applications. *Adv. Mater.* **2010**, *22* (2), 190–218.
(219) Wilms, D.; Stiriba, S.-E.; Frey, H. Hyperbranched Polyglycerols: From the Controlled Synthesis of Biocompatible Polyether Polyols to Multipurpose Applications. *Acc. Chem. Res.* **2010**, *43* (1), 129–141.
(220) Kainthan, R. K.; Muliawan, E. B.; Hatzikiriakos, S. G.; Brooks, D. E. Synthesis, Characterization, and Viscoelastic Properties of High Molecular Weight Hyperbranched Polyglycerols. *Macromolecules* **2006**, *39* (22), 7708–7717.
(221) Krause, S.; Scholz, T.; Temmler, U.; Lösche, W. Monitoring the Effects of Platelet Glycoprotein IIb/IIIa Antagonists with a Microtiter Plate Method for Detection of Platelet Aggregation. *Platelets* **2001**, *12* (7), 423–430.
(222) Ahmed, M.; Lai, B. F. L.; Kizhakkedathu, J. N.; Narain, R. Hyperbranched Glycopolymers for Blood Biocompatibility. *Bioconjug. Chem.* **2012**, *23* (5), 1050–1058.
(223) Schmidtchen, A.; Ringstad, L.; Kasetty, G.; Mizuno, H.; Rutland, M. W.; Malmsten, M. Membrane Selectivity by W-Tagging of Antimicrobial Peptides. *Biochim. Biophys. Acta - Biomembr.* **2011**, *1808* (4), 1081–1091.
(224) Shenoi, R. A.; Lai, B. F. L.; Kizhakkedathu, J. N. Synthesis, Characterization, and Biocompatibility of Biodegradable Hyperbranched Polyglycerols from Acid-Cleavable Ketal Group Functionalized Initiators. *Biomacromolecules* **2012**, *13* (10), 3018–3030.

(225) Johnson, W. C. Analyzing Protein Circular Dichroism Spectra for Accurate Secondary Structures. *Proteins* **1999**, *35* (3), 307–312.
(226) Provencher, S. W.; Glöckner, J. Estimation of Globular Protein Secondary Structure from Circular Dichroism. *Biochemistry* **1981**, *20* (1), 33–37.
(227) Sreerama, N.; Venyaminov, S. Y.; Woody, R. W. Estimation of the Number of Alpha-Helical and Beta-Strand Segments in Proteins Using Circular Dichroism Spectroscopy. *Protein Sci.* **1999**, *8* (2), 370–380.
(228) Gao, G.; Cheng, J. T. J.; Kindrachuk, J.; Hancock, R. E. W.; Straus, S. K.; Kizhakkedathu, J. N. Biomembrane Interactions Reveal the Mechanism of Action of Surface-Immobilized Host Defense IDR-1010 Peptide. *Chem. Biol.* **2012**, *19* (2), 199–209.
(229) Zhao, J.; Zhao, C.; Liang, G.; Zhang, M.; Zheng, J. Engineering Antimicrobial Peptides with Improved Antimicrobial and Hemolytic Activities. *J. Chem. Inf. Model.* **2013**, *53* (12), 3280–3296.
(230) Fox, M. A.; Thwaite, J. E.; Ulaeto, D. O.; Atkins, T. P.; Atkins, H. S. Design and Characterization of Novel Hybrid Antimicrobial Peptides Based on Cecropin A, LL-37 and Magainin II. *Peptides* **2012**, *33* (2), 197–205.
(231) Yu, K.; Lai, B. F. L.; Foley, J. H.; Krisinger, M. J.; Conway, E. M.; Kizhakkedathu, J. N. Modulation of Complement Activation and Amplification on Nanoparticle Surfaces by Glycopolymer Conformation and Chemistry. *ACS Nano* **2014**, *8* (8), 7687–7703.
(232) Chan, D. I.; Prenner, E. J.; Vogel, H. J. Tryptophan- and Arginine-Rich Antimicrobial Peptides: Structures and Mechanisms of Action. *Biochim. Biophys. Acta - Biomembr.* **2006**, *1758* (9), 1184–1202.
(233) Haney, E. F.; Brito-Sánchez, Y.; Trimble, M. J.; Mansour, S. C.; Cherkasov, A.; Hancock, R. E. W. Computer-Aided Discovery of Peptides That Specifically Attack Bacterial Biofilms. *Sci. Rep.* **2018**, *8* (1), 1871.
(234) Frank, R. The SPOT-Synthesis Technique: Synthetic Peptide Arrays on Membrane Supports - Principles and Applications. *J. Immunol. Methods* **2002**, *267* (1), 13–26.
(235) Kumar, P.; Shenoi, R. A.; Lai, B. F. L.; Nguyen, M.; Kizhakkedathu, J. N.; Straus, S. K. Conjugation of Aurein 2.2 to HPG Yields an Antimicrobial with Better Properties. *Biomacromolecules* **2015**, *16* (3), 913–923.
(236) Greenfield, N. J. Using Circular Dichroism Spectra to Estimate Protein Secondary Structure. *Nat. Protoc.* **2006**, *1* (6), 2876–2890.
(237) Schiffer, M.; Edmundson, A. B. Use of Helical Wheels to Represent the Structures of Proteins and to Identify Segments with Helical Potential. *Biophys. J.* **1967**, *7* (2), 121–135.
(238) Killian, J. A. Synthetic Peptides as Models for Intrinsic Membrane Proteins. *FEBS Lett.* **2003**, *555* (1), 134–138.
(239) Scheinpflug, K.; Wenzel, M.; Krylova, O.; Bandow, J. E.; Dathe, M.; Strahl, H. Antimicrobial Peptide CWFW Kills by Combining Lipid Phase Separation with Autolysis. *Sci. Rep.* **2017**, *7* (February), 44332.
(240) Mugabe, C.; Matsui, Y.; So, A. I.; Gleave, M. E.; Baker, J. H. E.; Minchinton, A. I.; Manisali, I.; Liggins, R.; Brooks, D. E.; Burt, H. M. In Vivo Evaluation of Mucoadhesive Nanoparticulate Docetaxel for Intravesical Treatment of Non-Muscle-Invasive Bladder Cancer. *Clin. Cancer Res.* **2011**, *17* (9), 2788–2798.
(241) M.C. Chung, E.; Dean, S. N.; Propst, C. N.; Bishop, B. M.; van Hoek, M. L. Komodo

Dragon-Inspired Synthetic Peptide DRGN-1 Promotes Wound-Healing of a Mixed-Biofilm Infected Wound. *npj Biofilms Microbiomes* **2017**, *3* (1), 9.
(242) Carmona, G.; Rodriguez, A.; Juarez, D.; Corzo, G.; Villegas, E. Improved Protease Stability of the Antimicrobial Peptide Pin2 Substituted with D-Amino Acids. *Protein J.* **2013**, *32* (6), 456–466.
(243) Svenson, J.; Stensen, W.; Brandsdal, B. O.; Haug, B. E.; Monrad, J.; Svendsen, J. S. Antimicrobial Peptides with Stability toward Tryptic Degradation. *Biochemistry* **2008**, *47* (12), 3777–3788.
(244) Knappe, D.; Henklein, P.; Hoffmann, R.; Hilpert, K. Easy Strategy to Protect Antimicrobial Peptides from Fast Degradation in Serum. *Antimicrob. Agents Chemother.* **2010**, *54* (9), 4003–4005.
(245) Hamley, I. W. PEG-Peptide Conjugates. *Biomacromolecules* **2014**, *15* (5), 1543–1559.
(246) Harris, J. M.; Chess, R. B. Effect of Pegylation on Pharmaceuticals. *Nat. Rev. Drug Discov.* **2003**, *2* (3), 214–221.
(247) Amarnath, L. P.; Srinivas, A.; Ramamurthi, A. In Vitro Hemocompatibility Testing of UV-Modified Hyaluronan Hydrogels. *Biomaterials* **2006**, *27* (8), 1416–1424.
(248) Hansson, K. M.; Tosatti, S.; Isaksson, J.; Wetterö, J.; Textor, M.; Lindahl, T. L.; Tengvall, P. Whole Blood Coagulation on Protein Adsorption-Resistant PEG and Peptide Functionalised PEG-Coated Titanium Surfaces. *Biomaterials* **2005**, *26* (8), 861–872.
(249) Gorbet, M. B.; Sefton, M. V. Biomaterial-Associated Thrombosis: Roles of Coagulation Factors, Complement, Platelets and Leukocytes. *Biomaterials* **2004**, *25* (26), 5681–5703.
(250) Morris, C. J.; Beck, K.; Fox, M. A.; Ulaeto, D.; Clark, G. C.; Gumbleton, M. Pegylation of Antimicrobial Peptides Maintains the Active Peptide Conformation, Model Membrane Interactions, and Antimicrobial Activity While Improving Lung Tissue Biocompatibility Following Airway Delivery. *Antimicrob. Agents Chemother.* **2012**, *56* (6), 3298–3308.
(251) Sahariah, P.; Sørensen, K. K.; Hjálmarsdóttir, M. Á.; Sigurjónsson, Ó. E.; Jensen, K. J.; Másson, M.; Thygesen, M. B. Antimicrobial Peptide Shows Enhanced Activity and Reduced Toxicity upon Grafting to Chitosan Polymers. *Chem. Commun.* **2015**, *51* (58), 11611–11614.
(252) Donlan, R. M. Biofilms: Microbial Life on Surfaces. *Emerg. Infect. Dis.* **2002**, *8* (9), 881–890.
(253) Kolar, S. L.; Liu, G. Y. Targeting Bacterial Abscess Formation. *EBioMedicine* **2016**, *12*, 16–17.
(254) Kobayashi, S. D.; Malachowa, N.; DeLeo, F. R. Pathogenesis of Staphylococcus Aureus Abscesses. *Am. J. Pathol.* **2015**, *185* (6), 1518–1527.
(255) Mohamed, M. F.; Abdelkhalek, A.; Seleem, M. N. Evaluation of Short Synthetic Antimicrobial Peptides for Treatment of Drug-Resistant and Intracellular Staphylococcus Aureus. *Sci. Rep.* **2016**, *6* (1), 29707.
(256) Mohammad, H.; Thangamani, S.; Seleem, M. N. Antimicrobial Peptides and Peptidomimetics - Potent Therapeutic Allies for Staphylococcal Infections. *Curr. Pharm. Des.* **2015**, *21* (16), 2073–2088.
(257) Kumar, P.; Takayesu, A.; Abbasi, U.; Kalathottukaren, M. T.; Abbina, S.; Kizhakkedathu, J. N.; Straus, S. K. Antimicrobial Peptide–Polymer Conjugates with High Activity: Influence of Polymer Molecular Weight and Peptide Sequence on Antimicrobial Activity, Proteolysis, and Biocompatibility. *ACS Appl. Mater. Interfaces* **2017**, acsami.7b09471.

(258) Haney, E. F.; Mansour, S. C.; Hilchie, A. L.; de la Fuente-Núñez, C.; Hancock, R. E. W. High Throughput Screening Methods for Assessing Antibiofilm and Immunomodulatory Activities of Synthetic Peptides. *Peptides* **2015**, *71*, 276–285.
(259) Hancock, R. E.; Carey, A. M. Outer Membrane of Pseudomonas Aeruginosa: Heat- 2-Mercaptoethanol-Modifiable Proteins. *J. Bacteriol.* **1979**, *140* (3), 902–910.
(260) Cheng, K.; Smyth, R. L.; Govan, J. R.; Doherty, C.; Winstanley, C.; Denning, N.; Heaf, D. P.; van Saene, H.; Hart, C. A. Spread of β-Lactam-Resistant Pseudomonas Aeruginosa in a Cystic Fibrosis Clinic. *Lancet* **1996**, *348* (9028), 639–642.
(261) Centers for Disease Control and Prevention (CDC). Outbreaks of Community-Associated Methicillin-Resistant Staphylococcus Aureus Skin Infections--Los Angeles County, California, 2002-2003. *MMWR. Morb. Mortal. Wkly. Rep.* **2003**, *52* (5), 88.
(262) Pletzer, D.; Mansour, S. C.; Wuerth, K.; Rahanjam, N.; Hancock, R. E. W. New Mouse Model for Chronic Infections by Gram-Negative Bacteria Enabling the Study of Anti-Infective Efficacy and Host-Microbe Interactions. *MBio* **2017**, *8* (1), e00140-17.
(263) Mohamed, M. F.; Brezden, A.; Mohammad, H.; Chmielewski, J.; Seleem, M. N. A Short D-Enantiomeric Antimicrobial Peptide with Potent Immunomodulatory and Antibiofilm Activity against Multidrug-Resistant Pseudomonas Aeruginosa and Acinetobacter Baumannii.
(264) Yu, K.; Lo, J. C. Y.; Mei, Y.; Haney, E. F.; Siren, E.; Manu, ⊥; Kalathottukaren, T.; Hancock, R. E. W.; Lange, D.; Kizhakkedathu, J. N. Toward Infection-Resistant Surfaces: Achieving High Antimicrobial Peptide Potency by Modulating the Functionality of Polymer Brush and Peptide.
(265) Flemming, H.-C.; Wingender, J.; Szewzyk, U.; Steinberg, P.; Rice, S. A.; Kjelleberg, S. Biofilms: An Emergent Form of Bacterial Life. *Nat. Rev. Microbiol.* **2016**, *14* (9), 563–575.
(266) Mah, T. F.; O'Toole, G. A. Mechanisms of Biofilm Resistance to Antimicrobial Agents. *Trends Microbiol.* **2001**, *9* (1), 34–39.
(267) Holm, T.; Räägel, H.; Andaloussi, S. EL; Hein, M.; Mäe, M.; Pooga, M.; Langel, Ü. Retro-Inversion of Certain Cell-Penetrating Peptides Causes Severe Cellular Toxicity. *Biochim. Biophys. Acta - Biomembr.* **2011**, *1808* (6), 1544–1551.
(268) Jiang, Z.; Vasil, A.; Vasil, M.; Hodges, R. "Specificity Determinants" Improve Therapeutic Indices of Two Antimicrobial Peptides Piscidin 1 and Dermaseptin S4 Against the Gram-Negative Pathogens Acinetobacter Baumannii and Pseudomonas Aeruginosa. *Pharmaceuticals* **2014**, *7* (4), 366–391.
(269) Haney, E. F.; Wu, B. C.; Lee, K.; Hilchie, A. L.; Hancock, R. E. W. Aggregation and Its Influence on the Immunomodulatory Activity of Synthetic Innate Defense Regulator Peptides. *Cell Chem. Biol.* **2017**, *24* (8), 969–980.e4.
(270) Yang, Q.; Moulder K, R.; Cohen, M. S.; Cai, S.; Forrest, L. M. Cabozantinib Loaded DSPE-PEG2000Micelles as Delivery System: Formulation, Characterization and Cytotoxicity Evaluation. *BAOJ Pharm. Sci.* **2015**, *1*.
(271) Nygaard, R.; Romaniuk, J. A. H.; Rice, D. M.; Cegelski, L. Whole Ribosome NMR: Dipolar Couplings and Contributions to Whole Cells. *J. Phys. Chem. B* **2017**, *121* (40), 9331–9335.
(272) Vidovic, V.; Prongidi-Fix, L.; Bechinger, B.; Werten, S. Production and Isotope Labeling of Antimicrobial Peptides in Escherichia Coli by Means of a Novel Fusion Partner That

Enables High-Yield Insoluble Expression and Fast Purification. *J. Pept. Sci.* **2009**, *15* (4), 278–284.
(273) Yap, K. L.; Kim, J.; Truong, K.; Sherman, M.; Yuan, T.; Ikura, M. Calmodulin Target Database. *J. Struct. Funct. Genomics* **2000**, *1* (1), 8–14.
(274) Vogel, H. J. The Merck Frosst Award Lecture 1994. Calmodulin: A Versatile Calcium Mediator Protein. *Biochem. Cell Biol.* **1994**, *72* (9–10), 357–376.
(275) Ishida, H.; Vogel, H. J. Protein-Peptide Interaction Studies Demonstrate the Versatility of Calmodulin Target Protein Binding. *Protein Pept. Lett.* **2006**, *13* (5), 455–465.
(276) Tropea, J. E.; Cherry, S.; Waugh, D. S. Expression and Purification of Soluble His6-Tagged TEV Protease. *Methods Mol. Biol.* **2009**, *498*, 297–307.
(277) Li, J.; Sha, Y. A Convenient Synthesis of Amino Acid Methyl Esters. *Molecules* **2008**, *13* (5), 1111–1119.
(278) Palmer, A. G.; Cavanagh, J.; Wright, P. E.; Rance, M. Sensitivity Improvement in Proton-Detected Two-Dimensional Heteronuclear Correlation NMR Spectroscopy. *J. Magn. Reson.* **1991**, *93* (1), 151–170.
(279) Kay, L.; Keifer, P.; Saarinen, T. Pure Absorption Gradient Enhanced Heteronuclear Single Quantum Correlation Spectroscopy with Improved Sensitivity. *J. Am. Chem. Soc.* **1992**, *114* (26), 10663–10665.
(280) Schleucher, J.; Schwendinger, M.; Sattler, M.; Schmidt, P.; Schedletzky, O.; Glaser, S. J.; Sørensen, O. W.; Griesinger, C. A General Enhancement Scheme in Heteronuclear Multidimensional NMR Employing Pulsed Field Gradients. *J. Biomol. NMR* **1994**, *4* (2), 301–306.
(281) Kuliopulos, A.; Walsh, C. T. Production, Purification, and Cleavage of Tandem Repeats of Recombinant Peptides. *J. Am. Chem. Soc.* **1994**, *116* (11), 4599–4607.
(282) Bommarius, B.; Jenssen, H.; Elliott, M.; Kindrachuk, J.; Pasupuleti, M.; Gieren, H.; Jaeger, K.-E.; Hancock, R. E. W.; Kalman, D. Cost-Effective Expression and Purification of Antimicrobial and Host Defense Peptides in Escherichia Coli. *Peptides* **2010**, *31* (11), 1957–1965.
(283) Bornhorst, J. A.; Falke, J. J. Purification of Proteins Using Polyhistidine Affinity Tags. *Methods Enzymol.* **2000**, *326*, 245–254.
(284) Zhang, Z.-Z.; Yang, S.-S.; Dou, H.; Mao, J.-F.; Li, K.-S. Expression, Purification, and C-Terminal Amidation of Recombinant Human Glucagon-like Peptide-1. *Protein Expr. Purif.* **2004**, *36* (2), 292–299.
(285) Cottingham, I. R.; Millar, A.; Emslie, E.; Colman, A.; Schnieke, A. E.; McKee, C. A Method for the Amidation of Recombinant Peptides Expressed as Intein Fusion Proteins in Escherichia Coli. *Nat. Biotechnol.* **2001**, *19* (10), 974–977.
(286) Avitabile, C.; D'Andrea, L. D.; Romanelli, A. Circular Dichroism Studies on the Interactions of Antimicrobial Peptides with Bacterial Cells. *Sci. Rep.* **2015**, *4* (1), 4293.
(287) Foster, M. P.; McElroy, C. A.; Amero, C. D. Solution NMR of Large Molecules and Assemblies. *Biochemistry* **2007**, *46* (2), 331–340.
(288) Lippens, G.; Cahoreau, E.; Millard, P.; Charlier, C.; Lopez, J.; Hanoulle, X.; Portais, J. C. In-Cell NMR: From Metabolites to Macromolecules. *Analyst* **2018**, *143*.
(289) Luchinat, E.; Banci, L. A Unique Tool for Cellular Structural Biology: In-Cell NMR. *J. Biol. Chem.* **2016**, *291* (8), 3776–3784.
(290) Hartmann, M.; Berditsch, M.; Hawecker, J.; Ardakani, M. F.; Gerthsen, D.; Ulrich, A. S.

Damage of the Bacterial Cell Envelope by Antimicrobial Peptides Gramicidin S and PGLa as Revealed by Transmission and Scanning Electron Microscopy. *Antimicrob. Agents Chemother.* **2010**, *54* (8), 3132–3142.
(291) Mahlapuu, M.; Håkansson, J.; Ringstad, L.; Björn, C. Antimicrobial Peptides: An Emerging Category of Therapeutic Agents. *Front. Cell. Infect. Microbiol.* **2016**, *6*, 194.
(292) Gaspar, D.; Veiga, A. S.; Castanho, M. A. R. B. From Antimicrobial to Anticancer Peptides. A Review. *Front. Microbiol.* **2013**, *4*, 294.
(293) Kumar, P.; Kizhakkedathu, J.; Straus, S. Antimicrobial Peptides: Diversity, Mechanism of Action and Strategies to Improve the Activity and Biocompatibility In Vivo. *Biomolecules* **2018**, *8* (1), 4.
(294) Jiang, Z.; Vasil, A.; Vasil, M.; Hodges, R. "Specificity Determinants" Improve Therapeutic Indices of Two Antimicrobial Peptides Piscidin 1 and Dermaseptin S4 Against the Gram-Negative Pathogens Acinetobacter Baumannii and Pseudomonas Aeruginosa. *Pharmaceuticals* **2014**, *7* (4), 366–391.
(295) Bacalum, M.; Radu, M. Cationic Antimicrobial Peptides Cytotoxicity on Mammalian Cells: An Analysis Using Therapeutic Index Integrative Concept. *Int. J. Pept. Res. Ther.* **2015**, *21* (1), 47–55.
(296) Subbalakshmi, C.; Sitaram, N. Mechanism of Antimicrobial Action of Indolicidin. *FEMS Microbiol. Lett.* **1998**, *160* (1), 91–96.
(297) Hsu, C.-H.; Chen, C.; Jou, M.-L.; Lee, A. Y.-L.; Lin, Y.-C.; Yu, Y.-P.; Huang, W.-T.; Wu, S.-H. Structural and DNA-Binding Studies on the Bovine Antimicrobial Peptide, Indolicidin: Evidence for Multiple Conformations Involved in Binding to Membranes and DNA. *Nucleic Acids Res.* **2005**, *33* (13), 4053–4064.
(298) Singh, M.; Kim, S. J.; Sharif, S.; Preobrazhenskaya, M.; Schaefer, J. REDOR Constraints on the Peptidoglycan Lattice Architecture of Staphylococcus Aureus and Its FemA Mutant. *Biochim. Biophys. Acta - Biomembr.* **2015**, *1848* (1), 363–368.
(299) Romaniuk, J. A. H.; Cegelski, L. Bacterial Cell Wall Composition and the Influence of Antibiotics by Cell-Wall and Whole-Cell NMR. *Philos. Trans. R. Soc. Lond. B. Biol. Sci.* **2015**, *370* (1679), 20150024.
(300) de la Fuente-Núñez, C.; Reffuveille, F.; Haney, E. F.; Straus, S. K.; Hancock, R. E. W. Broad-Spectrum Anti-Biofilm Peptide That Targets a Cellular Stress Response. *PLoS Pathog.* **2014**, *10* (5), e1004152.
(301) Pletzer, D.; Coleman, S. R.; Hancock, R. E. Anti-Biofilm Peptides as a New Weapon in Antimicrobial Warfare. *Curr. Opin. Microbiol.* **2016**, *33*, 35–40.
(302) Li, L.-L.; Xu, J.-H.; Qi, G.-B.; Zhao, X.; Yu, F.; Wang, H. Core–Shell Supramolecular Gelatin Nanoparticles for Adaptive and "On-Demand" Antibiotic Delivery. *ACS Nano* **2014**, *8* (5), 4975–4983.
(303) Maeda, H. Role of Microbial Proteases in Pathogenesis. *Microbiol. Immunol* **1996**, *40* (10), 685–699.
(304) Vanlaere, I.; Libert, C. Matrix Metalloproteinases as Drug Targets in Infections Caused by Gram-Negative Bacteria and in Septic Shock. *Clin. Microbiol. Rev.* **2009**, *22* (2), 224–39, Table of Contents.
(305) Qi, G.-B.; Zhang, D.; Liu, F.-H.; Qiao, Z.-Y.; Wang, H. An "On-Site Transformation" Strategy for Treatment of Bacterial Infection. *Adv. Mater.* **2017**, *29* (36), 1703461.
(306) Ashok, B.; Arleth, L.; Hjelm, R. P.; Rubinstein, I.; Onyüksel, H. In Vitro Characterization

of PEGylated Phospholipid Micelles for Improved Drug Solubilization: Effects of PEG Chain Length and PC Incorporation. *J. Pharm. Sci.* **2004**, *93* (10), 2476–2487.
(307) Bulbake, U.; Doppalapudi, S.; Kommineni, N.; Khan, W. Liposomal Formulations in Clinical Use: An Updated Review. *Pharmaceutics* **2017**, *9* (4), 12.

Appendix A

A.1 HPLC trace of Aurein 2.2Δ3-cys

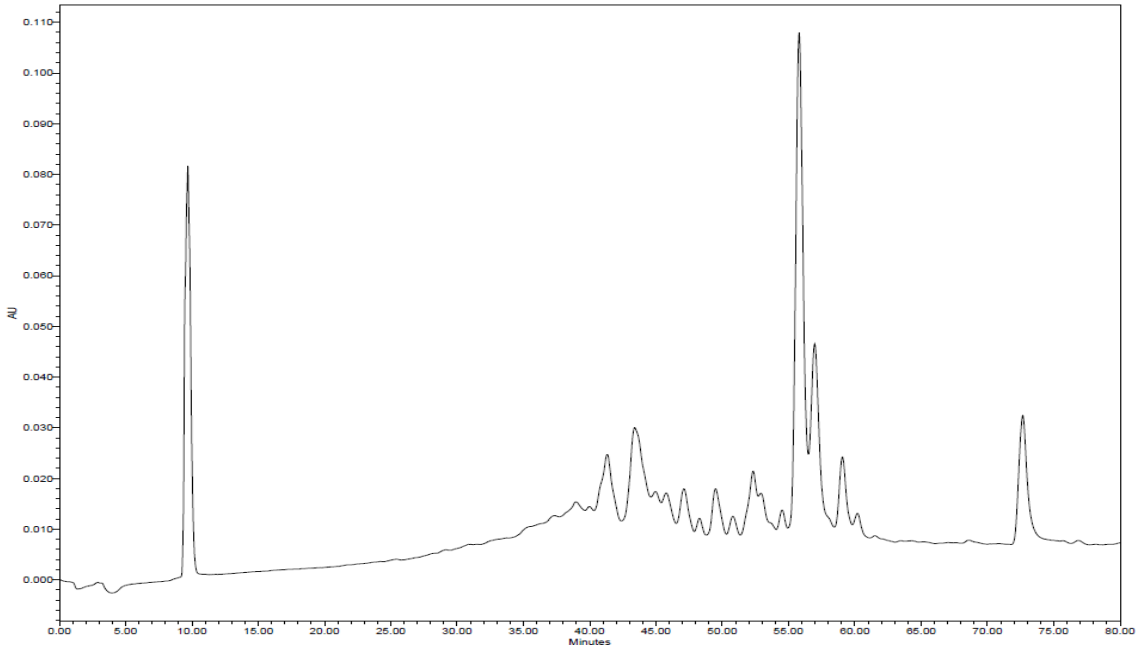

Figure A.1: HPLC purification of the Aurein 2.2Δ3cys. Peptide elutes between 55-57mins.

A.2 Proton NMR of amine functionalized HPG

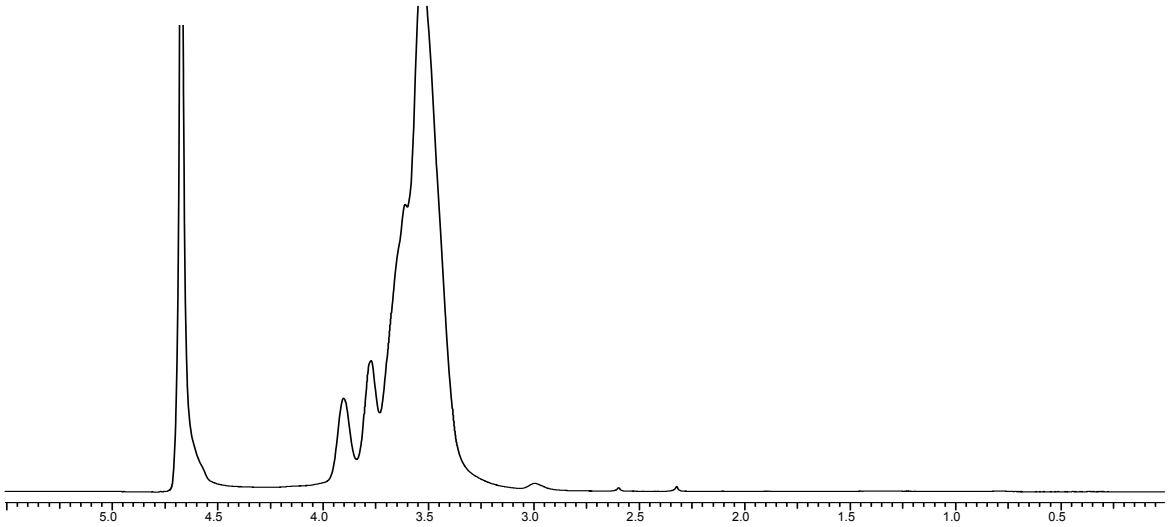

Figure A.2: Proton NMR (in D_2O) of amine modified HPG. Protons from the CH_2 group next to the amine show around 3.0ppm (A).

A.3 Proton NMR of HPG-bifunctional linker

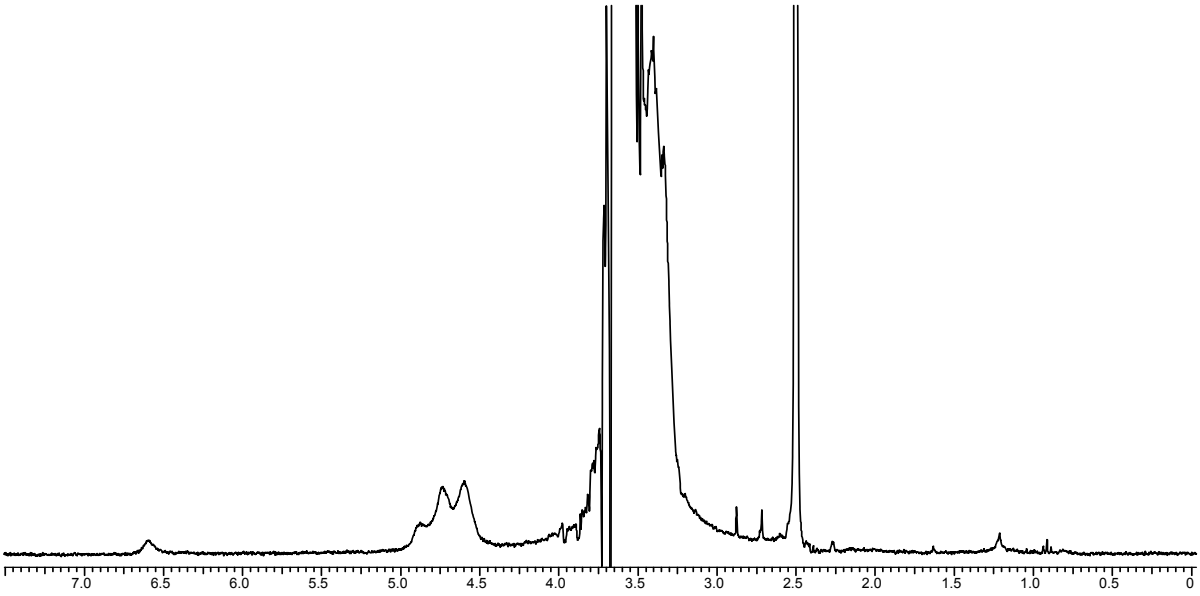

Figure A.3: Proton NMR (in deuterated DMSO) of HPG-bifunctional Linker. The Amide (NH) peak at 6.5ppm indicates the formation of an amide bond. In deuterated DMSO the protons from the hydoxyl groups of HPG can also be observed between 4.5-5.0ppm

A.4 UV spectra of the HPG-bifunctional linker

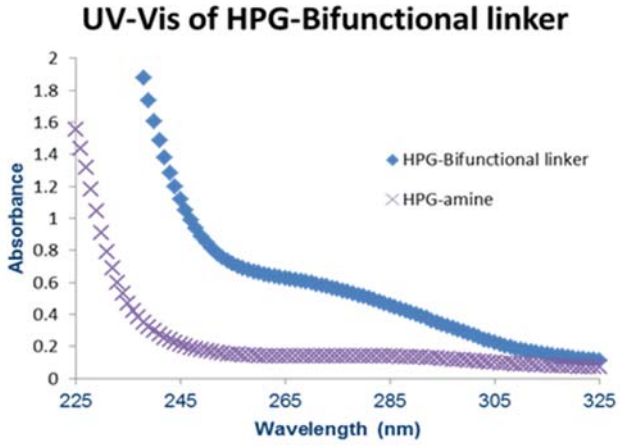

Figure A.4: UV-Vis of HPG-Bifunctional linker. Amine modified HPG does not absorb light in the UV-Vis region. However, once conjugated to the bifunctional linker it absorbs between 250-280 nm. Concentration of both the compounds was constant at 1 mg/mL.

A.5 HPLC purification of the conjugate

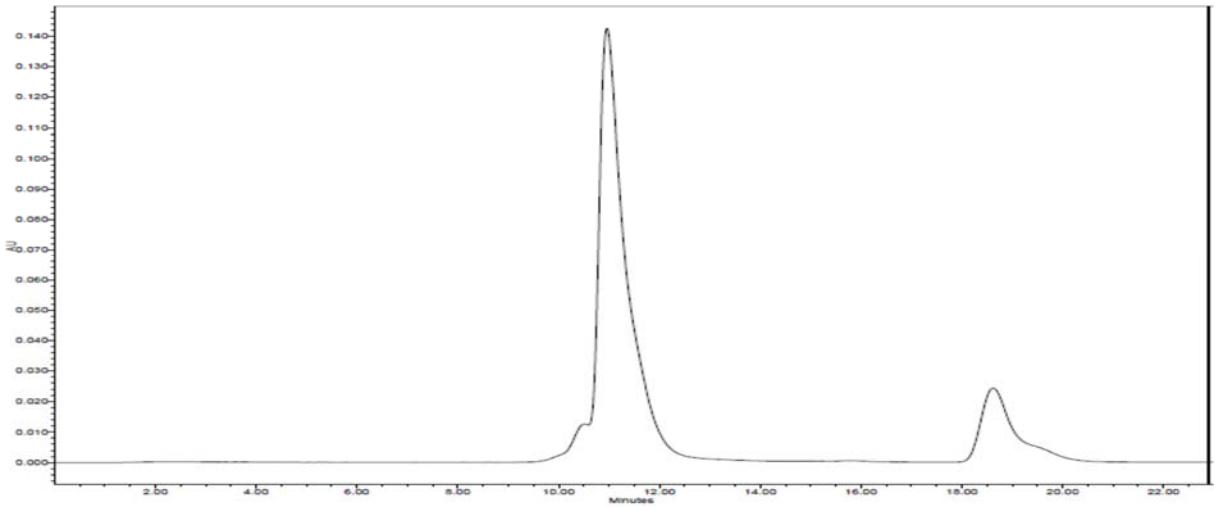

Figure A.5: Size exclusion HPLC purification of the bioconjugates. HPH-Aurein 2.2Δ3-cys elutes between 10-12min whereas the unreacted peptide elutes around 18-20min.

A.6 Proton NMR of HPG-Aurein 2.2Δ3-cys

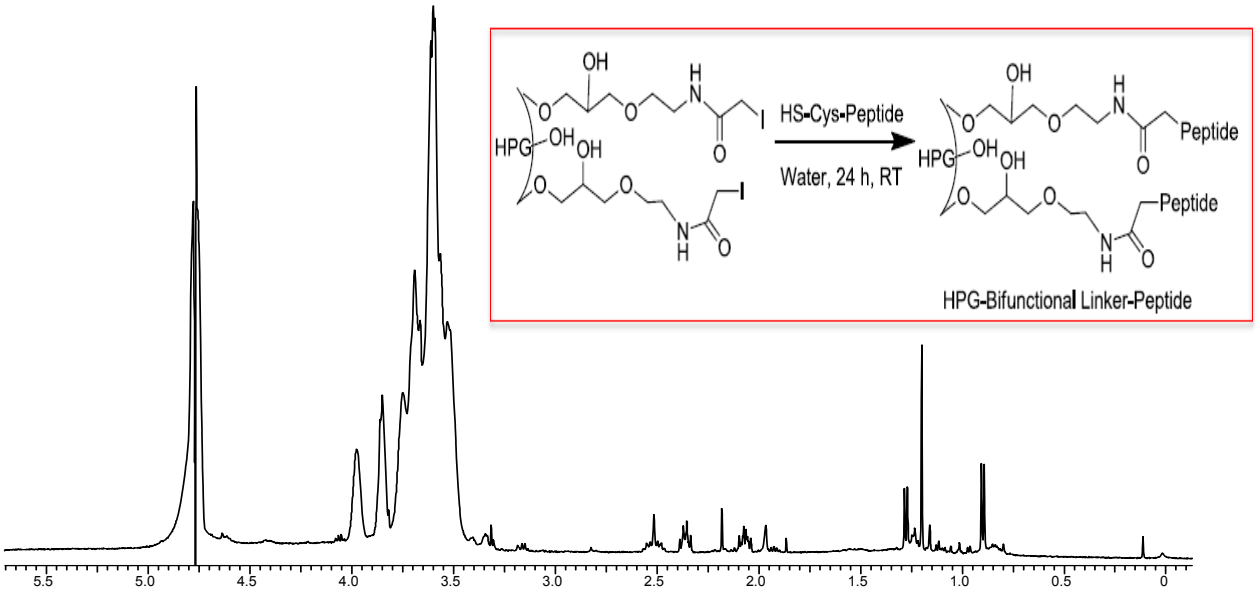

Figure A.6: Proton NMR (in D_2O) of HPG-Aurein 2.2Δ3-cys. The peak that eluted around 10-12minutes in the HPLC trace (figure A.5) was used for Proton NMR experiment. Additional peaks from the peptides can be observed between 0-5.0 ppm.

A.7 Size exclusion chromatography of conjugates

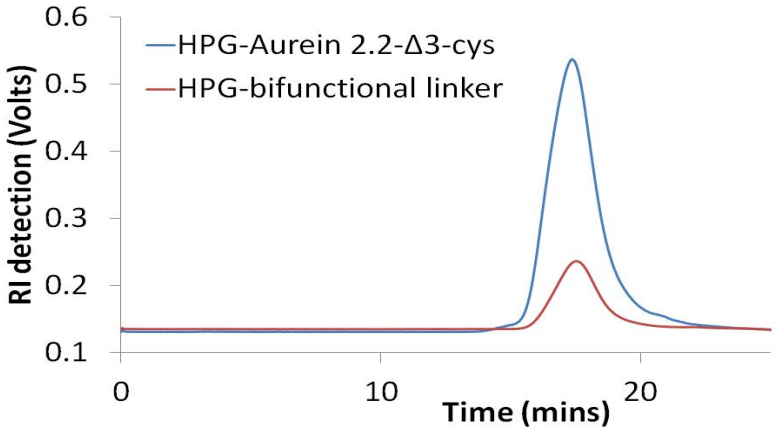

Figure A.7: Size exclusion chromatographs of HPG-Aurein 2.2Δ3-cys (M_n = 56,000) and HPG-Bifunctional linker (M_n = 44,000) at flow rate 0.8 mL/min at 25°C.

A.8 CD spectroscopy of Aurein 2.2Δ3-cys

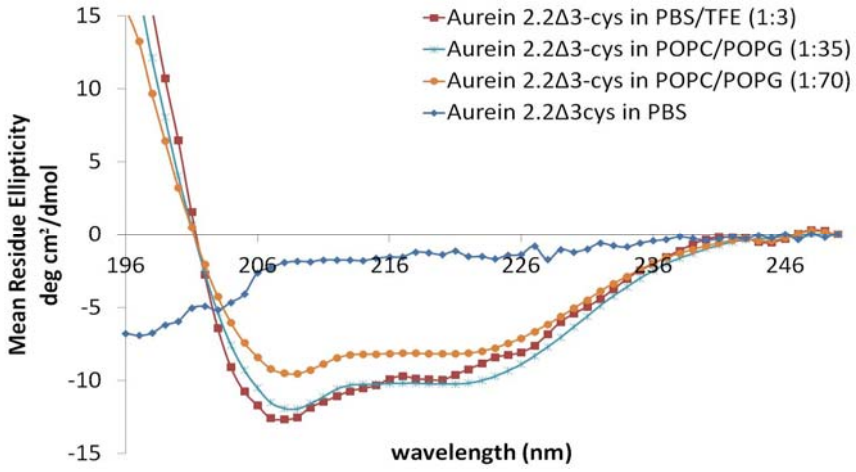

Figure A.8: CD spectra of the Aurein 2.2Δ3-cys in and trifluroethanol (TFE) and lipids (POPC/POPG).

A.9 CD spectroscopy of the conjugates

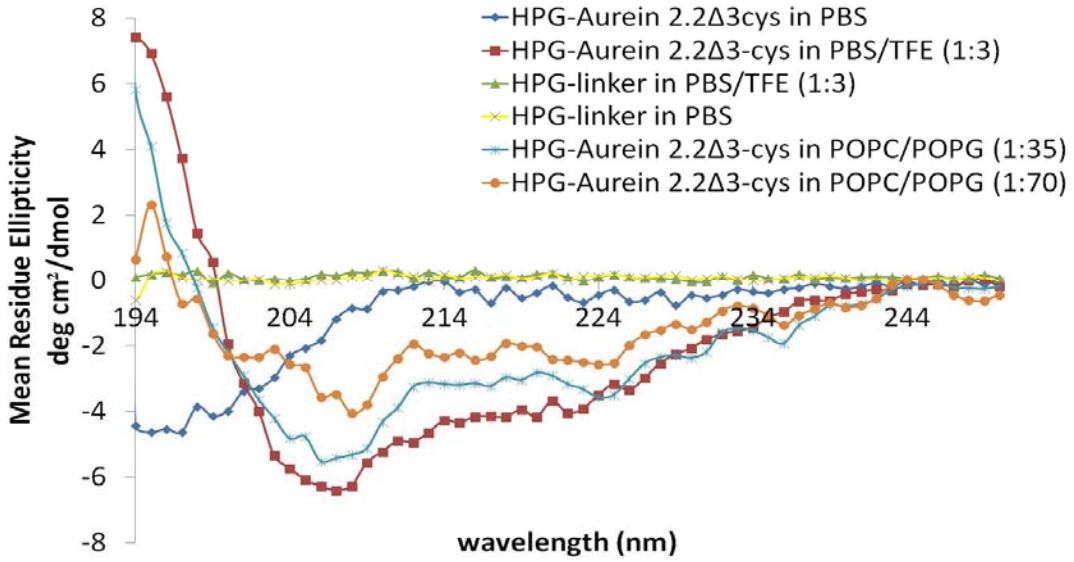

Figure A.9: CD spectra of the HPG-Aurein 2.2Δ3-cys in PBS buffer, Trifluroethanol (TFE) and lipids (POPC/POPG). In the presence of TFE and lipids the peptides conjugated to the polymer is still able to adopt a alpha helical structure.

A.10 Platelet aggregation by the bioconjugates

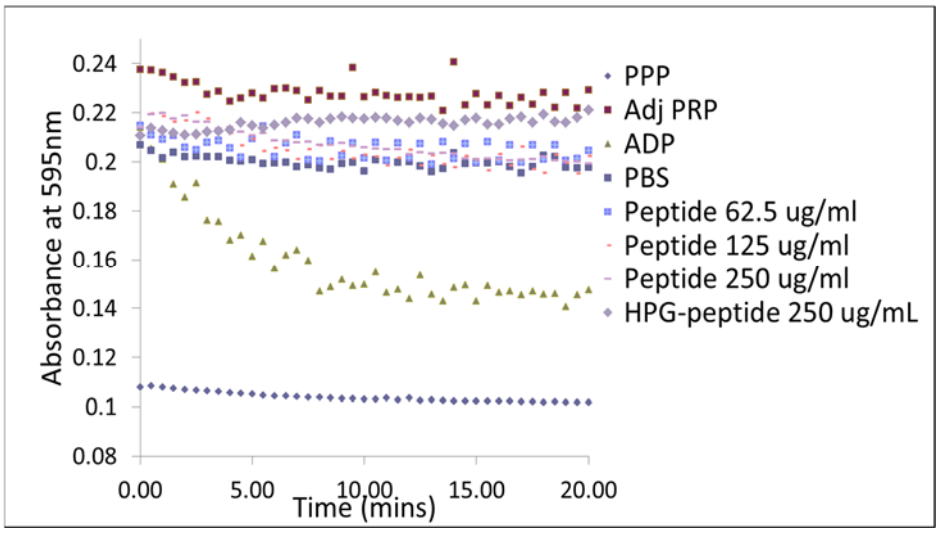

Figure A.10: Platelet aggregation by the bioconjugates. Aggregation was measured by measuring absorbance at 595 nm. Adjusted Platelet rich plasma (PRP) was incubated with peptides or conjugates and the absorbance was measured for 20 minutes. As aggregation increases the absorbance decreases as more light can pass through. The rate of aggregation

can be measured by calculating the slope during the first 5 minutes. The end point (total amount of platelet aggregated) can be calculated by plateau phase (last 5 minutes). 5 μM ADP was used as a positive control and PBS buffer as normal control. The absorbance of adjusted PRP and PPP is used as theoretical 100% aggregation and no aggregation respectively for calculation of percent aggregation.

Appendix B

B.1 Proton NMR of HPG-phthalimide

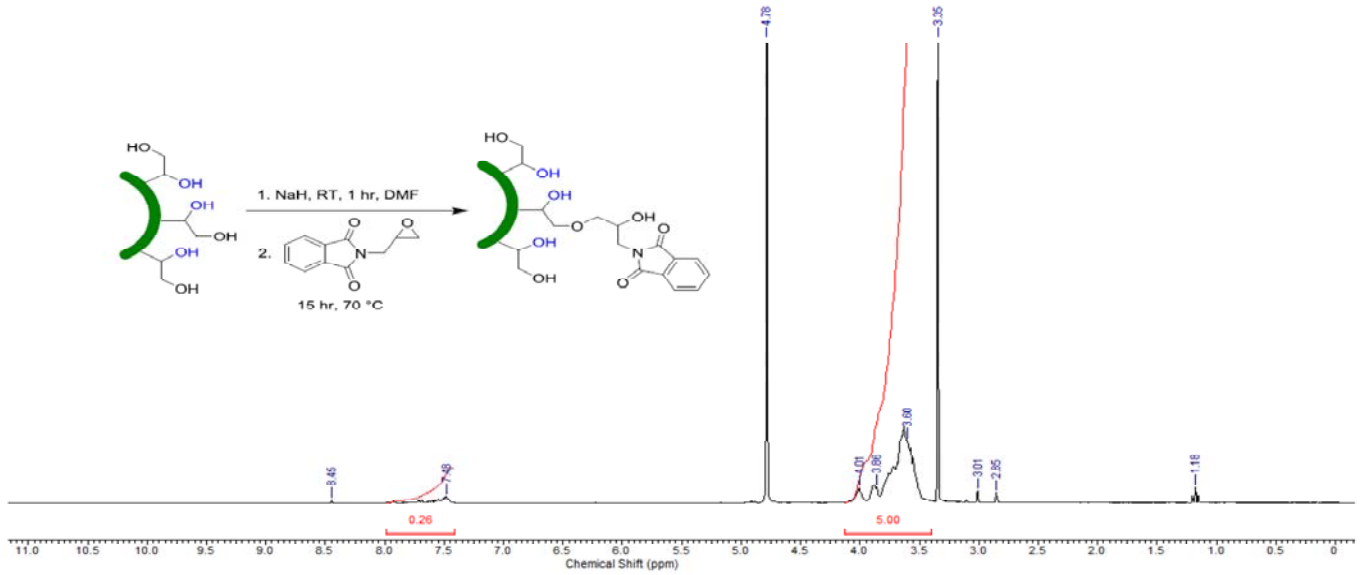

Figure B.1: ^{1}H NMR (in 100% DMSO-d6) of phthalimide modified 22k HPG. Protons from the phthalimide group appear around 7.5-8 ppm.

B.2 Proton NMR of HPG-Amine

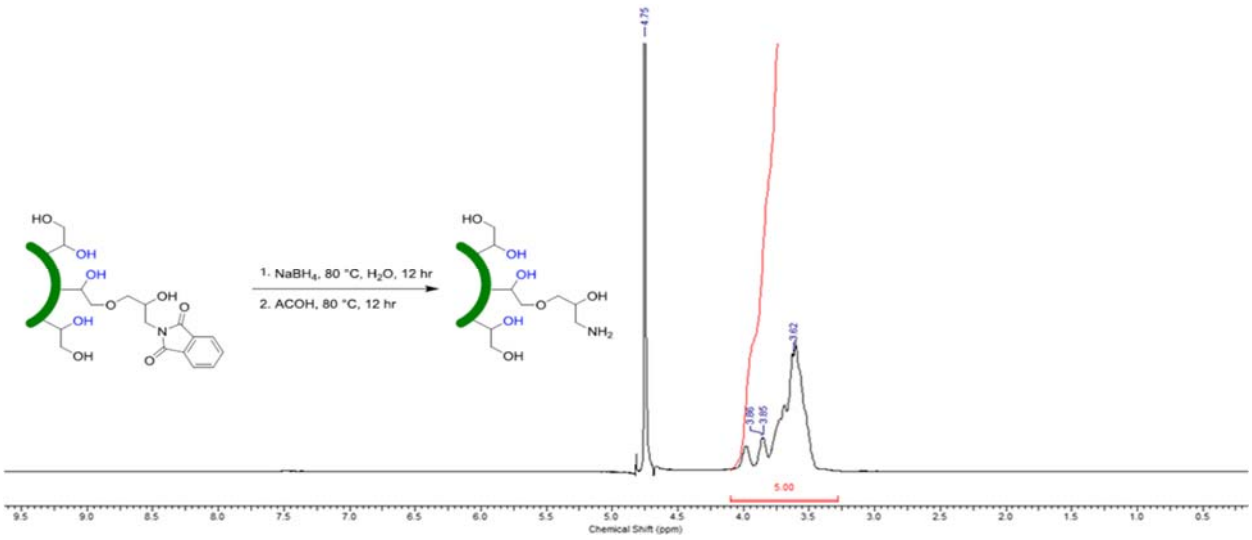

Figure B. 2: ^{1}H NMR (in 100% DMSO-d6) of 22k HPG-NH_2 after deprotection of the phthalimide.

B.3 Proton NMR of HPG maleimide

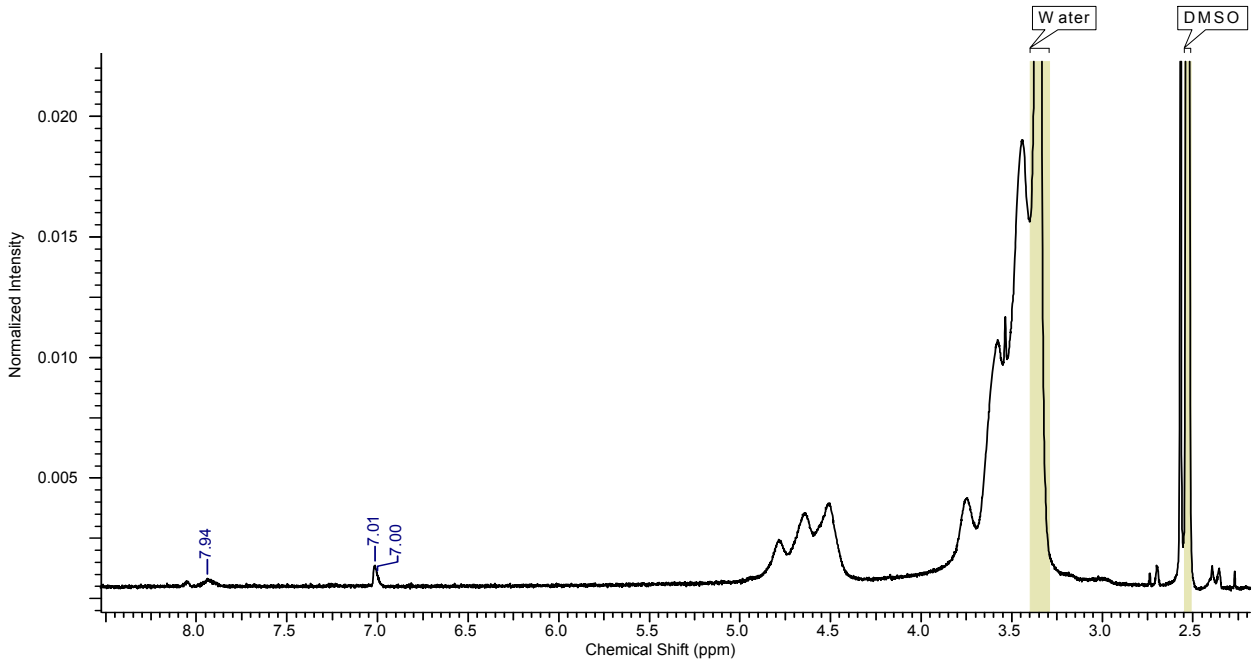

Figure B.3: ^{1}H NMR (in 100% DMSO-d6) of 22k HPG maleimide.

B.4 Proton NMR of HPG 77c

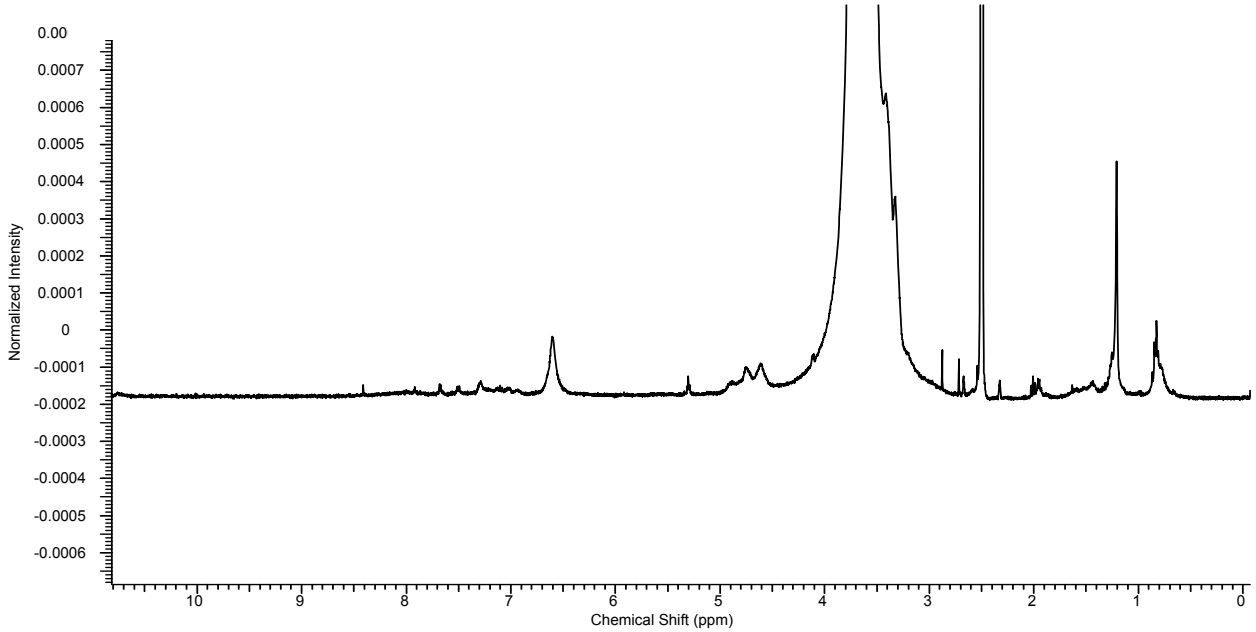

Figure B.4: ^{1}H NMR (in 100% DMSO- d6) of 22k HPG 77c.

B.5 Proton NMR of PEG 77c

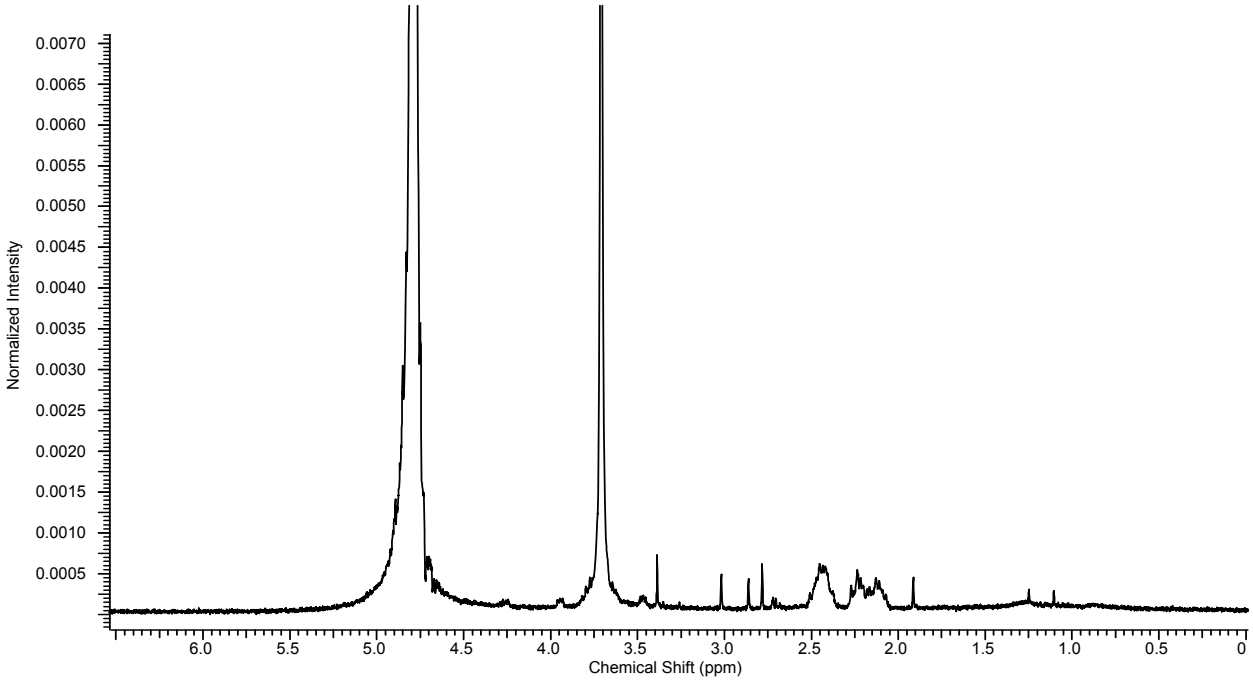

Figure B. 5: ^{1}H NMR (in 100% D_2O) of 5k mPEG 77c

B.6 Bacteria killing and RBC lysis in whole blood/bacteria mixture

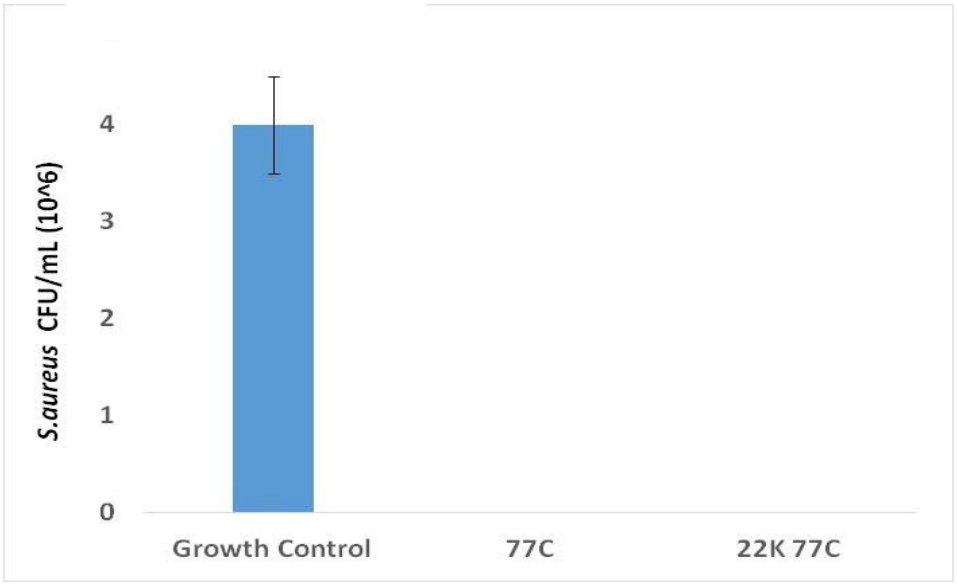

Figure B.6a: Bacterial colony forming units per milliliters (CFU/mL) in whole blood in presence of peptide/conjugates. No bacterial counts were detected for the 77c and 22k 77c (125 µg/mL). In the combined blood and bacteria experiment, bacteria (*S. aureus* C622) was diluted to $2x10^6$ CFU/mL in LB. Forty five microliters of 50% citrated blood (1:1

whole blood:PBS) was added and to 45 µL of the diluted bacterial suspension followed by 10 µL of peptide 77c or 22k 77c (125 µg/mL final concentration) and incubated at 37 °C for 1 h. The incubation mixture (5 µL) was serial diluted in LB and plated on LB agar, followed by incubation for 18-24 hours at 37 °C for CFU determination. Percent lysis for the mixture was measured by the Drabkin's method as described in the main text.

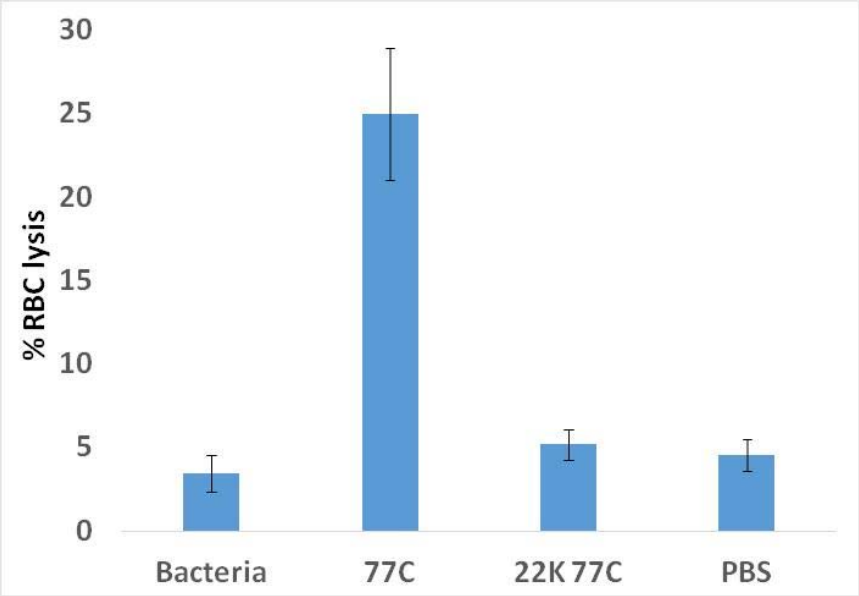

Figure B.6b: Percent RBC lysis in the whole blood in presence of bacteria and peptide/conjugate. Combined RBC lysis in the presence of bacterial cells. Peptide/conjugates (125 ug/mL) were added to the 50% citrated RBC/bacterial mixture (1:1). Lysis was determined by Drabkin's method.

B.7 Bacteria killing in serum/bacteria mixture

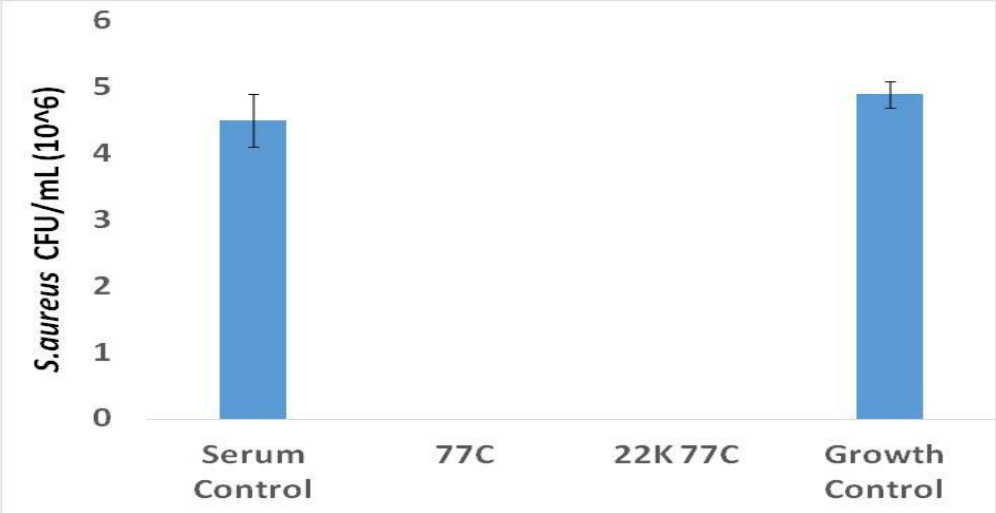

Figure B.7: The ability for the peptide and conjugates to kill bacteria in serum. Both 77c (125 µg/mL) and 22K 77c (125 µg/mL) cleared bacteria in serum efficiently. Bacteria killing assay was performed the same way as the combined blood lysis study. Instead of adding whole blood, 45 µL of serum was added to forty five microliters of the diluted bacteria. Mixture was incubated for 1 h at 37 °C and five microliters of the incubation mixture was serial diluted in LB and plated on LB agar to determine the CFU count.

B.8 Maldi of Matrix

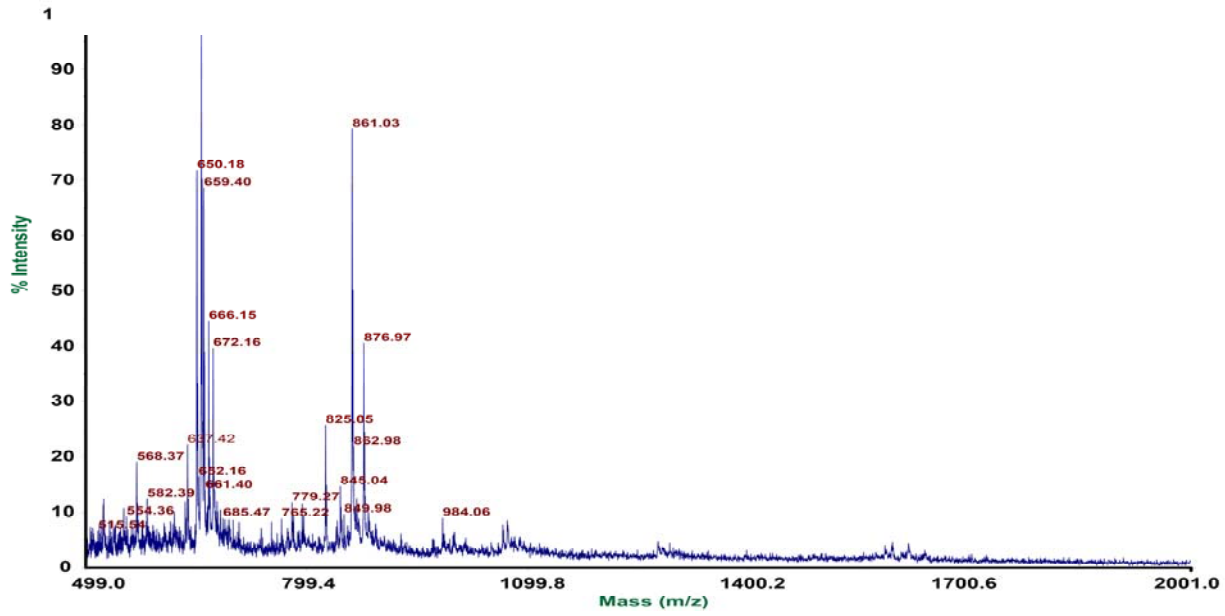

Figure B.8: MALDI of matrix.

B.9 aPTT analaysis of 77c and the conjugates

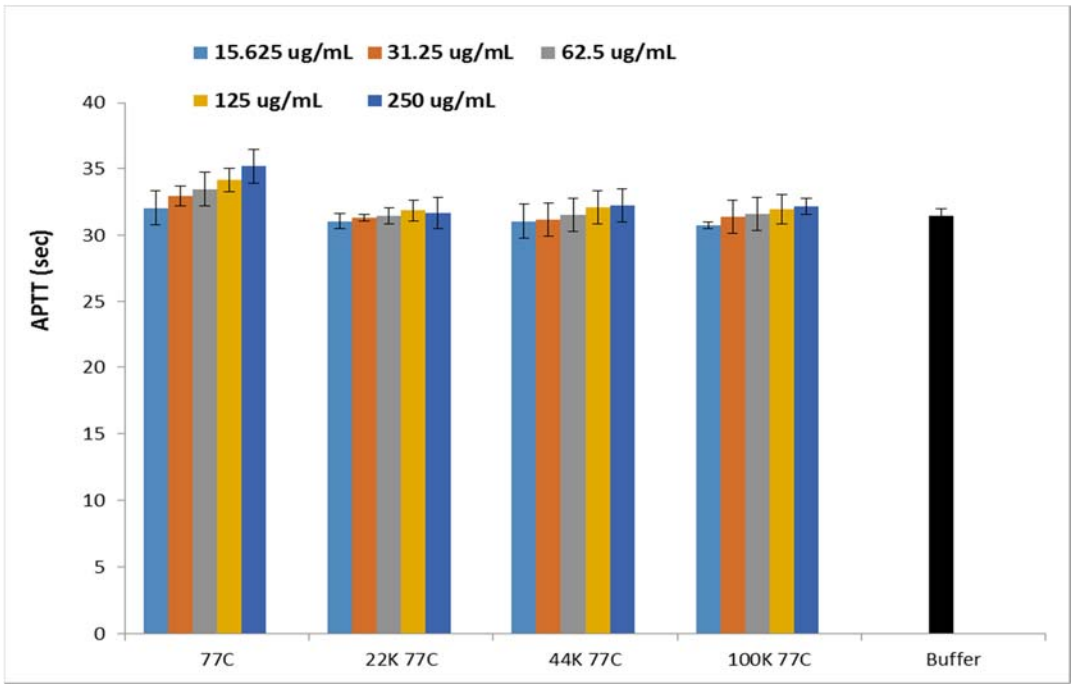

Figure B.9: Influence of free peptide and HPG peptide conjugates on activated Partial Thromboplastin Time (aPTT). Results are courtesy of Dr. Manu Thomas Kalathottukaren.

B.10 Thromboelastometry of conjugates and peptides

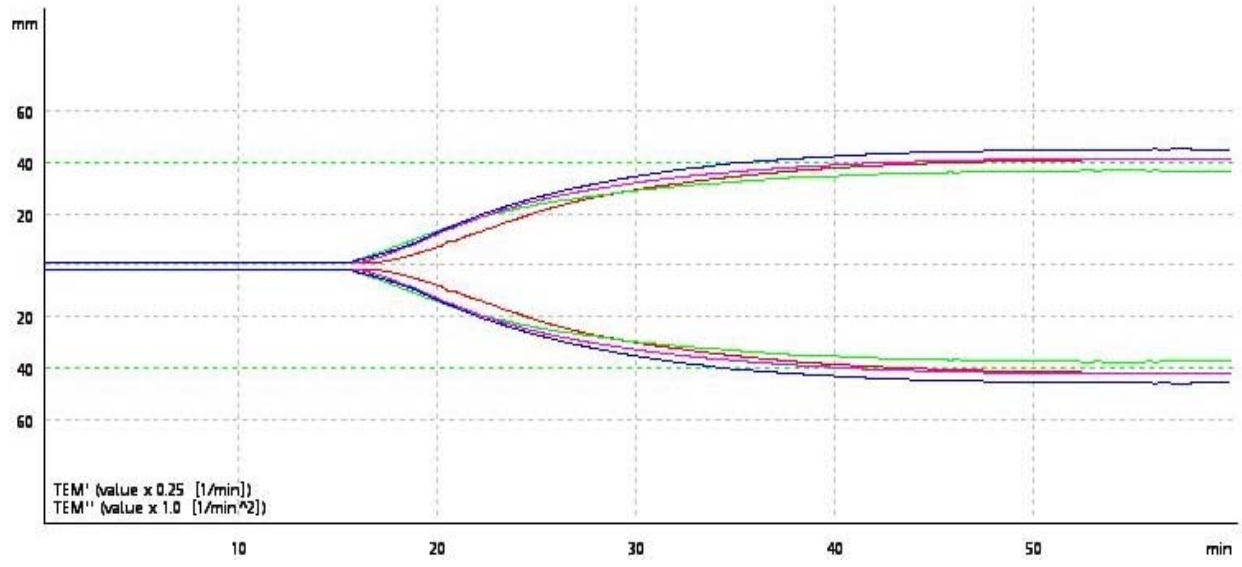

Figure B.10: Typical thromboelastometry of the HEPES-buffered saline (HBS) (red), 22K 77c (purple) and 77c (green), all at 125 µg/mL.

B.11 aPTT analaysis of 77c and the conjugates

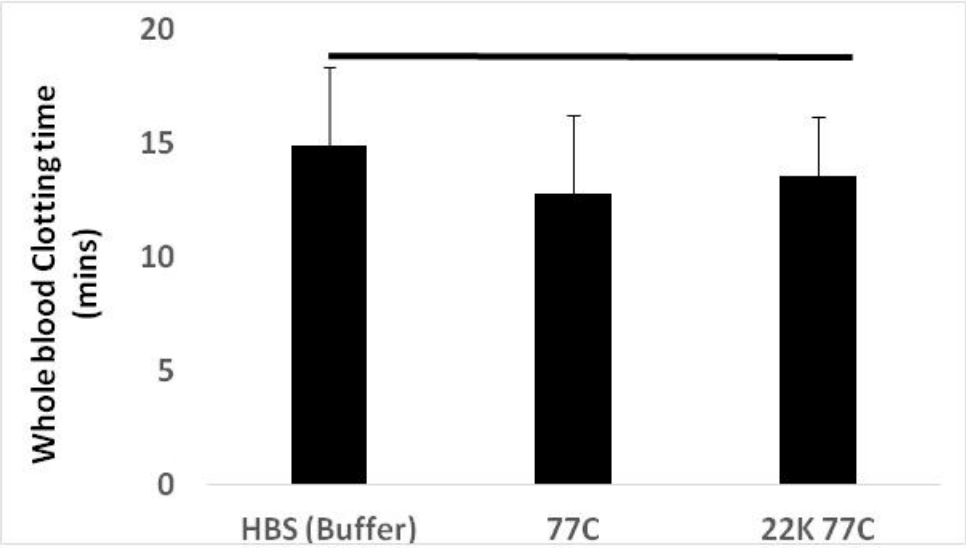

Figure B.11: Whole blood clotting time by Thromboelastometry of the 22k 77c and 77c, all at 125 µg/mL (n=3). No significant (ns) difference was observed in the clotting time of 22k 77c and 77c compared to buffer.

Appendix C

C.1 Toxicity and precipitation of D-peptides at various concentrations in saline.

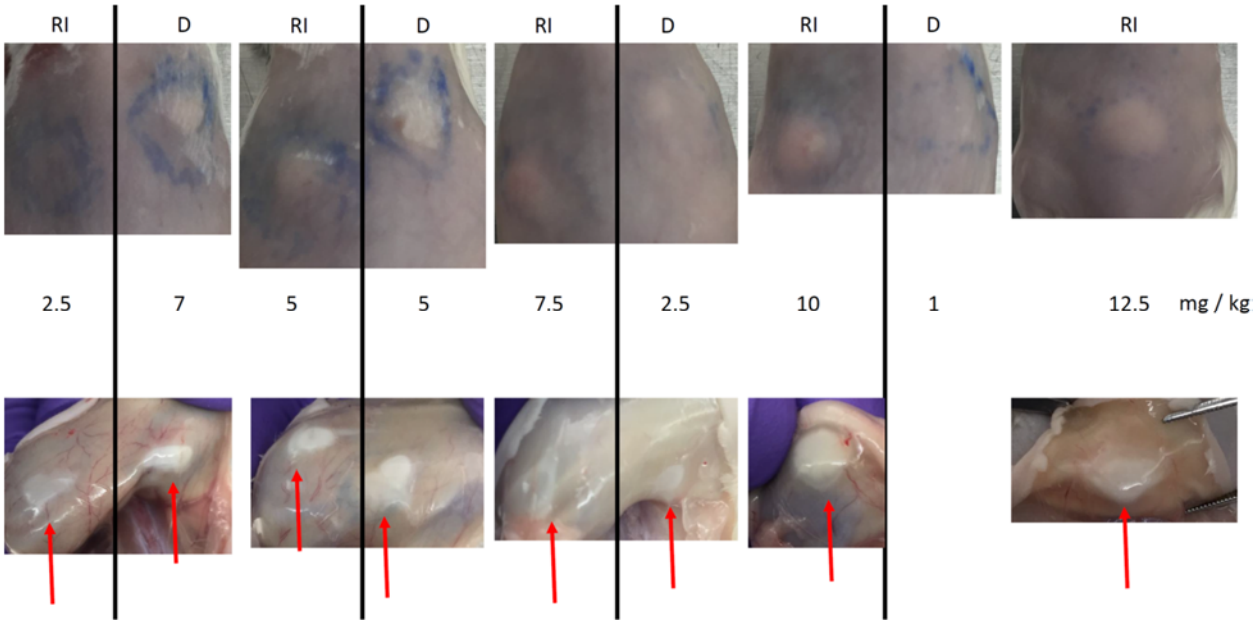

Figure C. 1: CD-1 mice were injected with 50 ul of different peptide concentrations on the left and right side of the dorsum. The skin inspected three days post injection. Upper panel: The backside of the mice. Lower panel: Skin flap to show the injection side under the skin. The red arrows point to peptide precipitation. Results are courtesy of Dr. Daniel Pletzer from the Hancock lab (UBC).

C.2 Toxicity and precipitation of D-peptides at various concentrations in DSPE-PEG2000

Stock 10 mg/ml in DSPE-PEG2000:
- D-73
- RI-73
- HPG-73

Toxicity test concentrations (D,RI):
- 10 mg/kg
- 8 mg/kg
- 6 mg/kg
- 4 mg/kg
- 2 mg/kg

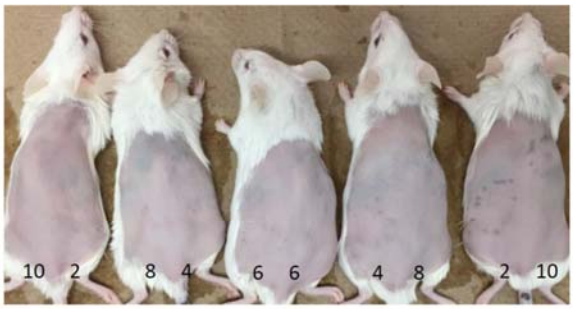

Left: D-73
Right: RI-73

Toxicity test concentrations (HPG):
- 10 mg/kg
- 5 mg/kg

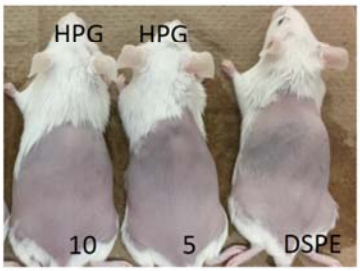

Figure C.2: CD-1 mice were injected with 50 ul of different peptide concentrations on the left and right side of the dorsum. The skin inspected three days post injection. No visible peptide/conjugate precipitation at various concentration in DSPE-PEG2000. Results are courtesy of Dr. Daniel Pletzer from the Hancock lab (UBC).

C.3 Average hydrodynamic size of peptide 73c in water and DSPE-PEG2000.

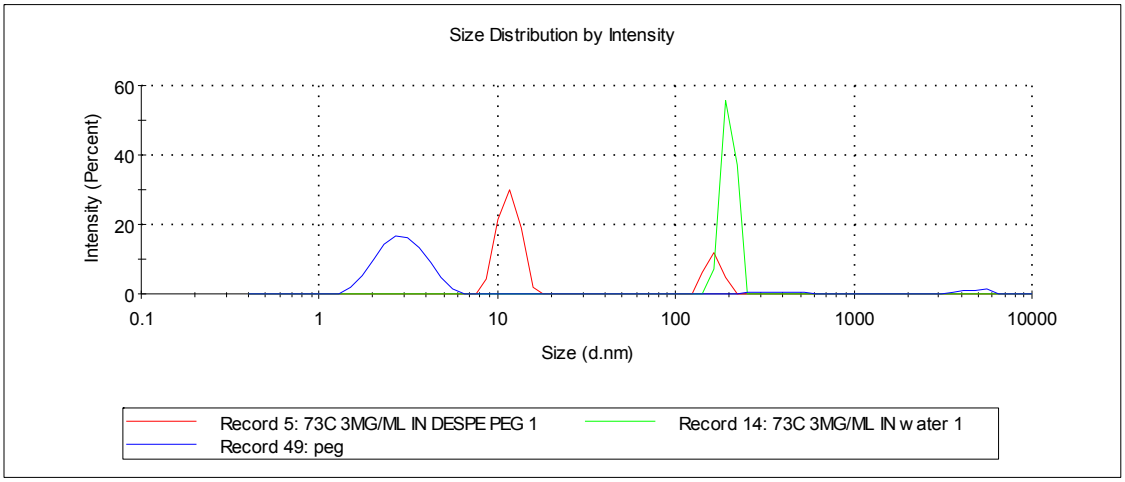

Figure C.3: Average hydrodynamic size and the intensity percent of peptide 73c in water and DSPE-PEG2000.

Appendix D

D.1 MS/MS spectra of aurein 2.2 and diesterified aurein 2.2

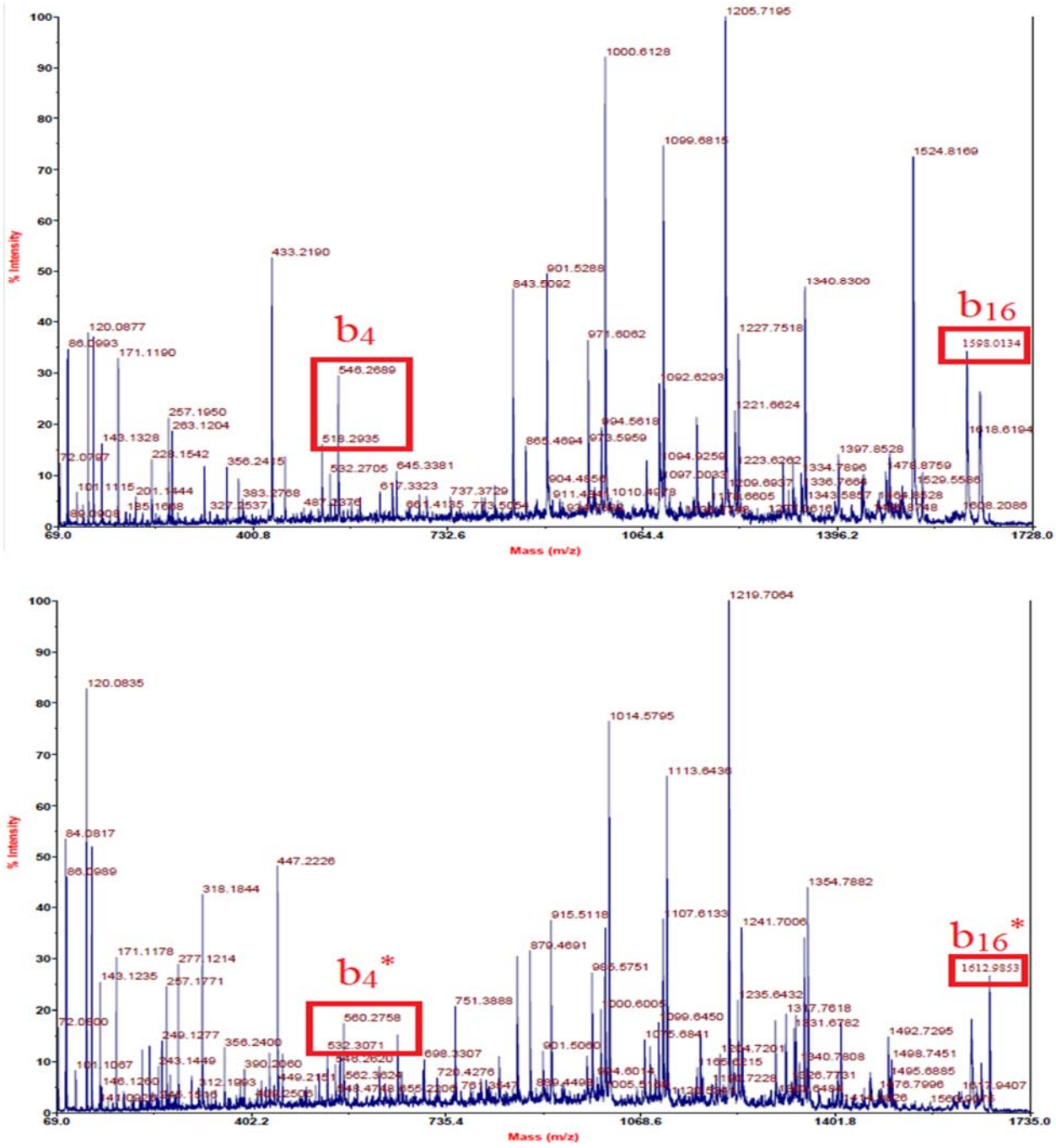

Figure D.1: MS/MS spectra of aurein 2.2 (top) and diesterified aurein 2.2 (bottom). The corresponding b ions for the C-terminus (L16) and aspartic acid (D4) residues are denoted and with an asterisk (*) to indicate an increase of +15 Da.